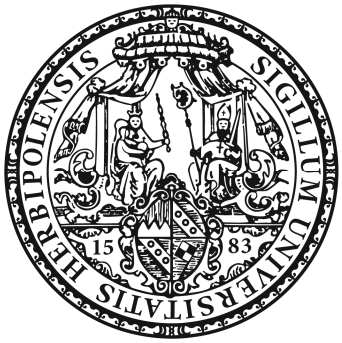

AN *IN VITRO* SYSTEM FOR THE BIOGENESIS OF SMALL NUCLEAR RIBONUCLEOPROTEIN PARTICLES

by

Nils Neuenkirchen

from Bremen, Germany

A thesis submitted to the Faculty of Pharmacy and Chemistry of the University of Würzburg, Germany, in partial fulfilment of the requirement for the degree of

Doctor rerum naturalium (Dr. rer. nat.)

Chair of Biochemistry

Würzburg, Germany, 2012

Date of submission: 27 April 2012

PhD thesis examiners:

1st Examiner: Prof. Dr. Utz Fischer

2nd Examiner: Prof. Dr. Alexander Buchberger

Members of the oral defence commission:

1st Examiner: Prof. Dr. Utz Fischer

2nd Examiner: Prof. Dr. Alexander Buchberger

3rd Examiner: Prof. Dr. Manfred Gessler

Date of the oral defence: 4 June 2012

Delivery of Dr. rer. nat. certificate:

Declaration

By this I declare on oath that I have written the dissertation "AN *IN VITRO* SYSTEM FOR THE BIOGENESIS OF SMALL NUCLEAR RIBONUCLEOPROTEIN PARTICLES" by myself and that no other means than those mentioned were used.

Furthermore, I assert not having submitted this dissertation in identical or other form to another examination board.

I did neither acquire nor tried to acquire any other academic degrees than those provided in the admission application.

Würzburg, Germany, 27 April 2012

…….

Nils Neuenkirchen

Summary

Most protein-encoding genes in Eukaryotes are separated into alternating coding and non-coding sequences (exons and introns). Following the transcription of the DNA into pre-messenger RNA (pre-mRNA) in the nucleus, a macromolecular complex termed spliceosome removes the introns and joins the exons to generate mature mRNA that is exported to the cytoplasm. There, it can be interpreted by ribosomes to generate proteins.

The spliceosome consists of five small nuclear ribonucleic acids (snRNAs) and more than 150 proteins. Integral components of this complex are RNA-protein particles (RNPs) composed of one or two snRNAs, seven common (Sm) and a various number of snRNP-specific proteins. The Sm proteins form a ring-structure around a conserved site of the snRNA called Sm site. *In vitro*, Sm proteins (B/B', D1, D2, D3, E, F, G) and snRNA readily assemble to form snRNPs. In the context of the cell, however, two macromolecular *trans*-acting factors, the PRMT5 (protein arginine methyltransferases type 5) and the SMN (survival motor neuron) complex, are needed to enable this process.

Initially, the Sm proteins in the form of heterooligomers D1/D2, D3/B and F/E/G are sequestered by the type II methyltransferase PRMT5. pICln, a component of the PRMT5 complex, readily interacts with Sm proteins to form two distinct complexes. Whereas the first one comprises pICln and D3/B the second one forms a ring consisting of pICln, D1/D2 and F/E/G (6S). It has been found that pICln prevents the premature interaction of snRNAs with the Sm proteins in these complexes and thus functions as an assembly chaperone imposing a kinetic trap upon the further assembly of snRNPs. PRMT5 catalyzes the symmetrical dimethylation of arginine residues in B/B', D1 and D3 increasing their affinity towards the SMN complex. Finally, the SMN complex interacts with the pICln-Sm protein complexes, expels pICln and mediates snRNP assembly in an ATP-dependent reaction.

So far, only little is known about the action of PRMT5 in the early phase of snRNP assembly and especially how the 6S complex is formed. Studies of this have so far been hampered by the unavailability of soluble and biologically active PRMT5 enzyme. The composition of the SMN complex and possible functions of individual subunits have been elucidated or hypothesized in recent years. Still, the exact mechanism of the entire

machinery forming snRNPs is poorly understood. *In vivo*, reduced production of functional SMN protein results in the neurodegenerative disease spinal muscular atrophy (SMA). How specific SMN mutations that have been found in SMA patients cause the disease remains elusive, yet, are likely to interfere with either SMN complex stability or snRNP assembly.

The aim of this work was to establish an *in vitro* system to recapitulate the cytoplasmic assembly of snRNPs. This was enabled by the recombinant production of all PRMT5 and SMN complex components as well as Sm proteins in a combination of bacterial and insect cell expression systems.

Co-expression of human PRMT5 and its direct interaction partner WD45 (WD-repeat domain 45) in *Sf*21 (*Spodoptera frugiperda* 21) insect cells resulted for the first time in soluble and biologically active enzyme. Recombinant PRMT5/WD45 formed complexes with Sm protein heterooligomers as well as pICln-Sm protein complexes but not with F/E/G alone. Also, the enzyme exhibited a type II methyltransferase activity catalyzing the mono- (MMA) and symmetrical dimethylation (sDMA) of Sm proteins B, D1 and D3. Two experimental setups were devised to quantitatively analyze the overall methylation of substrates as well as to identify the type and relative abundance of specific methylation types. Methylation of Sm proteins followed Michaelis-Menten kinetics. Complex reconstitutions and competition of the methylation reaction indicate that 6S is formed in a step-wise manner on the PRMT5 complex.

The analysis of the methylation type could be applied to deduce a model of sequential MMA and sDMA formation. It was found that large Sm protein substrate concentrations favored monomethylation. Following a distributive mechanism this leads to the conclusion that PRMT5 most likely confers partial methylation of several different substrate proteins instead of processing a single substrate iteratively until it is completely dimethylated.

Finally, the human SMN complex was reconstituted from recombinant sources and was shown to be active in snRNP formation. The introduction of a modified SMN protein carrying a mutation (E134K) present in spinal muscular atrophy (SMA) proved that mutated complexes can be generated *in vitro* and that these might be applied to elucidate the molecular etiology of this devastating disease.

Zusammenfassung

Der Großteil der Protein-kodierenden Gene in Eukaryoten ist in kodierende und nicht-kodierende Regionen unterteilt - sogenannte Exons und Introns. Damit aus einem Gen ein Protein hergestellt werden kann, muss zunächst die genomische DNA im Rahmen der Translation in prä-messenger RNA (prä-mRNA; Boten-RNA) übersetzt werden. Aus dieser prä-mRNA werden anschließend durch einen makromolekularen Komplex (Spleißosom) die Introns entfernt und die kodieren Exons zusammengefügt. Die daraus resultierende gereifte mRNA dient letztendlich den Ribosomen als Vorlage zur Herstellung von Proteinen.

Das Spleißosom besteht aus fünf snRNAs (small nuclear ribonucleic acids) und über 150 weiteren Proteinen. Zentrale Komponenten dieses Komplexes sind RNA-Protein Partikel (RNPs), die aus einer bzw. zwei snRNAs, sieben gemeinsamen (Sm) und weiteren snRNP-spezifischen Proteinen bestehen. Die Sm Proteine (B/B', D1, D2, D3, E, F and G) bilden eine Ringstruktur um eine konservierte Sequenz (Sm-site) der snRNA aus. *In vitro* erfolgt die Ausbildung dieser Struktur spontan. Im zellulären Kontext wird die Zusammenlagerung dieser snRNPs allerdings erst durch zwei makromolekulare, *trans*-agierende Proteinkomplexe, den PRMT5 und den SMN Komplex, ermöglicht.

Zu Beginn interagieren die Sm Proteine als heterooligomere Strukturen bestehend aus D1/D2, D3/B und F/E/G mit der Typ II Methyltransferase PRMT5. pICln, eine Komponente des PRMT5 Komplexes, interagiert mit den Sm Proteinen und bildet zwei spezifische Komplexe aus. Während der erste aus pICln und D3/B besteht, lagern sich im zweiten die Sm proteine D1/D2 und F/E/G mit pICln zu einem Ring zusammen (6S Komplex). Diese Interaktion erzeugt eine kinetische Falle, so dass die Sm Proteine sich nicht mehr spontan an die snRNA anlagern können und somit die snRNP Biogenese verzögert wird. PRMT5 katalysiert die symmetrische Dimethylierung von Argininresten in B/B', D1 und D3, wodurch deren Affinität zum SMN Komplex erhöht wird. Letztendlich assoziert der SMN Komplex mit den zuvor erzeugten pICln-Sm Protein Komplexen, entlässt pICln und ermöglicht im weiteren die Zusammenlagerung von snRNPs in einer ATP-abhängigen Reaktion.

Aktuell ist über die Funktion von PRMT5 in der frühen Phase der snRNP Biogenese wenig bekannt. Dies trifft insbesondere auf die Zusammenlagerung des 6S Komplexes zu. Biochemische Untersuchungen waren bis jetzt nahezu unmöglich, da rekombinant hergestelltes Protein entweder unlöslich oder biochemisch inaktiv war.

In den vergangenen Jahren wurde viel über die Zusammensetzung des SMN Komplexes sowie über die Funktionen einzelner Untereinheiten herausgefunden aber auch spekuliert. Trotz alledem ist der genaue Mechanismus der snRNP Biogenese noch nahezu unbekannt. *In vivo* sind verringerte Mengen an funktionalem SMN Protein der Ausschlaggeber für die neurodegenerative Krankheit Spinale Muskelatrophie (SMA). Welchen Effekt Mutationen im SMN Protein haben, die in SMA Patienten festgestellt wurden ist ungewiss. Es ist allerdings zu vermuten, dass diese entweder die Integrität des SMN Komplexes negativ beeinflussen oder störend auf die snRNP Biogenese wirken.

Das Ziel dieser Arbeit war es ein *in vitro*-System zu generieren, um die zytoplasmatische snRNP Biogenese biochemisch zu untersuchen. Dies geschah durch die rekombinante Produktion aller PRMT5 und SMN Komplex Komponenten sowie der Sm Proteine in einer Kombination von bakterieller und Insektenzell-Expression.

Durch die Ko-Expression von humanem PRMT5 und dem Interaktionspartner WD45 (WD-repeat domain 45) in *Sf*21 (*Spodoptera frugiperda* 21) Insekten Zellen konnte erstmals lösliches und enzymatisch aktives Protein hergestellt werden. Rekombinantes PRMT5/WD45 bildete Komplexe mit heterooligomeren Sm Proteinen sowie pICln-Sm Protein Komplexen, allerdings nicht mit F/E/G. Zusätzlich konnte eine Typ II Methyltransferase Aktivität dadurch nachgewiesen werden, dass die Sm Protein B, D1 und D3 monomethyliert (MMA) und symmetrisch dimethyliert (sDMA) werden können. Zur weiteren Untersuchung wurden zwei experimentelle Ansätze erarbeitet, um die allgemeine Methylierungsaktivität sowie das relative Vorhandensein von Mono- und Dimethylargininen zu bestimmen. Es konnte gezeigt werden, dass die Methylierung der Sm Proteine einer Michael-Menten Kinetik folgt. Die Rekonstitution von PRMT-Sm Protein Komplexen sowie the Methylierungsreaktionen deuten auf eine schrittweise Zusammenlagerung von 6S auf dem PRMT5 Komplex hin.

Die Untersuchung der unterschiedlichen Arten der Methylierung konnte herangezogen werden, um ein sequenzielles Modell der MMA und sDMA Bildung zu herzuleiten. Dabei wurde festgestellt, dass die Monomethylierung bei hoher Substratkonzentration bevorzugt wird. PRMT5 folgt einem distributiven Mechanismus und entlässt das Substrat nach jeder Methylierungsreaktion. Dementsprechend lässt sich schlussfolgern, dass eher unterschiedliche Substrate methyliert werden, anstatt dass zunächst ein bestimmtes Substratmolekül vollständig dimethyliert wird.

Neben dem PRMT5 Komplex konnte auch der humane SMN Komplex aus rekombinanten Proteinen rekonstituiert werden. Dieser Komplex war in der Lage snRNPs *in vitro* zusammenzulagern. Zudem konnte ein SMN Komplex mit einem mutierten SMN Protein erstellt werden, das in SMA Patienten auftritt. Somit konnte gezeigt werden, dass dieses System die Untersuchung von molekularen Ursachen dieser verheerenden Krankheit ermöglicht.

Table of Contents

1 Introduction

1.1 The spliceosome

The genetic information of a human cell is stored in the form of deoxyribonucleic acid (DNA) in its nucleus. In order to generate a protein which is encoded by a specific gene, a messenger ribonucleic acid (mRNA) depicting the blue print of this protein is prepared and exported to the cytoplasm. There, the ribosome, a large RNA-protein (ribonucleoprotein, RNP) complex that facilitates the translation into functional protein, is assembled onto the mRNA.

It was found that the majority of protein coding genes in human consist of alternating coding (exonic) and non-coding (intronic) DNA sequences (Sakharkar *et al.*, 2004). Consequently, most genes express precursor messenger RNAs (pre-mRNAs) which further have to be modified by splicing in order to specifically excise the non-coding introns and rejoin the coding exons (Rino and Carmo-Fonseca, 2009). This occurs through two sequential *trans*-esterification reactions that are mediated by the spliceosome, a multi-megadalton complex consisting of four small nuclear RNPs (snRNPs) and further proteins. Both the composition and conformation of the spliceosome are highly dynamic. One differentiates between two types of spliceosomes. The U2-dependent spliceosome catalyzes the majority of pre-mRNA splicing, whereas the U12-dependent one is only responsible for the removal of a subclass of introns (Patel and Steitz, 2003).

The assembly of the U2-dependent spliceosome on the pre-mRNA is an ordered process that requires the U1, U2, U4/U6 and U5 snRNPs as well as a large number of additional proteins (Will and Lührmann, 2011). In comparison, the U12-dependent spliceosome applies the U11, U12, U4atac/U6atac and U5 snRNPs. Each snRNP performs a distinct function in the spliceosome and consists of one or two eponymous snRNAs, a set of seven common (Sm) and snRNP-specific proteins. Being a major target for autoimmune antibodies in systemic lupus erythematosus (SLE), the common proteins have been named “Sm proteins” after one of the first patients, Stephanie Smith (Talken *et al.*, 2001). The seven Sm proteins, namely B/B’ (B’ is splicing variant of B), D1, D2, D3, E, F and G form a heptameric ring-structure around a specific uridine-rich sequence on the snRNA called the “Sm site” ($PuAU_{4–6}GPu$) forming the Sm core (Figure 1) (Urlaub *et al.*, 2001).

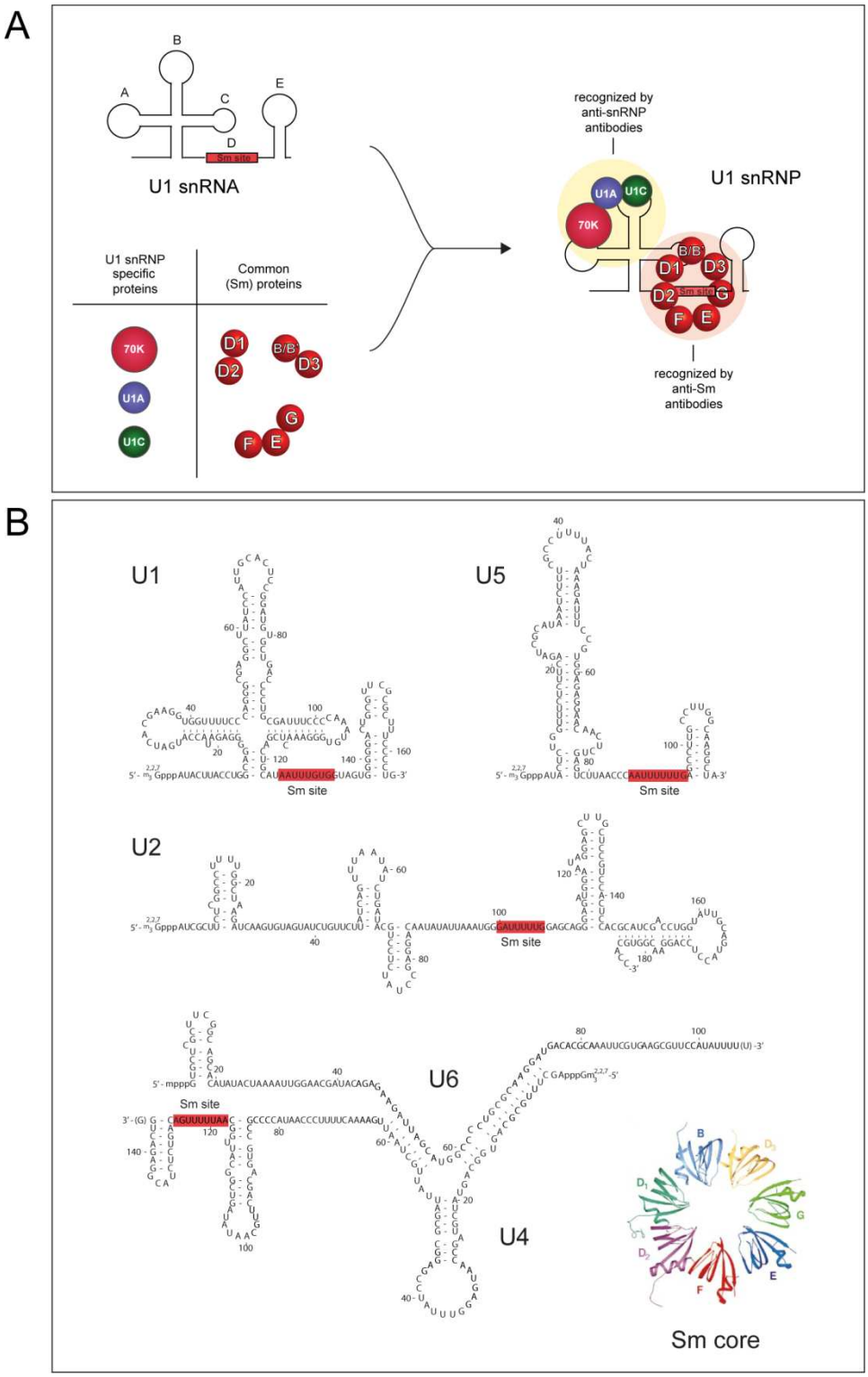

Figure 1 – Composition of uridine-rich small nuclear ribonucleoprotein particles (U snRNPs)

(A) The U1 snRNP consists of the U1 snRNA, a set of common (Sm) proteins that form a heptameric ring around a conserved uridine-rich sequence element termed the Sm site, and U1 snRNP specific proteins. **(B)** Secondary structures of U snRNAs belonging to the major spliceosome. U1, U2, U4 and U5 snRNA comprise an Sm site (indicated in red) around which the Sm core is assembled. The U snRNAs and the Sm core are not depicted in scale. For clarity reasons no U snRNP-specific proteins are shown. Adapted from Kambach et al. (1999) and Patel and Steitz (2003) with permission from Nature publishing group.

1.2 Biogenesis of small nuclear ribonucleoprotein particles (snRNPs)

A large number of studies performed mainly in *Xenopus laevis* oocytes but also in somatic cells has contributed to the understanding of the transport pathways enabling the biogenesis of spliceosomal U snRNPs (Will and Lührmann, 2001, 2011). These studies showed that the biogenesis of U snRNPs can be divided into individual steps some of which may actually be coupled.

Initially, the U1, U2, U4 and U5 snRNAs are transcribed as precursor-snRNAs (pre-snRNAs) in the nucleus by RNA polymerase II (pol II) and co-transcriptionally acquire a monomethylguanosine (m^7G) cap at their 5' end (Figure 2, step 1). In contrast to the 5'-3' orientation of phosphodiester bonds which are commonly observed in RNA and DNA elongation, the cap structure exhibits a 5'-5' triphosphate linkage protecting the snRNA from exonucleolytic cleavage (Reddy *et al.*, 1992). Transcription extends beyond the mature end of the snRNA and is terminated via endonucleolytic cleavage at the 3' box by the Integrator complex (Baillat *et al.*, 2005).

The m^7G cap facilitates the binding of the heterodimeric cap-binding complex (CBC) consisting of two cap-binding proteins with a molecular weight of 20 and 80 kDa (CBP20 and CBP80) (Izaurralde *et al.*, 1995). PHAX, a phosphorylated adaptor protein that specifically mediates RNA export, associates with both the cap binding complex as well as the snRNA (Ohno *et al.*, 2000). Carrying a nuclear export signal (NES), it interacts with the export receptor CRM1 (Chromosome region maintenance 1), also known as Exportin 1. The GTP-bound form of Ran associates with CRM1 resulting in the export complex which is then transported through the nuclear pore complex (NPC) into the cytoplasm (Figure 2, step 2). U6 snRNA, on the other hand, is transcribed by RNA polymerase III (pol III) and obtains a 5'-γ-methylphosphate cap. Consequently, the U6 snRNA is not exported to the cytoplasm and U6 snRNP maturation occurs only in the nucleus (Singh and Reddy, 1989). At its 3'-terminal end it contains a recognition motif around which Sm-like proteins Lsm2-8 form a heptameric ring (Achsel *et al.*, 1999).

In the cytoplasm, PHAX is dephosphorylated and Ran-GTP hydrolyzed to its GDP-bound form ensuring the directionality of the process. The export complex dissociates and thus releases the free snRNA (Figure 2, step 3). The snRNA and the Sm proteins, which occur as the heterooligomers D1/D2, D3/B and F/E/G, specifically interact with the SMN complex. In an ATP-driven reaction the Sm proteins are assembled as a heptameric ring onto the

Sm site of the snRNA (Figure 2, step 4). The formation of this Sm core structure is the prerequisite for the hypermethylation of the m^7G-cap to a 2,2,7-tri-methylated guanosine (m_3G = TMG) cap by the methyltransferase Tgs1 (trimethylguanosine synthase 1) (Plessel *et al.*, 1994). Tgs1 not only interacts with the cap structure but also contacts Sm proteins of the core domain thereby sensing correct Sm core assembly. Additionally, the 3' end of the snRNA is processed by a yet unidentified exo-ribonuclease (Figure 2, step 5) (Dahlberg *et al.*, 1990).

In the next step, the nuclear import complex consisting of snurportin-1 (SPN1) and importin β interacts with a bipartite nuclear localization signal (NLS) comprising both the m_3G cap and the SMN complex (Fischer *et al.*, 1991; Fischer and Lührmann, 1990; Hamm *et al.*, 1990a; Narayanan *et al.*, 2002). Once both transport factors have bound to their respective signals, nuclear import can be effected (Figure 2, step 6). The import complex dissociates in the nucleus and the transport factors are recycled into the cytoplasm (Figure 2, step 7). Subsequently, the snRNP, probably still associated to the SMN complex, accumulates in subnuclear domains termed Cajal bodies (Figure 2, step 8). In the Cajal bodies, the snRNA is further modified by the introduction of site-specific pseudouridylation (ψ) and 2'-O-methylation (m) by small Cajal body RNAs (scaRNAs) (Darzacq *et al.*, 2002; Jady *et al.*, 2003). This completes the processing of the U snRNAs (Figure 2, step 9). It is still unknown for most snRNPs whether the U snRNP-specific proteins join the complex already in the cytoplasm or following the nuclear import. Mature spliceosomal U snRNPs eventually accumulate in interchromatin regions in structures referred to as splicing speckles (Figure 2, step 10). It is assumed that the SMN complex dissociates from the snRNP and returns to the cytoplasm (Figure 2, step 11) in order to engage in a new round of cytoplasmic snRNP assembly (Figure 2, step 12).

Figure 2 – Biogenesis pathway of spliceosomal U snRNPs.

Pre-U snRNA (uridine-rich small nuclear RNA) is transcribed by RNA polymerase II (pol II) and m^7G-capped in the nucleus (step 1). After the export complex, consisting of pre-U snRNA, CBC (cap-binding complex), PHAX (phosphorylated adaptor for RNA export), CRM1 (Chromosome region maintenance 1) and RanGTP (Ras-related nuclear protein bound to GTP), has formed, it is actively transported into the cytoplasm via the nuclear pore complex (NPC; step 2). There, export factors and pre-U snRNA dissociate from each other (step 3) and Sm proteins provided by the SMN complex are assembled onto the "Sm-site" of pre-U snRNA (step 4).

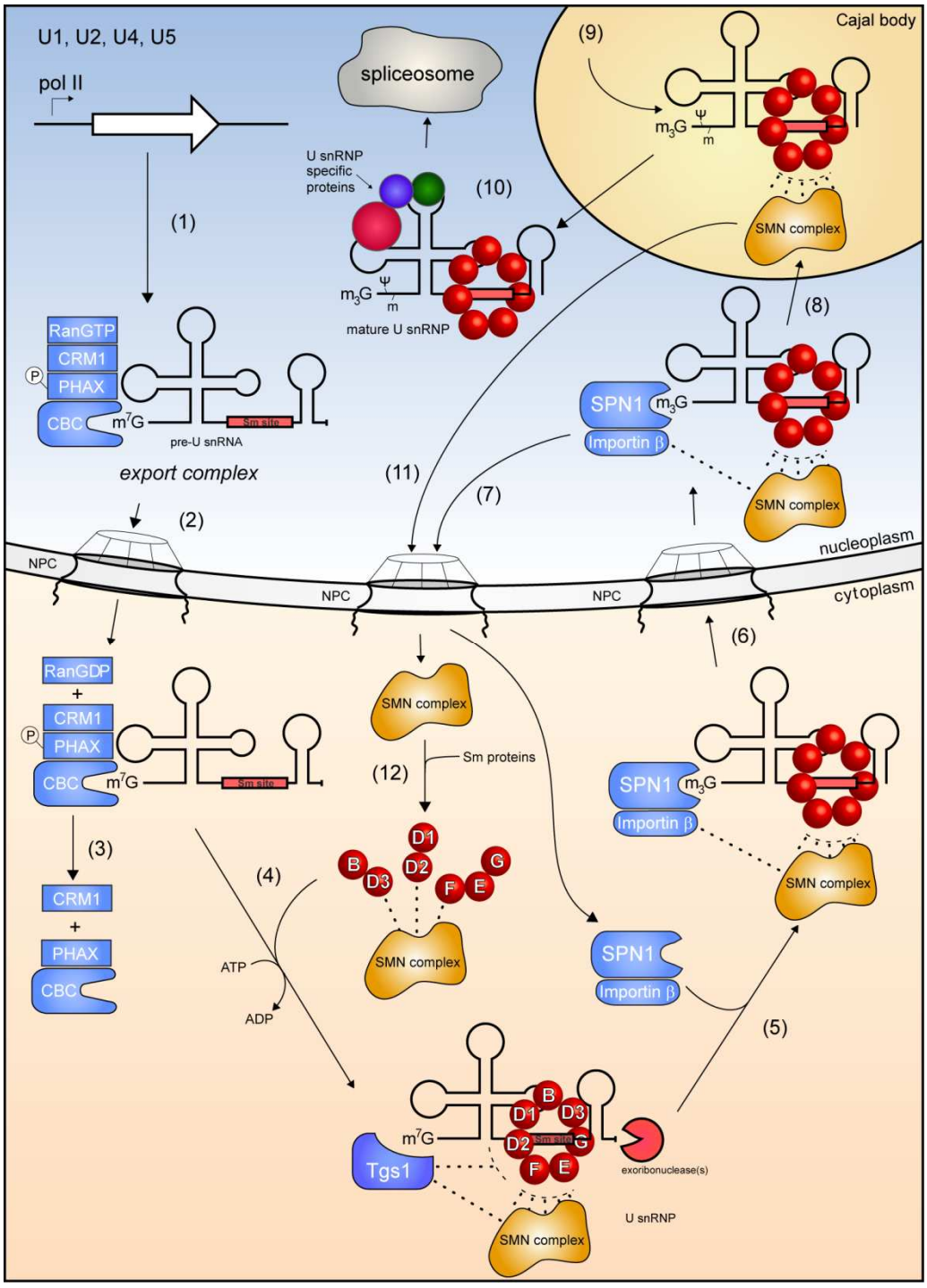

Following recruitment by the SMN complex and Sm core domain, the hypermethylase Tgs1 modifies the m^7G-cap to m_3G (step 5), before the import factors snurportin-1 (SPN1) and importin β mediate translocation into the nucleus (step 6). There, both factors dissociate and are recycled into the cytoplasm (step 7), and U snRNPs associated with the SMN complex enrich in Cajal bodies (step 8). After scaRNA guided pseudouridylation (Ψ) and 2'-O-methylation (m; step 9), the mature U snRNP is directed to the spliceosome, (step 10), whereas the SMN complex is believed to be exported into the cytoplasm (step 11), where it can re-enter the biogenesis cycle (step 12). Adapted from Neuenkirchen et al. (2008) with permission from Elsevier.

1.2.1 Two distinct protein complexes assist in cytoplasmic snRNP assembly

The assembly of snRNP core particles, yet spontaneous *in vitro* (Raker, 1996; Raker, 1999), has been shown to depend on two protein complexes, namely the PRMT5 and the SMN complex, *in vivo* (Figure 3) (Bühler *et al.*, 1999; Fischer *et al.*, 1997; Meister *et al.*, 2001b). These complexes act sequentially in the biogenesis process. Initially, newly synthesized Sm proteins are bound to the PRMT5 complex. Thereafter, they are transferred, presumably in a pre-assembled stage, onto the SMN complex. This serves at least two purposes. First, the PRMT5 complex prevents Sm protein aggregation and simultaneously pre-arranges them for their subsequent loading onto snRNA. Second, the SMN complex confers specificity to Sm proteins and hence prevents mis-assembly onto non-snRNA molecules.

Although the principal contribution of these *trans*-acting factors has been well established, many mechanistic aspects of the assisted assembly reaction remain to be elucidated.

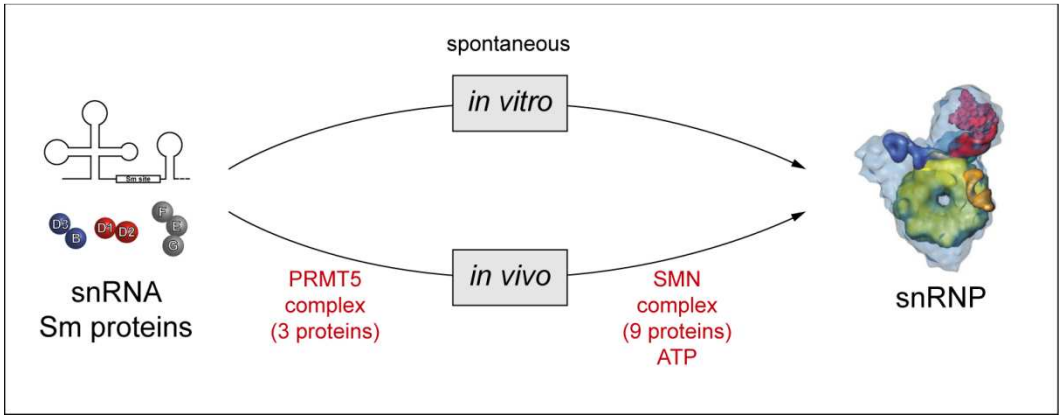

Figure 3 – *In vitro* and *in vivo* snRNP assembly

In vitro, snRNA and Sm proteins are able to assemble spontaneously and form snRNPs. The same reaction *in vivo* requires the orchestrated action of two distinct protein complexes (PRMT5 and SMN complex) and ATP hydrolysis.

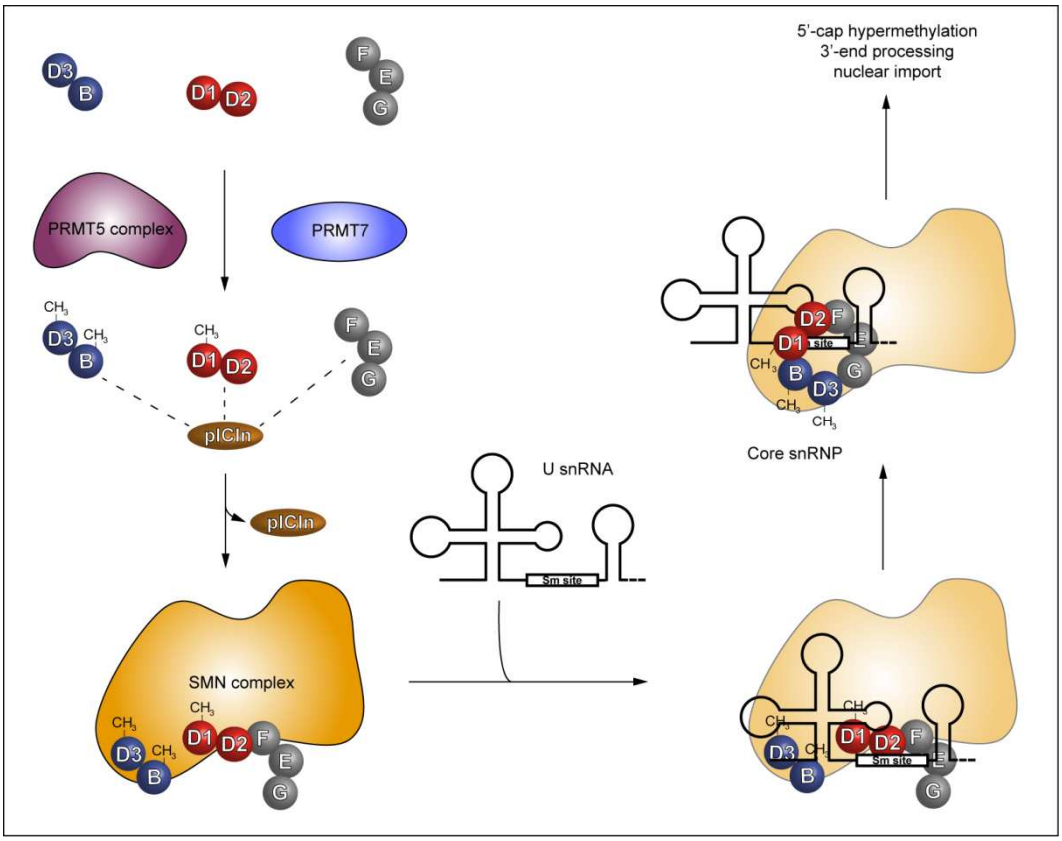

Figure 4 – Model of assisted assembly of U snRNPs.

Sm proteins are initially translated in the cytoplasm and sequestered by the PRMT5 complex (protein arginine methyltransferase type 5), consisting of the type II methyltransferase PRMT5, WD45 (WD repeat domain 45; also termed MEP50) and pICln (Chloride conductance regulatory protein). PRMT5 promotes symmetric dimethylation of arginines (sDMA) on Sm proteins B/B', D1 and D3. Recently, PRMT7 has been identified to catalyze the formation of sDMA in B/B' and D3. Yet, the scope of its participation is contentious (see Discussion 6.2.4, page 170). Next, the Sm proteins are transferred onto the SMN complex and are assembled onto the "Sm-site" of U snRNAs to form U snRNPs (uridine-rich small nuclear ribonucleoproteins). Finally, the U snRNA is hypermethylated at its 5'-cap and the mature U snRNP together with the SMN complex is imported to the nucleus. The proteins and protein complexes depicted in the schematic are not depicted in scale. The cryo-electron microscopy image of the snRNP has been adapted from Stark et al. (2001) with permission from Nature publishing group.

1.3 Protein arginine methyltransferases (PRMTs)

1.3.1 Introductory notes

In the initial phase of the snRNP assembly, the PRMT5 complex catalyzes the post-translational modification of Sm proteins. Following the addition of methyl groups onto arginine residues, altered Sm proteins are more likely to associate with the SMN complex. In general, post-translational modification of proteins is known to influence protein properties and thus expand the structural and functional diversity of the proteome. The

by far most studied and best understood kind of post-translational modification is phosphorylation (Pawson and Scott, 2005): Two antagonistic enzymes are capable of adding a phosphate group to a protein (kinase) or removing one from it (phosphatase) and thus influence its activity. So far, more than 200 different posttranslational modifications are known (Walsh, 2006).

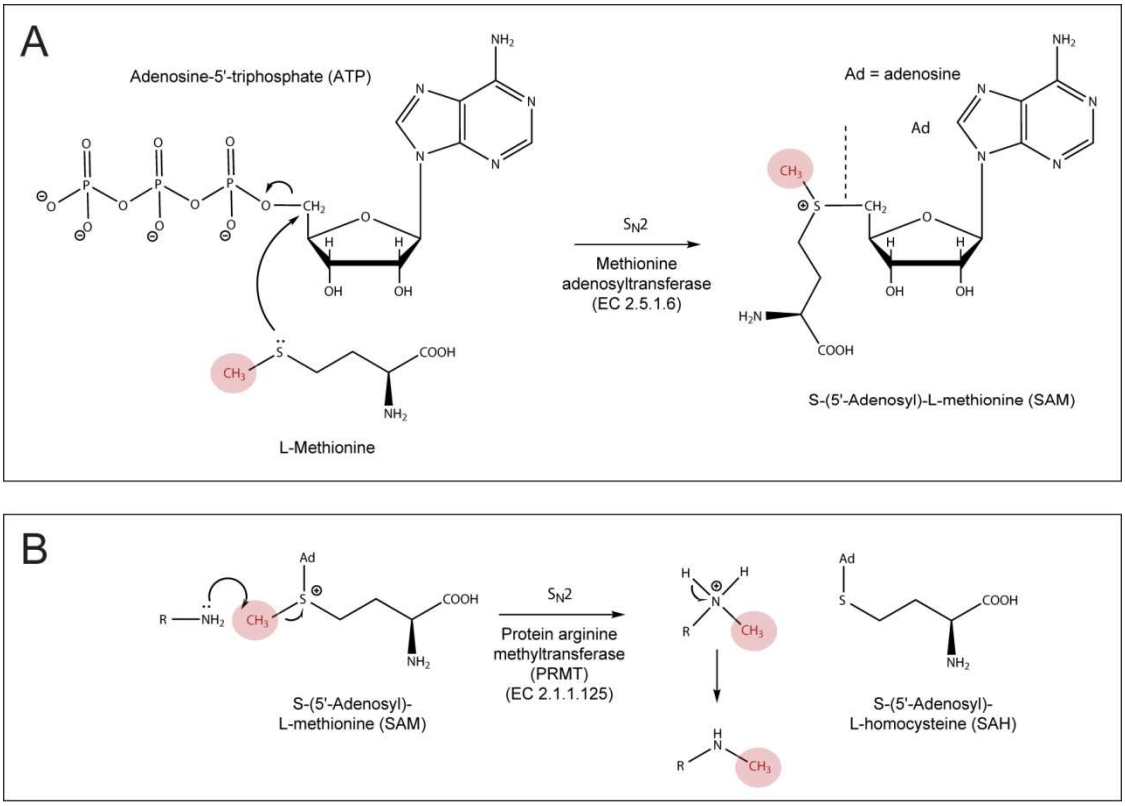

Figure 5 – Activation of the methyl group donor and methyl group transfer onto an arginine residue.

(A) Formation of S-adenosylmethionine (SAM): The enzyme methionine adenosyltransferase (E.C. 2.5.1.6) catalyzes the transfer of the adenosine of ATP onto the sulfur group of the methionine side chain in an S_N2 reaction. **(B)** Methylation of an amino group using SAM: The methyl group of SAM is passed onto the ω-N^G amino group in an arginine side by a protein arginine methyltransferase (PRMT) in an S_N2 reaction.

In protein methylation, methyl groups are covalently linked to lysine, arginine, histidine and proline residues as well as to carboxy groups (Lee *et al.*, 2005a). The specific methylation of arginine residues has first been recognized in histones in 1967 (Paik and Kim, 1967), yet, the responsible enzymes have only been identified during the past 15 years. Protein arginine methyltransferases (PRMTs) influence cellular processes like gene transcription, RNA processing, cellular transport, protein translocation and signal transduction (Wolf, 2009). These enzymes catalyze the transfer of a methyl group from

the universal methyl group donor S-adenosylmethionine (SAM = AdoMet) onto a nitrogen atom of an arginine residue (McBride and Silver, 2001). SAM is formed by the activation of the amino acid methionine through adenosine triphosphate (ATP) by the methionine adenosyltransferase (EC 2.5.1.6). The adenosine moiety of ATP is transferred onto the sulfur atom of the methionine (Figure 5 A). Upon methylation of the arginine residue SAM is altered to S-adenosylhomocysteine (SAH = AdoHcy) (Figure 5 B). Both reactions the activation of SAM as well as the arginine methylation follow an S_N2 mechanism.

1.3.2 The four types of protein arginine methyltransferase activities

Arginine residues comprise one δ- and two ω- (guanidino) nitrogen atoms that are receptive to methylation. Being a positively charged amino acid, arginine is known to mediate hydrogen bonding and van der Waals contacts (Jones *et al.*, 2001). The overall charge of the arginine side chain is retained upon methylation (Boisvert *et al.*, 2005). One differentiates between four types of protein arginine methyltransferases depending on which nitrogen atom is methylated (δ or ω) as well as the number of methyl groups added to the ω-nitrogen and the resulting stereochemistry (Figure 6) (Bedford and Clarke, 2009; Wang and Li, 2012; Wolf, 2009).

Most methyltransferases belong to the type I PRMTs and catalyze the formation of monomethylarginine (MMA, ω-N^G -Monomethyl-L-arginine) as well as asymmetrical dimethylarginine (aDMA, ω-N^G,N^G-Dimethyl-L-arginine). PRMT1, PRMT2, PRMT3, CARM1/PRMT4, PRMT6 and PRMT8 are type I methyltransferases (Chen *et al.*, 1999; Frankel *et al.*, 2002; Katsanis *et al.*, 1997; Lee *et al.*, 2005b; Scorilas *et al.*, 2000; Tang *et al.*, 1998).

Type II methyltransferases introduce monomethylarginine (MMA) as well as symmetrically dimethylated arginine (sDMA, ω-N^G,N'^G-Dimethyl-L-arginine). The major representative of type II methyltransferases is PRMT5. Even though PRMT7 and PRMT9 have been identified as type II methyltransferases, their contribution to sDMA formation is contemporarily disputed (Zurita-Lopez *et al.*, 2012) (see Discussion 6.2.4, page 170).

Enzymes that mediate only the incorporation of MMA belong to the type III methyltransferases. The only representative of this type that has been identified is PRMT7 (Miranda *et al.*, 2004b). In *Saccharomyces cerevisiae* but not in human the

enzyme arginine methyltransferase 2 (RMT2) was shown to catalyze the monomethylation of the δ-nitrogen atom of arginine side chains and has been defined as a type IV methyltransferase (Niewmierzycka and Clarke, 1999).

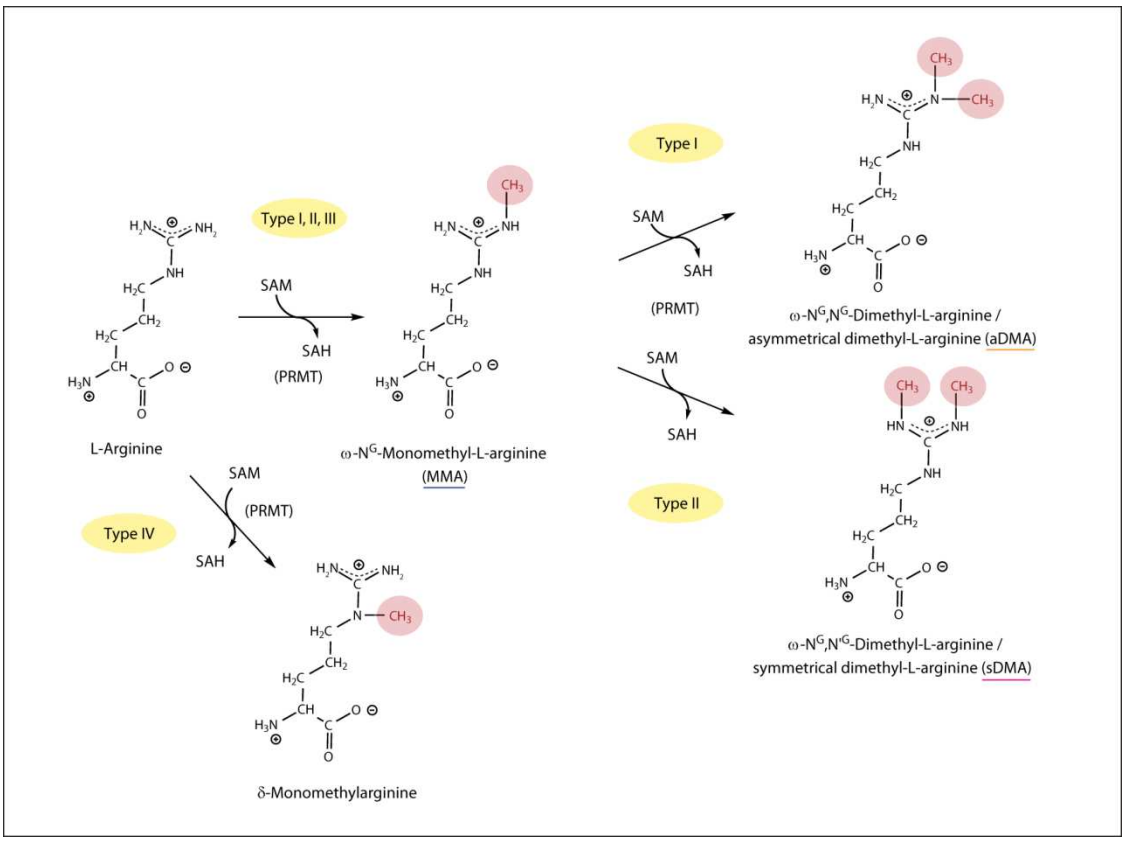

Figure 6 – Arginine methylation by protein arginine methyltransferases (PRMTs)

Protein arginine methyltransferases are categorized as type I, II, III and IV enzymes. While monomethylation of the ω-nitrogen atom is mediated by type I, II and III methyltransferases, incorporation of a methyl group to the δ-nitrogen atom is caused by a type IV enzyme. Only type I and type II PRMTs are capable of introducing a second methyl group. Whereas type I enzymes methylate the already modified ω-nitrogen atom resulting in an asymmetrically dimethylated arginine (aDMA), type II enzymes alter the second ω-nitrogen atom causing symmetrical dimethylated arginines (sDMA). The differently modified arginines can be specifically separated and thus distinguished from each other by thin layer chromatography (see Results 5.5.6, page 119). For clarity reasons the arginine residues are depicted as individual amino acids. In a methylation substrate the arginine residues are integral components of the amino acid sequence.

PRMT1 (type I) and PRMT5 (type II) are most strictly conserved throughout eukaryotic evolution (Bachand, 2007; Wang and Li, 2012). In bacteria, on the other hand, PRMTs are absent (Bachand, 2007). Nearly all PRMT substrates harbor glycine and arginine rich (GAR) motifs (Najbauer *et al.*, 1993). Whereas some substrates are unique for specific PRMTs, others can be processed in the same arginine residue by different enzymes. PRMT1 and PRMT5 both catalyze the dimethylation of histone H4 in arginine residue 3

(H4R3). PRMT1 introduces aDMA resulting in activation of gene transcription (Strahl *et al.*, 2001; Wang *et al.*, 2001). Addition of sDMA by PRMT5, in contrast, has the opposite effect and causes gene silencing (Pal *et al.*, 2004; Wang *et al.*, 2007; Zhao *et al.*, 2009). The specificity of PRMT5 for H3R8 and H4R3 can be altered by its interaction with the cooperator of PRMT5 (COPR5) (Lacroix *et al.*, 2008). Also, myelin basic protein (MBP) is processed differently by PRMT1 and PRMT5 (Branscombe *et al.*, 2001). Consequently, the type of arginine methylation is not coded by the substrate itself but strongly depends on the active site of the respective methyltransferase and the co-factor. The GAR motif merely indicates the target site (Branscombe *et al.*, 2001; Kuhn and Xu, 2009).

1.3.3 Arginine demethylation

Arginine methylation has long been thought of as being an irreversible alteration that could only be removed by complete protein degradation. Peptidylarginine deiminases have been found to convert arginine, in the context of a protein, to citrullin, yet do not affect methylated arginine residues (Raijmakers *et al.*, 2007). Recently, the Jumonji-domain-containing protein 6 (JMJD6) has been identified to specifically demethylate asymmetrically and symmetrically dimethylated arginines in histone H3 and H4 (Chang *et al.*, 2007). The availability of arginine demethylation enzymes provides a new aspect of how proteins containing methylarginines might be regulated.

1.3.4 Eukaryotic arginine methyltransferases

In RAT1 fibroblast and mouse liver cells PRMT1 is responsible for 85% of aDMA formation (Kuhn and Xu, 2009). It was shown *in vivo* that 59% of all arginine methylation corresponds to aDMA, 29% to MMA and 12% to sDMA (Paik and Kim, 1980). All PRMTs contain either one (PRMTs 1-6, 8, 9 and 11) or two (PRMTs 7 and 10) catalytic domains of which only one is active in each enzyme (Figure 7 A). Crystal structures of rat PRMT1 and PRMT3, mouse CARM1/PRMT4 as well as biochemical data indicate that PRMTs in general form homooligomers (Rho *et al.*, 2001; Yue *et al.*, 2007; Zhang and Cheng, 2003; Zhang *et al.*, 2000). The N-terminus is variable in length and contains domains responsible for protein-protein interactions or plasma membrane association (PRMT8) (Figure 7).

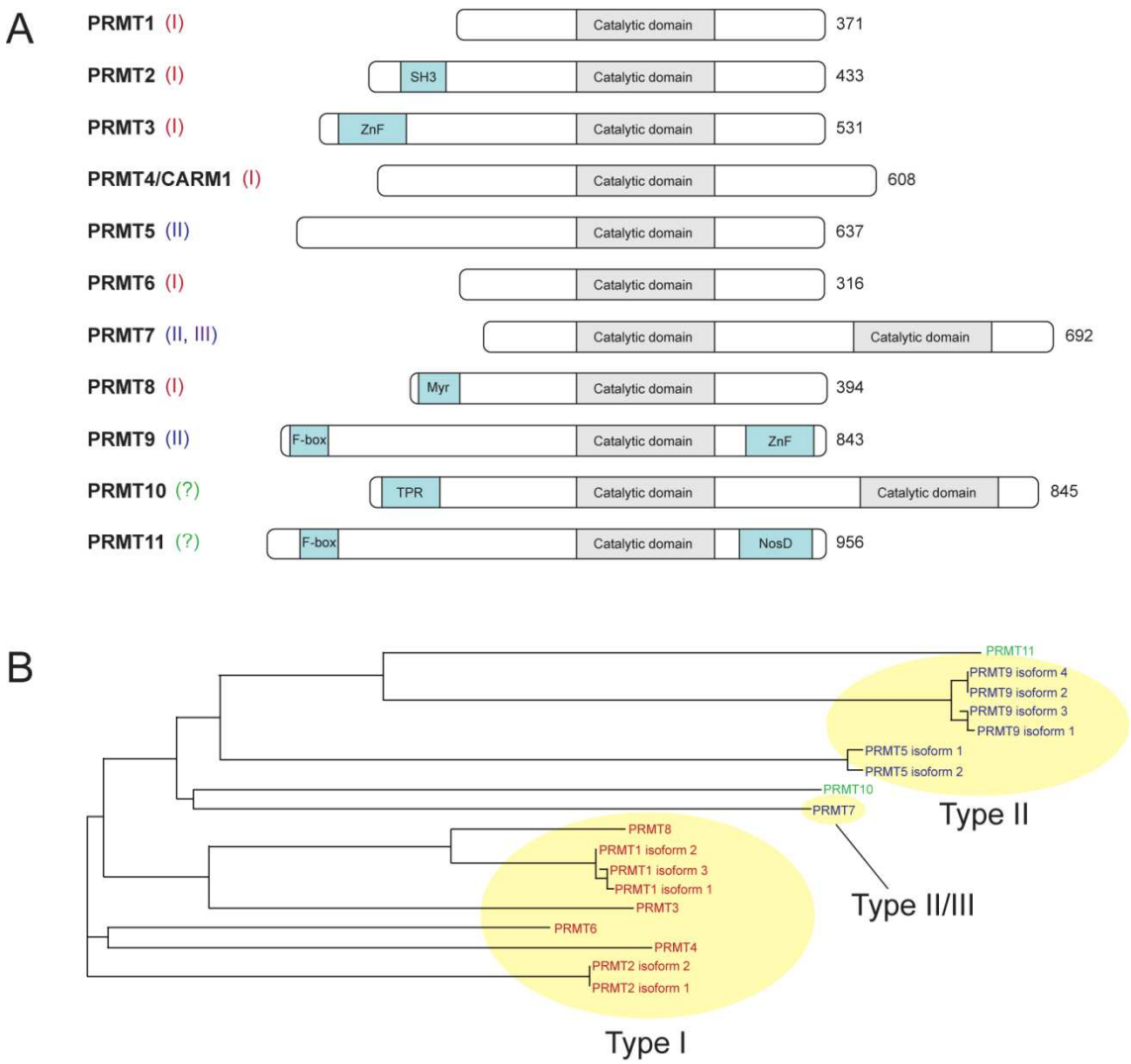

Figure 7 – Overview of the human protein arginine methyltransferase (PRMT) family.

(A) Human PRMTs 1-11 are depicted as boxes with the length corresponding to the number of amino acids in the primary sequence. The methylation type caused by the individual enzyme is indicated as I (MMA/aDMA, red), II (MMA/sDMA, blue) or III (δ-MMA, purple). Biochemical evidence of the types of PRMT10 and 11 is yet elusive. All methyltransferases contain at least one catalytic domain (gray boxes). PRMT2, 3 and 8–11 contain additional domains (blue boxes): Src homology 3 (*SH3)*, *ZnF* zinc finger, *Myr* myristoylation, *F-box*, tetratricopeptide (*TPR*) and nitrous oxidase accessory protein (*NosD*). **(B)** Phylogenetic analysis of all known human PRMTs. The length of lines refers to both the relationship as well as the distance between the individual proteins and isoforms. Adapted from Wolf (2009) with permission from Springer.

PRMTs are ubiquitously expressed but can be enriched in certain tissues. PRMT8, for instance, is solely expressed in the brain. In the cell, PRMTs are distributed both in the nucleus and the cytoplasm. According to the individual PRMT, the local concentration of the enzyme can be elevated in either compartment. PRMT6 is the only enzyme that is restricted to the nucleus (Frankel *et al.*, 2002). It was found that several isoforms of each

PRMT exist in human (Figure 7 B) and are expressed in a tissue-specific manner (Scorilas *et al.*, 2000).

PRMT activity has been found to be regulated by interacting proteins. These proteins are capable of inhibiting, activating or changing the substrate specificity of PRMTs (Jelinic *et al.*, 2006; Lacroix *et al.*, 2008; Lin *et al.*, 1996; Pal *et al.*, 2004; Robin-Lespinasse *et al.*, 2007; Singh *et al.*, 2004; Xu *et al.*, 2004). Whereas some protein-protein interactions are permanent others are only transitory (Bedford and Clarke, 2009). Very recently, phosphorylation of PRMT5 by JAK2V617F was shown to down-regulate its methylation activity and promoted myeloproliferation (Liu *et al.*, 2011).

1.3.5 The PRMT5 complex

From all these methyltransferases only PRMT5 plays a major role in the assembly of snRNPs. In the cytoplasm, PRMT5 is the eponymous member of the PRMT5 complex (also known as the methylosome) catalyzing the symmetrical dimethylation of Sm proteins B/B', D1 and D3 (Brahms *et al.*, 2000; Friesen *et al.*, 2001). Gel filtration chromatography and gradient ultracentrifugation provided a molecular weight of the endogenous PRMT5 complex of about 500 kDa (Meister *et al.*, 2001b). Furthermore, it was shown that PRMT5 is capable of forming homooligomers (Rho *et al.*, 2001) indicating the presence of several copies of the enzyme in the PRMT5 complex. In cooperation with the SMN complex it participates in the cytoplasmic assembly of spliceosomal U snRNPs (Meister *et al.*, 2001a). In *Drosophila melanogaster* symmetrical dimethylation of Sm proteins was shown to be dispensable (Gonsalvez *et al.*, 2006).

Apart from PRMT5, the complex is composed of pICln (Meister *et al.*, 2001a) and the WD-repeat protein WD45 (= MEP50) (Figure 8) (Friesen *et al.*, 2002). The chloride conductance regulatory protein ICln (pICln) is a phosphoprotein with a sole cytoplasmic distribution (Emma *et al.*, 1998; Pu *et al.*, 1999). It was found to bind directly to PRMT5 and the Sm protein heterooligomers D1/D2 and D3/B. Since B/B', D1 and D3 are methylation substrates of PRMT5, pICln has been termed an Sm protein recruitment factor (Friesen *et al.*, 2001). Recently, the kinase RioK1 has been shown to associate with PRMT5 via the same binding site as pICln in a mutual exclusive manner (Guderian *et al.*, 2011).

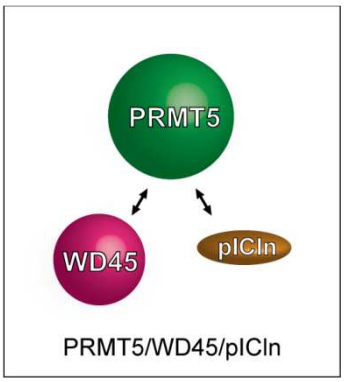

Figure 8 – Schematic of the protein arginine methyltransferase type 5 (PRMT5) complex.

The PRMT5 complex, which is also referred to as the methylosome, consists of the name-giving component, the protein arginine methyltransferase type 5 (PRMT5 = JBP1), a WD-repeat protein of 45 kDa (WD45 = MEP50 = WDR77) and the chloride conductance regulatory protein ICln (pICln). Whereas WD45 and pICln interact directly with PRMT5, they do not associate with each other.

1.3.6 Sm proteins form distinct RNA-free complexes with pICln *in vivo*

During the cytoplasmic assembly of U snRNPs the PRMT5 complex transiently interacts with Sm proteins and symmetrically dimethylates arginine residues at their C-terminal part (Brahms *et al.*, 2000). The methylated Sm proteins have in turn a higher affinity for the SMN complex (Meister *et al.*, 2001b). Initially, Sm proteins are translated in the cytoplasm and form heterooligomeric complexes comprising D1/D2, D3/B and F/E/G (Figure 9, upper panel) (Raker *et al.*, 1996). All Sm proteins contain two conserved structural domains, the so-called Sm-folds. These have been shown to provide the interface of their mutual binding (Appendix 12.2, page 208) (Kambach *et al.*, 1999). Still, the order in which these proteins interact with each other is highly specific. Other proteins, such as pICln, Gemin6 and Gemin7 have been found to also contain Sm-folds that might mediate the association with Sm proteins (Ma *et al.*, 2005; Pu *et al.*, 1999). The major adaptor for Sm proteins is pICln which is able to directly interact with D1/D2 via D1, with both proteins in D3/B but not with F/E/G alone (Figure 9, lower panel) (Chari *et al.*, 2008; Pu *et al.*, 1999). Consequently, the complexes pICln/D1/D2 as well as pICln/D3/B are formed which are incapable of binding to U snRNA (Meister *et al.*, 2001a; Pesiridis *et al.*, 2009; Pu *et al.*, 1999). Recently, a third RNA-free Sm protein intermediate has been identified *in vivo* consisting of a six-membered ring of pICln, D1/D2 and F/E/G (Figure 9, lower panel) (Chari *et al.*, 2008). According to its migration properties in gradient

ultracentrifugation it has been termed 6S complex. Previous studies showed that the 6S complex from cytoplasmic L929 mouse fibroblast extract contained only symmetrically dimethylated arginines (Miranda *et al.*, 2004a). Whereas mouse pICln shows a sequence identity of 88.8% to the human homolog, the Sm proteins of both are identical. Furthermore, it was demonstrated that D1 is fully symmetrically dimethylated in mature U snRNPs (Brahms *et al.*, 2000). Therefore, a type II methyltransferase, probably PRMT5, has to process the D1 protein previous to the assembly of the 6S complex. Biochemical evidence supporting this scenario, however, is lacking.

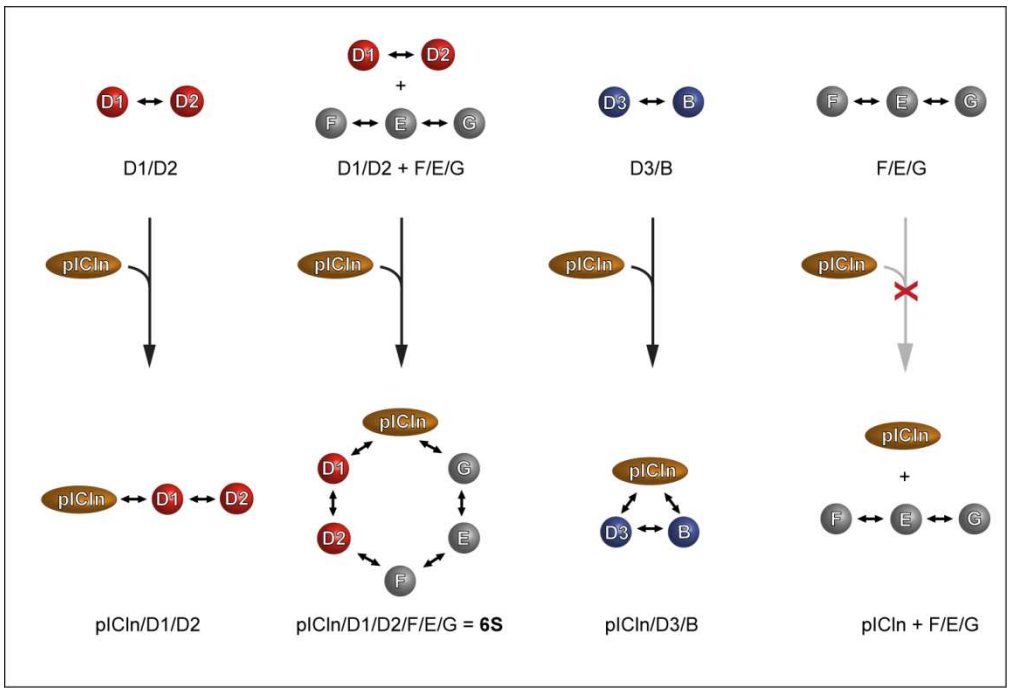

Figure 9 – Heterooligomeric Sm proteins interact with pICln *in vivo* to form distinct RNA-free complexes.

In vivo, Sm proteins form heterooligomeric complexes consisting of D1/D2, F/E/G and D3/B (Raker *et al.*, 1996). These interact with pICln to generate distinct complexes comprising pICln/D1/D2, a closed ring of pICln/D1/D2/F/E/G (6S complex) and pICln/D3/B. F/E/G alone does not bind to pICln (Chari *et al.*, 2008). Neither of these complexes is capable of binding to snRNA.

1.3.7 Sm proteins B/B', D1 and D3 contains several methylation sites

Only three Sm proteins, namely B/B', D1 and D3 are symmetrically dimethylated by PRMT5 (Friesen *et al.*, 2001). Immunoprecipitations of assembled snRNPs from HeLa extracts showed that B/B' is methylated in 6, D1 in 9 and D3 in 4 or 5 distinct arginine residues (Brahms *et al.*, 2000). Most of these methylation sites occur in GRG tripeptides (Figure 10). Whereas these sites are adjacent to each other in the amino acid sequence in

D1 and D3, GRG tripeptides in B spread over a distance of 200 amino acids. The three-dimensional structure of the N-terminal part of each Sm protein has been solved (Kambach *et al.*, 1999), however, the spatial orientation of the region containing the GRG tripeptides remains elusive. Consequently, the receptive arginine residues in B could still be close to each other in the final protein structure.

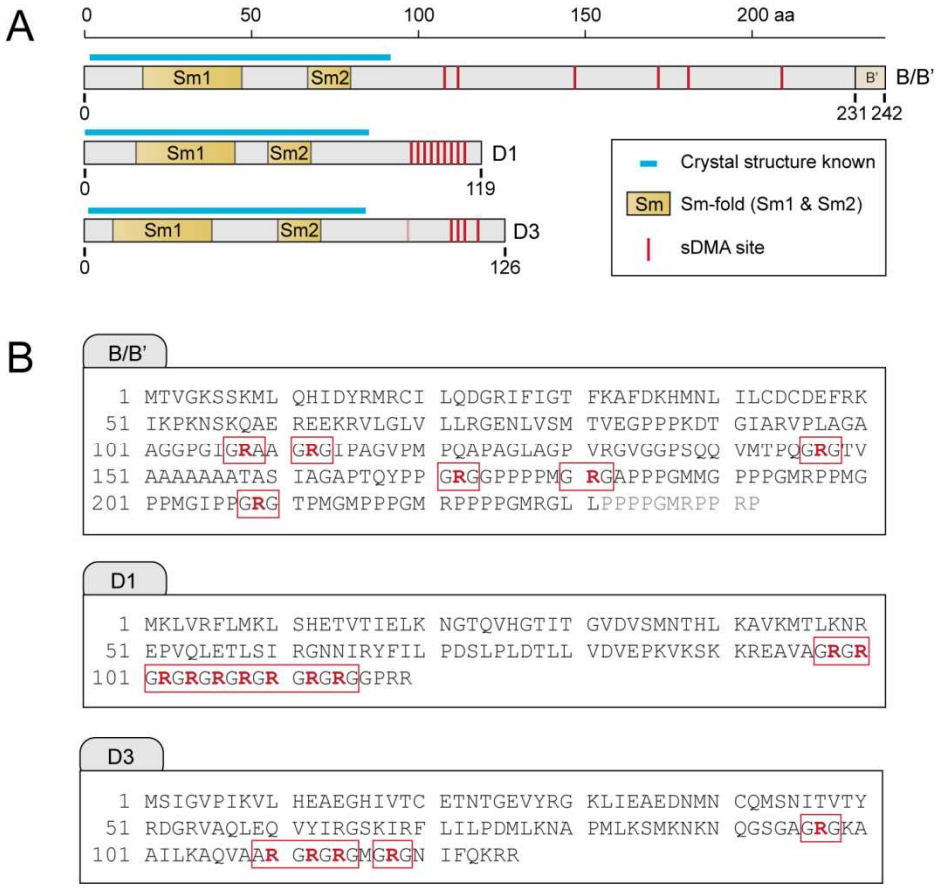

Figure 10 – Arginine methylation sites in the human Sm proteins B/B', D1 and D3.

Sm proteins B/B', D1 and D3 contain symmetrical dimethylarginines (sDMAs) *in vivo*. **(A)** Schematic overview of Sm protein amino acid sequences. The Sm-folds by which Sm protein-Sm protein interaction occurs are indicated by yellow boxes. Arginine residues that are symmetrically dimethylated in mature snRNPs are shown in red. D3 exhibits a theoretical methylation site at position 97 which could not be verified experimentally (light red). Crystal structures obtained from Sm protein heterooligomers D1/D2 (PDB ID: 1B34), D3/B (PDB ID: 1D3B) as well as the entire U1 snRNP (PDB IDs: 3CW1, 3PGW) resolve only the first 85–90 amino acids of each protein (light blue lines). The three-dimensional orientation of the C-terminal regions is unknown. **(B)** Primary sequences of B/B', D1 and D3. Symmetrically dimethylated arginines are highlighted in red.

1.4 The SMN complex

1.4.1 Spinal muscular atrophy (SMA)

The early phase of cytoplasmic snRNP assembly is characterized by the methylation of Sm proteins mediated by PRMT5 and a kinetic trap that is imposed by pICln. In the late phase, the SMN complex enables the removal of pICln and thus guarantees the snRNP assembly to proceed. Historically, the elucidation of this phase is closely connected to the neurodegenerative disease spinal muscular atrophy (SMA). SMA is one of the leading genetic causes of infant mortality in humans with an incidence of 1:6,000 to 1:10,000 in live births (Lunn and Wang, 2008). It is an autosomal recessive disease and was initially described by Guido Werdnig in the early 1890s. The disease is characterized by degeneration of α-motor neurons in the anterior horns of the spinal cord and by progressive muscle weakness and wasting (Bergin *et al.*, 1997).

The causative gene for SMA is the *survival motor neuron* (*SMN*) that is localized in two copies (*SMN1*: telomeric, *SMN2*: centromeric) in an inverted repeat of 500 kilobases (kb) on the long arm of chromosome 5 (5q13) (Lefebvre *et al.*, 1995; Markowitz *et al.*, 2012). Both copies of this gene are nearly identical and encode for the same protein. *SMN2* contains five nucleotide exchanges one of which results in inefficient splicing of exon7. As a result, only 10% of functional SMN protein is generated from this gene locus (Lorson and Androphy, 2000). Whereas 95% of all SMA patients have a compound heterozygous deletion of the *SMN1* gene, 3% carry a mutation (Lefebvre *et al.*, 1995). When *SMN1* is affected resulting in decreased levels of the SMN protein, the gene product of *SMN2* alone is not sufficient to compensate for the loss. The absence of *SMN1* as well as *SMN2* is lethal. Consequently, SMA is caused by low levels of functional SMN. Four clinical forms (type I-IV) of SMA are currently known based on their severity and age of disease onset (Coady and Lorson, 2011).

Common mutations observed in the SMN protein are single amino acid exchanges such as D44V, E134K and Y272C. D44V was identified to prevent the interaction of SMN with Gemin2 (Ogawa *et al.*, 2007). A mutation of the glutamic acid at position 134 to lysine (E134K) resulted in decreased association with Sm proteins (Selenko *et al.*, 2001). Y272C was shown to prevent SMN oligomerization as well as Sm protein binding and weakened the interaction between SMN and Gemin3 (Charroux *et al.*, 1999; Lefebvre *et al.*, 1997;

Lorson *et al.*, 1998; Pellizzoni *et al.*, 1999). Recently, the stoichiometry of individual components of the SMN complex revealed that the Y272C mutation decreased Gemin6, Gemin7 and Gemin8 levels by 50% (Wiesner, 2011).

Even though SMN is ubiquitously expressed in all body cells, the actual phenotype occurs only in neuron tissue. It could be shown in the zebrafish (*Danio reo*) model system that disruption of the *SMN* gene in the entire organism led to developmental defects in α-motor neurons. These could be completely alleviated by the addition of human SMN-free spliceosomal U snRNPs (Winkler *et al.*, 2005).

1.4.2 Composition of the SMN complex

The human SMN complex consists of the eponymous component SMN and eight additional proteins termed Gemin2–8 and unrip (Figure 11) (Baccon *et al.*, 2002; Carissimi *et al.*, 2005; Carissimi *et al.*, 2006a; Charroux *et al.*, 1999; Charroux *et al.*, 2000; Grimmler *et al.*, 2005; Gubitz *et al.*, 2002; Liu and Dreyfuss, 1996; Pellizzoni *et al.*, 2002). An overview of protein domains, motifs and regions involved in protein-protein interaction of each component is provided in the Appendix (Appendix 12.3, page 213).

SMN is a ubiquitously expressed protein of 294 amino acids (aa) that directly interacts with Gemin2, Gemin3 as well as Gemin8, and is able to form homooligomers (Carissimi *et al.*, 2006a; Charroux *et al.*, 1999; Liu *et al.*, 1997; Lorson *et al.*, 1998; Pellizzoni *et al.*, 1999). Its most prominent feature is the so-called Tudor domain which has a negative surface charge and binds specifically to symmetrically dimethylated arginine residues in RG repeats of Sm proteins B/B', D1, D3 and other proteins such as coilin (Bühler *et al.*, 1999; Chen *et al.*, 2011; Hebert *et al.*, 2001; Selenko *et al.*, 2001; Tripsianes *et al.*, 2011). In the nucleus, SMN is enriched in distinct regions adjacent to Cajal bodies that are therefore referred to as Gemini of Cajal bodies (Gems) (Carvalho *et al.*, 1999; Young *et al.*, 2001). Gems contain more than 200 proteins involved in pre-mRNA splicing (Liu and Dreyfuss, 1996; Morse *et al.*, 2007).

Complete loss or decreased levels of SMN have been linked to the devastating neurodegenerative disease spinal muscular atrophy (SMA; see: Introduction 1.4.1, page 17) (Burghes and Beattie, 2009; Lefebvre *et al.*, 1995). The major and so far best categorized function of the SMN complex is its involvement in the cytoplasmic assembly

of spliceosomal U snRNPs (Fischer *et al.*, 2011). A second function that has been devised for SMN is its role in axonal transport of mRNAs (Coady and Lorson, 2011; Rossoll and Bassell, 2009).

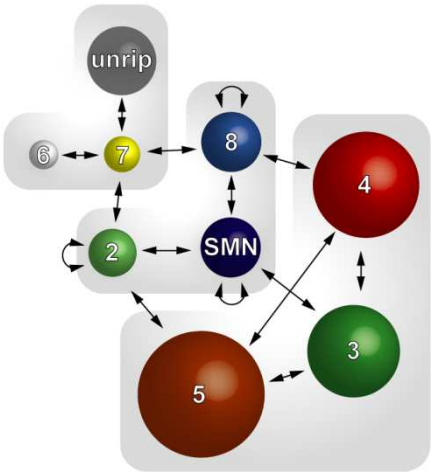

Figure 11 – Interaction map of the human SMN complex.

Schematic of protein interactions within the human SMN complex (Survival Motor Neuron) as described in Otter et al. (2007) and with additional information from Ogawa et al. (2009). The SMN protein together with Gemin2, Gemin7 and Gemin8 form a core scaffold of the SMN complex by which the remaining components are recruited. All core units but Gemin7 are capable of oligomerization. Gemin3, Gemin4 and Gemin5 are directly associated with SMN, Gemin8 and Gemin2, respectively. Furthermore, both Gemin6 and unrip are recruited by Gemin7. Within the cell, distinct subcomplexes of the SMN complex have been identified consisting of SMN/Gemin2, Gemin3/Gemin4/Gemin5 and Gemin6/Gemin7/unrip. Specific information of each individual subunit is presented in the Appendix (Appendix 12.3, page 213). Adapted from Neuenkirchen et al., (2008) with permission from Elsevier.

Recent studies showed that distinct subunits of the SMN complex are formed *in vivo*. These comprised SMN/Gemin2, Gemin3–5, Gemin5 as well as Gemin6–7/unrip (Battle *et al.*, 2007). Gemin2 and SMN are highly conserved and form the smallest entity that is active in snRNP assembly (Battle *et al.*, 2007; Fischer *et al.*, 1997; Kroiss *et al.*, 2008). Lately, the crystal structure of SMN, Gemin2 and the Sm proteins D1, D2, F, E and G has been solved (Zhang *et al.*, 2011). It could be shown that the Sm proteins that interact with Gemin2 form an open ring conformation.

Gemin3, Gemin4 and Gemin5 were shown to be associated with each other in the cytoplasm, whereas all three proteins were underrepresented in the nucleus (Gubitz *et al.*, 2004). Gemin3 is a putative ATPase/RNA helicase and binds directly to SMN and Gemin4 (Charroux *et al.*, 1999; Charroux *et al.*, 2000). Whereas the recombinantly

expressed mouse homolog of Gemin3 (dp103) could be shown to exhibit both activities, the human protein did not (Charroux *et al.*, 1999; Yan *et al.*, 2003). Since Gemin3 and Gemin4 are components of the SMN complex as well as micro ribonucleoprotein particles (miRNPs) it has been proposed that Gemin4 might be necessary for Gemin3 activity (Cauchi *et al.*, 2008; Charroux *et al.*, 2000). It has been hypothesized that Gemin3 might cause a conformational change of the SMN complex upon ATP hydrolysis and thus provide the catalytic activity in snRNP assembly (Meister *et al.*, 2002).

Gemin5 is the largest component of the SMN complex and is directly associated with Gemin2, Gemin3 and Gemin4 (Battle *et al.*, 2007; Gubitz *et al.*, 2002). Recently, Gemin5 has been identified as a scaffold for protein-RNA interaction (Lau *et al.*, 2009). The N-terminal region of Gemin5 comprising 13 WD-repeats specifically recognizes snRNAs via the Sm site and the adjacent 3'-stem loop (in U4, U5 and U11 snRNA) or the 5'-stem loop (in U1 snRNA) (Battle *et al.*, 2006; Lau *et al.*, 2009; Yong *et al.*, 2004). Consequently, Gemin2 and Gemin5 provide major functions in binding the Sm proteins as well as the snRNA. It has been hypothesized that singular Gemin5 captures snRNA molecules in the cell and guides them to the SMN complex (Workman *et al.*, 2012).

Gemin8 directly interacts with SMN as well as Gemin4 (Carissimi *et al.*, 2006b; Otter *et al.*, 2007) and bridges the Gemin6/Gemin7/unrip subcomplex via Gemin7 to the SMN protein (Figure 11) (Carissimi *et al.*, 2006a; Carissimi *et al.*, 2006b). Gemin6 and Gemin7 show no sequence similarities to Sm proteins, yet exhibit an Sm-fold which provides the structural basis for their mutual binding (Ma *et al.*, 2005). Correspondingly, it has been proposed that the Gemin6/Gemin7 dimer might serve as a surrogate for D3/B forming a heteroheptameric ring with D1, D2, F, E and G on the SMN complex (Ma *et al.*, 2005; Zhang *et al.*, 2011). It has been proclaimed that unrip (unr-interacting protein) finally replaces Gemin6/Gemin7 enabling the binding of D3/B and thus the correct assembly of the snRNP on the SMN complex (Ogawa *et al.*, 2009).

2 Aim of the study

The aim of this study was to establish an *in vitro* system recapitulating the cytoplasmic assembly of spliceosomal snRNPs. Since both the PRMT5 and the SMN complex play a major role in this process, expression and purification protocols for the individual components were to be devised. The strategy was to apply a combination of the bacterial and the insect cell expression system. For the latter, the MultiBac system was chosen as this is especially suited for the expression of protein complexes. Thus *in vitro* reconstituted complexes were to be assessed with respect to their contribution to core snRNP assembly.

In the early phase of snRNP assembly, PRMT5 mediates the symmetrical dimethylation of Sm proteins B/B', D1, and D3 improving their binding affinity towards the SMN complex. Since the mechanism of Sm protein methylation by PRMT5 as well as the timely order of these events remain elusive, biochemical and methylation kinetic studies were to be carried out. Biochemical studies would provide evidence of oligomerization states, possible protein-protein interactions and would indicate whether the reaction followed a specific order. Methylation kinetic analyses would yield information on enzymatic constants and the methylation efficiencies of the various Sm protein substrates (B, D1 and D3) with respect to their interaction partners. *In vivo*, D1/D2 readily interacts with the adaptor protein pICln that itself associates with PRMT5. Since a cytoplasmic pool of a six-membered ring consisting of the pICln, D1, D2, F, E and G (termed the 6S complex) has been found, it is intriguing to illuminate the process of how this complex is formed. Even though speculations of its generation have been accumulating in the literature recently, supporting biochemical evidence has been lacking.

The late phase of cytoplasmic core snRNP assembly is mediated by the SMN complex. All seven Sm proteins are present in a pICln-bound form, unable to assemble onto the snRNA. Following the ejection of pICln, the SMN complex catalyzes the specific transfer of the Sm proteins onto the snRNA forming a heptameric ring around the Sm site. Having all of the participating protein complexes and the U snRNA available *in vitro* would provide a strong tool to identify the specific contributions of SMN complex components. In particular, mutants occurring in the SMN protein found in patients suffering from SMA would provide evidence on the molecular etiology of this devastating disease.

Furthermore, the putative ATPase and RNA helicase Gemin3 and Gemin5, which was recently found to be a specific identifier of snRNAs, are interesting candidates to elaborate on the final steps of cytoplasmic core snRNP formation.

3 Materials

3.1 Devices

Device	Supplier
Äkta prime/prime plus	GE Healthcare, Giles, UK
Äkta purifier	GE Healthcare, Giles, UK
Amersham Hyperfilm™ MP	GE Healthcare, Giles, UK
Avanti® J-20-XP Centrifuge	Beckman-Coulter, Brea, CA, USA
Avanti® J-HC Centrifuge	Beckman-Coulter, Brea, CA, USA
Biofuge pico	Heraeus Instruments, Hanau, Germany
BioPhotometer	Eppendorf, Hamburg, Germany
CEA RP NEW Medical X-ray Screen (Blue sensitive)	AGFA Healthcare, Mortsel, Belgium
Cell culture ware	BD BioSciences, Franklin Lakes, NJ USA
CERTOMAT® BS-1 Incubator shaker	Sartorius stedim biotech, Göttingen, Germany
Certomat® R shaker	Sartorius stedim biotech, Göttingen, Germany
CL-1000 Crosslinker	UVP, Upland, CA, USA
Cryo vials	Sigma-Aldrich, St. Louis, MO, USA
Dry-block cooling thermostat Sample cooler SC-2M	Talron Biotech. L.T.D., Rehovot, Israel
Ehret Incubator KLT/S4	EHRET Labor- und Pharmatechnik, Emmendingen, Germany
Eppendorf Centrifuge 5415R	Eppendorf, Hamburg, Germany
Eppendorf Centrifuge 5424	Eppendorf, Hamburg, Germany
Eppendorf Centrifuge 5804R	Eppendorf, Hamburg, Germany
Fuchs-Rosenthal hemocytometer	Hartenstein, Würzburg, Germany
Gel Dryer Model 583	Bio-Rad, Hercules, CA, USA
GeneAmp® PCR System 9700	Applied Biosystems, Carlsbad, CA, USA
Head over tail (H.O.T.)	Carl Roth GmbH + Co. KG, Karlsruhe, Germany
Heraeus TK 6060 incubator	Heraeus Instruments, Hanau, Germany
HiTrap Q 1 ml anion exchange column	GE Healthcare, Giles, UK
HT Labotron shaker	Infors AG, Bottmingen, Switzerland
Incubator BK600	Kendro Laboratory Products, Langensebold,

	Germany
Innova™ 4300 Incubator shaker	New Bruinswick Scientific, Edison, NJ, USA
Innova® 44 Incubator shaker	New Bruinswick Scientific, Edison, NJ, USA
LaminAir HB 2448K	Heraeus Instruments, Hanau, Germany
LB1210B radioactive surface counter	Berthold Technologies, Bad Wildbad, Germany
Memmert drying oven	Memmert, Schwabach, Germany
MN TLC CEL DEAE/HR-Mix-20 (TLC plates)	Macherey-Nagel, Düren, Germany
Optima™ L-80XP Ultracentrifuge	Beckman-Coulter, Brea, CA, USA
Optima™ L-90K Ultracentrifuge	Beckman-Coulter, Brea, CA, USA
OPTIMAX X-Ray Film Processor	PROTEC® Medical Systems
PEI Cellulose F (TLC plates)	Merck, Darmstadt, Germany
Phosphorimager 400E	Molecular Dynamics/GE Healthcare, Giles, UK
Poly-Prep columns	Bio-Rad, Hercules, CA, USA
Rotors – Centrifuges (JS 4.2, JLA 8.1000, JA 25.50)	Beckman-Coulter, Brea, CA, USA
Rotors – Ultracentrifuges (45Ti, 60Ti, 70Ti)	Beckman-Coulter, Brea, CA, USA
Semidry blotting apparatus	Bio-Rad, Hercules, CA, USA
SilverFast32 scanner	Seiko Epson Corporation, Tokio, Japan
Slide-A-Lyzer® dialysis caps	Pierce/VWR, Radnor, PA, USA
Sonifier 250	Branson, Danbury, CT, USA
Specord 50, UV Vis spectrophotometer	Analytik Jena, Jena, Germany
SpeedVac Concentrator	Savant/Thermo Scientific, Waltham, MA, USA
Superdex200 10/300GL gel filtration column	GE Healthcare, Giles, UK
Superose6 10/300GL gel filtration column	GE Healthcare, Giles, UK
Thermomixer compact	Eppendorf, Hamburg, Germany
Vacupack Plus (vacuum sealing device)	Krups GmbH, Offenbach am Main, Germany
Vacuum pump	Greifenberger Antriebstechnik, Marktredwitz, Germany
Varioklav® Steam Sterilizer	H + P Labortechnik, Oberschleißheim, Germany
Variomag Biomodul 40B	H + P Labortechnik, Oberschleißheim, Germany
Variomag Biosystem	H + P Labortechnik, Oberschleißheim, Germany
Wallac 1410 Scintillation Counter	Pharmacia/GE Healthcare, Giles, UK
Whatman paper	VWR, Radnor, PA, USA

Wheaton EC vials for protein hydrolysis	Pierce/VWR, Radnor, PA, USA
Wheaton NextGen™ V Vial® for protein hydrolysis	Pierce/VWR, Radnor, PA, USA
Zeiss Axiovert 200M Microscope	Carl Zeiss AG, Jena, Germany
Zeiss Axiovert 25 Microscope	Carl Zeiss AG, Jena, Germany

3.2 Chemicals and enzymes

Chemical	**Supplier**
[^{3}H] S-adenosylmethionine (10 Ci/mmol)	Perkin Elmer, Waltham, MA, USA
[α-^{32}P]-ATP (3,000 Ci/mmol)	Perkin Elmer, Waltham, MA, USA
[α-^{32}P]-UTP (3,000 Ci/mmol)	Perkin Elmer, Waltham, MA, USA
Acetic acid (99%)	VWR, Radnor, PA, USA
Acrylamide (Rotiphorese Gel A)	Carl Roth GmbH + Co. KG, Karlsruhe, Germany
Acrylamide/bisacrylamide (Rotiphorese 30)	Carl Roth GmbH + Co. KG, Karlsruhe, Germany
Acrylamide/bisacrylamide (Rotiphorese 40)	Carl Roth GmbH + Co. KG, Karlsruhe, Germany
Acrylamide/Bisacrylamide, 30% (w/v) – Rotiphorese 30	Carl Roth GmbH + Co. KG, Karlsruhe, Germany
AEBSF (4-(2-Aminoethyl) benzenesulfonyl fluoride hydrochloride)	Sigma-Aldrich, St. Louis, MO, USA
Agar	Carl Roth GmbH + Co. KG, Karlsruhe, Germany
Agarose	Carl Roth GmbH + Co. KG, Karlsruhe, Germany
Amido black	Merck, Darmstadt, Germany
Ammonium acetate	Merck, Darmstadt, Germany
Ammonium hydroxide	VWR, Radnor, PA, USA
Ammonium persulfate (APS)	Carl Roth GmbH + Co. KG, Karlsruhe, Germany
Ampicillin	Carl Roth GmbH + Co. KG, Karlsruhe, Germany
Aprotinin	Sigma-Aldrich, St. Louis, MO, USA
Asymmetrical dimethyl-L-arginine	Sigma-Aldrich, St. Louis, MO, USA
ω-N^{G},N^{G}-Dimethyl-L-arginine (aDMA)	
Bacto™ Tryptone	BD BioSciences, Franklin Lakes, NJ USA
Bacto™ Yeast Extract	BD BioSciences, Franklin Lakes, NJ USA
Betaine	Sigma-Aldrich, St. Louis, MO, USA
β-mercaptoethanol	Carl Roth GmbH + Co. KG, Karlsruhe, Germany
Bisacrylamide (Rotiphorese Gel B)	Carl Roth GmbH + Co. KG, Karlsruhe, Germany
Boric acid	Carl Roth GmbH + Co. KG, Karlsruhe, Germany
Bovine Serum Albumin (BSA)	PAA Laboratories GmbH, Pasching, Austria
Bromophenol blue	Serva, Heidelberg, Germany
Calcium chloride ($CaCl_2$)	Carl Roth GmbH + Co. KG, Karlsruhe, Germany
Cellfectin II	Invitrogen, Carlsbad, CA, USA
Chloramphenicol	Carl Roth GmbH + Co. KG, Karlsruhe, Germany
Chloroform	Carl Roth GmbH + Co. KG, Karlsruhe, Germany

Coumaric acid	Carl Roth GmbH + Co. KG, Karlsruhe, Germany
Disodium tetraborate (Borax)	Carl Roth GmbH + Co. KG, Karlsruhe, Germany
Dulbecco's Modified Eagle Medium (DMEM)	Gibco®; Invitrogen, Carlsbad, CA, USA
DMF (N,N-Dimethylformamide)	Sigma-Aldrich, St. Louis, MO, USA
DMP (dimethyl pimelimidate)	Sigma-Aldrich, St. Louis, MO, USA
DMSO (Dimethylsulfoxide)	Carl Roth GmbH + Co. KG, Karlsruhe, Germany
dNTP mix	Fermentas, St. Leon-Rot, Germany
DTT (Dithiothreitol)	Carl Roth GmbH + Co. KG, Karlsruhe, Germany
EDTA (Ethyleneaminetetraacetic acid)	Carl Roth GmbH + Co. KG, Karlsruhe, Germany
Ethanol, denatured	VWR, Radnor, PA, USA
Ethanol, p.a.	Sigma-Aldrich, St. Louis, MO, USA
Ethidium bromide	Carl Roth GmbH + Co. KG, Karlsruhe, Germany
Fetal calf serum (FCS)	Gibco®; Invitrogen, Carlsbad, CA, USA
Formaldehyde	Carl Roth GmbH + Co. KG, Karlsruhe, Germany
Formamide	Carl Roth GmbH + Co. KG, Karlsruhe, Germany
Galactose	Sigma-Aldrich, St. Louis, MO, USA
Gelatin	Merck, Darmstadt, Germany
GeneRuler™ 100 bp Plus DNA Ladder	Fermentas, St. Leon-Rot, Germany
Gentamycin	Carl Roth GmbH + Co. KG, Karlsruhe, Germany
Glucose	Carl Roth GmbH + Co. KG, Karlsruhe, Germany
Glutathione sepharose™ 4B	QIAGEN, Hilden, Germany
Glycerol 86% (v/v)	Carl Roth GmbH + Co. KG, Karlsruhe, Germany
Glycine	Carl Roth GmbH + Co. KG, Karlsruhe, Germany
Heparin	Sigma-Aldrich, St. Louis, MO, USA
Hepes (4-(2-hydroxyethyl)-1-piperazineethanesulfonic acid)	Carl Roth GmbH + Co. KG, Karlsruhe, Germany
Hybond PVDF membrane. Protein Transfer membrane	VWR, Radnor, PA, USA
Hydrochloric acid (HCl) 37% (v/v)	Carl Roth GmbH + Co. KG, Karlsruhe, Germany
Hydrogen peroxide	Merck, Darmstadt, Germany
Imidazole	Sigma-Aldrich, St. Louis, MO, USA
IPTG (Isopropyl-β-D-1-thiogalactopyranoside)	Carl Roth GmbH + Co. KG, Karlsruhe, Germany
Isopropanol	VWR, Radnor, PA, USA
Kanamycin	Carl Roth GmbH + Co. KG, Karlsruhe, Germany
L-arginine (L-arg)	Sigma-Aldrich, St. Louis, MO, USA
Leupeptin	Sigma-Aldrich, St. Louis, MO, USA
Luminol	Carl Roth GmbH + Co. KG, Karlsruhe, Germany
MassRuler™ DNA Ladder Mix	Fermentas, St. Leon-Rot, Germany
Methanol	VWR, Radnor, PA, USA
Monomethyl-L-arginine ω-N^G -Monomethyl-L-arginine (MMA)	Sigma-Aldrich, St. Louis, MO, USA
NAMP100 Amplify Fluorographic Reagent	GE Healthcare, Giles, UK
Nickelchloride $NiCl_2$	Merck, Darmstadt, Germany
Ninhydrin	Fluka/Sigma-Aldrich, St. Louis, MO, USA

Ni-NTA Superflow	QIAGEN, Hilden, Germany
Non-Ident P40	Carl Roth GmbH + Co. KG, Karlsruhe, Germany
PageRuler™ Plus Prestained Protein Ladder	Fermentas, St. Leon-Rot, Germany
PageRuler™ Unstained Protein Ladder	Fermentas, St. Leon-Rot, Germany
Penicillin/Streptomycin	PAA, Farnborough, Hampshire, UK
Pepstatin	Sigma-Aldrich, St. Louis, MO, USA
Phenol (Roti®-Aqua-Phenol for RNA isolation)	Carl Roth GmbH + Co. KG, Karlsruhe, Germany
PIPES (Piperazine-1,4-bis(2-ethanesulfonic acid))	Carl Roth GmbH + Co. KG, Karlsruhe, Germany
PMSF (phenylmethylsulfonyl fluoride)	Sigma-Aldrich, St. Louis, MO, USA
Polyadenylic acid (potassium salt) – polyA	Sigma-Aldrich, St. Louis, MO, USA
Polycytidylic acid (potassium salt) – polyC	Sigma-Aldrich, St. Louis, MO, USA
Polyguanylic acid (potassium salt) – polyG	Sigma-Aldrich, St. Louis, MO, USA
Polyuridylic acid (potassium salt) – polyU	Sigma-Aldrich, St. Louis, MO, USA
Potassium chloride	Carl Roth GmbH + Co. KG, Karlsruhe, Germany
Potassium ferricyanide (III) $K_3[Fe(CN)_6]$	Merck, Darmstadt, Germany
Potassium phosphate monobasic (KH_2PO_4)	Carl Roth GmbH + Co. KG, Karlsruhe, Germany
RNase Q1	Promega, Madison, WI, USA
RNAsin	Promega, Madison, WI, USA
Rotiszint liquid scintillation solution	Carl Roth GmbH + Co. KG, Karlsruhe, Germany
S-adenosylmethionine	New England Biolabs, Ipswich, MA, USA
SDS (Sodium dodecyl sulfate)	Carl Roth GmbH + Co. KG, Karlsruhe, Germany
Serva Blue R	Serva, Heidelberg, Germany
Silver nitrate	Degussa AG, Frankfurt, Germany
Sodium acetate	Carl Roth GmbH + Co. KG, Karlsruhe, Germany
Sodium azide (NaN_3)	Sigma-Aldrich, St. Louis, MO, USA
Sodium carbonate anhydrous	Fluka/Sigma-Aldrich, St. Louis, MO, USA
Sodium chloride (NaCl)	VWR, Radnor, PA, USA
Sodium hydroxide (NaOH)	Carl Roth GmbH + Co. KG, Karlsruhe, Germany
Sodium phosphate dibasic (Na_2HPO_4)	Carl Roth GmbH + Co. KG, Karlsruhe, Germany
Sodium thiosulfate	Sigma-Aldrich, St. Louis, MO, USA
Sorbitol	Carl Roth GmbH + Co. KG, Karlsruhe, Germany
Sulfuric acid (H_2SO_4)	Carl Roth GmbH + Co. KG, Karlsruhe, Germany
Symmetrical dimethyl-L-arginine ω-N^G,N'^G-Dimethyl-L-arginine (sDMA)	Sigma-Aldrich, St. Louis, MO, USA
TCEP (tris(2-carboxyethyl)phosphine)	Sigma-Aldrich, St. Louis, MO, USA
TEMED (N,N,N,N-Tetramethylethylenediamine)	Carl Roth GmbH + Co. KG, Karlsruhe, Germany
Tetracycline	Carl Roth GmbH + Co. KG, Karlsruhe, Germany
Trichloroacetic acid (TCA)	Carl Roth GmbH + Co. KG, Karlsruhe, Germany
TRIS (Tris(hydroxymethyl)aminomethane)	Carl Roth GmbH + Co. KG, Karlsruhe, Germany
Triton X-100	Carl Roth GmbH + Co. KG, Karlsruhe, Germany
Trypan blue	Merck, Darmstadt, Germany
Tween 20 (Polyoxyethylene-sorbitan monolaurate)	Carl Roth GmbH + Co. KG, Karlsruhe, Germany
Urea	Carl Roth GmbH + Co. KG, Karlsruhe, Germany
Virkon® S	DuPont, Sudbury, Suffolk, UK

X-Gal (5-Bromo-4-chloro-3-indolyl β-D-galactopyranoside)	Carl Roth GmbH + Co. KG, Karlsruhe, Germany
Xylene cyanol	Serva, Heidelberg, Germany

Enzyme	Supplier
Tobacco Etch Virus protease (TEV)	Bacterial expression
T4 DNA ligase	Fermentas, St. Leon-Rot, Germany
Restriction Enzymes	Fermentas, St. Leon-Rot, Germany
Shrimp Alkaline Phosphatase (SAP)	Fermentas, St. Leon-Rot, Germany
T7 RNA polymerase	Fermentas, St. Leon-Rot, Germany
RNase A	Sigma-Aldrich, St. Louis, MO, USA
Restriction Enzymes (*Acc*65I, *Avr*II=*Xma*JI, *Bam*HI, *Bss*HII, *Dpn*I, *Eco*RI, *Hin*dIII, *Nco*I, *Nde*I, *Not*I, *Nru*I=*Bsp*68I, *Pag*I, *Pme*I=*Mss*I, *Pvu*I, *Sma*I, *Spe*I=*Bcu*I, *Stu*I, *Xho*I)	Fermentas, St. Leon-Rot, Germany
Pfu DNA polymerase	Fermentas, St. Leon-Rot, Germany
2× PCR MasterMix	Roche, Basel, Switzerland
SP6 RNA polymerase	Fermentas, St. Leon-Rot, Germany
T3 RNA polymerase	Fermentas, St. Leon-Rot, Germany

3.3 Kits

Kit System	Supplier
NucleoSpin® Plasmid QuickPure	Macherey-Nagel, Düren, Germany
NucleoSpin® Extract II	Macherey-Nagel, Düren, Germany
NucleoBond® PC100	Macherey-Nagel, Düren, Germany
NucleoBond® PC500	Macherey-Nagel, Düren, Germany

3.4 Oligonucleotides

Oligonucleotides were synthesized and purified using high pressure liquid chromatography (HPLC) by Biomers (biomers.net GmbH, Ulm, Germany).

Sequencing Primers

Primer	DNA sequence (5'-->3')	Tm (°C)
T7 forward	TAATACGACTCACTATAGG	44.6
T7 reverse	GCTAGTTATTGCTCAGCG	48.0
M13 forward (-20)	GTAAAACGACGGCCAG	45.9
M13 reverse	CAGGAAACAGCTATGAC	44.6
MultiBac_MCS1_fwd	GGATTATTCATACCGTCCCA	49.7

MultiBac_MCS1_rev	CAAATGTGGTATGGCTGATT	47.7
MultiBac_MCS2_fwd	CGGACCTTTAATTCAACCC	48.9
MultiBac_MCS2_rev	GTCTCCTTCCGTGTTTCAG	51.1
GEX fwd	GGGCTGGCAAGCCACGTTTGGTG	62.4
GEX rev	CCGGGAGCTGCATGTGTCAGAGG	62.4
His_6_NcoI_fwd	CATGCCATGGGACATCACCATCACCATCACG	65.7

Primer orientations – fwd: forward; rev: reverse

Modified multiple cloning sites for pFBDM vectors

Oligonucleotide	Primer orientation	DNA sequence (5'-->3')
MultiBac_mod_MCS1	lower	AGCTTCTCGAGACTGCAGGCTCTAGATTCGAAAGCGTAGGCCTTT CATATGGAATTCGCGCGCTTCGGACCGG
MultiBac_mod_MCS1	upper	GATCCCGGTCCGAAGCGCGCGAATTCCATATGAAAGGCCTACGCT TTCGAATCTAGAGCCTGCAGTCTCGAGA
MultiBac_mod_MCS2	lower	GGGATTCCATGGTGCTAGCAGCTGGTCGACGCGGCCGCG
MultiBac_mod_MCS2	upper	GTACCGCGGCCGCGTCGACCAGCTGCTAGCACCATGGAATCCC

See Results 5.1.3, page 85, for specific modifications of the pFBDM multiple cloning sites.

Mutagenesis primers

Target gene	Modified RE site/ mutation	Primer orientation	DNA sequence (5'-->3')
Gemin3	+*Nco*I	forward	CATGCCATGGCGGCGGCAGTTGAAGCCTC
Gemin3	+*Not*I	reverse	ATTTGCGGCCGCTTATCACTGGTTACTATGCATCATTTCTTGTAG
Gemin4	+*Eco*RI	forward	CCGGAATTCATGGACCTAGGACCCTTGAACATCTGAAG
Gemin4	+*Xho*I	reverse	CCGCTCGAGTCAGAAGCTGCTCATCTTCTGCAACAG
Gemin5	+*Nco*I	forward	CATGCCATGGGGCAGGAGCCGCGGACG
Gemin5	+*Not*I	reverse	ATTTGCGGCCGCTTTATCACATACAGAAGGTCTGGCAGTG
EGFP	+*Nco*I	forward	GCCACCATGGTGAGCAAGGGCGAG
EGFP	+*Not*I	reverse	TGATTGCGGCCGCTTATCTAGATCCGGTGGATCC
EGFP	+*Nde*I	forward	GTCGCCCATATGGTGAGCAAGGGCGAG
EGFP	+*Stu*I	reverse	GATTATAGGCCTTTATCTAGATCCGGTGGATCC
PRMT5	+*Eco*RI	forward	CCGGAATTCATGGCGGCGATGGCGGTCG
PRMT5	+*Xho*I	reverse	CCGCTCGAG CTAGAGGCCAATGGTATATGAGCGG
WD45	+*Eco*RI	forward	CCGGAATTCATGCGGAAGGAAACCCCACCCC
WD45	+*Xho*I	reverse	CCGCTCGAGCTACTCAGTAACACTTGCAGGTCCAG
Gemin3	K112N	lower	CTATGGTGGAGAACACACAGGT**G**TTCCCGGTGCCAGATTTAGC
Gemin3	K112N	upper	GCTAAATCTGGCACCGGGAA**C**ACCTGTGTGTTCTCCACCATAG
Gemin4	+*Eco*RI/-*Avr*II	forward	GGAATTCATGGA**T**CTAGGACCCTTGAACATCTGTGAAG
Gemin4	(*Stu*I)	reverse	TAGGCCTCCACGATGGGCCGTCCAAC

Newly introduced restriction sites are highlighted in light gray, removed ones in dark gray. DNA mutations generated by the QuikChange methods are underlined. Non-modified restriction sites for further cloning procedures are indicated by a black-bordered square.

Primers for protein affinity tags

Tag	Protease cleavage site	5'-RS	3'-RS	Primer orientation	DNA sequence (5'-->3')
His_6	TEV	*Bss*HII	*Eco*RI	upper	CGCGCATGAAACATCACCATCACCATCACG AGAATCTTTATTTTCAGGGCG
				lower	AATTCGCCCTGAAAATAAAGATTCTCGTGA TGGTGATGGTGATGTTTCATG
His_6	TEV	*Eco*RI	*Nde*I	upper	AATTCATGGGACATCACCATCACCATCACG AGAATCTTTATTTTCAGCA
				lower	TATGCTGAAAATAAAGATTCTCGTGATGGT GATGGTGATGTCCCATG
His_6	TEV	*Nco*I	*Pag*I(X)	upper	CATGGGACATCACCATCACCATCACGAGAA TCTTTATTTTCAGGG
				lower	CATGCCCTGAAAATAAAGATTCTCGTGATG GTGATGGTGATGTCC
His_6	TEV	*Pag*I(X)	*Nco*I	upper	CATGCATCACCATCACCATCACGAGAATCT TTATTTTCAGGC
				lower	CATGGCCTGAAAATAAAGATTCTCGTGATG GTGATGGTGATG
His_6GST	TEV	*Bss*HII	-	forward	TTGGCGCGCCAAATGAAACATCACCATCAC CATCACAACACTAG
GST	TEV	*Bss*HII	-	forward	TTGGCGCGCCAAATGTCCCCTATACTAGGT TATTGGAAAATTAAGG
GST	TEV	-	*Eco*RI	reverse	CCGGAATTCCGGCTGAAAATAAAGATTCTC GCTCATCCATCCG
His_6GST	TEV	*Pag*I(X)	-	forward	CATGTCATGAAACATCACCATCACCATCAC AACACTAGTAGC
GST	TEV	*Pag*I(X)	-	forward	CATGTCATGAAATCCCCTATACTAGGTTAT TGGAAAATTAAGGGC
GST	TEV	-	*Nco*I	reverse	CATGCCATGGCGCCCTGAAAATAAAGATTC TCG

Gray background: protein affinity tag for MCS1 in pFBDM derivative; White background: protein affinity tag for MCS2 in pFBDM derivative; *Pag*I(X): disruption of restriction site using overlapping ends of *Pag*I in oligonucleotide and *Nco*I in vector DNA. The restriction sites (RS) for further cloning procedures are indicated by a black-bordered square.

Oligonucleotides for recombinant bacmid analysis by PCR

Primer	DNA sequence (5'-->3')	Tm (°C)
M13 forward (-20)	GTAAAACGACGGCCAG	45.9
M13 reverse	CAGGAAACAGCTATGAC	44.6
MB_AvrII	ATTAAAGGTCCGTATACTAGGCTCAAGCAGTGATCAGATCCAG	67.4
MB_NruI	CGACCTACTCCGGAATATTAATAGATCATG	58.9
MB_PmeI	ATATTCCGGAGTAGGTCGAAACAAAGCTGGCTATGGCAGGGC	70.4
MB_SpeI	AGTATACGGACCTTTAATTCAACCCAACAC	58.9

3.5 Plasmid vectors

Plasmid	Description	Reference/Supplier
pET28a	Bacterial expression vector	Novagen, Madison, WI, USA
pET21a	Bacterial expression vector	Novagen, Madison, WI, USA
pETM-30	Bacterial expression vector	EMBL protein expression group

pGEX-6P-1	Bacterial expression vector	GE Healthcare, Giles, UK
pFBDM	MultiBac system: bacterial transfer vector	(Berger *et al.*, 2004)
pFBDM4	MultiBac system: modified bacterial transfer vector	This work
pEGFP-C1	Mammalian expression vector encoding enhanced green fluorescent protein (EGFP)	Clonetech, Mountain View, CA, USA

3.6 Transcription vectors

RNA	Vector	Promoter	Reference/Supplier
U1	pUC9	T7	(Zeller *et al.*, 1984)
U1ΔD	pUC9	T7	(Hamm *et al.*, 1990b)
U1ΔE	pUC9	T7	(Jarmolowski and Mattaj, 1993)

3.7 Baculovirus system transfer vectors

Plasmid	Protein	Amino acids	MCS*	5'-/internal/3'- Restriction site
pFBDM4	EGFP	1–266	MCS1	*Nde*I/*Stu*I
pFBDM4	EGFP	1–266	MCS2	*Nco*I/*Not*I
pFBDM4	His_6[TEV]	1–15	>MCS1	*Bss*HII/*Eco*RI
pFBDM4	GST[TEV]	1–236	>MCS1	*-/-*
pFBDM4	GST[TEV]	1–236	>MCS2	*-/Nco*I
pFBDM4	His_6GST[TEV]	1–250	>MCS1	*-/-*
pFBDM4	His_6GST[TEV]	1–250	>MCS2	*-/Nco*I
pFBDM4	GST[TEV]	1–236	>MCS1	*-/-*
	EGFP	1–266	MCS2	*Nco*I/*Not*I
pFBDM4	EGFP	1–266	MCS1	*Nde*I/*Stu*I
	GST[TEV]	1–236	>MCS2	*-/Nco*I
pFBDM4	His_6GST[TEV]	1–250	>MCS1	*-/-*
	EGFP	1–266	MCS2	*Nco*I/*Not*I
pFBDM4	EGFP	1–266	MCS1	*Nde*I/*Stu*I
	His_6GST[TEV]	1–250	>MCS2	*-/Nco*I
pFBDM4	EGFP	1–266	MCS1	*Nde*I/*Stu*I
	His_6[TEV]Gemin3	1–840	MCS2	*Nco*I/*-/Not*I
pFBDM4	EGFP	1–266	MCS1	*Nde*I/*Stu*I
	His_6[TEV]Gemin3(K112N)	1–840	MCS2	*Nco*I/*-/Not*I
pFBDM4	His_6[TEV]Gemin4	1–1,076	MCS1	*Bss*HII/*Eco*RI/*Xho*I
	EGFP	1–266	MCS2	*Nco*I/*Not*I
pFBDM4	EGFP	1–266	MCS1	*Nde*I/*Stu*I

	His_6[TEV]Gemin5	1–1,524	MCS2	*Nco*I/-/*Not*I
pFBDM4	EGFP	1–266	MCS1	*Nde*I/*Stu*I
	GST[TEV]Gemin3	1–1,063	MCS2	*Nco*I/-/*Not*I
pFBDM4	EGFP	1–266	MCS1	*Nde*I/*Stu*I
	GST [TEV]Gemin3(K112N)	1–1,063	MCS2	*Nco*I/-/*Not*I
pFBDM4	EGFP	1–266	MCS1	*Nde*I/*Stu*I
	GST[TEV]Gemin5	1–1,747	MCS2	*Nco*I/-/*Not*I
pFBDM4	His_6[TEV]PRMT5	1–655	MCS1	*Bss*HII/*Eco*RI/*Xho*I
	WD45	1–343	MCS1'	*Bss*HII/*Eco*RI/*Xho*I
	EGFP	1–266	MCS2'	*Nco*I/*Not*I

*: MCS1 is under the control of the polyhedrin promoter, MCS2 under the control of the p10 promoter.

3.8 Bacterial expression vectors

Plasmid	Protein	Amino acids	MCS	5'-/internal/3'- Restriction site
pET28b*	GST[TEV]SMN	1–531	poly-cistron	*Nco*I/*Not*I
	Gemin8	1–243		*Nde*I/*Not*I
	Gemin2	1–281		*Nde*I/*Not*I
pET28b*	GST[TEV]SMN(E134K)	1–531	poly-cistron	*Nco*I/*Not*I
	Gemin8	1–243		*Nde*I/*Not*I
	Gemin2	1–281		*Nde*I/*Not*I
pET21a	His_6[Thrombin]Gemin6	1–185	poly-cistron	*Eco*RI/*Xho*I
	Gemin7	1–132		*Nde*I/*Not*I

*: MCS of pET28b with swapped *Nco*I and *Nde*I restriction sites (Chari *et al.*, 2008)

3.9 Antibodies

Antibody	Antigen	Source	Reference
7B10	SMN1–30	Mouse, monoclonal	(Meister *et al.*, 2000)
α-His	penta-histidine	Mouse, monoclonal	QIAGEN, Hilden, Germany
α-Gemin3	Gemin3, C-terminus	Rat, monoclonal	Friedrich Grässer
α-Gemin4	Gemin4, C-terminus	Goat, monoclonal	Santa Cruz Biotechnology, Santa Cruz, CA, USA
α-PRMT5	hPRMT5(1–291)	Rabbit, polyclonal	This work
α-pICln	pICln, full-length	Rabbit, polyclonal	This work
α-mouse	mouse IgG	Goat, polyclonal	Sigma-Aldrich, St. Louis, MO, USA
α-rabbit	rabbit IgG	Goat, polyclonal	Sigma-Aldrich, St. Louis, MO, USA
α-rat	rat IgG	Rabbit, polyclonal	Sigma-Aldrich, St. Louis, MO, USA
α-goat	goat IgG	Rabbit, polyclonal	Sigma-Aldrich, St. Louis, MO, USA

3.10 Organisms and cell lines

Bacterial cells

Strain	Chromosomal genotype	Reference
E. coli DH5α	F-φ80*lac*ZΔM15 Δ(*lac*ZYA-*arg*F)U169 *deo*R *rec*A1 *end*A1 *hsd*R17(rk^-, mk^+) *pho*A *sup*E44 *thi*-1 *gyr*A96 *rel*A1 λ^-	Invitrogen, Carlsbad, CA, USA (Horii *et al.*, 1980; Taylor *et al.*, 1993)
E. coli XL1 Blue	F´ ::Tn10 $proA^+B^+$ $lacI^q$ Δ(lacZ)M15/recA1 endA1 gyrA96 (Nal^r) thi hsdR17 (r_K^- m_K^+) glnV44 relA1 lac	Stratagene, La Jolla, CA, USA (Bullock *et al.*, 1987)
E. coli BL-21 pRARE	B F- dcm *ompT hsdS*(r_B- m_B-) *gal dcm* pRARE (Cam^R)	GE Healthcare, Giles, UK (Novy *et al.*, 2001; Phillips *et al.*, 1984)
E. coli DH10MultiBac	F- *mcr*A Δ(*mrr-hsd*RMS-*mcr*BC) ϕ80*lac*ZΔM15 Δ*lac*X74 *rec*A1 *end*A1 *ara*D139 Δ (*ara*, *leu*)7697 *gal*U *gal*K λ- *rps*L *nup*G /pMON14272 Δ (*chiA, v-cath*) / pMON7124	(Berger *et al.*, 2004)

Eukaryotic cell lines

Cell type	Description	Supplier	Reference
*Sf*9	*Sf*9 (*Spodoptera frugiperda*) insect cells	European Collection of Cell Cultures (ECACC)	(Smith *et al.*, 1985; Vaughn *et al.*, 1977)
*Sf*21	*Sf*21 (*Spodoptera frugiperda*) insect cells, derivative of *Sf*9 cells	European Collection of Cell Cultures (ECACC)	(Smith *et al.*, 1985; Vaughn *et al.*, 1977)
*Tn*5	*Tn*5 B1-4 (*Trichoplusia ni*) insect cells	European Collection of Cell Cultures (ECACC)	(Granados *et al.*, 1994)
HeLa S3	Human cervix carcinoma cell line	European Collection of Cell Cultures (ECACC)	(Puck *et al.*, 1956)

3.11 Eukaryotic cell culture media

Medium	Description	Supplier
EX-CELL® TiterHigh™	Insect cell medium for *Sf*9 and *Sf*21 cells	Sigma-Aldrich, St. Louis, MO, USA
EX-CELL® 405	Insect cell medium for *Tn*5 cells	Sigma-Aldrich, St. Louis, MO, USA
EX-CELL® 420	Insect cell medium for *Sf*9 and *Sf*21 and *Tn*5 cells	Sigma-Aldrich, St. Louis, MO, USA
DMEM	Dulbecco's Modified Eagle's Medium, Culture medium for mammalian cells	PAA, Farnborough, Hampshire, UK

3.12 Buffers and solutions

3.12.1 Agarose gel electrophoresis

Buffer/Solution	Composition
5× TBE (Tris/EDTA/borate)	445 mM Tris-HCl, pH 8.3 445 mM boric acid 10 mM Na_2EDTA
1× TBE (running buffer)	200 ml 5× TBE 800 ml ddH_2O
Agarose gel	0.5%–2.0% (w/v) agarose 1× TBE 5 µg/ml ethidium bromide
6× DNA sample loading buffer	10 mM Tris-HCl, pH 7.5 60% (v/v) glycerol 60 mM EDTA, pH 8.0 0.03% (w/v) xylene cyanol 0.03% (w/v) bromophenol blue Sterile filtered (0.2 µm)

3.12.2 Antibiotics

Antibiotic stock solutions

Antibiotic	Concentration	Solvent
Ampicillin	100 mg/ml	ddH_2O
Chloramphenicol	50 mg/ml	ethanol
Gentamycin	50 mg/ml	ethanol
Kanamycin	50 mg/ml	ddH_2O
Tetracycline	10 mg/ml	ddH_2O
Penicillin/Streptomycin	100× stock solution (PAA)	-

3.12.3 Bacterial cell culture

Buffer/Solution	Composition
LB medium (Luria Broth)	1% (w/v) tryptone 0.5% (w/v) yeast extract 1% (w/v) NaCl

Agar plates	LB medium 1.5% (w/v) agar antibiotics
SB medium (Super Broth)	3.5% (w/v) tryptone 2.0% (w/v) yeast extract 0.5% (w/v) NaCl set pH to 7.5 using NaOH
$CaCl_2$ solution (preparation of chemically competent cells)	60 mM $CaCl_2$ 15% (v/v) glycerol 10 mM PIPES, pH 7.0 set pH to 7.0 using NaOH sterile filtration (0.2 µm)
E. coli DH10MultiBac culture medium	LB medium 50 µg/ml kanamycin 7 µg/ml gentamycin 100 µg/ml ampicillin 10 µg/ml tetracycline
Agar plates for *E. Coli* DH10MultiBac blue/white screening	*E. coli* DH10MultiBac culture medium 1.5% (w/v) agar 0.179 mg/ml IPTG (= 0.75 mM) 32 µg/ml X-Gal
SMNΔGemin3–5 complex expression medium	SB medium 100 µg/ml ampicillin 50 µg/ml kanamycin 50 µg/ml chloramphenicol 500 mM sorbitol 2% (w/v) glucose 1 mM betaine

3.12.4 Bacmid DNA isolation

Solution	**Composition**
Bacmid isolation (S1) – cell resuspension solution	50 mM Tris-HCl, pH 8.0 10 mM EDTA 100 µg/ml Rnase A
Bacmid isolation (S2) – cell lysis solution	200 mM NaOH 1% (w/v) SDS
Bacmid isolation (S3) – neutralization solution	2.8 M potassium acetate, pH 5.1

TE buffer	10 mM Tris-HCl, pH 7.5 1 mM EDTA

3.12.5 Insect cell culture

Buffer/Solution	Composition
Trypan blue staining solution	0.4% (w/v) trypan blue in 1× PBS sterile filtered (0.2 µm)
Insect cell lysis buffer	62.5 mM Tris, pH 6.8 2% (w/v) SDS
Insect cell cryo-preservation buffer	45% (v/v) EX-CELL® TiterHigh™ medium 45% (v/v) culture supernatant 10% (v/v) DMSO
Insect cell disinfection solution	1% (w/v) Virkon® S

3.12.6 Mammalian cell culture

Buffer/Solution	Composition
HeLa culture medium	Dulbecco's Modified Eagle Medium (DMEM) 10% (v/v) Fetal Calf Serum 2 mM L-Glutamin 50 µg/ml Penicillin/Streptomycin

3.12.7 SDS-PAGE

Buffer/Solution	Composition
SDS-PAGE stacking gel – 5%	5% (v/v) acrylamide/bisacrylamide (37.5:1), Rotiphorese 30 0.125 M Tris-HCl, pH 6.8 0.001% (w/v) SDS 0.0005% (w/v) APS 0.0025% (v/v) TEMED
SDS-PAGE separating gel – (8–13%) – high TEMED	8%, 10%, 12%, 13% (v/v) Acrylamide/ bisacrylamide (37.5:1), Rotiphorese 30 0.375 M Tris-HCl, pH 8.8 0.001% (w/v) SDS

	0.0005% (w/v) APS 0.005% (v/v) TEMED
10× Laemmli running buffer	0.25 M Tris 1.92 M glycine 1% (w/v) SDS
1× Laemmli running buffer	100 ml 10× Laemmli running buffer 900 ml ddH_2O
6× SDS-PAGE protein sample buffer	300 mM Tris-HCl, pH 6.8 12% (w/v) SDS 30% (v/v) glycerol 600 mM DTT or β-mercaptoethanol 0.04% (w/v) bromophenol blue

3.12.8 Protein gel staining (Coomassie staining)

Buffer/Solution	Composition
Coomassie staining solution I	50% (v/v) methanol 10% (v/v) acetic acid 0.15% (w/v) Serva blue R
Coomassie staining solution II	20% (v/v) isopropanol 10% (v/v) acetic acid 0.15% (w/v) Serva blue R
Coomassie de-staining solution I	30% (v/v) methanol 10% (v/v) acetic acid
Coomassie de-staining solution II	20% (v/v) acetic acid

3.12.9 Protein gel staining (Silver staining)

Buffer/Solution	Composition
Fixation solution	50% (v/v) methanol 12% (v/v) acetic acid 0.185% (v/v) formaldehyde (add directly before use)

Washing solution	50% (v/v) ethanol, degassed
Sodium thiosulfate solution (staining)	0.02% (w/v) sodium thiosulfate
Silver solution	0.2% (w/v) silver nitrate 0.02775% (v/v) formaldehyde (add directly before use)
Developing solution	6% (w/v) sodium carbonate anhydrous 0.185% (v/v) formaldehyde (add directly before use)
Stopping solution	50% (v/v) ethanol, degassed
Potassium ferricyanide solution	0.5 M potassium ferricyanide (III)
Sodium thiosulfate solution (de-staining)	0.5 M sodium thiosulfate pentahydrate
Background de-staining	0.5 ml 0.5 M potassium ferricyanide (III) 10 ml 0.5 M sodium thiosulfate pentahydrate 89.5 ml ddH_2O
Complete de-staining	3 ml 0.5 M potassium ferricyanide 10 ml 0.5 M sodium thiosulfate pentahydrate 87 ml ddH_2O

3.12.10 Western Blotting

Buffer/Solution	**Composition**
10× Towbin electrotransfer buffer	0.25 M Tris 1.92 M glycine
1× Towbin buffer	25 mM Tris 192 mM glycine 20% (v/v) methanol 0.1% (w/v) SDS
Amido black staining solution	0.2% (w/v) amido black 10% (v/v) methanol 2% (v/v) acetic acid
De-staining solution	90% (v/v) methanol

	3% (v/v) acetic acid
10× NET	1.5 M NaCl 0.05 M NaEDTA, pH 8.0 0.5 M Tris, pH 7.5 0.5% (v/v) Triton X-100 sterile filtered (0.45 µm)
1× NET-gelatin solution (blocking solution)	100 ml 10× NET 900 ml ddH_2O 0.25% (w/v) gelatin
Primary antibody solution	1× NET-gelatin solution primary antibody (1:500 – 1:100) 0.01% (w/v) Sodium azide
10× PBS	1.37 M NaCl 27 mM sodium phosphate dibasic (Na_2HPO_4) 20 mM potassium phosphate monobasic (KH_2PO_4)
1× PBS	100 ml 10× PBS 900 ml ddH_2O
Western Blotting washing solution (1× PBST)	1× PBS 0.05% (v/v) Tween 20 0.2% (v/v) Triton X-100
Secondary antibody solution	1× PBST secondary antibody (1:45,000 – 1:1,000)
ECL reagent I (Coumaric acid)	6.8 mM coumaric acid in DMSO
ECL reagent II (Luminol)	1.25 mM luminol 100 mM Tris-HCl, pH 8.5
ECL reagent III (hydrogenperoxide)	30% (v/v) hydrogen peroxide

3.12.11 Protein purification buffers

Buffer/Solution	**Composition**
Insect cell pellet resuspension buffer (I)	20 mM Hepes-NaOH, pH 7.5/pH 8.5 1 M NaCl 10% (v/v) glycerol 5 mM β-mercaptoethanol 20 mM imidazole, pH 7.5/pH 8.5

	1 mM PMSF 20 mg/l aprotitin 20 mg/l leupeptin/pepstatin 0.2 mM AEBSF sterile filtered (0.45 µm)
Ni-NTA purification – washing buffer	Identical with the resuspension buffer lacking protease inhibitors
Ni-NTA purification – elution buffer	Identical with the washing buffer containing a higher imidazole concentration 250 mM imidazole, pH 7.5/pH 8.5
Anion exchange – low salt dialysis buffer	20 mM Hepes-NaOH, pH 7.5/pH 8.5 90 mM NaCl 10% (v/v) glycerol 5 mM β-mercaptoethanol sterile filtered (0.45 µm) and degassed
Anion exchange – high salt dialysis buffer	20 mM Hepes-NaOH, pH 7.5/pH 8.5 1 M NaCl 10% (v/v) glycerol 5 mM β-mercaptoethanol sterile filtered (0.45 µm) and degassed
Gel filtration – running buffer (I)	20 mM Hepes-NaOH, pH 7.5/pH 8.5 200 mM NaCl 5 mM DTT sterile filtered (0.45 µm) and degassed
GST-purification of GST-tagged Gemin3/Gemin4 and Gemin3/Gemin4/Gemin5 complexes – resuspension buffer	50 mM sodium-phosphate, pH 7.5 500 mM NaCl 10% (v/v) glycerol 5 mM β-mercaptoethanol 1 mM PMSF 20 mg/l aprotitin 20 mg/l leupeptin/pepstatin 0.2 mM AEBSF sterile filtered (0.45 µm)
GST-purification of GST-tagged Gemin3/Gemin4 and Gemin3/Gemin4/Gemin5 complexes – washing buffer	50 mM sodium-phosphate, pH 7.5 500 mM NaCl 10% (v/v) glycerol 5 mM β-mercaptoethanol sterile filtered (0.45 µm)
GST-purification of GST-tagged Gemin3/Gemin4 and Gemin3/Gemin4/Gemin5 complexes –	50 mM sodium-phosphate, pH 7.5 500 mM NaCl

elution buffer	10% (v/v) glycerol 20 mM glutathione 5 mM β-mercaptoethanol sterile filtered (0.45 µm), set pH to 7.5
GST-purification of GST-tagged Gemin3/Gemin4 and Gemin3/Gemin4/Gemin5 complexes – gel filtration buffer	50 mM sodium-phosphate, pH 7.5 500 mM NaCl 10% (v/v) glycerol 5 mM β-mercaptoethanol sterile filtered (0.45 µm) and degassed
GST-purification of pentameric SMN complex – resuspension buffer	20 mM Hepes-NaOH, pH 6.8 300 mM sodium sulfate 10 mM EDTA 20% (w/v) sucrose 0.5 mM TCEP (added fresh before use) 1 mM PMSF 20 mg/l aprotitin 20 mg/l leupeptin/pepstatin 0.2 mM AEBSF spatula tip of RNase Q1 sterile filtered (0.2 µm)
GST-purification of pentameric SMN complex – washing buffer I	as resuspension buffer but lacking protease inhibitors and RNase Q1
GST-purification of pentameric SMN complex – washing buffer II	20 mM sodium/potassium phosphate, pH 6.8 100 mM sodium sulfate 5% (w/v) galactose sterile filtered (0.2 µm)

3.12.12 Protein chromatography matrix regeneration

Solution	**Composition**
Ni-NTA regeneration solution (I) – EDTA	0.5 M NaEDTA
Ni-NTA regeneration solution (II) – Urea	8.75 M urea
Ni-NTA regeneration solution (III) – Nickel chloride solution	0.2 M nickel chloride hexahydrate
GSH bead regeneration solution	0.08% (w/v) SDS 20 mM DTT 8.225 M urea

3.12.13 Protein complex reconstitution

Buffer/Solution	Composition
4× Reconstitution buffer	80 mM Hepes-NaOH, pH 7.5 4 M NaCl 20 mM DTT
Reconstitution dialysis buffer	20 mM Hepes-NaOH, pH 7.5 200 mM NaCl 5 mM DTT

3.12.14 Immunoprecipitation (IP)

Buffer	Composition
IP dialysis buffer/binding buffer	20 mM Hepes-NaOH, pH 7.5 200 mM NaCl
IP wash buffer (I)	20 mM Hepes-NaOH, pH 7.5 300 mM NaCl 0.01% (v/v) NP40
IP wash buffer (II)	20 mM Hepes-NaOH, pH 7.5 300 mM NaCl

3.12.15 Protein methylation

Buffer/Solution	Composition
Methylation buffer	100 mM Hepes-NaOH, pH 8.2 200 mM NaCl 5 mM DTT sterile filtered (0.45 µm)
S-adenosylmethionine (SAM) stock solution	32 mM SAM, 5 mM H_2SO_4:EtOH (9:1)
SAM dilution solution	5 mM H_2SO_4:EtOH (9:1)
S-adenosylmethionine (SAM) working solution	110 µM SAM (34.4 µl 32 mM SAM + 9.965 ml SAM dilution solution)
[^{3}H]-S-adenosylmethionine (SAM) solution	55 µM [^{3}H]-SAM, 5 mM H_2SO_4:EtOH (9:1), 10 µCi/mmol
Amplifying solution	NAMP100 Amplify Fluorographic Reagent

SDS-gel slice dissolution solution	hydrogen peroxide (H_2O_2):Sodium hydroxide (NH_4OH) (99:1)
Liquid scintillation counting solution	Rotiszint liquid scintillation counting solution (Roth)

3.12.16 Protein hydrolysis

Solution	Composition
BSA solution	10 µM bovine serum albumin (BSA) in ddH_2O
TCA precipitation solution	25% (w/v) trichloroacetic acid (TCA)
Protein hydrolysis solution	6 M hydrochloric acid (HCl)

3.12.17 Amino acid thin layer chromatography

Buffer/Solution	Composition
L-arginine standard	0.4 mM L-arginine (Sigma-Aldrich)
MMA standard	0.4 mM N^G-methyl-L-arginine (Sigma-Aldrich)
aDMA standard	0.4 mM N^G,N^G-dimethyl-L-arginine (Sigma-Aldrich)
sDMA standard	0.4 mM N^G,$N^{G'}$-dimethyl-L-arginine (Sigma-Aldrich)
TLC running buffer for amino acid separation	75% (v/v) ethanol 25% (v/v) ammonium hydroxide
Ninhydrin staining solution	0.5% (w/v) ninhydrin in ethanol

3.12.18 Denaturing RNA polyacrylamide gel electrophoresis

Buffer/Solution	Composition
Denaturing RNA polyacrylamide gel	5% acrylamide/bis-acrylamide (Rotiphorese 40) 8 M urea 0.5× TBE 500 µl 10% (w/v) APS per 100 ml gel solution 50 µl TEMED per 100 ml gel solution

RNA loading buffer (denaturing)	90% (v/v) formamide 0.025% (w/v) xylene cyanol 0.025% (w/v) bromophenol blue
RNA elution buffer (AES buffer)	300 mM sodium acetate 2 mM EDTA 0.1% (w/v) SDS

3.12.19 Non-denaturing/native RNA polyacrylamide gel electrophoresis

Buffer/Solution	Composition
20% acrylamide/bisacrylamide (80:1)	66.7 ml 30% (v/v) acrylamide (Rotiphorese Gel A) 12.5 ml 2% (v/v) bisacrylamide (Rotiphorese Gel B) 20.8 ml ddH_2O
Native RNA polyacrylamide gel	6% acrylamide/bisacrylamide (80:1) 4% (v/v) glycerol 0.5× TBE 0.001% (w/v) APS 0.001% (v/v) TEMED
Native RNA sample buffer with heparin	16% (v/v) glycerol 10 mg/ml heparin 0.025% (w/v) xylene cyanol 0.025% (w/v) bromophenol blue
Native RNA sample buffer without heparin	16% (v/v) glycerol 0.025% (w/v) xylene cyanol 0.025% (w/v) bromophenol blue

3.12.20 ATP-crosslink and ATPase assay

Buffer/Solution	Composition
ATPase reaction buffer	50 mM Sodium phosphate, pH 7.5 50 mM NaCl 3 mM $MgCl_2$ 2.5 mM DTT
ATPase reaction stopping solution	0.5 M EDTA, pH 8.0
TLC running buffer for nucleotide separation	0.75 M potassium phosphate monobasic (KH_2PO_4)

3.13 Software

Software	**Supplier**
Photoshop	Adobe Systems, San Jose, California, USA
Illustrator	Adobe Systems, San Jose, California, USA
Excel	Microsoft Corporation, Redmond, WA, USA
ImageJ 1.44	National Institutes of Health, Bethesda, MD, USA
Origin 8.6	OriginLab Corporation, Northampton, MA, USA
PyMOL Molecular Graphics System, Version 1.3	Schrödinger LLC, Portland, OR, USA
ÄktaPrimeView 5.0	GE Healthcare, Giles, UK
Äkta Prime Program Generator	David Cooper, Ph.D., University of Virginia, Charlottesville, VA, USA http://ginsberg.med.virginia.edu/akta.html
OligoCalc: Oligonucleotide Properties Calculator	Warren A. Kibbe, Ph.D., Northwestern University, Chicago, IL, USA http://www.basic.northwestern.edu/biotools/oligocalc.html
ImageQuant	Molecular Dynamics, now: GE Healthcare, Giles, UK
Quantum-Capt	Vilber-Lourmat ,Marne-la-Vallée Cedex 1, France

4 Methods

4.1 Molecular biological methods

4.1.1 Preparation of chemically competent *E. coli* DH5α

Fifty milliliters of LB medium without antibiotics were inoculated with *E. coli* DH5α cells in a 500 ml shaker flask and incubated at 37°C overnight shaking at 180 rpm. Of this solution, 4 ml were transferred into a 2,000 ml baffled shaker flask containing 400 ml culture medium and were incubated likewise until an optical density of A_{590nm} = 0.375 was reached. The culture was cooled on ice for 10 min and centrifuged at 1,600 *×g* and 2°C for 7 min without deceleration. Then, the cell pellet was resuspended in 80 ml of $CaCl_2$ solution (60 mM $CaCl_2$, 15% (v/v) glycerol, 10 mM PIPES, pH 7.0) and centrifuged once more. After repetition of the previous step, the cells were incubated on ice for 30 min, centrifuged as before and resuspended in 16 ml of $CaCl_2$ solution. Finally, the cells were aliquoted at 250 µl, frozen on dry ice and permanently stored at -80°C.

4.1.2 Preparation of bacterial glycerol cultures

Glycerol cultures are used to preserve bacteria in a frozen form. Five hundred microliters of a bacterial suspension culture were added to 750 µl of sterile 86% (v/v) glycerol, vortexed and stored at -80°C.

4.1.3 Agarose gel electrophoresis

Agarose gel electrophoresis is used to separate DNA and RNA molecules by size. Agarose is a linear polymer consisting of repeating units of agarobiose (1,3-linked β-D-galactose and 1,4-linked 3,6-anhydro-α-L-galactose) which accumulates in the cell walls of agarophyte red algae (Narayan, 2009). Whereas agarose is water-soluble at high temperatures, at low temperatures a gel is formed. The porosity of this gel is inversely proportional to the agarose concentration. DNA samples are supplemented with DNA loading buffer containing glycerol to increase the sample density and dyes to track to progress of the separation. Molecules are separated by applying an electric charge. The

ethidium bromide added to the gel intercalates between the stack of DNA bases in the double helix. UV-light is used to visualize the DNA fragments on the gel.

TBE buffer was mixed with agarose to a final concentration of 0.5% (for large DNA fragments such as bacmid DNA), 1.0% (standard concentration) or 2.0% (small DNA fragments) and heated until all the agarose was dissolved. After cooling the agarose solution, ethidium bromide was added to a final concentration of 5 µg/ml and the gel was poured. Gels were run at 120V for 45 min and analyzed by a Quantum Gel documentation device (peqlab).

4.1.4 Isolation of DNA fragments from agarose gels

DNA fragments were excised from agarose gels using a scalpel and processed as described in the PCR clean-up gel extraction manual by Macherey-Nagel.

4.1.5 Restriction hydrolysis of DNA fragments

Restriction endonucleases are enzymes that specifically cleave palindromic 4-/6-/8-sequences in double stranded DNA (dsDNA). One differentiates between analytical and preparative restriction hydrolysis. Whereas the first is used to verify specific hydrolysis patterns, the second one is used for subcloning of DNA fragments. Restriction hydrolysis was carried out as recommended by the manufacturer (Fermentas) by using 1 U of enzyme to cleave 1 µg DNA at 37°C within 60 min applying the appropriate reaction buffer. If more than one enzyme was used (double/triple digestion), the reaction buffers were adjusted accordingly or the enzymes were used sequentially diluting the reaction with the optimal buffers.

4.1.6 Hybridization of double-stranded DNA oligomers

Single-stranded DNA oligomers were synthesized by Biomers. Lyophilized DNA was resuspended in ddH_2O to a final concentration of 100 µM. For hybridization reactions, two complementary DNA oligomers were diluted in 10 mM Tris, pH 7.4, to a final concentration of 10 µM each, incubated at 70°C for 10 min and cooled down at RT for 30 min.

4.1.7 Preparative polymerase chain reaction (PCR)

In the polymerase chain reaction the enzyme DNA polymerase is used to amplify specific DNA fragments in large amounts. Two short DNA oligomers with complementary sequences toward the template DNA are extended with deoxyribonucleotides at the free 3'-OH group of the primer. In general, the reaction comprises repetitive steps of DNA double strand separation (denaturation), binding of the complementary primers (annealing) and DNA amplification mediated by the DNA polymerase (extension). For the preparative amplification of DNA sequences the Pfu (*Pyrococcus furiosus*) DNA polymerase - which contains a 3'-5'-exonuclease activity (proofreading activity) - was used.

The common setup of a PCR reaction and the accompanying PCR program were as follows:

PCR reaction setup:	
Template DNA (50 ng/µl)	1 µl
Primer A (10 µM)	1 µl
Primer B (10 µM)	1 µl
dNTP mix (10 mM)	1 µl
ddH_2O	13 µl
10× *Pfu* DNA polymerase buffer	2 µl
Pfu DNA polymerase (2.5 U/µl)	1 µl

PCR program:		
Temperature	**Time**	**Cycles**
95°C	3 min	1×
95°C	30 s	┐
T_m - 5°C	30 s	30×
68°C	1 min/1,000 bp	┘
68°C	5 min	1×
4°C	∞	

Initially, the template DNA was denatured for 3 min at 95°C, then 30 PCR cycles followed in which (1) the DNA double strands were denatured for 30 s at 95°C, (2) specific primers bound at a temperature 5 degrees below the melting temperature of the primers for 30 s and (3) the DNA was amplified at 68°C for 1 min per 1,000 base pairs of DNA to be copied. After a final extension step, the samples were cooled to 4°C, supplemented with 6× DNA sample loading buffer and separated by agarose gel electrophoresis (Methods 4.1.3, page 47).

4.1.8 Dephosphorylation of DNA fragments

In order to release 5'- and 3'-phosphate groups from DNA, Shrimp Alkaline Phosphatase (SAP; Fermentas) was added to the recipient vector in DNA cloning to prevent recircularization. After restriction hydrolysis of the recipient vector, 1 µl of SAP was added to the reaction setup and incubated for 60 min at 37°C.

4.1.9 Ligation of DNA fragments

T4 DNA ligase is an enzyme that catalyzes the formation of a phosphodiester bond between juxtaposed 5'-phosphate and 3'-hydroxyl termini in duplex DNA as well as RNA and is used to fuse single strand nicks in duplex DNA, RNA or DNA/RNA hybrids. In molecular biology it is commonly applied to covalently introduce a donor DNA fragment into a recipient vector sequence both of which have been previously treated with restriction enzymes to leave cohesive ends. One hundred nanograms of recipient vector were incubated with a 10-fold molar excess of donor DNA and 1 Weiss-unit T4 DNA ligase (Fermentas) in the appropriate buffer at 14°C overnight or at room temperature (RT) for 2 h.

4.1.10 DNA mutagenesis

DNA sequences were specifically modified using the polymerase chain reaction. The first method comprised the introduction of modified DNA bases into the primer sequences of a preparative PCR. Thus prepared DNA fragments carried for example additional restriction sites at the 5’- or 3’- ends enabling further subcloning into recipient vectors. The second method, the so called Quikchange method (Stratagene) used primers harboring mutations which are complementary to each other. During the amplification each primer attached to one of the vector DNA strands amplifying the entire vector sequence.

The reaction setup of the Quikchange method was as follows:

PCR reaction setup:	
Template DNA (5 ng/µl)	3 µl
Primer A (4 µM)	2 µl
Primer B (4 µM)	2 µl
dNTP mix (1 mM)	4 µl
ddH_2O	6 µl
10× *Pfu* DNA polymerase buffer	2 µl
Pfu DNA polymerase (2.5 U/µl)	1 µl

PCR program:		
Temperature	**Time**	**Cycles**
95°C	3 min	1×
95°C	30 s	┐
T_m - 5°C	1 min	15×
68°C	8 min	┘
68°C	7 min	1×
4°C	∞	

Finally, the methylated template DNA was hydrolyzed by the addition of 10 units of *Dpn*I and incubation at 37°C for 1 h.

4.1.11 Transformation of chemically competent *E. coli* DH5α

One hundred microliters of chemically competent *E. coli* DH5α were thawed on ice, incubated with 100 ng of vector DNA on ice for 15 min, transferred to 42°C for exactly 90 s, placed on ice for 2 min, supplemented with 500 µl LB medium and incubated at 37°C shaking at 1,000 rpm for 1 h. Then, 1/5 and 4/5 of the bacterial solution were transferred onto agar plates containing antibiotics with respect to the type of vector DNA. Common antibiotic concentrations were 50 µg/ml kanamycin, 100 µg/ml ampicillin, 7 µg/ml gentamycin and 10 µg/ml tetracycline.

4.1.12 Polymerase chain reaction (PCR) colony screen

The successful integration of a novel DNA fragment into a vector can be verified by a PCR colony screen. In this, individual bacterial colonies are analyzed by a polymerase chain reaction. Whereas one of the PCR primers binds to the inserted DNA fragment, the other one interacts with the recipient vector. Therefore, only vectors with a correctly inserted sequence give rise to a DNA fragment in the PCR colony screen.

Reactions were set up as follows:

PCR reaction setup:	
Bacterial colony	
Primer A (5 µM)	1 µl
Primer B (5 µM)	1 µl
2× Roche MasterMix (incl. *Taq* DNA pol)	10 µl
ddH_2O	8 µl

PCR program:		
Temperature	**Time**	**Cycles**
95°C	3 min	1×
95°C	30 s	┐
T_m - 5°C	30 s	30×
72°C	1 min/1,000 bp	┘
72°C	5 min	1×
4°C	∞	

Resulting samples were analyzed on a 1% (w/v) agarose gel.

4.1.13 DNA isolation and purification

Plasmid DNA was prepared from bacterial suspension cultures using Macherey-Nagel DNA purification kit systems. For 3 ml cultures "Nucleospin Plasmid QuickPure" and for 500 ml cultures "Nucleobond PC500" kits were applied according the manual of the manufacturer.

4.1.14 DNA sequencing

DNA sequencing was performed by Medigenomix and GATC.

4.1.15 Preparation of bacterial transfer vectors for the insect cell expression system

The MultiBac system is a baculovirus expression vector system (BEVS) that was specifically designed for eukaryotic multiprotein expression (Berger *et al.*, 2004; Fitzgerald *et al.*, 2006). Two distinct transfer vectors provide the incorporation of gene expression cassettes via the Tn7 transposase (pFBDM: plasmid FastBacDual-derived MultiBac) or the Cre recombinase (pUCDM: plasmid pUC-derived Dual MultiBac) (Figure 12). Both vectors contain two multiple cloning sites (MCS1 and MCS2) in a head-to-head orientation. MCS1 is enclosed by the polyhedrin promoter and the SV40 terminator, whereas MCS2 is

surrounded by the p10 promoter and the HSVtk terminator. The pFBDM vector carries a gentamycin and ampicillin resistance; the pUCDM vector confers the restistance against chloramphenicol. Containing a replication of origin derived from R6Kγ, pUCDM can only replicate in host cells expressing the *pir* gene (Metcalf *et al.*, 1994).

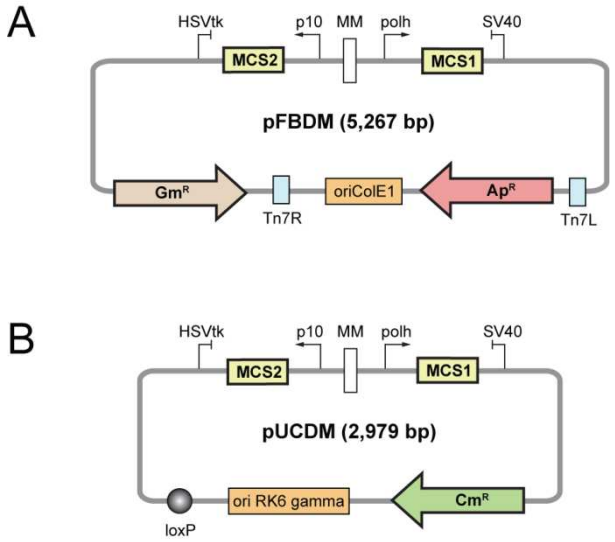

Figure 12 – Bacterial transfer vectors of the MultiBac system.

The MultiBac transfer vectors pFBDM and pUCDM contain two multiple cloning sites (MCS) each, one of which is under the control of the polyhedrin promoter (polh) and the Simian Virus 40 terminator (SV40). The second multiple cloning site is regulated by the p10 promoter and the Herpes Simplex Virus thymidine kinase terminator (HSVtk). In between the multiple cloning sites lies the Multiplication Module (MM) which provides the possibility to insert additional coding sequences (see Figure 14). **(A)** The pFBDM vector contains two transposon sites (Tn7R, Tn7L) which are used to transfer the coding sequence and the gentamycin resistance into the bacmid DNA (Figure 13, (1)). **(B)** pUCDM is entirely incorporated into the bacmid DNA via its loxP site using the Cre/Lox System (Figure 13, (2)). (X^R: antibiotic resitance gene; Ap^R: ampicillin, Gm^R: gentamycin, Cm^R: chloramphenicol).

4.1.16 Modification of multiple cloning sites

The given multiple cloning sites MCS1 and MCS2 did not suit for further cloning procedures and were replaced by new ones. For this, single stranded DNA oligomers were synthesized and assembled as described above (Methods 4.1.6, page 48). The resulting multiple cloning sites MCS1* and MCS2* were sequentially introduced into the pFBDM vector.

Five micrograms of pFBDM vector DNA was hydrolyzed using 10 units of *Bam*HI and *Hin*dIII (Fermentas) at 37°C for 1 h. DNA fragments were separated by agarose gel

electrophoresis and purified using the DNA extraction kit from Macherey-Nagel. The previously prepared double-stranded modified MCS1 was then introduced into 100 ng of pFBDM vector. Likewise, restriction enzymes *Acc*65I and *Sma*I (Fermentas) were applied to exchange the MCS2 with a modified one. The resulting pFBDM4 vector was verified by DNA sequencing.

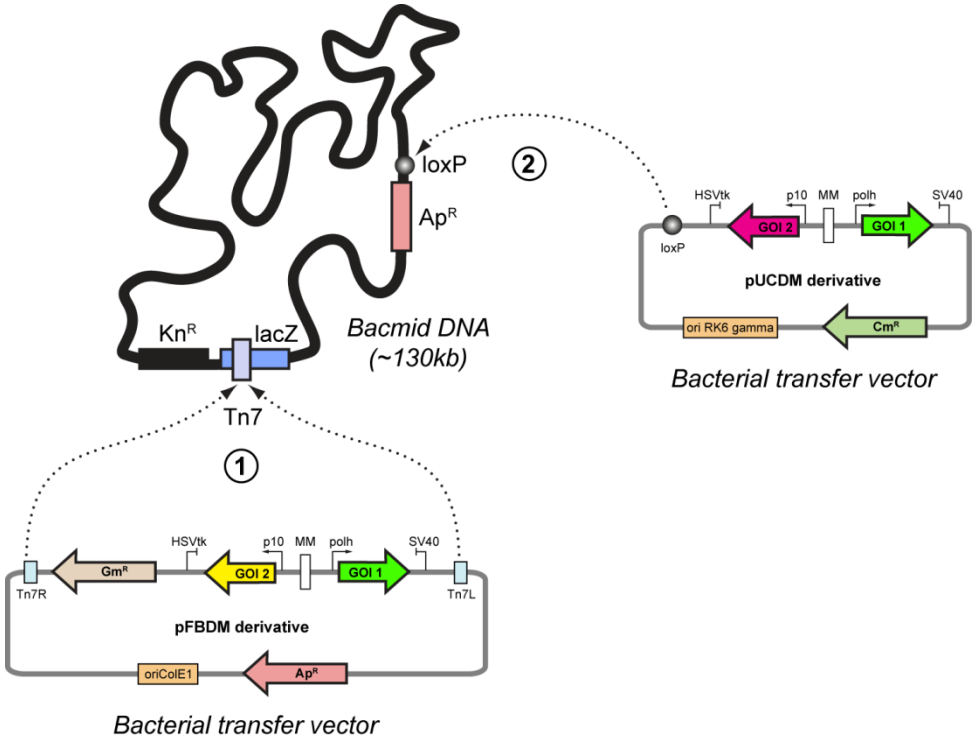

Figure 13 – Construction of recombinant bacmid DNA.

The coding sequence of the bacterial transfer vectors are either introduced into the bacmid DNA by transposition from the pFBDM derivative (1) or by the Cre/Lox system from the pUCDM derivative (2). Successful uptake of recombinant DNA is then verified by blue/white screening (in case of 1) or chloramphenicol selection (in case of 2) as well as PCR analysis. (Kn: kanamycin, lacZ: β-D-galactosidase gene, GOI: gene of interest). Adapted from Berger et al. (2004) with permission from Nature publishing group.

4.1.17 Introduction of EGFP as a transfection marker

In order to follow the transfection of insect cells, EGFP was introduced into the transfer vector as a transfection marker. Insect cells that are infected with an EGFP encoding baculovirus will show a strong green fluorescence under a UV microscope. The EGFP gene sequence was amplified by PCR from the pEGFP-C1 vector (Clonetech) using the primer sets EGFP_NdeI_fwd and EGFP_StuI_rev as well as EGFP_NcoI_fwd and EGFP_NotI_rev (Materials 3.4, page 28). Amplified gene sequences and the pFBDM4 vector were

hydrolyzed using the restriction enzymes *Nde*I and *Stu*I (Fermentas) as well as *Nco*I and *Not*I (Fermentas) and ligated to yield pFBDM4 constructs containing EGFP either in MCS1 or MCS2.

4.1.18 Introduction of protein affinity tags

To simplify late protein expression, DNA sequences coding for N-terminal protein affinity tags with accompanying protease recognition sites were introduced into the individual multiple cloning sites. DNA oligomers coding for a His_6-tag with a TEV cleavage site were synthesized and assembled as described above (for oligomer sequences see Materials 3.4, page 28). The resulting DNA was introduced into MCS1 by *Bss*HII and *Eco*RI (Fermentas) and into MCS2 by *Nco*I (Fermentas) hydrolysis.

GST-TEV and His_6-GST-TEV-tag-coding sequences were inserted into pFBDM4 by PCR amplification of the appropriate tag sequences from the pETM-30 vector (EMBL) and restriction hydrolysis using *Bss*HII and *Eco*RI (Fermentas) for MCS1 as well as *Pag*I and *Nco*I (Fermentas) for MCS2. Finally, EGFP sequences were introduced into the empty multiple cloning sites of these four vectors by subcloning from the EGFP_pFBMD4 derivatives that have been described before. Resulting constructs were verified by analytic restriction hydrolysis and DNA sequencing.

4.1.19 Construction of multi-cassette transfer vectors

The major advantage of the MultiBac system is the possibility to iteratively introduce cloning cassettes enabling the expression of protein complexes. These cloning cassettes comprise both multiple cloning sites with the appropriate promoter and terminator sequences and can be excised from the transfer vector by the restriction enzymes *Pme*I and *Avr*II (Fermentas). A different transfer vector can then be linearized in the multiplication module in between the two multiple cloning sites using the enzymes *Nru*I and *Spe*I (Fermentas).

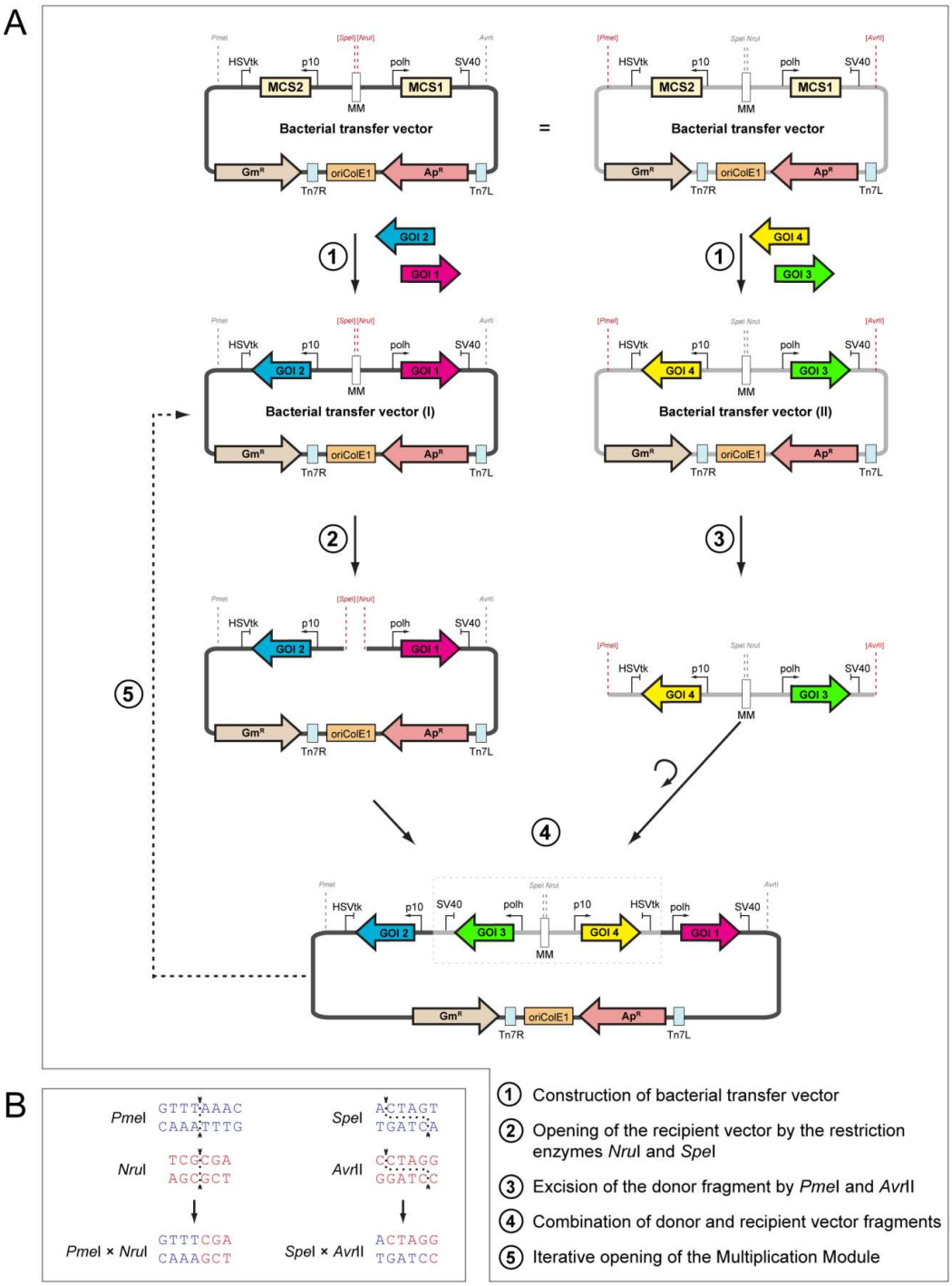

Figure 14 – Construction of multi-cassette transfer vectors.

(A) Schematic of multi-cassette cloning. Initially, one to four genes of interest (GOI) are introduced into bacterial transfer vectors (1). In the given example a pFBDM-derived vector is used. The vector containing GOI 1 and GOI 2 is then linearized by the restriction endonucleases *Spe*I and *Nru*I in the Multiplication Module (MM) forming the recipient vector (2), whereas the other vector containing GOI 3 and GOI 4 is hydrolyzed by the restriction enzymes *Pme*I and *Avr*II. By this, a donor fragment comprising only the coding and regulatory region is excised (3). Since *Avr*II and *Spe*I as well as *Pme*I and *Nru*I are isocaudamers or blunt cutters, respectively, the fragment obtained in (3) can be introduced into the linearized vectors from (2) forming a new vector containing all four genes of interest (4). Due to the inactivation of the restriction sites used for ligation the resulting vector can iteratively serve as a recipient vector for other coding sequences (5). **(B)** Once the donor fragment is ligated into the recipient vector the respective restriction sites are lost.

Since *Pme*I and *Nru*I are blunt cutters and *Avr*II and *Spe*I are isocaudamers, ligation of the cloning cassette into the multiplication module will result in the destruction of these restriction sites and in a pFBDM4 derivative containing four multiple cloning sites. Consequently, these steps can be repeated iteratively. As a matter of fact, the corresponding gene sequences have to be inserted into the transfer vector before multi-cassette vectors can be prepared. Also, it is essential that the restriction enzymes are unique cutters with respect to the donor or recipient vector.

DNA sequences were introduced into the pFBDM4 transfer vectors as described above. Whereas the donor vector was hydrolyzed using the enzymes *Pme*I and *Avr*II, the recipient vector was linearized using *Nru*I and *Spe*I. Depending on the size of the resulting DNA fragments the insert:vector ratio for ligation was either 10:1 (for large inserts, 100 ng vector) or 1:1 (for identical size of both DNA sequences, 500 ng vector).

4.1.20 Preparation of chemically competent *E. coli* DH10MultiBac cells

Chemically competent *E. coli* DH10MultiBac cells were prepared containing the unmodified bacmid DNA with an ampicillin and a kanamycin resistance gene as well as a helper plasmid encoding the transposase and a tetracycline resistance gene. The *v-cath* gene coding for the viral protease V-CATH and *chiA* encoding a chitinase are inactivated on the given bacmid DNA (Berger *et al.*, 2004). Competent cells were generated as *E. coli* DH5α cells only that the culture medium contained 50 µg/ml kanamycin and 10 µg/ml tetracycline (see Methods 4.1.1, page 47).

4.1.21 Transformation of *E. coli* DH10MultiBac cells

Eighty microliters of chemically competent *E. coli* DH10MultiBac were thawed on ice, incubated with 5 µg of recombinant transfer vector for 15 min, transferred to 42°C for exactly 90 s, placed on ice for 2 min, supplemented with 500 µl LB medium and incubated at 37°C shaking at 1,000 rpm for at least 8 h or overnight.

4.1.22 Blue/white screening of *E. coli* DH10MultiBac cells

Chemically competent *E. coli* DH10MultiBac cells were transformed with a pFBDM-derived transfer vector as described above, transferred onto agar plates containing 50 µg/ml kanamycin, 7 µg/ml gentamycin, 100 µg/ml ampicillin, 10 µg/ml tetracycline, 0.179 mg/ml (= 0.75 mM) IPTG as well as 32 µg/ml X-Gal and were incubated for 24–48 h at 37°C. Successful integration of the recombinant DNA disrupts the *lacZ* gene on the bacmid DNA and results in white colonies. If the transposition reaction is ineffective, the IPTG-induced *lacZ* gene will be transcribed to produce β-galactosidase which in turn will be able to cleave X-Gal to yield galactose and 5-bromo-4-chloro-3-hydroxyindole. Oxidation of the latter results in 5,5'-dibromo-4,4'-dichloro-indigo, an insoluble blue product.

4.1.23 Isolation of recombinant bacmid DNA

Bacterial colonies containing recombinant bacmid DNA showed a white color and were used to inoculate 15 ml of LB medium supplemented with 50 µg/ml kanamycin, 7 µg/ml gentamycin, 100 µg/ml ampicillin and 10 µg/ml tetracycline. Cultures were incubated at 150 rpm in 500 ml shaker flasks at 37°C overnight. Following centrifugation at 4,500 *×g* at RT for 5 min, the bacterial cell pellets were resuspended in 500 µl resuspension buffer S1 (50 mM Tris/HCl (pH 8.0), 10 mM EDTA, 100 µg/ml RNase A). Cell lysis was caused by addition of 500 µl of buffer S2 (200 mM NaOH, 1% (w/v) SDS) and 5 min incubation at RT. Dropwise supplementation of 500 µl ice-cold buffer S3 (2.8 M potassium acetate, pH 5.1) and 10 min incubation on ice caused the neutralization of the solution and the precipitation of potassium dodecyl sulfate in combination with cellular debris. The bacmid DNA-containing fraction was separated from this by centrifugation for 10 min at 20,000 *×g* and RT. Equal amounts of the supernatant and isopropanol (RT) were combined, incubated on ice for 10 min and centrifuged for 30 min at 13,000 *×g* and 4°C. Finally, the bacmid DNA was washed with 800 µl 70% (v/v) ethanol (p.a.), dried in a SpeedVac Concentrator (Savant, no heat) and rehydrated in 150–300 µl 10 mM Tris/HCl (pH 7.4) overnight. Thus prepared bacmid DNA could be used for PCR verification as well as insect cell transfection.

4.1.24 Verification of recombinant bacmid DNA and baculovirus titer using PCR

One method to identify whether a bacterial colony contains recombinant bacmid DNA is blue/white screening to analyze the disruption of the *lacZ* gene. To verify the correct insertion of a specific DNA fragment a PCR colony screen can be performed using one primer binding to the inserted DNA sequence (gene specific primer) and one interacting with the bacmid DNA (M13 primer).

A general approach to detect recombinant bacmid DNA as well as recombinant baculoviruses in cell culture supernatants is the use of primers specifically covering the MCS1 and MCS2 of the inserted transfer vector DNA. One hundred nanograms of bacmid DNA or 1 µl of baculovirus titer were added to either the primers MB_NruI and MB_AvrII (to analyze MCS1) or MB_SpeI and MB_PmeI (to analyze MCS2) and processed in a PCR colony screen. Consequently, one can specifically identify whether a single transfer vector or an assembled multi-cassette module has been taken up by the bacmid as well as the size of the inserted DNA. The primers used are vector-specific but not gene-specific; therefore, one can only compare the sizes of integrated DNA fragments. Gene specific primers could be used to distinguish between wild-type and mutant forms of baculovirus titers.

4.2 Eukaryotic cell culture methods

4.2.1 Propagation of insect cells

Insect cells (*Sf*9 and *Sf*21: *Spodoptera frugiperda* as well as *Tn*5: *Trichoplusia ni*) were seeded at 0.5×10^6 cells/ml in the appropriate culture media (see Materials 3.12.5, page 36) and incubated in suspension culture at 27°C using either shaker flasks without baffles at 100 rpm or stirrer bottles at 120 rpm. The cell density and viability was measured using a hemocytometer (Fuchs-Rosenthal) and applying trypan blue staining. Thirty microliters of an insect cell culture were mixed with 270 µl of 0.4% (w/v) trypan blue in 1× PBS and immediately applied to a hemocytometer. Whereas viable cells have intact membranes and exclude the dye, dead cells readily take up the blue dye through their leaky membranes and thus appear blue under the microscope. This method actually proves the membrane integrity but is commonly used to identify viable cells.

Once the cell density exceeded 3×10^6 cells/ml (*Sf*9 and *Sf*21) or 1.5×10^6 cells/ml (*Tn*5), cells were diluted to 0.5×10^6 cells/ml. Cell cultures with a viability below 60% were discarded and with a viability of at least 95% were used for recombinant protein expression and virus titer generation. After 20 propagations (approximately 3 months), the insect cells were replaced by fresh ones.

4.2.2 Freezing and thawing of insect cells

In order to prepare a backup of uninfected insect cells, exponentially growing cells were centrifuged, resuspended in 10% (v/v) DMSO, 45% (v/v) culture supernatant and 45% (v/v) fresh culture medium, aliquoted as samples of 2.5×10^7 cells in 1 ml and transferred to cryo vials (Nalgene). To provide a slow cooling process, Cryo Freezing Containers (Nalgene) containing isopropanol were used to cool the insect cells down 1°C/min for 90 min in a -80°C freezer. Then, the cells were transferred to the vaporous phase of a liquid nitrogen storage container.

For starting a new culture from frozen insect cells a vial (2.5×10^7 cells) was thawed rapidly in a 37°C water bath, cells were washed with 10 ml of culture medium to remove any remaining DMSO and finally seeded into 50 ml of fresh medium at a concentration of 0.5×10^6 cells/ml.

4.2.3 Transfection of insect cells with recombinant bacmid DNA

To transfect *Sf*9 or *Sf*21 insect cells, 12 µg of recombinant bacmid DNA and 36 µl of Cellfectin II solution (Invitrogen) were incubated with 1.2 ml of EX-CELL® TiterHigh™ medium (Sigma-Aldrich) for 30 min at RT. Meanwhile, 3×10^6 insect cells were seeded into a 75 cm^2 tissue culture flasks (Falcon). The culture medium was exchanged by 3 ml of medium and the transfection solution before the cells were incubated at 27°C for 3–5 hours. Eventually, the transfection solution was replaced by 10 ml of fresh EX-CELL® TiterHigh™ medium und incubated for 9–10 days at 27°C. *Tn*5 cells can be transfected as *Sf*9 and *Sf*21 cells, however, do not produce infectious virus particles.

4.2.4 Amplification of baculoviruses

After the transfection of the insect cells with recombinant bacmid DNA, the cells generate infectious viral particles which are delivered to the culture medium by budding. These baculoviruses are then able to infect further insect cells that again produce more viruses. The initial transfection generates the P1 viral stock within 9–10 days, whereas the following virus amplification rounds (*i.e.* P2 and P3) last 72–79 hours. Propagation for more than three generations might cause an accumulation of mutations in the recombinant virus that has an advantage over the non-mutated form.
For the generation of the P2 baculovirus titer, the entire supernatant of the P1 titer was transferred to a 200 ml uninfected suspension culture of *Sf*21 insect cells (2.0×10^6 cells/ml; viability > 95%) and incubated for 72–79 h at 27°C. In order to produce the P3 baculovirus titer, 2.5 ml of P2 baculovirus titer were added to 500 ml *Sf*21 insect cells (2.0×10^6 cells/ml; viability > 95%) and incubated likewise. Both P2 and P3 baculovirus titers were analyzed for the number of infectious particles per milliliter.

4.2.5 Determination of the number of infectious viral particles by end-point dilution

Previous to protein expression, the number of infectious virus particles in the cell culture supernatant (baculovirus titer) has to be determined. Since all recombinant baculoviruses in this study carry a gene for the enhanced green fluorescent protein (EGFP), successful transfection can be monitored by fluorescence microscopy.
The end-point dilution was performed as described by O'Reilly (1993) with some modifications. Ten-fold serial dilutions (10^{-1} to 10^{-8}) of the baculovirus titer were prepared and uninfected insect cells were diluted to a concentration of 0.5×10^6 cells/ml. Then, 10 µl of the virus dilution and 60 µl of the uninfected cells were mixed and seeded into a 96 well plate. In total, 12 replicates of each virus dilution were added. The 96 well plates were either wrapped in plastic foil or placed in a humidified environment to prevent evaporation during the incubation at 27°C for 9–10 d. After the incubation, each well was checked for infection, whereas wells containing at least one cell expressing EGFP were scored as positive. The number of infectious particles per volume was determined by the method of Reed and Muench (1938) assuming that infected cultures would have been

infected at any higher and all uninfected cultures not have been infected at any lower virus concentration. From this, the actual virus titer concentration was calculated (see Excel spreadsheet in Appendix 12.8, page 223).

4.2.6 Disinfection of baculovirus-infected insect cell cultures

Insect cells infected by recombinant baculoviruses produce infectious viral particles that are exported out of the cells into the culture medium. To inactivate these baculoviruses the culture supernatant was either autoclaved twice or incubated with 1% (w/v) Virkon® S (final concentration) for 16 h at RT. Contaminated surfaces were sprayed with a 1% (w/v) Virkon® S solution.

4.3 Protein biochemistry

4.3.1 SDS-polyacrylamide gel electrophoresis (SDS-PAGE)

Proteins were separated by size using the denaturing discontinuous SDS-polyacrylamide gel electrophoresis (SDS-PAGE). The polyanion SDS binds stoichiometrically to the protein causing its denaturation and a constant mass to charge ratio. When applying an electrical charge, proteins are thus solely separated by their molecular weight. Generally, SDS-polyacrylamide gels (SDS-PAAGs) were run using the tris/glycine system (Laemmli, 1970) at 75 mA for 90 min.

Table 1 – Composition of SDS-PAGE separation gel (8% and 10% acrylamide).

High-TEMED gel	8%			10%			
Separating gel	**1 gel**	**2 gels**	**4 gels**	**1 gel**	**2 gels**	**4 gels**	
Rotiphorese Gel 30 Acrylamide/Bisacrylamide (37.5:1)	5.0000	10.0000	20.0000	6.2500	12.5000	25.0000	**ml**
1.0 M Tris-HCl, pH 8.8	7.0313	14.0625	28.1250	7.0313	14.063	28.1250	**ml**
ddH_2O	6.4375	12.8750	25.7500	5.1875	10.375	20.7500	**ml**
20% (w/v) SDS	0.09375	0.1875	0.3750	0.0938	0.1875	0.3750	**ml**
10% (w/v) APS	0.09375	0.1875	0.3750	0.0938	0.1875	0.3750	**ml**
TEMED	0.09375	0.1875	0.3750	0.0938	0.1875	0.3750	**ml**
Total	18.75	37.5	75	18.75	37.5	75	**ml**

Table 2 – Composition of SDS-PAGE separation gel (12% and 13% acrylamide).

High-TEMED gel	12%			13%			
Separating gel	**1 gel**	**2 gels**	**4 gels**	**1 gel**	**2 gels**	**4 gels**	
Rotiphorese Gel 30 Acrylamide/Bisacrylamide (37.5:1)	7.5000	15.0000	30.0000	8.1250	16.2500	32.5000	**ml**
1.0 M Tris-HCl, pH 8.8	7.0313	14.0625	28.1250	7.0313	14.0625	28.1250	**ml**
ddH_2O	3.9375	7.8750	15.7500	3.3125	6.6250	13.2500	**ml**
20% (w/v) SDS	0.09375	0.1875	0.3750	0.09375	0.1875	0.3750	**ml**
10% (w/v) APS	0.09375	0.1875	0.3750	0.09375	0.1875	0.3750	**ml**
TEMED	0.09375	0.1875	0.3750	0.09375	0.1875	0.3750	**ml**
Total	18.75	37.5	75	18.75	37.5	75	**ml**

Table 3 – Composition of SDS-PAGE stacking gel.

	5%			
Stacking gel	**1 gel**	**2 gels**	**4 gels**	
Rotiphorese Gel 30 Acrylamide/Bisacrylamide (37.5:1)	1.5000	3.0000	6.0000	**ml**
0.5 M Tris-HCl, pH 6.8	2.2500	4.5000	9.0000	**ml**
ddH_2O	5.1375	10.275	20.5500	**ml**
20% (w/v) SDS	0.0450	0.0900	0.1800	**ml**
10% (w/v) APS	0.0450	0.0900	0.1800	**ml**
TEMED	0.0225	0.0450	0.0900	**ml**
Total	9	18	36	**ml**

4.3.2 Coomassie staining and de-staining of SDS-polyacrylamide gels

Coomassie Brilliant Blue (CBB) is a triphenylmethane dye that interacts with basic side chains of amino acids and thus unspecifically stains proteins. Of the two known forms, R-250 and G-250, the R-form is commonly used to stain SDS-polyacrylamide gels.

After the separation of the proteins in SDS-PAGE, the gels were incubated with 100 ml Coomassie staining solution for 1 h at RT (see Materials 3.12.8, page 37). Then, the staining solution was replaced by either de-staining solution I (containing methanol) or de-staining solution II (lacking methanol). The de-staining solution was sequentially exchanged by a fresh one until the gel was de-stained.

4.3.3 Regeneration of Coomassie de-staining solution

Used Coomassie de-staining solution II was mixed with activated charcoal and given through a folding filter. The Coomassie Brilliant Blue in the solution binds to the charcoal and is thus removed.

4.3.4 Silver staining of SDS-polyacrylamide gels

Silver staining is a sensitive method for detecting proteins as little as 50–100 pg and is based on the interaction of silver ions with target molecules (see Materials 3.12.9, page 37). During the developing step, these ions are reduced to metallic silver (Merril *et al.*, 1981).

Unstained or de-stained polyacrylamide gels were fixed for 1 h in fixation solution, washed three times for 15 min in 50% (v/v) ethanol and incubated with 0.2 g/l sodium thiosulfate for 60 s. After washing the gel 3× with ddH_2O, it was soaked in silver staining solution for 20 min. Following two more washing steps with ddH_2O, protein bands were visualized by incubation in developing solution. Once the signal was strong enough, 25% (v/v) acetic acid was added. Finally, the gel was briefly washed in ddH_2O and scanned immediately.

4.3.5 Silver de-staining of SDS-polyacrylamide gels

Silver staining is the method of choice to detect small amounts of proteins. However, inadvertent effects such as background staining, negative staining or over-development of protein bands often occur. These problems can be alleviated by the addition of two reducing agents (potassium ferricyanide (III) and sodium thiosulfate) to the stained gel in order to remove background noise or to de-stain the entire gel (Gharahdaghi *et al.*, 1999; Junge and Hübner, 1989; Meywald *et al.*, 1996). First, potassium ferricyanide (III) oxidizes metallic silver which in turn is reduced to silver ferricyanide (II). Second, this complex reacts with sodium thiosulfate to form a water-soluble complex. The amount of added ferricyanide, therefore, gives rise to the de-staining intensity. Staining and de-staining of the protein gels can be repeated for several times.

According to the de-staining needs either the solution for background de-staining or total de-staining of the gel was added followed by incubation at RT for 5–10 min (see Materials 3.12.9, page 37). Finally, the gel was washed 5× with ddH_2O to remove the yellow background staining. An alternative to speed up the total de-staining procedure is to apply the potassium ferricyanide (III) and sodium thiosulfate solutions sequentially.

4.3.6 Dissolution of SDS-PAGE gel slices

SDS-PAGE gels were stained with Coomassie staining solution and the background was de-stained with 20% (v/v) acetic acid. Then, protein bands were excised from the gel using a scalpel, transferred to a liquid scintillation counting tube containing 3 ml of 30% (v/v) hydrogenperoxide and 30% (v/v) ammoniumhydroxide in a ratio of 99:1. Samples were incubated with a lose lid at 70°C for 16 h in a Heraeus oven (L'Annunziata, 2003). Ten milliliters of Rotiszint solution (Roth) were added and the tritium signal was recorded in a Wallac 1410 liquid scintillation counter.

4.3.7 Protein expression in insect cells

Protein expression in the insect cell system offers the advantage of posttranslational modifications comparable to the mammalian system such as glycosylation (Kakker *et al.*, 1999), phosphorylation (Hericourt *et al.*, 2000) or disulfide bond formation (Hodder *et al.*, 1996; Smith *et al.*, 1985) which is not possible in the bacterial system. Additionally, expression under the polyhedrin promoter results in expression levels of up to 30% of total cellular protein (BacPAK™ Baculovirus Expression System User Manual 2009, Clonetech).

For reproducible protein expression, the number of infectious virus particles has to be determined by end-point dilution (see above – Methods 4.2.5, page 61). The number of baculovirus particles per insect cell (Multiplicity Of Infection = MOI) serves as a major criterion for protein expression.

Uninfected and exponentially growing *Sf*21 insect cells were pelleted at 600 ×*g* for 5 min at RT, resuspended in fresh EX-CELL® TiterHigh™ medium (Sigma) and diluted to a final concentration of 1.0–4.0 × 10^6 cells/ml. Expression cultures were prepared in 2,000 ml shaker flasks without baffles containing culture volumes of 100–300 ml. Recombinant baculovirus was added to obtain a multiplicity of infection (MOI) of 3.0–5.0. Depending on the number of proteins to be expressed, the recombinant baculoviruses carried either a single or several foreign genes apart from the EGFP gene sequence. Therefore, co-expression of two proteins could be achieved by using either a single bacmid with two coding sequences or two bacmids carrying one each. The insect cells were incubated

depending on the type of recombinant protein to be expressed for 60–79 h at 27°C at 100 rpm and were finally harvested by centrifugation at 4°C and 600 ×*g* for 30 min.

4.3.8 Purification of proteins expressed in insect cell

4.3.8.1 Purification of His_6-tagged proteins and protein complexes

Insect cell pellets were resuspended in 20 mM Hepes-NaOH(pH 7.5/pH 8.5), 1 M NaCl, 10% (v/v) glycerol and 5 mM β-mercaptoethanol, 20 mM imidazole (pH 7.5/pH 8.5), 1 mM PMSF, 20 mg/l aprotitin, 20 mg/l leupeptin/pepstatin and 0.2 mM AEBSF (100 ml per liter expression culture). The resuspension buffer either had a pH-value of 7.5 (PRMT5/WD45 and Gemin5) or 8.5 (Gemin3/Gemin4). To disrupt the cells, they were sonicated in 5 cycles of 30 s pulse and 30 s cooling on ice using a Sonifier 250 (Branson; output: 8, duty-cycle: 50). Finally, the cell lysate was cleared by ultracentrifugation using a 45Ti rotor (Beckman) at 25,000 rpm (49,000 ×*g*) at 4°C for 1 h.

The cell lysate was subsequently incubated with 2 ml of Ni-NTA agarose beads per liter culture for 90 min by head-over-tail rotation. After the beads were washed with 50 CVs (column volumes) of washing buffer (identical to the resuspension buffer but lacking protease inhibitors), bound proteins were eluted by the addition of elution buffer (= washing buffer with 250 mM imidazole, pH 7.5/pH 8.5).

Eluted proteins were then dialyzed against 20 mM Hepes-NaOH (pH 7.5/pH 8.5), 90 mM NaCl, 10% (v/v) glycerol and 5 mM β-mercaptoethanol (low-salt buffer) and applied to an anion exchange chromatography column (HiTrap Q, 1 ml, GE Healthcare). Bound proteins were released by gradually increasing the NaCl concentration to 1 M.

Finally, the elution fractions containing the corresponding proteins were pooled, concentrated using a VivaSpin protein concentrator and further submitted to gel filtration chromatography (Superose6 10/300GL; GE Healthcare).

4.3.8.2 Regeneration of Ni-NTA agarose beads

Used Ni-NTA beads were washed with ddH_2O. Then, 10 CV of 0.5 M EDTA, pH 8.0 (a chelating agent removing the Ni^{2+} ions), 10 CV of 8.75 M urea (eluting precipitated proteins) and 20–30 CV of ddH_2O (washing) were added sequentially. To regenerate the

nickel ions on the agarose-NTA beads, the beads were incubated with 2–3 CV of 0.2 M $NiCl_2$ hexahydrate for 20–30 min or overnight at RT. Finally, unbound nickel chloride was removed by washing with 20–30 CV of ddH_2O and the beads were stored in 20% (v/v) ethanol (p.a.) until further use.

4.3.8.3 Purification of GST-tagged proteins and protein complexes

Insect cells containing recombinant proteins carrying a GST-tag were resuspended in 50 mM sodium-phosphate, pH 7.5, 500 mM NaCl, 10% (v/v) glycerol, 5 mM β-mercaptoethanol, 1 mM PMSF, 20 mg/l aprotitin, 20 mg/l leupeptin/pepstatin and 0.2 mM AEBSF (100 ml per liter expression culture). In analogy to the Ni-NTA purification, the cells were lyzed by sonication and centrifuged before the supernatant was incubated with 2 ml of glutathione sepharose® 4B (GE Healthcare). The sepharose beads were washed with 50 CVs of the resuspension buffer. Finally, proteins were eluted using the same buffer containing 20 mM glutathione. The elution fractions were pooled, supplemented with TEV protease (33 µl of 2mg/ml TEV protease per 1 ml elution fraction) and dialyzed against the resuspension buffer lacking protease inhibitors for 2 days at 4°C. TEV-cleavage separates the N-terminal affinity tag as well as the protease recognition site leaving an extra glycine residue on the remaining protein sequence (Kapust *et al.*, 2002; Phan *et al.*, 2002) (for specific overview of the proteolytic cleavage site see Appendix 12.5.2, page 219). Finally, the sample was concentrated and applied to gel filtration chromatography (Superose6 10/300GL; GE Healthcare).

4.3.8.4 Regeneration of glutathione sepharose (GSH) beads

Used GSH beads were washed with 20 CV of ddH_2O. Then, the beads were incubated at RT for 30 min in 10 CVs of GSH bead regeneration solution (0.08% (w/v) SDS, 20 mM DTT and 8.225 M urea). After washing with 20–30 CVs of ddH_2O, the beads were stored in 20% (v/v) ethanol (p.a.).

4.3.9 Expression and purification of SMNΔGemin3–5 and SMN(E134K)ΔGemin3–5 in bacterial cells

E. coli BL21*(DE3) (pLysS) pRARE cells were sequentially transformed with GST(TEV)SMN,Gemin8,Gemin2_pET28b or a variant containing the E134K mutant of SMN and His_6(Thrombin)Gemin6,Gemin7_pET21a. Cultures were grown in SMNΔGemin3–5 complex expression medium (see Materials 3.12.3, page 34) at 37°C until an absorbance (A_{600}) of 0.25 was reached. Then, the temperature was reduced to 15°C and protein expression was induced with 0.5 mM IPTG at an absorbance (A_{600}) of 0.4. After twenty hours, cells were pelleted, resuspended in SMNΔGemin3–5 complex resuspension buffer (see Materials 3.12.11, page 39) and disrupted by sonication. Following separation by ultracentrifugation, the supernatant was incubated with glutathione sepharose beads and washed with washing buffer I and II. Finally, pentameric SMN complex was eluted from the sepharose matrix by proteolytic cleavage using the tobacco etch virus (TEV) protease.

4.3.10 Sizing of protein complexes

Protein standards of known molecular weight (Dextran blue: 2000 kDa, Thyroglobulin: 669 kDa, Ferritin: 440 kDa, BSA: 67 kDa, Ovalbumin: 43 kDa and RNase A: 13.7 kDa) were applied to gel filtration chromatography (Superdex200 10/300GL, Superose6 10/300GL – GE Healthcare). The molecular weight of each protein was plotted against the elution volume (see Appendix 12.6, page 221). Purified protein complexes were submitted to gel filtration chromatography and their elution volumes were compared to the previously run standard samples.

4.3.11 *In vitro* protein complex reconstitution

To reconstitute protein complexes *in vitro*, equimolar amounts of proteins were resuspended in 20 mM Hepes-NaOH(pH 7.5), 1 M NaCl, 10% (v/v) glycerol and 5 mM β-mercaptoethanol or 5 mM DTT and dialyzed against the same buffer containing 200 mM NaCl. Finally, the protein complexes were purified by gel filtration chromatography (Superose6 10/300GL or Superdex200 10/300GL; GE Healthcare). The correct formation of protein complexes was verified by SDS-PAGE.

4.3.12 Replacement of protein complex components

Once a protein complex is formed *in vitro*, individual subunits can be replaced by the addition of proteins that have a higher affinity towards the initial complex.

Protein complexes were reconstituted *in vitro* and purified by gel filtration chromatography. Elution fractions were pooled, concentrated and supplemented with the competing proteins. After an overnight dialysis, the newly formed complex was again purified by gel filtration chromatography and analyzed by SDS-PAGE.

4.3.13 Preparation of HeLa S3 total cell extract

HeLa S3 cells (Puck *et al.*, 1956) were grown in Dulbecco's Modified Eagle Medium (DMEM) supplemented with 50 µg/ml penicillin and 50 µg/ml streptomycin and 2 mM L-glutamine at 37°C with 5% CO_2. After centrifugation of the cells at 600 ×*g* at 4°C for 5 min, they were resuspended in 3 ml of 1× PBS, pH 7.4, per gram of cells and incubated on ice for 10 min. The suspension was transferred to a glass homogenizer (Pyrex) and disrupted with 30–50 strokes of the pestle. Finally, the supernatant was separated from the cellular debris by ultracentrifugation at 40,000 ×*g* for 45 min at 4°C. For methylation reactions, the extract was diluted 1:200 in the methylation reaction buffer.

4.3.14 TCA precipitation

Trichloroacetic acid (TCA) causes the precipitation of proteins in solution and is based on hydrophobic aggregation (Sivaraman *et al.*, 1997; Xu *et al.*, 2003). As a result, one can increase the protein concentration of a solution by resuspending the precipitated sample in a smaller volume of buffer. Additionally, it is possible to separate proteins from non-used radioactive co-factors that are not precipitated by TCA, such as [^{3}H]-SAM in a methylation reaction. To aid in the precipitation of small amounts of proteins BSA is added to the reaction as a carrier molecule.

For TCA precipitation, 1 volume of 10 µM BSA and 3 volumes of 25% (v/v) TCA were added sequentially to the sample, incubated at 4°C overnight, centrifuged at 4°C for 30 min at 13,000 ×*g* and washed once with ice-cold acetone. Dried protein samples were directly applied to protein hydrolysis.

4.3.15 Autoradiography

Following gel electrophoresis, either dried SDS gels or wet native RNA gels were exposed to Amersham Hyperfilm™ MP (GE Healthcare) or CEA RP NEW medical X-ray screens (AGFA Healthcare) at -80°C for the appropriate amount of time (1 min – several weeks). Methylation reactions were commonly exposed for 5, 9 and 16 h.

4.3.16 Phosphorimaging

Dried SDS-gels containing cross-linked proteins or dried thin layer chromatography plates were exposed to Storage Phosphor Screens (MD: Molecular Dynamics) in Exposure Cassettes (MD) for 30 min to several days. Phosphor screens were analyzed by a PhosphorImager (MD) using the computer program ImageQuant (MD) and erased using the Eraser (MD) for 8 min.

4.3.17 Total hydrolysis of proteins

Proteins are very stable molecules and can only be destroyed at high temperatures and acidic conditions. Posttranslational modifications of proteins mainly occur on the side chains of amino acids. In order to analyze these, proteins have to be separated into individual amino acids by acidic hydrolysis.

Dried protein samples were resuspended in 100 µl 6 M HCl and boiled at 110°C for 20 h in a Heraeus oven using a micro reaction vial (VWR, Pierce). The vial was shortly centrifuged at RT and the sample transferred to a microcentrifuge tube for drying in a SpeedVac Concentrator (Savant). After the sample was dried completely, the pellet was resuspended in 50 µl ddH_2O. This sample could then be either used directly in scintillation counting or was applied to thin layer chromatography.

4.3.18 Thin layer chromatography of individual amino acids

Thin layer chromatography can be used to separate non-modified as well as posttranslationally modified amino acids from each other.

Thee microliters of the hydrolyzed protein sample were mixed with 1 µl of total arginine standard mix (0.1 mM of each L-arginine, MMA, aDMA and sDMA) or MMA-sDMA

standard mix (0.1 mM of MMA and sDMA) and loaded onto a Cellulose DEAE/HR-Mix-20 TLC plate (Macherey-Nagel). Subsequently, the plate with the dried sample spots was placed for 8–10 h into a TLC chamber with 75% (v/v) ethanol and 25% (v/v) ammonium hydroxide as a running buffer. The plate was removed from the chamber, dried under a ventilation hood and sprayed with 0.5% (w/v) ninhydrin solution. Consequently, amino acids were visualized by the formation of Ruhemann's purple. Stained TLC plates could be further analyzed by either autoradiography or scraping of the individual amino acids for liquid scintillation counting.

When radioactively labeled co-factor was used to induce mono- or dimethylation of arginine residues, the separated amino acids on the TLC plate contained a radioactive label. Therefore, the amount of radioactivity in the form of MMA or sDMA can be directly measured.

Stained and dry TLC plates were marked with a pencil indicating the individual lanes as well as small fragments covering the entire migration distance. A sharpened lab spatula (width: 1 cm) was used to scrape off the TLC plate surface and transfer it into a liquid scintillation counting tube. This was then supplemented with 5 ml of scintillation solution (Roth) and measured in the ^{3}H-spectrum of a Wallac 1410 liquid scintillation counter. From this, the relative abundance of MMA and sDMA could be determined.

4.3.19 *In vitro* methylation of protein substrates

Methylation of arginine side chains is catalyzed by protein arginine methyltransferases (PRMTs) *in vivo*. In this work, insect cell expressed and purified recombinant PRMT5/WD45 as well as total HeLa S3 cell extract was used to methylate Sm proteins B, D1 and D3 *in vitro*.

The amounts of enzyme, substrate and co-factor varied according to the type of experiment performed. In general, to check methylation activity of the enzyme, 1 pmol PRMT5/WD45, 20 pmol Sm protein substrates and 219 pmol [^{3}H]-SAM/SAM were combined in 100 mM Hepes-NaOH, pH 8.2, at 37°C for 60 min. Samples were further processed either in gel filtration (non-radioactive), SDS-PAGE or TCA precipitation. For SDS-PAGE analysis, reactions were stopped by the addition of 6× SDS-PAGE loading buffer

and boiling at 95°C. Gels were dried and finally applied to autoradiography and densitometry.

4.3.19.1 Methylation of protein substrates increasing the incubation time

The reaction velocity in enzyme catalysis is defined by the formation of product per time. In order to do any kinetic analyses, the time point of the methylation reaction should lie in the initial linear range of product formation.

Constant amounts of enzyme (0.5 pmol) or total HeLa S3 extract resulting in approximately the same methylation rate, Sm protein substrates (40 pmol) and [^{3}H]-SAM/SAM co-factor (438 pmol) were incubated at 37°C for 0–90 min. Reactions were split and either processed by SDS-PAGE and autoradiography or TCA precipitation, total hydrolysis and thin layer chromatography.

4.3.19.2 Methylation of protein substrates increasing the enzyme concentration

Increasing amounts of PRMT5/WD45 (0–1 pmol) were used to methylate 20 pmol protein substrate with 219 pmol [^{3}H]-SAM/SAM co-factor at 37°C for 60 min. Reactions were submitted to SDS-PAGE, autoradiography and densitometry.

4.3.19.3 Methylation of protein substrates increasing the co-factor concentration

The arginine methylation reaction is a bi-substrate reaction, whereas the first substrate is the methyl group donor, S-adenosylmethionine (SAM), and the second one the protein to be methylated. Thus, both substrates follow saturation kinetics as long as the other substrate is available in an exceeding amount.

Fixed amounts of protein substrate (20 pmol) and enzyme (1 pmol) were incubated with increasing amounts of [^{3}H]-SAM/SAM co-factor (0–584 pmol) at 37°C for 60 min. After SDS-PAGE and autoradiography the samples were analyzed by densitometry.

4.3.19.4 Methylation of protein substrates increasing the substrate concentration

Increasing amounts of protein substrates (0–200 pmol) were incubated with 2 pmol of PRMT5/WD45 and 438 pmol [^{3}H]-SAM/SAM co-factor at 37°C for 60 min. Reactions were split equally and processed by either SDS-PAGE, autoradiography and densitometry or TCA precipitation, total hydrolysis and thin layer chromatography. Finally, the

densitometry results were used for enzyme kinetic analyses to obtain K_m, V_{max} and k_{cat} values.

4.3.19.5 Methylation of competing protein substrates

Methyltransferases often have several different methylation substrates. This can be used to evaluate relative binding affinities of these substrates with respect to each other. In an initial experiment, 5 pmol of each Sm protein substrates were methylated with 219 pmol of co-factor at 37°C for 60 min using 1 pmol of PRMT5/WD45. Additionally, 5 pmol of Sm protein substrate were supplemented with equal amounts of each of the other substrates or all substrates together and methylated likewise.

In a second experiment, constant amounts of Sm protein substrates (5 pmol) were methylated as described before with increasing amounts of competing Sm protein substrates (0–100 pmol, 0–20-fold excess). Samples were analyzed by SDS-PAGE, autoradiography and densitometry.

4.3.19.6 Analysis of processive and distributive methylation mechanisms

One differentiates between distributive and processive enzymes. Whereas the former release the modified substrate after each catalytic event, the latter stay attached to the substrate for several rounds of catalysis (such as DNA polymerases). Five picomoles Sm protein substrates were incubated with 1 pmol PRMT5/WD45 and 219 pmol [^{3}H]-SAM/SAM at 37°C for 0–90 min. In a second experiment, an identical reaction setup was supplemented with 100 pmol of competing Sm protein substrates to completely inhibit the methylation of the initial Sm protein substrate. Finally, in a third experiment, the initial reaction setup was run for 15 min before a 20-fold excess (100 pmol) of competitor was added. The reactions were analyzed by SDS-PAGE autoradiography and densitometry.

4.3.20 ATPase assay

Protein samples with a putative ATPase activity were dialyzed against the ATPase reaction buffer (50 mM Na-phosphate (pH 7.5), 50 mM NaCl, 3 mM $MgCl_2$, 2.5 mM DTT) overnight. Then, 5 µCi α-^{32P}-ATP (Perkin Elmer) and RNA homooligopolymers (A, C, G and U - Sigma Aldrich) at a final concentration of 1 mg/ml were added to 50 µl of protein solution.

Whereas half of the reaction was immediately stopped by the addition of 25 µl 0.5 M EDTA (pH 8.0), the other half was incubated for 15 to 60 min at 37°C before stopping the reaction. Of the solution, 1 µl of each time point was applied to a PEI Cellulose F thin layer chromatography plate (20×20 cm, Merck) to separate ATP, ADP, AMP and inorganic phosphate. The plate was dried, run in 0.75 M KH_2PO_4 for 50 min, dried once more under a fume hood at RT and exposed to ^{32}P-storage screens (Molecular Dynamics) for 1–2 h. Finally, the screens were analyzed using a Molecular Dynamics 400E PhosphorImager.

4.3.21 UV-crosslinking of radioactively labeled ATP to protein molecules

Proteins for UV-crosslinking were treated as in the ATPase assay. After the addition of the radioactively labeled ATP, the sample was incubated for 10 min at 30°C and placed into a CL-1000 Crosslinker (UVP) for 5 min. Samples were processed in SDS-PAGE, followed by Coomassie staining, gel drying and autoradiography.

4.4 RNA biochemical methods

4.4.1 Preparation of DEPC ddH_2O

100 µl of DEPC (diethylpyrocarbonate) were added to 100 ml of de-ionized water and stirred overnight under a fume hood at RT. DEPC causes unspecific alkylation of proteins and thus inactivates any RNases present in the solution that could interfere in experiments with RNA. Autoclaving results in the elimination of the remaining DEPC.

4.4.2 Phenol-Chloroform extraction

Phenol-chloroform extraction is a liquid-liquid extraction technique for isolating DNA, RNA and protein. Samples containing a mixture of DNA, RNA and protein were combined with one volume of phenol (Roth, RNA grade) and vortexed for 30 s. One volume of chloroform/isoamyl alcohol (24:1) was added, vortexed and centrifuged at 13,000 ×*g* at RT for 10 min resulting in two phases. Whereas the upper (aqueous) phase contains the DNA and RNA, the lower (organic) phase includes the protein. The upper phase was treated once more with one volume of chloroform/isoamyl alcohol (24:1). After

centrifugation, the supernatant was transferred to 3 volumes of 100% (v/v) ethanol. Nucleic acids were precipitated at RT for 5 min and centrifuged at 13,000 ×*g* for 25 min. Finally, RNA and DNA samples were washed with 1 volume 70% (v/v) ethanol and resuspended in 0.1 volume TE buffer (10 mM Tris-HCl (pH 7.5), 1 mM EDTA).

4.4.3 Preparative *in vitro* transcription of U snRNAs

For the *in vitro* transcription of the *Xenopus laevis* U1 wild-type, U1ΔD and U1ΔE snRNA, pUC9 vectors containing the coding sequences were linearized with *Bam*HI and purified by phenol-chloroform extraction. The transcription reaction setup using the Promega transcription kit was as follows:

10 µl 5× transcription buffer (Promega)
5 µl DTT (100 mM)
10 µl Cap- analogue (m^7GpppG, Promega)
2.5 µl GTP (5 mM)
2.5 µl ATP (5 mM)
2.5 µl CTP (5 mM)
1.5 µl UTP (1 mM)
1 µl [α-^{32}P]-UTP, 10 µCi/µl (Perkin Elmer)
5 µl Linearized template (0.5 µg/µl)
3 µl T7 polymerase
2 µl RNAsin (40 U/µl) (Promega)
5 µl DEPC H_2O

The transcription was carried out at 37°C for 3 h with an intermittant addition of 3 µl of T7 RNA polymerase after 90 min of incubation. Finally, RNA loading buffer for denaturing gels was added, the sample boiled at 95°C for 2 min, and the RNAs were separated by denaturing RNA electrophoresis on a 5% polyacrylamide gel (see Materials 3.12.18, page 43).

4.4.4 Purification of radioactively labeled RNAs from denaturing polyacrylamide gels

Following gel electrophoresis, the upper glass plate was removed and the denaturing RNA gel was wrapped in saran wrap. After exposure to a Biomax MR X-ray film for 1–3 min, the developed film was used as a template to excise the RNA band from the gel with a scalpel. The RNA was eluted from the gel slice by incubation with 400 µl RNA elution buffer (AES buffer) on a head-over-tail rotor overnight at 4°C. Then, the supernatant was sequentially combined with 100 µl 3 M ammonium acetate (pH 5.2) and 1 ml of 100% (v/v) ethanol. RNA was precipitated by centrifugation at 13,000 *×g* for 30 min at 4°C. Finally, the RNA pellet was washed with 1 ml 70% (v/v) ethanol, dried in a SpeedVac and resuspended in 20 µl DEPC ddH_2O.

4.4.5 Electrophoretic mobility shift assay (EMSA)

The electrophoretic mobility shift assay, or band shift assay, is a technique to analyze protein-DNA and protein-RNA interactions. Proteins and DNA or RNA are incubated with each other and separated by non-denaturing gel electrophoresis. Successful interaction of protein and DNA or RNA manifests itself in the upward shift of the according gel band.
Proteins were incubated with radioactively-labeled *Xenopus laevis* U1 wild-type and mutant snRNAs in the respective protein buffer at 30°C for 1 h. Subsequently, the samples were separated by native RNA-gel electrophoresis (see Materials 3.12.19, page 44).

4.4.6 *In vitro* assembly small nuclear ribonucleoprotein particles (snRNPs)

In vivo, the Sm proteins B/'B, D1, D2, D3, E, F and G form a heptameric ring around the Sm site of snRNA. The assembly of this so-called Sm core could be recapitulated *in vitro* by incubating radioactively labeled U1 snRNA with recombinantly expressed Sm protein. The formation of this RNA-protein complex was analyzed in the absence or presence of recombinant SMN complex using an electron mobility shift assay. Reactions were incubated for 30 min at 37°C and separated in native gel electrophoresis (see Materials 3.12.19, page 44).

4.5 Statistic analysis and enzyme kinetics

4.5.1 ImageJ analysis of autoradiographic signals

Band intensities of methylated proteins were analyzed by the program ImageJ (NIH). MS films (GE Healthcare) were scanned in document mode using a SilverFast32 scanner (EPSON) without applying any image correction setting. In ImageJ, a rectangular shape of a defined size was used to select individual autoradiography signals as well as a background signal. Each shape was processed by the Histogram function to count the number of pixels corresponding to a specific gray color and multiplied with a correlation factor of (black = 1; white = 0) to obtain gray values. Finally, the difference of all gray values of a radioactive signal and the background intensity resulted in the grayscale value of this signal. See Results 5.5.5, page 117, for the application of the ImageJ analysis.

4.5.2 Correlation of grayscale value of autoradiography signals and number of transferred methyl groups

The major goal in any arginine methylation reaction is to identify the number of methyl groups that are transferred in a certain amount of time to an arginine residue on a protein substrate. Experimentally, methylated proteins were separated by SDS-PAGE and visualized by autoradiography. Therefore, the grayscale value of a certain protein band on the film had to be correlated to the actual number of transferred methyl groups.

Forty picomoles of protein substrate (pICln/D1/D2) were methylated using 438 pmol [^{3}H]-SAM/SAM as co-factor with increasing enzyme concentrations (0.5–3 pmol recombinant PRMT5/WD45) for 60 min at 37°C. Then, the samples were equally split and applied to SDS-PAGE. The first gel was fixed with 30% (v/v) methanol and 10% (v/v) acetic acid for 30 min at RT, the radioactive signal was amplified using amplifying reagent (GE Healthcare), the gel was dried for 2 h at 80°C and exposed to MS films (GE Healthcare) for 5, 9 or 15 h at -80°C. Films were developed, scanned and densitometrically analyzed using the program ImageJ (NIH) (see previous section). The second gel was Coomassie-stained, individual protein bands were excised, dissolved (Methods 4.3.6, page 65) and analyzed by liquid scintillation counting. Consequently, the result of the densitometric analysis (grayscale values over enzyme concentration) was correlated to the outcome of the liquid

scintillation counting of the dissolved protein bands (counts per minute over enzyme concentration). To obtain a direct relation between the [^{3}H]-SAM/SAM concentration and the number of dissociations per minute, increasing amounts of co-factor (0–17.5 pmol) were mixed with 3 ml of 30% (v/v) hydrogenperoxide and 30% (v/v) ammoniumhydroxide in a ratio of 99:1 - to achieve identical conditions as in the dissolved protein bands - and 10 ml of liquid scintillation counting solution. This resulted in the linear relation of counts per minute over picomoles of co-factor [^{3}H]-SAM/SAM. Three graphs were sequentially correlated to each other: (1) the graph obtained from SDS-PAGE and autoradiography, (2) the one stemming from the liquid scintillation counting of dissolved protein bands and (3) the one resulting from the direct liquid scintillation counting of co-factor. Consequently, a direct correlation of the grayscale value depending on the exposure time and the number of transferred picomoles of methyl groups could be obtained. This analysis was independent of the substrate concentration. For a graphical depiction of the correlation experiments see Figure 35 and Figure 36 (pages 115 and 116).

4.5.3 Kinetic analysis of methylation reactions

In order to obtain K_m, V_{max} and k_{cat} values and the methylation efficiency of various protein substrates, substrate concentrations and corresponding methylation rates were analyzed by the models of Michaelis-Menten $\left(V_0 = \frac{V_{max} \cdot [S]}{K_m + [S]}; y = V_0; x = [S]\right)$, Lineweaver-Burk $\left(\frac{1}{V_0} = \frac{K_m}{V_{max}} \cdot \frac{1}{[S]} + \frac{1}{V_{max}}; y = \frac{1}{V_0}; x = \frac{1}{[S]}\right)$, Hanes-Woolf $\left(V_0 = \frac{1}{V_{max}} \cdot [S] + \frac{K_m}{V_{max}}; y = V_0; x = [S]\right)$ and Eadie-Hofstee $\left(V_0 = -K_m \cdot \frac{V_0}{[S]} + V_{max}; y = V_0; x = \frac{V_0}{[S]}\right)$. Nonlinear fitting curves where calculated for the Michaelis-Menten model (Results 5.5.10, page 128), whereas linear graphs described the remaining models (for more information see Appendix 12.10.1, page 226).

4.6 Immunobiochemical methods

4.6.1 Affinity purification of 7B10 (anti-SMN) monoclonal antibody

GST-SMN(1–160) was bacterially expressed from the SMN(1–160)_pGEX-5X-1 plasmid. Cells were lyzed and the supernatant was separated from cellular debris, before it was

incubated with 1 ml of glutathione sepharose matrix (Qiagen) to achieve specific interaction of GST and GSH-sepharose (Smith and Johnson, 1988). First, the matrix was incubated with GSH washing buffer (20 mM Hepes (pH 7.5), 500 mM NaCl, 5 mM DTT), then washed with and resuspended in 10 ml of 0.2 M disodium tetraborate, pH 9.0. Finally, solid dimethyl pimelimidate (DMP; Sigma-Aldrich), a homobifunctional crosslinker of amine-reactive imidoester groups (Schneider *et al.*, 1982), was added at a final concentration of 10 mM. The reaction was incubated at RT for 30 min on a head-over-tail rotor and centrifuged at 2,500 *×g* for 2 min at RT (Eppendorf 5804R) in order to separate the supernatant from the matrix. The matrix was then washed with 0.2 M ethanolamine, pH 8.0, and incubated at RT for 2 h using the same buffer to saturate any remaining reactive groups. Eventually, the matrix was equilibrated in 1× PBS.

The matrix was incubated with 10 ml of 7B10 hybridoma culture supernatant at 4°C overnight and washed three times with 10 ml 1× PBS. Antibodies were eluted by rapidly decreasing the pH value by the addition of 100 mM glycine-HCl, pH 2.7. The eluate was supplemented with 1/10 of the elution volume of 1 M Tris, pH 8.8, to neutralize the antibody solution. Elution fractions were analyzed by SDS-PAGE and antibody containing fractions were dialyzed against a 50-fold volume of 1× PBS at 4°C overnight.

4.6.2 Immunoprecipitation of reconstituted protein complexes

Immunoprecipitation is a technique to precipitate a protein antigen out of a solution using an antibody that specifically binds to a particular protein.

7B10 (anti-SMN) antibody was coupled to protein G sepharose beads at a concentration of 2 mg/ml using DMP as described in the previous section. Protein complexes were reconstituted and dialyzed in a Slide-A-Lyzer® dialysis cap overnight against 20 mM Hepes-NaOH (pH 7.5), 200 mM NaCl, 5 mM DTT and for 3 h against the same buffer lacking DTT (IP binding buffer). After centrifugation at 13,000 *×g* for 30 min at 4°C, the supernatant was transferred to 40 µl 7B10-coupled protein G sepharose beads and incubated at 600 rpm at 4°C for 90 min. The beads were washed three times with IP wash buffer I (20 mM Hepes-NaOH (pH 7.5), 300 mM NaCl, 0.01% NP40) and twice with IP wash buffer II (20 mM Hepes-NaOH (pH 7.5), 300 mM NaCl lacking NP40).

4.6.3 Western blotting

The Western blot (WB), also referred to as immunoblot (IB), is an analytic method to detect specific proteins. Cell extracts or purified proteins are separated in SDS-PAGE and transferred onto a nitrocellulose or PVDF membrane. This membrane is sequentially incubated with a primary antibody directed against the specific protein and a secondary antibody coupled to horseradish peroxidase (HRP) that interacts with the primary antibody. Protein bands are finally detected by chemiluminescence.

After protein separation, the protein transfer reaction was set up as follows from bottom to top in a semi-dry blotting chamber: three layers of Whatman paper soaked in 1× Towbin buffer, a PVDF membrane previously incubated with 100% (v/v) methanol, the protein gel and three more layers of soaked Whatman paper. The blotting occurred at 0.8 mA/cm^2 of gel area for 1–2 h. Successful protein transfer was verified by subsequent incubation of the membrane with amido black staining and de-staining solution.

The PVDF membrane was blocked for 20 min with 1× NET-gelatin solution (blocking solution), washed in 1× PBST (Western blot washing solution) and incubated with the primary antibody (see Table 4) for 1 h at RT or overnight at 4°C. Following a washing step (3×), the membrane was incubated with the secondary antibody (see Table 5) for 1 h at RT. After a final washing step (3×), the ECL reagents I, II and III were added to detect the chemiluminescence signal generated by the secondary antibody using X-ray films.

Table 4 – Primary antibodies.

α-His antibody (mouse)	1:1,000 anti-His_6 (QIAGEN) 1× NET-gelatin 0.1% (v/v) sodium azide
α-Gemin3 antibody (rat)	1:100 anti-Gemin3 (Friedrich Grässer) 1× NET-gelatin 0.1% (v/v) sodium azide
α-Gemin4 antibody (goat)	1:250 anti-Gemin4 (Santa Cruz Biotechnology) 1× NET-gelatin 0.1% (v/v) sodium azide
α-PRMT5 antibody (rabbit)	1:500 anti-PRMT5 (this work) 1× NET-gelatin 0.1% (v/v) sodium azide
α-pICln antibody (rabbit)	1:500 anti-pICln (this work) 1× NET-gelatin 0.1% (v/v) sodium azide

Table 5 – Secondary antibodies.

α- mouse (goat) (horseradish peroxidase-coupled)	1:5,000 anti-mouse IgG (Sigma-Aldrich) 1× PBST
α- rabbit (goat) (horseradish peroxidase-coupled)	1:3,000 anti-rabbit IgG (Sigma-Aldrich) 1× PBST
α- goat (rabbit) (horseradish peroxidase-coupled)	1:45,000 anti-goat IgG (Sigma-Aldrich) 1× PBST
α- rat (rabbit) (horseradish peroxidase-coupled)	1:5,000 anti-rat IgG (Sigma-Aldrich) 1× PBST

5 Results

5.1 MultiBac system

5.1.1 Introductory notes

The assembly of spliceosomal snRNPs occurs in the cytoplasm and is mediated by the cooperation by the PRMT5 and the SMN complex. Initially, the PRMT5 complex catalyzes the symmetrical dimethylation of Sm proteins which hence acquire a higher binding affinity towards the SMN complex. The Sm proteins were found to be associated with a factor (pICln) that prevents their interaction with the snRNA. Finally, the SMN complex removes this kinetic trap, binds the Sm proteins and thus ensures the correct assembly of snRNPs.

In order to better understand the molecular mechanisms of this process, the application of an *in vitro* system using recombinant proteins is most promising. So far, such an approach has been hampered by difficulties in obtaining biologically active or correctly folded proteins from bacterial expression. In recent years, the insect cell-based MultiBac system has been established that is specifically suited for the expression of protein complexes (Berger *et al.*, 2004). Using a combination of both bacterial expression and the application of the MultiBac system recombinant proteins were to be generated. A step-by-step protocol of the MultiBac system can be found in the Methods section of this work (Methods 4.1.16 – 4.2.6 , pages 53 – 62). Also, a schematic overview of the applied insect cell system is shown at the end of this section (Figure 22, page 94).

5.1.2 Construction of the pFBDM4 transfer vector for the MultiBac system

The MultiBac system comprises distinct steps to generate recombinant proteins. Initially, a coding gene sequence is introduced into a transfer vector which is propagated in bacterial cells. This transfer vector contains baculovirus promoters which are active in insect cells but not in the bacterial host of the transfer vector. Once a coding gene sequence has been introduced into the transfer vector it can be specifically incorporated into the viral genome via Tn7 transposition (Methods 4.1.22, page 58). Recombinant

baculoviruses can then be used to transfect uninfected insect cells that in turn express the protein of interest.

The original pFBDM transfer vector of the MultiBac system contains two multiple cloning sites (MCS). According to the cloning strategy for the complex components of the PRMT5 and SMN complex both MCSs were to be modified (Figure 15 A–B). The original MCS sequences were excised by restriction hydrolysis and replaced by synthesized and hybridized double-stranded DNA (dsDNA) fragments (Methods 4.1.16, page, 53). Successful integration of the new MCSs resulted in a transfer vector termed pFBDM4 and was verified by DNA sequencing (Figure 15 C–D). The original pFBDM transfer vector contained a *Spe*I restriction site in MCS1 (Figure 15 A). Since this enzyme is used for the iterative integration of expression cassettes into the so-called Multiplication Module of the transfer vector, pFBDM4 cannot be inadvertently hydrolyzed in MCS1 (see Methods 4.1.19, page 55 for background information).

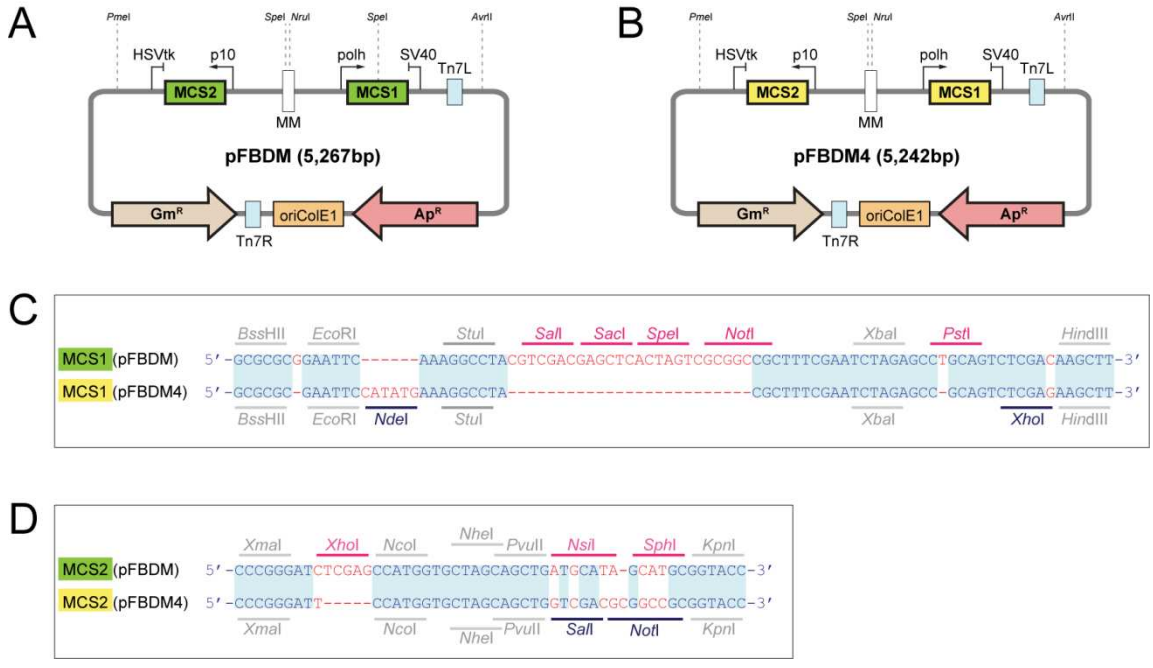

Figure 15 – Construction of the bacterial transfer vector pFBDM4.

Both multiple cloning sites (MCSs) of the original pFBDM transfer vector were excised by restriction hydrolysis and replaced by alternative ones. **(A)** Schematic of the pFBDM transfer vector (Berger *et al.*, 2004). **(B)** Schematic of the pFBDM4 transfer vector with two modified multiple cloning sites. The dashed lines indicate the recognition sites of the restriction enzymes used for iterative cloning of expression cassettes in the MultiBac system. **(C,D)** Aligned DNA sequences of initial (green) and modified (yellow) multiple cloning sites. Identical nucleotide sequences are highlighted in light blue. Newly introduced restriction sites are indicated in dark blue, deleted ones in pink and non-modified ones in gray.

5.1.3 Construction of pFBDM4 derivatives

Commonly, recombinant proteins that are expressed in insect cells and that are devoid of any localization signal accumulate in the cytoplasm. In order to easily identify infected cells that express foreign proteins, the coding sequence of enhanced green fluorescent protein (EGFP) was to be incorporated into the transfer vector. GFP, a protein initially isolated from jelly fish, absorbs light in the UV-range and has a single emission peak at 509 nm (green light). Correspondingly, successful infection can be verified using fluorescence microscopy (Results 5.2.2, page 90).

To set up an in *vitro* system for the study of snRNP biogenesis, recombinantly expressed proteins had to be specifically isolated from the insect cells. The most common method to purify proteins is the addition of so-called protein affinity tags. These are amino acid sequences that specifically bind to interaction partners covalently linked to an immobilized matrix. Proteins can thus be specifically enriched on this matrix and hence be eluted in a pure form.

Following the replacement of both multiple cloning sites, a set of modified transfer vectors was prepared. These alterations comprised the insertion of coding sequences for EGFP, sequences for protein affinity tags, and a combination thereof. For a detailed explanation see Methods 4.1.17/4.1.18, pages 54/55. EGFP-coding sequences were introduced under the control of the polyhedrin (polh) promoter (MCS1) as well as under the p10 promoter (MCS2) (Figure 16 A). The production of EGFP in insect cells had no effect on the co-expression of other recombinant proteins. Insect cell suspension cultures expressing EGFP showed a strong green color which could be observed by eye already after 48 hours post infection (hpi). Furthermore, time-consuming plaque assays to analyze the number of infectious viral particles in the supernatant could be replaced by non-invasive end-point dilution assays applying fluorescence microscopy (see Methods 4.2.5, page 61 and Results 5.2.3, page 92).

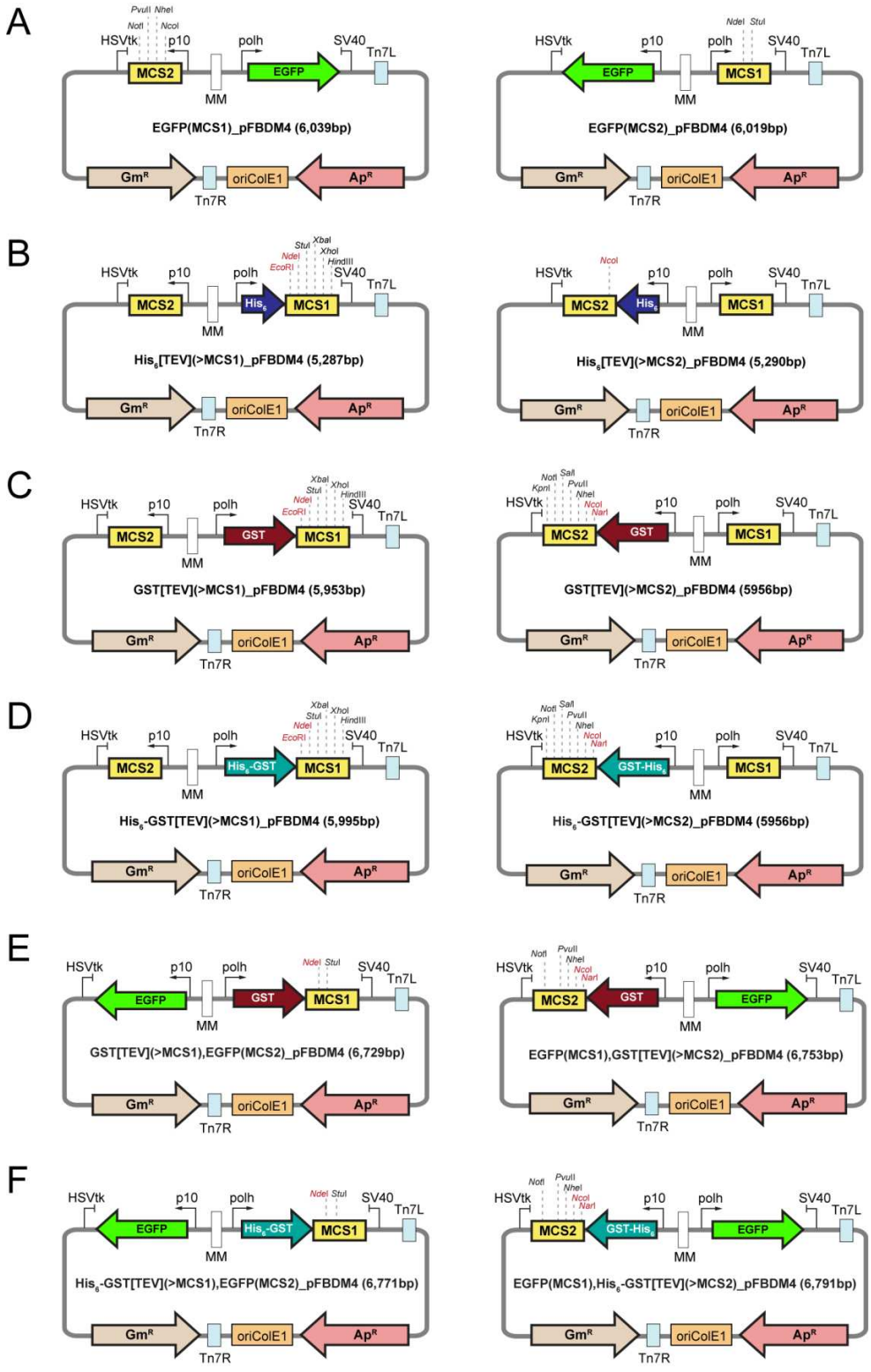

Figure 16 – Bacterial transfer vectors derived from pFBDM4.

Several bacterial transfer vectors have been prepared containing coding sequences in each multiple cloning site, respectively, for the enhanced green fluorescent protein (EGFP) serving as a transfection marker in the insect cells **(A)**, a His_6-tag for protein affinity purification **(B)**, a GST-tag **(C)**, a combined His_6-GST-tag **(D)**, as well as a combination of either the GST- or the His_6-GST-tag in one multiple cloning site and EGFP in the other **(E, F)**. Dashed lines indicate single-cutting restriction enzymes. DNA that is introduced by restriction enzymes labeled in red is in-frame with the preceding protein affinity tag.

Both multiple cloning sites were separately supplemented with DNA sequences coding for N-terminal affinity tags of His_6 (Figure 16 B), GST (Figure 16 C) and His_6GST (Figure 16 D). Finally, transfer vectors were prepared harboring the coding sequence for EGFP in one MCS as well as a sequence encoding GST (Figure 16 E) or His_6GST (Figure 16 F) in the other one. All protein affinity tags can be cleaved by the tobacco etch virus (TEV) protease leaving an N-terminal glycine residue on the recombinant protein (see Appendix 12.5.2, page 219).

5.1.4 Preparation and verification of recombinant bacmid DNA

Following the generation of recombinant transfer vectors, the expression cassettes had to be incorporated into the baculovirus genome. This transfer was carried out by Tn7 transposition. The integration of foreign DNA into the baculovirus genome disrupts the *lacZ* gene, which can be verified by blue/white screening (see Methods 4.1.22, page 58 for detailed information). In order to analyze the successful uptake of the respective DNA sequences, either bacmid-specific or transfer vector-specific primers could be applied to amplify distinct DNA fragments (Methods 4.1.24, page 59). During the preparation of recombinant baculovirus genomes using the MultiBac system, only three states of the bacmid DNA were possible: Wild-type baculoviruses, holding an intact *lacZ* gene, should register as negative (blue colonies) in blue/white screening. The resulting PCR fragment amounted to a size of about 450 bp when using M13 primers (Figure 17 A). Analysis of recombinant baculovirus DNA, on the other hand, resulted in much larger fragments stemming from the insertion of one (Figure 17 B) or two (Figure 17 C) expression cassettes. Transfer vector-specific primers could be used to explicitly analyze the inserted DNA in MCS1 and MCS2. With respect to the number of expression cassettes, two or four products were formed in the PCR. The sizes of these fragments directly depend on the inserted DNA sequences (Figure 17 D, Table 6).

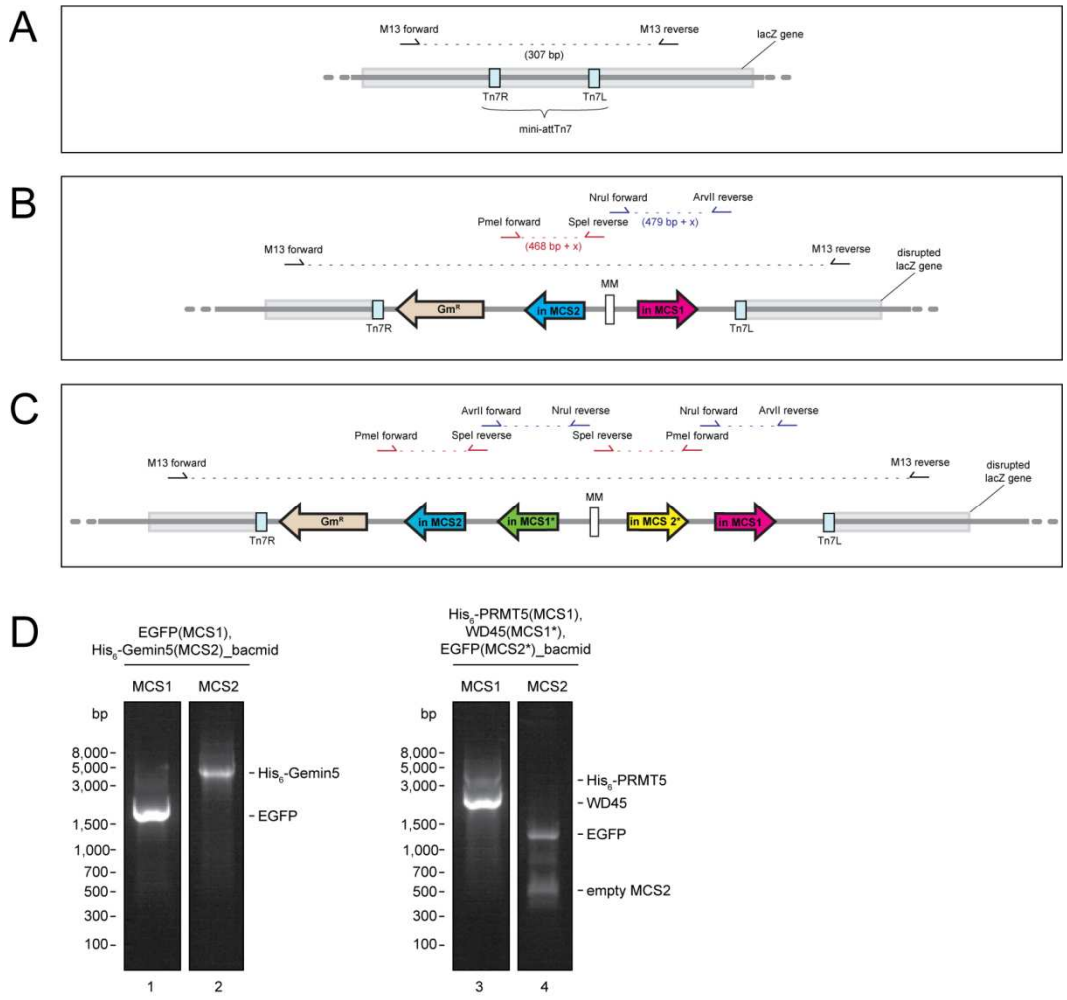

Figure 17 – Incorporation of recombinant DNA into the bacmid DNA by transposition.

The *Autographa californica* nuclear polyhedrosis virus (*Ac*MNPV) is used to introduce recombinant DNA into insect cells. The *lacZ* gene on the bacmid DNA contains a mini-attTn7 site at which DNA can be specifically incorporated by the enzyme transposase and subsequently disrupt gene expression **(A)**. In the MultiBac system this recombinant DNA stems either from a transfer vector with two multiple cloning sites **(B)** or multi-cassette variant containing at least four ones **(C)**. For a detailed protocol how to generate multiple expression cassettes see Methods 4.1.19, page 55. In each case, the gene for gentamycin resistance is taken up by the bacmid DNA. Positive incorporation can be tested by both blue/white screening, whereas white colonies indicate a disrupted *lacZ* gene, or by PCR. For this, M13 primers, which bind to the bacmid DNA, and transfer vector-specific primers can be used. **(D)** PCR verification of recombinant bacmids comprising a single expression cassette of EGFP and His_6-Gemin5 (lanes 1 and 2) and a double expression cassette harboring His_6-PRMT5, WD45 and EGFP (lanes 3 and 4) using the primer combinations MB_NruI/MB_AvrII (MCS1) and MB_PmeI/ MB_SpeI (MCS2). Schematic depictions of the modified bacmid DNA in A-C are not in scale to provide a better overview of the basic concept.

Table 6 – PCR verification of recombinant bacmid DNA

Bacmid construct	Forward primer	Reverse primer	Covered Multiple Cloning Site	Length of PCR fragment (bp)	5'-3' restriction sites of insert
Wild-type baculovirus	M13_fwd	M13_rev	-	307	-
Empty MCS1	MB_NruI	MB_AvrII	MCS1	524	-
Empty MCS2	MB_SpeI	MB_PmeI	MCS2	493	-
EGFP in MCS1	MB_NruI	MB_AvrII	MCS1	1321	*Nde*I, *Stu*I
EGFP in MCS2	MB_SpeI	MB_PmeI	MCS2	1269	*Nco*I, *Not*I
Any_insert in MCS1	MB_NruI	MB_AvrII	MCS1	479 + insert length	*Eco*RI, *Xho*I
Any_insert in MCS2	MB_SpeI	MB_PmeI	MCS2	468 + insert length	*Nco*I, *Not*I

5.2 Insect cell culture

5.2.1 Propagation of insect cell lines

In the insect cell expression system commonly cells derived from *Spodoptera frugiperda* (*Sf*9, *Sf*21) and *Trichoplusia ni* (*Tn*5) are used (Insect cell techniques are described in detail in Methods 4.2.1, page 59). These cells differ from each other by cell size, population doubling time (PDT), protein processing and the ability to generate infectious baculovirus progeny (Figure 18). In this work, only *Sf*21 insect cells were used for baculovirus amplification and recombinant protein expression. The advantages of this cell line lie in the population doubling time of 22.5 h compared to 45.6 h and 30.1 h in *Sf*9 and *Tn*5 cells (Table 7). Furthermore, only the *Sf*-derived cell lines were capable of generating infectious viral particles. Since the baculovirus system relies on this feature to produce baculoviruses for large scale protein expression, *Tn*5 cells were not used (Methods 4.3.7, page 65).

Table 7 – Insect cell properties

Cell line	μ (h^{-1})	Population doubling time (h)
*Sf*9	0.0152	45.6
*Sf*21	0.0308	22.5
*Tn*5	0.0230	30.1

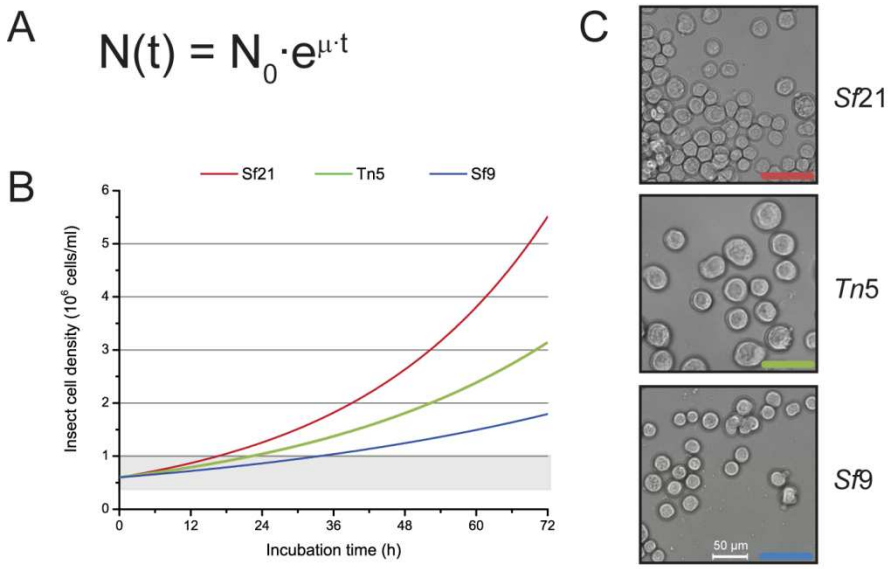

Figure 18 – Insect cell culture.

(A) Equation of exponential cell growth - N_0: initial cell concentration, N(t): cell concentration after an incubation of time t, µ: cell specific cell division factor (number of doublings per hour), t: incubation time (h). **(B)** Graph of insect cell concentrations of *Spodoptera frugiperda* 21 (*Sf*21, red), *Trichoplusia ni* (*Tn*5, green) and *Spodoptera frugiperda* 9 (*Sf*9, blue) cells after an incubation for 0–72 h with an identical initial cell density of $0.5 \cdot 10^6$ cells·ml^{-1}. The optimal cell density for seeding uninfected cells is $0.4–1.0 \cdot 10^6$ cells·ml^{-1} (indicated by the gray background). **(C)** Microscopic photographs of *Sf*21, *Tn*5 and *Sf*9 cells in the exponential growth phase. The images were obtained using a Zeiss Axiovert 200M microscope and a 10× phase contrast objective.

5.2.2 Transfection of insect cells using recombinant bacmid DNA

In order to express recombinant proteins in insect cells baculoviruses carrying the genes of interest were transfected into uninfected cells. These baculoviruses coded for at least one foreign protein and the transfection marker EGFP. Apart from the fluorescence microscopy, infection could be determined by morphological changes in the cell appearance and by the so-called plaque assay (see O'Reilly (1993) for detailed description of the respective methods). The availability of the non-invasive transfection marker EGFP provides a more rapid and reliable screening process in comparison to the other methods. *Sf*21 insect cells were infected with recombinant baculoviruses carrying sequences coding for EGFP and a foreign gene of interest. Depending on the cloning strategy these were either under the control of a polyhedrin (MCS1) or p10 (MCS2) promoter. Successful expression of EGFP was determined using fluorescence microscopy (Figure 19 A). Whether the protein of interest had also been expressed was verified by SDS polyacrylamide gel electrophoresis (SDS-PAGE) (Figure 19 B). The expression rate of

individual proteins depended on the passage number of the insect cell culture, the number of infectious baculovirus particles at the time of infection (multiplicity of infection = MOI), the time allocated for recombinant protein expression to pass (harvest time), the type of promoter used as well as the specific protein itself.

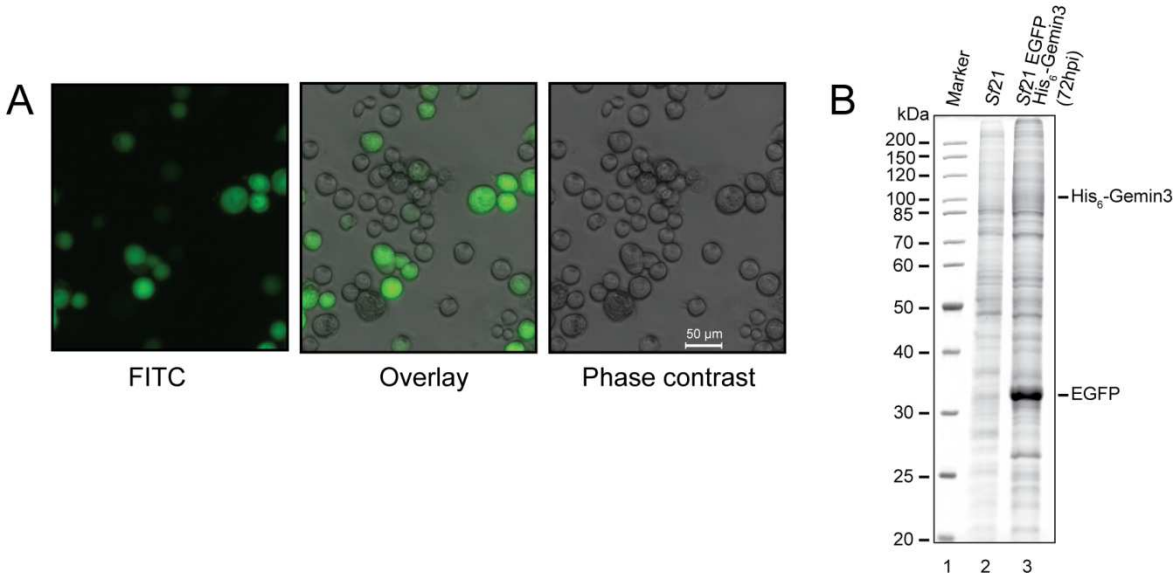

Figure 19 – Expression of recombinant proteins in insect cells.

(A) Fluorescence microscopy of baculovirus infected *Sf*21 insect cells expressing enhanced green fluorescent protein (EGFP) and His_6-Gemin3. Left panel: FITC channel, middle panel: overlay, right panel: phase contrast image. **(B)** SDS-PAGE of uninfected (lane 2) and baculovirus-infected (lane 3) *Sf*21 insect cells.

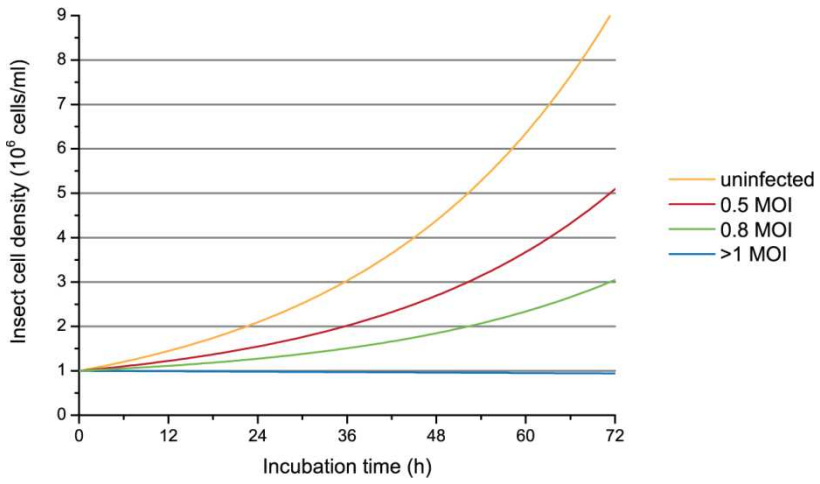

Figure 20 – Baculovirus infection inhibits insect cell division.

Once an insect cell has taken up a baculovirus particle, cell division discontinues. If the multiplicity of infection (MOI) is below 1, only a fraction of insect cells is infected (red and green line). Consequently, the percentage of infected cells decreases over time. If the number of viral particles exceeds the number of cells, *i.e.* MOI > 1, a maximal infection rate can be obtained (blue line).

Historically, insect cell infection was identified by the arrest of the insect cell cycle, the increase of the cell size as well as morphological changes within the cells. Fluorescent marker protein expression contributes to a much faster identification of infected insect cells. Once a cell has been infected by a baculovirus, cell division ceases and the major functions are related to virus replication. This is an important characteristic which is applied in the expression of recombinant proteins. A synchronous infection of cells could be achieved by adding a large excess of infectious baculovirus particles over the number of insect cells. If the ratio of baculoviruses to cells was smaller than one, uninfected cells continued to replicate (Figure 20). This effect is exploited in generating initial baculovirus titers. Insect cells are transfected at low cell densities. A fraction of the total cell number is infected and produces baculovirus progeny that in turn is capable of entering the yet uninfected cells. Consequently, this secondary infection is likely to result in the infection of the entire culture.

5.2.3 Amplification and determination of baculovirus titers

Baculoviruses infect insect cells and exploit their replication and protein expression system to generate baculovirus offspring. Once virion particles are formed, they are released to the culture supernatant by budding receiving a membrane envelop from the host cell. Consequently, recombinant proteins accumulate in the cytoplasm of infected cells while baculoviruses are exported to the surrounding culture medium. This can subsequently be used to infect a new insect cell culture and thus to generate a large titer stock volume (see Methods 4.2.4, page 61).

A second important step is to identify the exact number of infectious viral particles in the culture supernatant. Traditionally, these are referred to as plaque forming units (pfu) paying tribute to the plaque assay method that was initially used for the determination. In the advent of fluorescent marker proteins, baculovirus concentrations (baculovirus titers) are determined by end-point dilution combined with fluorescent microcopy (Figure 21; see Methods 4.2.5, page 61). Baculovirus concentrations of up to $3 \cdot 10^8$ pfu/ml were obtained following synchronous infections after an incubation time of 72–82 h (Figure 21 E).

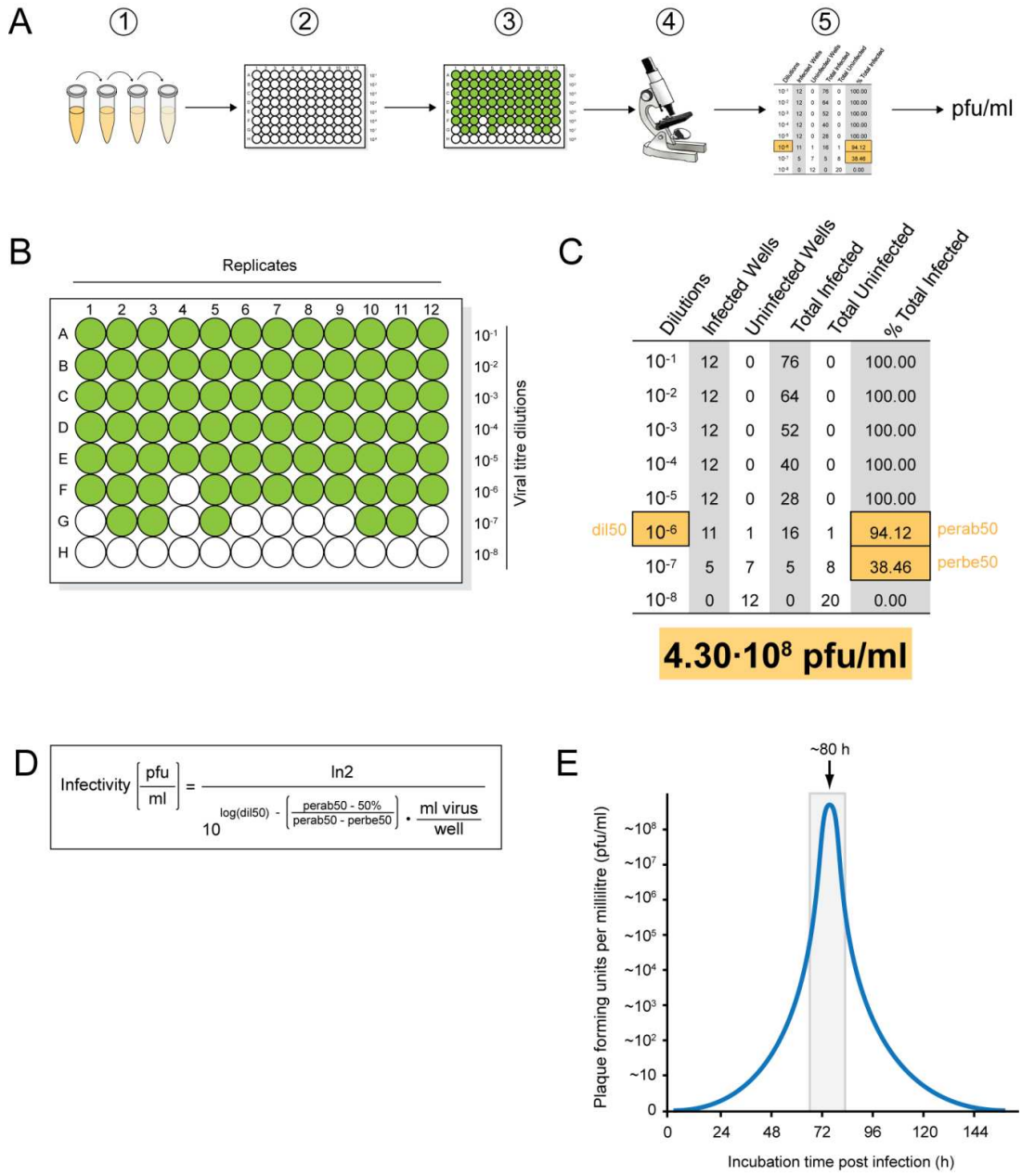

Figure 21 – Baculovirus titer screening by end-point dilution.

(A) Scheme of baculovirus titer determination: The baculovirus titer was diluted in culture medium (1), added to $5 \cdot 10^5$ *Sf*21 insect cells seeded on a 96-well microtiter plate (2) and incubated at 27°C. After 10 days of incubation, infected cells produced enhanced green fluorescent protein (3) which could be detected by fluorescence microscopy (4). Finally, the number of infected wells at the varying baculovirus titer dilutions was used to calculate the total number of infectious particles per milliliter of the initial baculovirus titer. **(B)** 96-well microtiter plate with infected wells. Each viral titer dilution was prepared in 12 replicates. **(C)** Statistical evaluation of the number of infected wells. **(D)** Equation to calculate the number of infectious particles per milliliter (infectivity). dil50: dilution at which 50% of the cells were infected; perab50/perbe50: percentage of total infected cells in the baculovirus titer dilution above/below 50% infection. Each well contained 10 µl of baculovirus titer solution. **(E)** Relationship of number of infectious particles per milliliter and incubation time of the insect cell culture producing these particles. The optimal harvesting time was about 80 hours post infection. The image of the microscope was taken with permission from http://images.all-free-download.com/ images/graphiclarge/microscope_clip_art_23280.jpg with permission.

5.2.4 Expression of recombinant proteins in insect cells

The insect cell system is very popular for the expression of recombinant proteins that are insoluble or biologically inactive following bacterial expression. Whereas recombinant proteins can be obtained in bacteria within a single day, several weeks are necessary in the insect cell system.

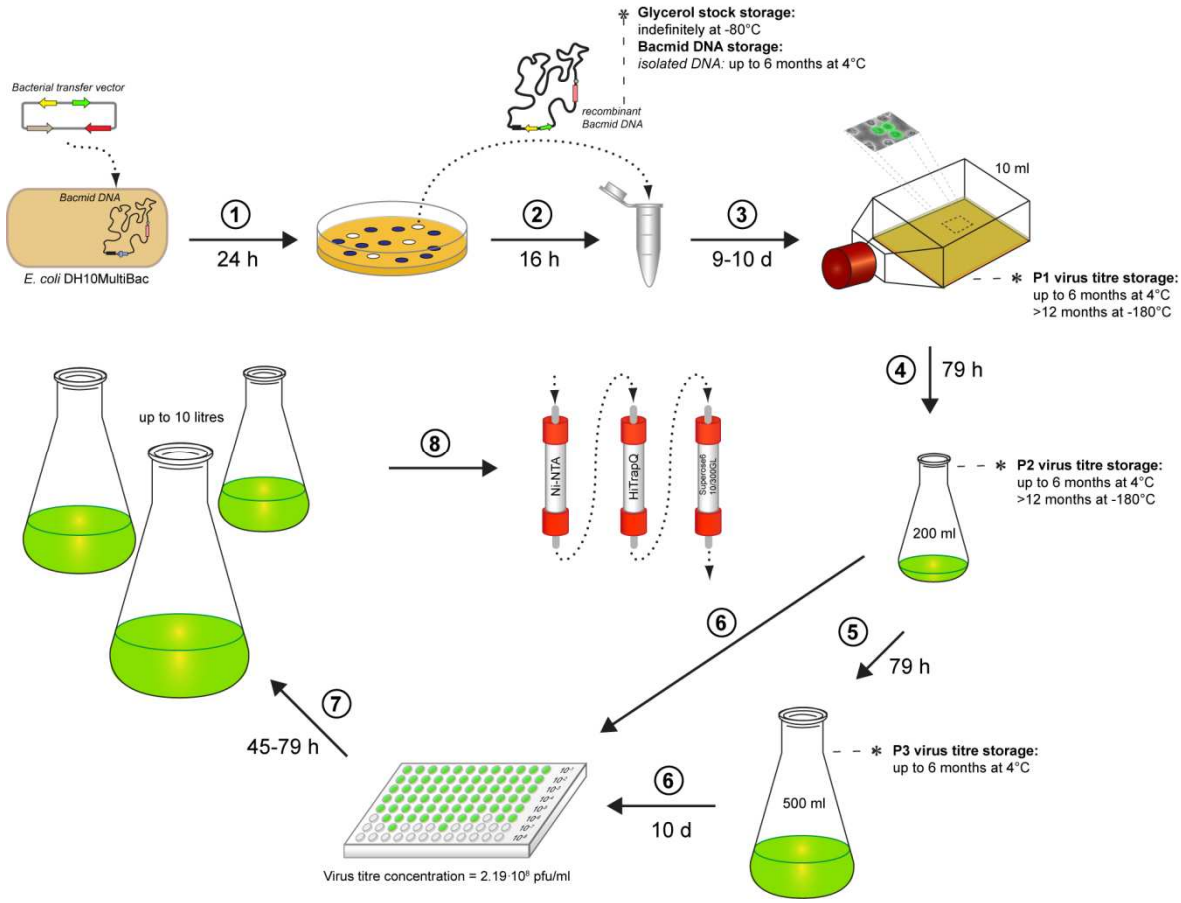

Figure 22 – Schematic of the insect cell expression system.

A recombinant transfer vector was introduced into *E. coli* DH10MultiBac cells by transformation (1). Positive constructs were analyzed by blue/white screening and PCR verification. Recombinant bacmid DNA was then isolated (2) and used to transfect *Sf*21 insect cells (3). The number of baculovirus particles was amplified from passage 1 to passage 3 (4–5) and determined by baculovirus titer screening using end-point dilution (6). After the exact number of infectious particles had been obtained, reproducible infections could be achieved for large scale protein expression (7). Finally, recombinant proteins were purified using standard purification procedures. (*) Asterisks indicate time points at which backups are recommended.

In this work, the MultiBac insect cell expression system was used applying EGFP as a transfection marker. The total amount of time between the transposition of the gene expression cassettes into the bacmid DNA and the harvest of the large scale protein

expression amounted to at least 4 weeks excluding the time necessary for the preparation of the transfer vector (Figure 22). Insect cells were generally cultured without antibiotics making the system prone to bacterial contamination. In order to sustain major contamination events, time points were identified at which preparations of reaction backups were possible. Bacmid DNA could be stored best in the bacterial host cell supplemented with glycerol at -80°C for several years. Once recombinant baculoviruses had been obtained from insect cell culture supernatants, these could be frozen in liquid nitrogen without the addition of cryopreservants such as glycerol or DMSO (Dimethyl sulfoxide).

In conclusion, the MultiBac system has been applied for the expression of protein complexes in insect cells. Transfer vector sequences were modified in accordance with the applied cloning strategy. The coding sequence for EGFP was introduced into the transfer vectors to later serve as a transfection marker. Furthermore, sequences of protein affinity tags were inserted to simplify subsequent protein purification. Following the incorporation of genes of interest into these vectors and transposition into viral DNA, the correct uptake could be verified by PCR analysis. *Sf*21 insect cells served as the host for baculovirus amplification as well as recombinant protein expression. Infection was monitored by fluorescence microscopy since all recombinant baculoviruses expressed EGFP. Furthermore, this transfection marker was exploited to identify the number of infectious baculovirus particles in cell culture supernatants. Constructs containing components of the PRMT5 and SMN complexes were generated and used for recombinant protein expression. The preparation of PRMT5/WD45 is presented in the following section, of Gemin3–5 in Results 5.6.3, page 143.

5.3 Expression and purification of PRMT5 complex components

5.3.1 Introductory notes

In the early phase of cytoplasmic snRNP assembly, the PRMT5 complex plays a major role in generating symmetrically dimethylated arginines in Sm proteins B/B', D1 and D3.

Biochemical analysis of this complex has so far been difficult as bacterial expression of single PRMT5 protein or even of the entire PRMT5 complex resulted in insoluble or biologically inactive protein. To overcome this problem, the heterodimeric PRMT5/WD45 was to be expressed in insect cells.

Following translation, Sm proteins exist as heterooligomeric complexes of D1/D2, D3/B and F/E/G. Furthermore, the adaptor protein pICln binds to most of these proteins to generate complexes of pICln/D1/D2, pICln/D3/B and pICln/D1/D2/F/E/G (6S complex). Whereas the former two were shown to be associated with PRMT5 in the cell in the 20S complex, the 6S complex forms a separate entity. Sm protein heterooligomers and pICln were thus to be expressed in bacteria since these cells lack protein arginine methyltransferases that might modify substrate proteins. Insect cell-expressed Sm proteins were shown to carry asymmetrically dimethylated arginine residues (Brahms *et al.*, 2000).

5.3.2 Insect cell co-expression of PRMT5/WD45

Recombinant baculoviruses were generated using the MultiBac system coding for His_6-tagged PRMT5 and WD45 under the control of the polyhedrin promoter and EGFP regulated by the p10 promoter. Proteins were expressed in *Sf*21 insect cells (see Methods 4.3.7, page 65) and sequentially purified by immobilized-metal affinity chromatography (IMAC, NiNTA), anion exchange chromatography (HiTrapQ) and gel filtration chromatography (Superose6) (Figure 23 A) (see Methods 4.3.8.1, page 66). According to the elution profile, PRMT5/WD45 forms a tetra- or pentameric complex (Figure 23 B). The resulting PRMT5/WD45 was further used in complex reconstitutions and methylation reactions (Results 5.4.2, page 100 and Results 5.5.2, page 110). Apart from the human PRMT5/WD45 heterodimer, the *Drosophila melanogaster* homologs Capsuleen/Dart5 (37.4% sequence identity with human PRMT5) and Valois (19.6% sequence identity with human WD45) could also be prepared using the MultiBac system (data not shown). Yet, biochemical analysis of these was not carried out.

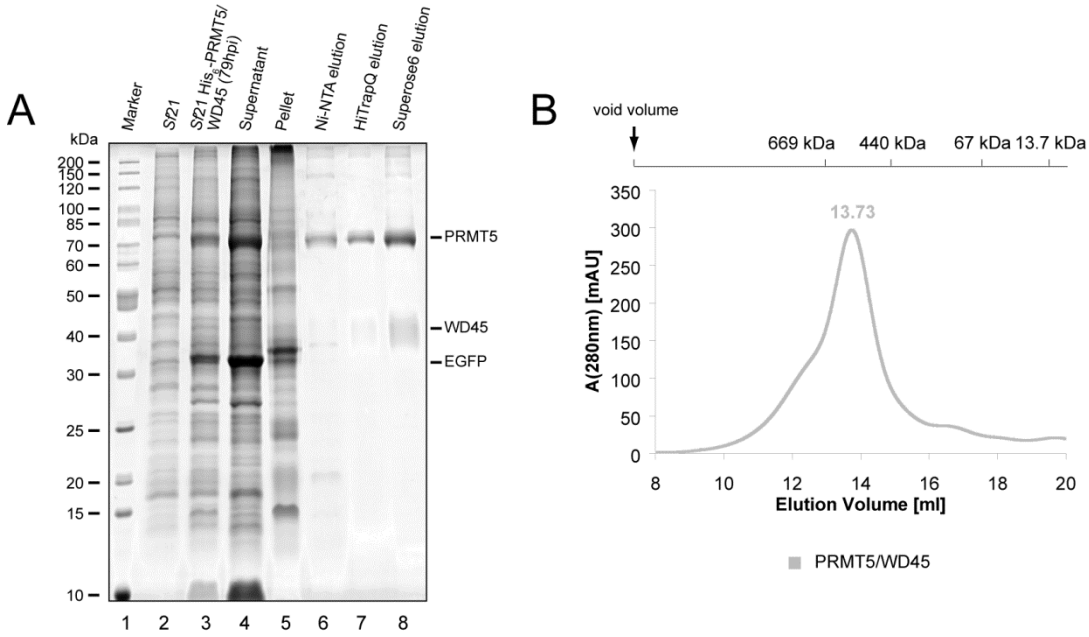

Figure 23 – Expression and purification of His_6-tagged PRMT5/WD45.

His_6-PRMT5 and WD45 were co-expressed in *Sf*21 insect cells at 3.0 MOI and 27°C for 79 h. Cells were harvested, lyzed and sequentially purified by immobilized-metal affinity (Ni-NTA), anion exchange (HiTrapQ 1 ml) and gel filtration chromatography (Superose6 10/300GL). Purified samples were used in methylation assays and PRMT5 complex reconstitutions. **(A)** SDS-PAGE of His_6-PRMT5/WD45 purification. **(B)** Gel filtration elution profile of His_6-PRMT5/WD45.

5.3.3 *In vitro* reconstitution of pICln-Sm protein complexes

Sm protein heterooligomers form complexes with pICln containing pICln/D1/D2, pICln/D3/B and pICln/D1/D2/F/E/G (6S complex). To reconstitute these complexes *in vitro*, recombinant Sm protein heterooligomers and pICln were bacterially expressed and purified as described (Chari *et al.*, 2008). Following an incubation of equimolar protein amounts (see Methods) pICln-Sm protein complexes were separated by gel filtration chromatography (Figure 24) (Superdex200 10/300GL; see Appendix 12.6, page 221 for a calibration graph using standard proteins). The protein complexes showed a Gaussian elution profile at an absorbance of 280 nm (Figure 24, right panel). Whereas the individual components of pICln/D1/D2 and the 6S eluted in the same fractions, B appeared to be underrepresented in pICln/D3/B (Figure 24, middle panel). Peak fractions were pooled and further used in PRMT5 complex reconstitutions (Results 5.4.2, page 100) and methylation reactions (Results 5.5.2, page 110).

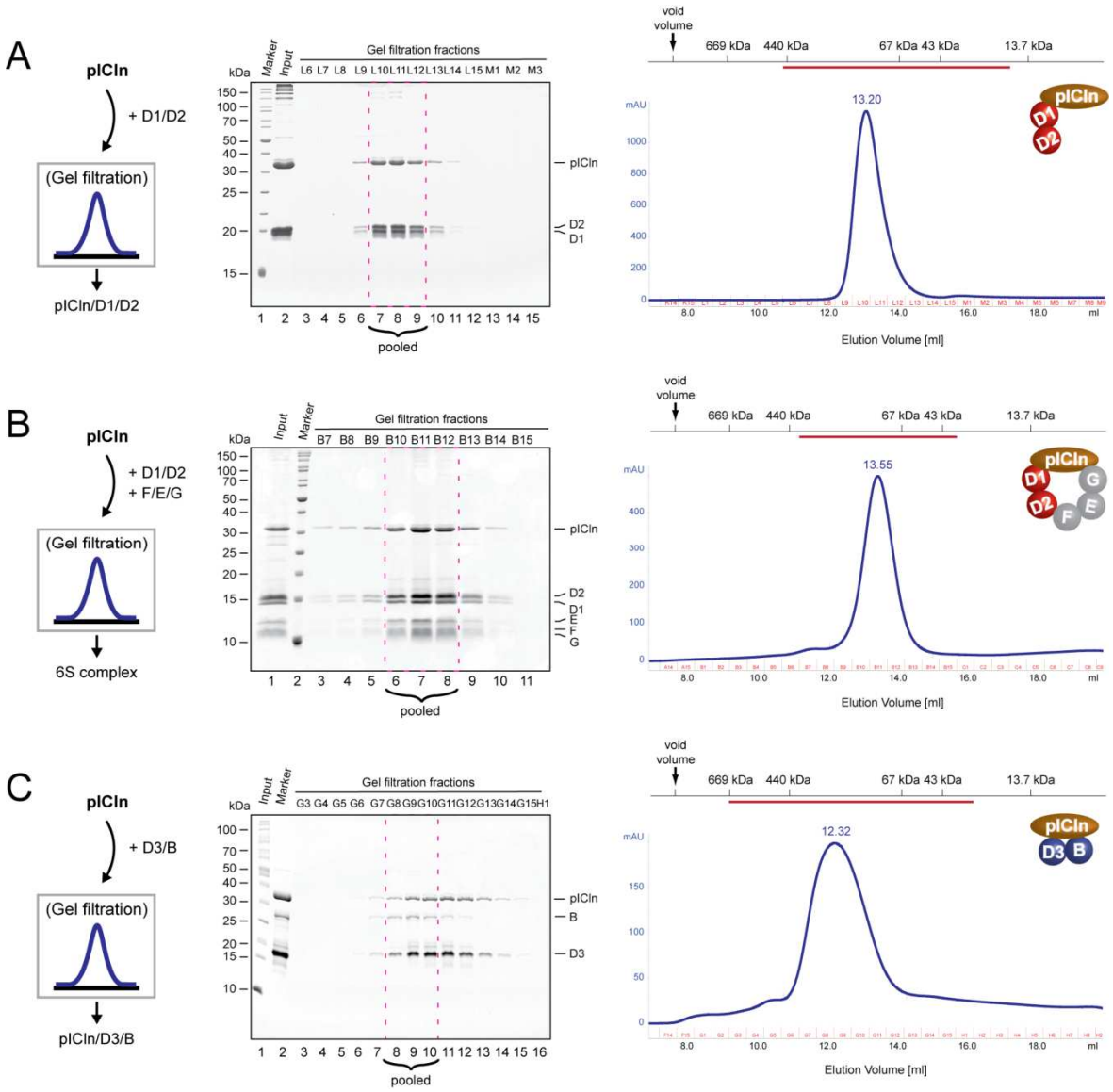

Figure 24 – *In vitro* reconstitution of pICln-Sm protein complexes.

Equimolar amounts of pICln and the Sm protein heterooligomers D1/D2 **(A)**, D1/D2 and F/E/G **(B)**, and D3/B **(C)** were combined and dialyzed overnight against 20 mM Hepes-NaOH (pH 7.5), 200 mM NaCl and 5 mM DTT. Samples were separated by gel filtration chromatography (Superdex200 10/300GL, right panel) and analyzed by SDS-PAGE (middle panel). The red line above the elution profile indicates the range of elution samples that were applied to SDS-PAGE.

5.3.4 Overview of recombinantly expressed and *in vitro* reconstituted protein complexes

In conclusion, in order to biochemically analyze the interactions of PRMT5 with its methylation substrates as well as the actual methylation kinetics, recombinant proteins were generated. The PRMT5/WD45 heterodimer was expressed in *Sf*21 insect cells using the MultiBac system (Figure 25, lane 1). The adaptor protein pICln and the Sm protein

heterooligomers D1/D2, F/E/G, and D3/B were bacterially expressed (Figure 25, lanes 2–5) and subsequently reconstituted to pICln-Sm protein complexes pICln/D1/D2, 6S and pICln/D3/B (Figure 25, lanes 6–8).

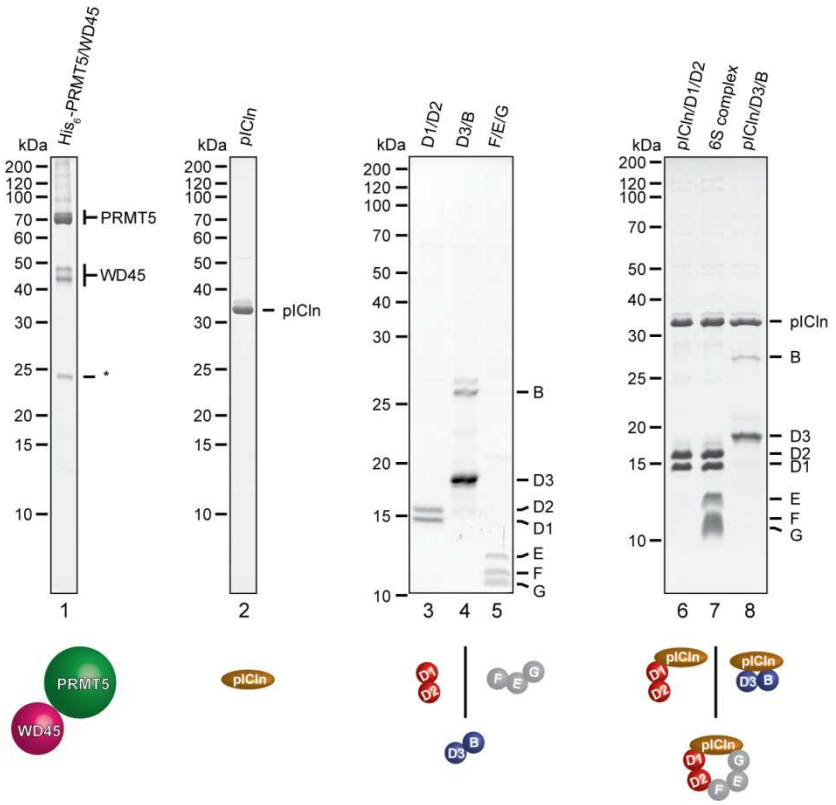

Figure 25 – Overview of purified proteins and reconstituted protein complexes (PRMT5 complex).

PRMT5 complex components: His_6-PRMT5 and WD45 were co-expressed in insect cells (lane 1). pICln was obtained from bacterial expression (lane 2). Sm protein complexes: The heterooligomeric Sm protein complexes D1/D2 (lane 3), D3/B (lane 4) and F/E/G (lane 5) were produced in bacterial cells. After the individual expression and purification of pICln and the heterooligomeric Sm protein complexes, pICln/D1/D2 (lane 6), pICln/D1/D2/F/E/G (= 6S complex; lane 7) and pICln/D3/B (lane 8) were reconstituted *in vitro* and separated by gel filtration chromatography. (*) The asterisk (A, lane 1) indicates a PRMT5 degradation product.

5.4 PRMT5 complex biochemistry

5.4.1 Introductory notes

The endogenous PRMT5 complex was shown to consist of its name-giving component PRMT5, WD45, pICln and the Sm proteins D1/D2 and D3/B. The Sm proteins F/E/G were not part of the 20S complex (Chari *et al.*, 2008) but were found to be associated with pICln and D1/D2 to form a distinct complex (6S complex). It could be shown previously

that the majority of Sm proteins are bound to pICln (Pu *et al.*, 1999). Furthermore, Sm protein D1 of the 6S complex carries symmetrically dimethylated arginine residues (Miranda *et al.*, 2004a). This brings up the question of how the 6S complex is formed. *In vitro*, it could be demonstrated that the 6S complex assembles readily if recombinant proteins are incubated at equimolar amounts (Figure 24). Since the D1 protein in the endogenous 6S complex contains sDMA, the D1 protein must have been in contact with a type II methyltransferase before its assembly. So far, PRMT5 is the only enzyme capable of introducing this modification. In order to identify how the 6S complex is assembled and what role the PRMT5 complex plays in this, various complexes containing PRMT5/WD45 and Sm proteins or pICln-bound Sm proteins were reconstituted *in vitro*.

5.4.2 *In vitro* reconstitution of complexes containing PRMT5/WD45 and Sm protein substrates

In order to identify which Sm protein complexes directly interacted with PRMT5, recombinant PRMT5 was to be immobilized on a stationary phase via its N-terminal His_6-tag and incubated with the respective protein complexes. This, however, was not possible since Sm proteins unspecifically bound to the Ni-NTA matrix (data not shown). To circumvent this problem, protein complexes containing PRMT5 and Sm protein substrates were reconstituted and analyzed for complex formation by gel filtration chromatography (see Appendix 12.6, page 221, for the calibration graph using standard proteins). Initially, all Sm protein heterooligomers (Figure 26) and pICln-Sm protein complexes (Figure 27) were subjected to gel filtration chromatography (Superose6 10/300GL; for a calibration graph of the gel filtration run see the Appendix 12.6, page 221) to obtain their elution profiles. Complex integrity was analyzed by SDS-PAGE.

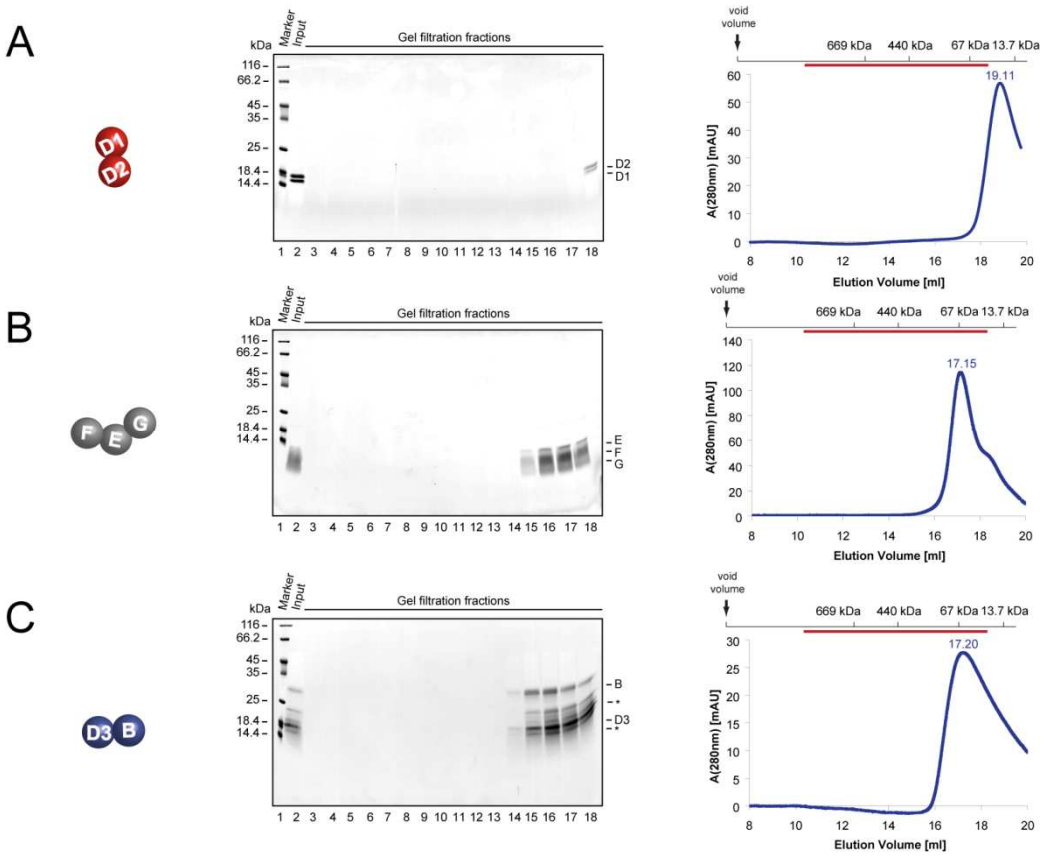

Figure 26 – Recombinantly expressed Sm protein heterooligomers.

Heterooligomeric complexes were expressed in bacterial cells and applied to gel filtration chromatography (Superose6 10/300GL). **(A)** D1/D2, **(B)** F/E/G, **(C)** D3/B. Left panel: schematic depiction of protein complex composition, middle panel: SDS-PAGE of gel filtration samples, right panel: elution profile of gel filtration runs. The red line above the elution profile indicates the range of elution samples that were applied to SDS-PAGE.

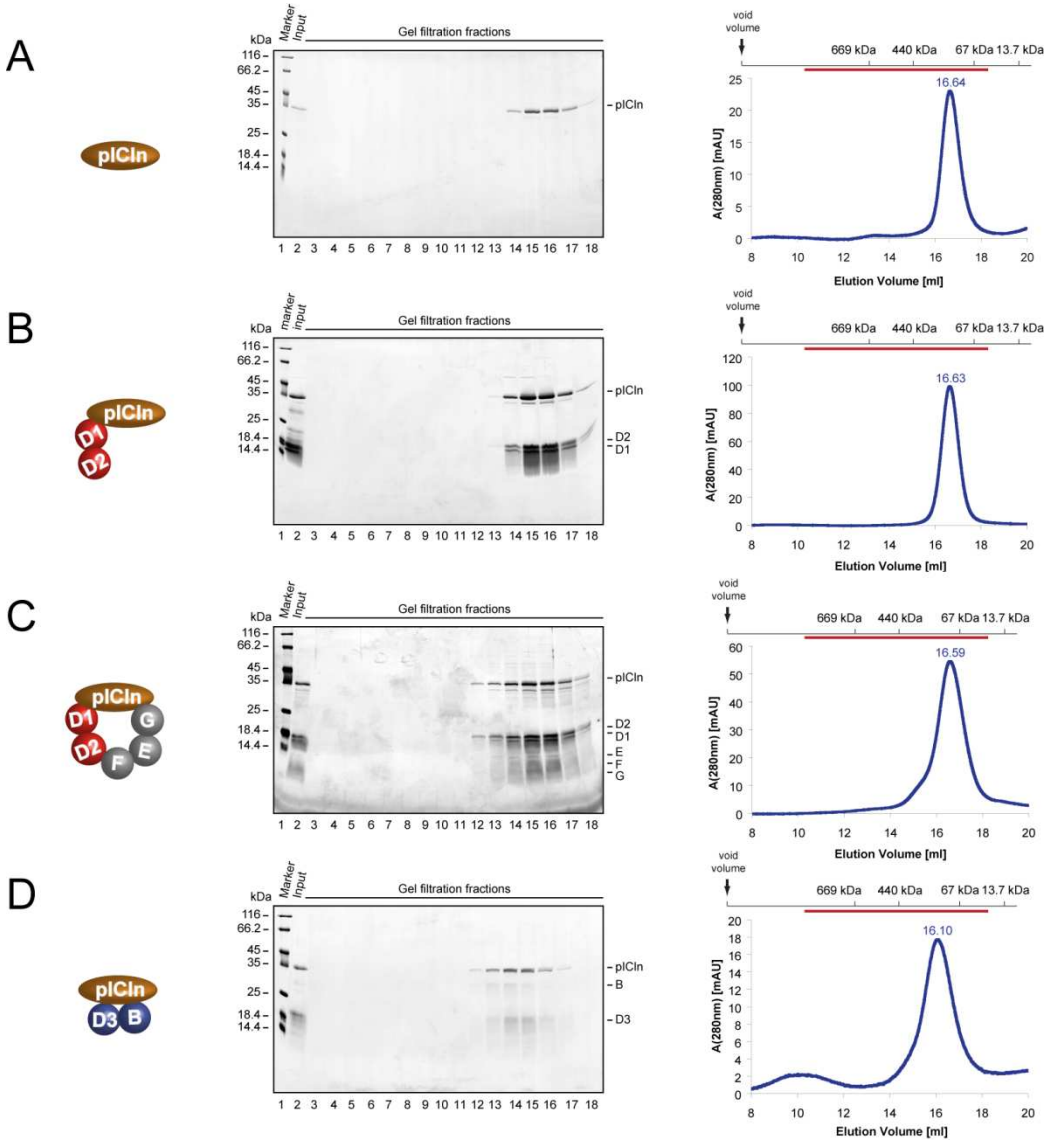

Figure 27 – *In vitro* reconstituted pICln-Sm protein complexes.

PICln alone or protein complexes containing a mixture of pICln and Sm proteins were applied to gel filtration chromatography (Superose6 10/300GL). **(A)** pICln, **(B)** pICln/D1/D2, **(C)** 6S complex (pICln/D1/D2/F/E/G), **(D)** pICln/D3/B. Left panel: schematic depiction of protein complex composition, middle panel: SDS-PAGE of gel filtration samples, right panel: elution profile of gel filtration runs. The red line above the elution profile indicates the range of elution samples that were applied to SDS-PAGE.

All protein complexes eluted in homogeneous peaks when measuring the absorbance at 280 nm. The addition of pICln to the Sm protein heterooligomers shifted the elution peak of the Sm proteins to smaller elution volumes indicating an interaction with pICln (compare the SDS-PAGE depictions in Figure 26 and Figure 27).

The recombinant PRMT5/WD45 complex was incubated with Sm protein heterooligomers, pICln and pICln-Sm protein complexes. Resulting protein complexes were again separated by gel filtration chromatography and analyzed by SDS-PAGE (Figure

28 and Figure 29). In order to compare the resulting sizes of the protein complexes the elution profiles of PRMT5/WD45 (green), the Sm protein heterooligomers and pICln-Sm protein complexes (blue) and the combination thereof (yellow) were overlaid (Figure 28 and Figure 29, right panel). Sm protein heterooligomers D1/D2 and D3/B directly interacted with PRMT5/WD45 (Figure 28 B and D), whereas F/E/G did not (Figure 28 C).

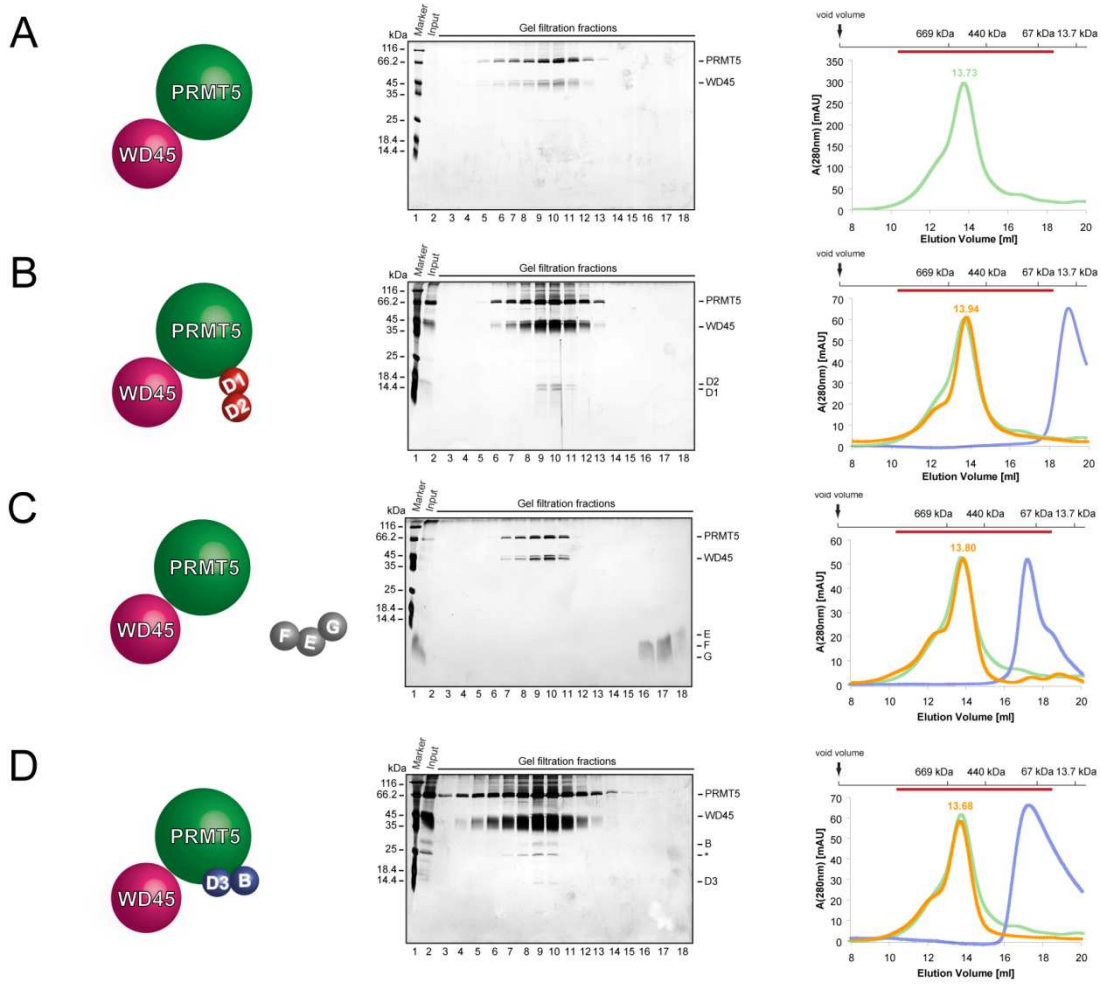

Figure 28 – Interaction of PRMT5/WD45 with Sm protein heterooligomers.

PRMT5/WD45 alone or together with Sm protein heterooligomers were incubated at 4°C overnight and applied to gel filtration chromatography (Superose6 10/300GL). **(A)** PRMT5/WD45 only, **(B)** +D1/D2, **(C)** +F/E/G, **(D)** +D3/B. Left panel: schematic depiction of protein complex composition, middle panel: SDS-PAGE of gel filtration samples, right panel: elution profile of gel filtration runs. The red line above the elution profile indicates the range of elution samples that were applied to SDS-PAGE. For better comparison, the elution profile of PRMT5/WD45 is depicted as a green line in all diagrams. The resulting protein complex is depicted in yellow; the elution profile of the respective substrates is shown in blue.

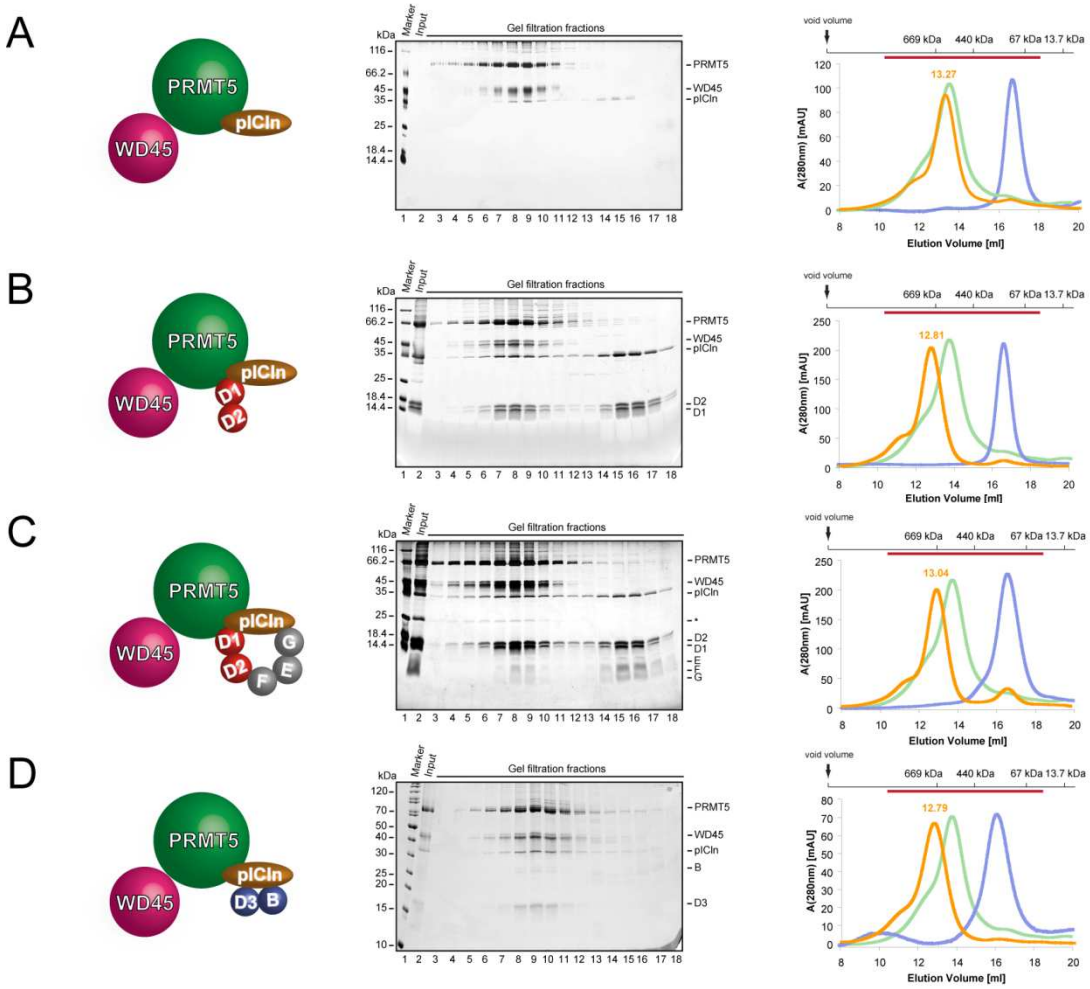

Figure 29 – Interaction of PRMT5/WD45 with pICln-Sm protein complexes.

PRMT5/WD45 and pICln alone or together with pICln-Sm protein complexes were incubated at 4°C overnight and applied to gel filtration chromatography (Superose6 10/300GL). **(A)** PRMT5/WD45 +pICln, **(B)** +pICln/D1/D2, **(C)** +6S complex (pICln/D1/D2/F/E/G), **(D)** +pICln/D3/B. Left panel: schematic depiction of protein complex composition, middle panel: SDS-PAGE of gel filtration samples, right panel: elution profile of gel filtration runs. The red line above the elution profile indicates the range of elution samples that were applied to SDS-PAGE. For better comparison, the elution profile of PRMT5/WD45 is depicted as a green line in all diagrams. The resulting protein complex is depicted in yellow; the elution profile of the respective substrates is shown in blue.

Finally, PRMT5/WD45 was incubated with pICln and pICln-Sm protein complexes, separated by gel filtration chromatography and subjected to SDS-PAGE (Figure 29). It could be shown that PRMT5/WD45 interacted with all pICln-Sm protein complexes including the 6S complex. Furthermore, D1/D2 or D3/B bound directly to PRMT5/WD45. When preformed pICln-Sm protein complexes were used, however, a larger amount of Sm proteins was found to be present in the complex. Both PRMT5/WD45 as well as pICln is capable of binding Sm proteins D1/D2 and D3/B. While pICln associates with Sm

proteins via its Sm-fold, PRMT5 likely binds to the C-terminal domains in Sm proteins that receive methyl groups.

5.4.3 6S is formed on the PRMT5 complex

The previous experiment showed that pICln/D1/D2, pICln/D3/B as well as 6S directly bind to PRMT5/WD45. In the cell, the former two correspond to the 20S complex components. The 6S complex, however, has previously not been shown to be associated with PRMT5/WD45. In a cellular context one could envisage that 6S is assembled on the PRMT5 complex in a step-wise manner using pICln/D1/D2 and F/E/G.

To analyze a possible assembly route of the 6S complex, protein complexes containing PRMT5, WD45, pICln, D1 and D2 were reconstituted *in vitro* (Figure 30 A). PRMT5/WD45 and pre-assembled pICln/D1/D2 were incubated and subjected to gel filtration chromatography (Superose6 10/300GL). Elution fractions of the resulting protein complex were pooled, concentrated, incubated with an excess of F/E/G and processed as before. Finally, a surplus of pICln/D1/D2 was added and again analyzed by gel filtration chromatography. Each reconstitution step was verified by SDS-PAGE.

Initially, the PRMT5/WD45/pICln/D1/D2 complex was assembled *in vitro*. Using a large excess of the interacting pICln/D1/D2 over PRMT5/WD45, a complex was formed containing stoichiometric amounts of all five proteins (Figure 30 B). This complex was then incubated with F/E/G to form the 6S complex (Figure 30 C). The amount of F/E/G incorporated into the resulting protein complex was comparable to the one in the previously directly reconstituted PRMT5/WD45/6S complex (Figure 29 C). Finally, an excess of pICln/D1/D2 caused the removal of the 6S complex from PRMT5/WD45 which was indicated by the shift of the F/E/G heterooligomer from the 20S to the 6S peak fractions (Figure 30 D).

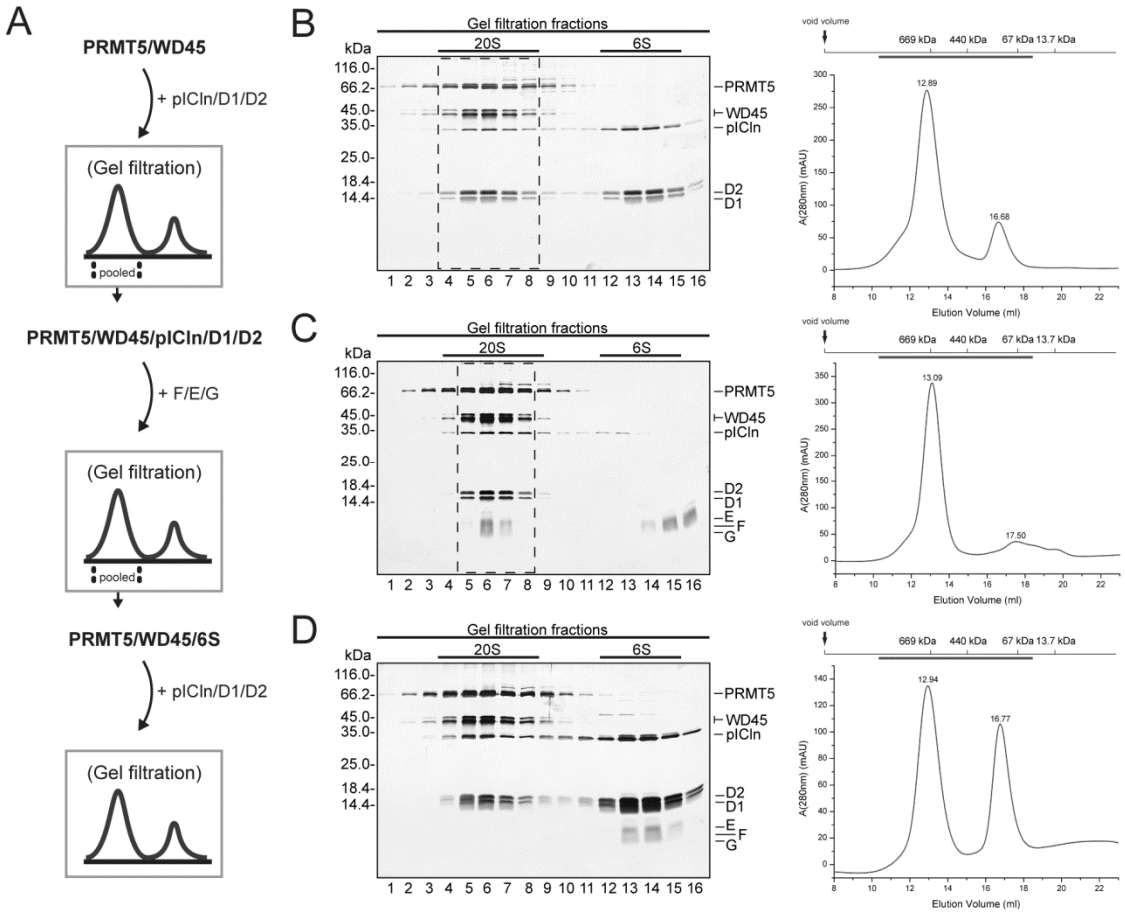

Figure 30 – Stepwise assembly of 6S on the PRMT5 complex.

(A) Schematic experimental outline. **(B)** PRMT5/WD45 and a 2-fold molar excess of pICln/D1/D2 were incubated at 4°C overnight and separated by gel filtration chromatography (Superose6 10/300GL). **(C)** Fractions containing PRMT5/WD45/pICln/D1/D2 were pooled (**B**, lanes 4–8), incubated with a 5-fold molar excess of F/E/G and separated by size. **(D)** Gel filtration fractions containing PRMT5/WD45/6S (**C**, lanes 5–8) were treated with a 3.5-fold molar excess of pICln/D1/D2 followed by another gel filtration chromatography. **(B-D)** Left panels: SDS-PAGE of gel filtration chromatographies. Right panels: Corresponding chromatograms observed at A280nm. The black line above the elution profile indicates the range of elution samples that was applied to SDS-PAGE.

It was shown that the 6S complex could not only self-assemble from individual Sm protein heterooligomers and pICln *in vitro*, but also that 6S can reconstituted in a step-wise manner on PRMT5/WD45. Following the initial addition of pICln/D1/D2, the 6S complex is formed by the addition of F/E/G. The structural details of this complex have not been addressed.

One question that immediately arose from the presence of the 6S complex on PRMT5/WD45 was its subsequent release as 6S was found to exist as a separate entity *in vivo*. It could be shown that the addition of pICln/D1/D2 caused the replacement of 6S from PRMT5/WD45.

5.4.4 6S is released from PRMT5/WD45 by pICln-containing complexes

Once a means for the formation of the 6S complex on PRMT5/WD45 and a possible subsequent release through the addition of pICln/D1/D2 was found, there could still be more possibilities to expel the 6S complex. Release of 6S might occur spontaneously, mediated by other binding partners or even driven by the methylation of the D1 protein in the 6S complex.

To identify other possibilities for 6S release, PRMT5/WD45 and the reconstituted 6S complex were incubated with each other and separated by gel filtration chromatography (Figure 31) (Superose6 10/300GL). The PRMT5/WD45/6S complex containing elution fractions were united and incubated in the presence of buffer only, pICln, pICln/D1/D2, pICln/D3/B or 1 mM SAM (Figure 31 A). Whereas the former setups were kept at 4°C throughout the experiment, SAM-treated PRMT5/WD45/6S was incubated for 1 h at 37°C to provide methylation conditions. These reactions were again separated by gel filtration chromatography to differentiate between the PRMT5/WD45-bound (20S) and the methyltransferase-free state (6S). Peak fractions of 20S and 6S were pooled, concentrated and analyzed by SDS-PAGE.

The PRMT5/WD45/6S complex that was incubated overnight at 4°C remained intact (compare: Figure 31 C, lanes 1 and 2). When adding pICln-containing protein complexes, however, F/E/G was quantitatively replaced from PRMT5/WD45 indicating the release of 6S (compare: Figure 31 C, lanes 3 and 4, 5 and 6 as well as 7 and 8). A residual amount of D1/D2 was still present in the 20S peak. Finally, the methylation of the D1 protein in the 6S complex had no effect on its release from the PRMT5/WD45 as F/E/G remained in the 20S peak (compare: Figure 31C, lanes 9 and 10).

It was shown that the release of the 6S complex from PRMT5/WD45 was mediated by pICln and pICln-containing complexes, whereas methylation of D1 alone was not sufficient to expel 6S.

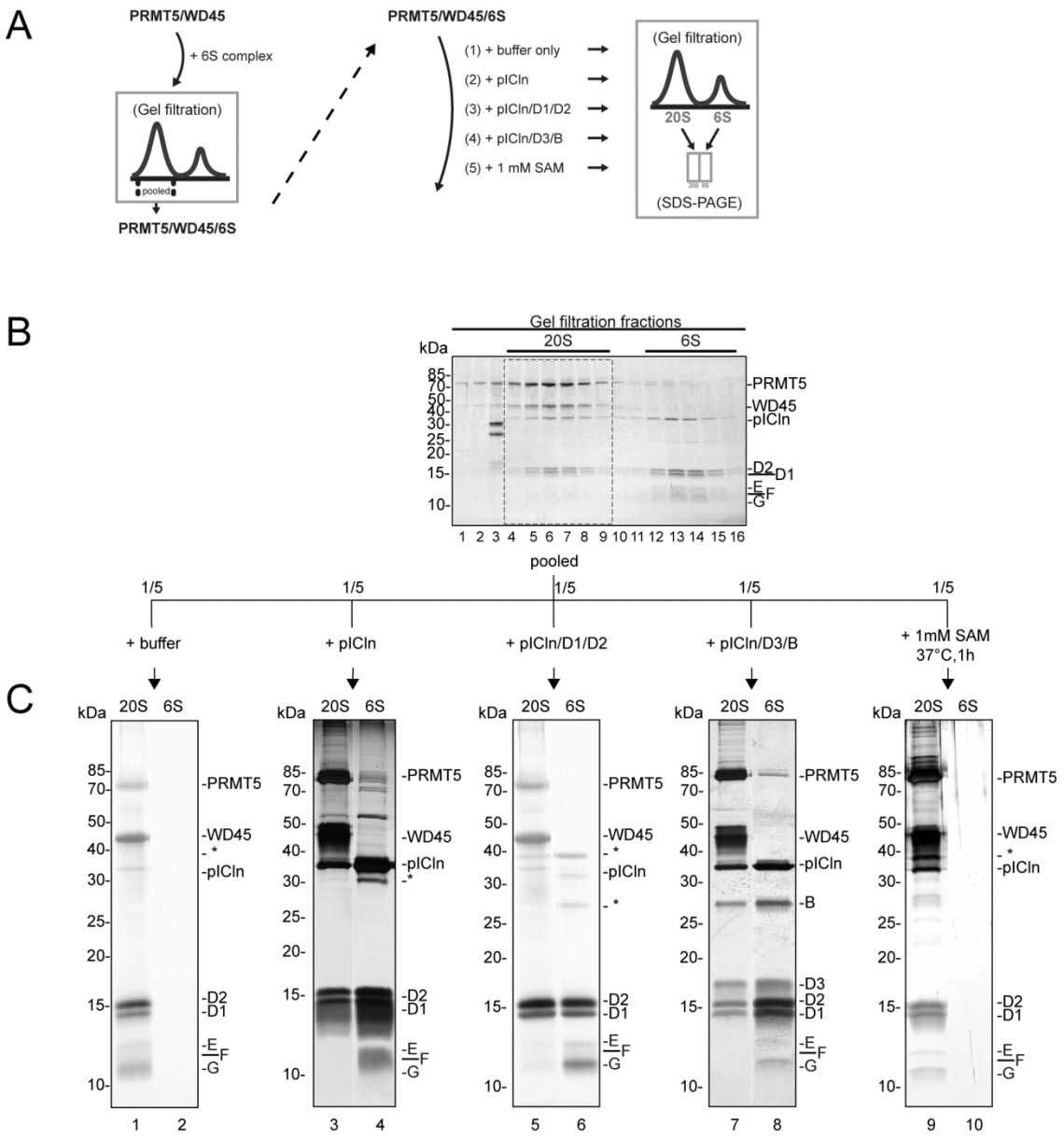

Figure 31 – 6S is replaced from the PRMT5/WD45 by pICln containing protein complexes.

PRMT5/WD45 was incubated with an excess of 6S overnight at 4°C and purified by gel filtration chromatography (Superose6 10/300GL). The elution fractions containing PRMT5/WD45/6S were pooled and incubated overnight at 4°C with buffer only (1), pICln (2), pICln/D1/D2 (3), pICln/D3/B (4) or for 1 h at 37°C with 1 mM SAM. **(A)** Experimental outline. **(B)** SDS-PAGE of the initial reconstitution of the PRMT5/WD45/6S complex. **(C)** SDS-PAGE of the 20S and 6S fractions following the second incubation. (*) The asterisks on the SDS gels show protein degradation products.

5.4.5 6S alone is unable to release pICln/D1/D2 from PRMT5/WD45

So far, it was found that the 6S complex could be assembled on PRMT5/WD45 and subsequently be released by the addition of pICln-Sm protein containing complexes. Since this might have only been due to a large amount of pICln, 6S might cause the same effect on pICln/D1/D2 and pICln/D3/B if it was provided in large excess.

PRMT5/WD45 was incubated with pICln/D1/D2, separated by gel filtration (Superose6 10/300GL) and incubated with an excess of 6S. This again was separated by size. The 20S and 6S peak fractions were pooled and subjected to SDS-PAGE (Figure 32 A).

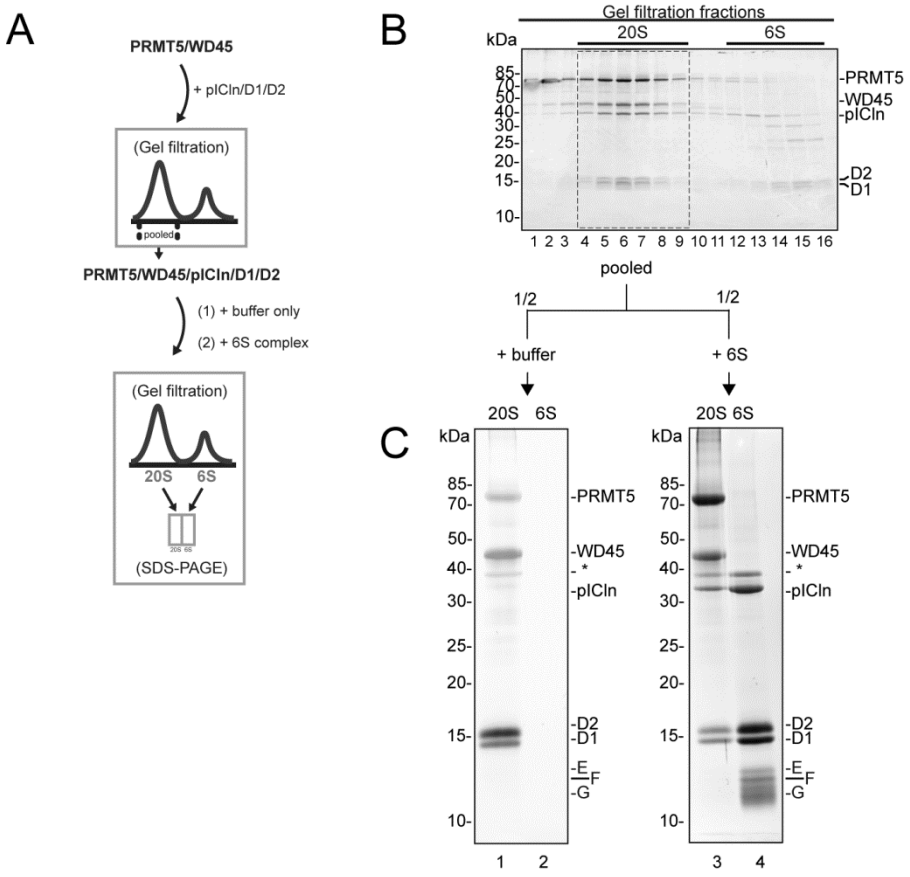

Figure 32 – The 6S complex is unable to replace pICln/D1/D2 from the PRMT5 complex.

PRMT5/WD45 was incubated with an excess of pICln/D1/D2 overnight at 4°C and purified by gel filtration chromatography (Superose6 10/300GL). The elution fractions containing PRMT5/WD45/pICln/D1/D2 were pooled and incubated overnight at 4°C with buffer only (1) or with 6S (2). **(A)** Experimental outline. **(B)** SDS-PAGE of the initial reconstitution of the PRMT5/WD45/pICln/D1/D2 complex. **(C)** SDS-PAGE of the 20S and 6S fractions following the second incubation. (*) The asterisks on the SDS gels show protein degradation products.

The pICln-Sm protein complex pICln/D1/D2 remained stably bound to the methyltransferase at longer incubation at 4°C (Figure 32, compare lanes 1 and 2) and also

upon addition of 6S (Figure 32, compare lanes 3 and 4). Consequently, once 6S is released from the PRMT5 complex by pICln/D1/D2 or pICln/D3/B it is unable to re-associate with the methyltransferase.

In summary, it could be shown that the 6S is assembled in a step-wise manner on the PRMT5 complex. Initially, pICln/D1/D2 binds to PRMT5/WD45 and is methylated before F/E/G associates to form the 6S complex. This complex can then be released by either pICln/D1/D2 or pICln/D3/B leading to two complexes of 6S and 20S that have also been observed *in vivo*. Still, the aspect of arginine methylation has so far been excluded in the *in vitro* analysis of the 6S complex formation.

5.5 PRMT5 complex methylation kinetics

5.5.1 Introductory notes

PRMT5 is the major type II methyltransferase in human. It catalyzes the symmetrical dimethylation of arginine side chains of a variety of substrate molecules by transferring a methyl groups from S-adenosylmethionine (SAM) (Introduction 1.3.5, page 13). In the cytoplasmic snRNP assembly, methylation substrates are the Sm proteins B/B', D1 and D3. So far, recombinant PRMT5 was either insoluble or lacked biological activity. To overcome this obstacle PRMT5/WD45 was co-expressed using the MultiBac system (Results 5.3.2, page 96). Sm protein heterooligomers were bacterially expressed and reconstituted to pICln-Sm protein containing complexes as described before (Results 5.3.3, page 97). These tools now provided the opportunity not only to analyze the methylation of specific Sm protein substrates but also to gain mechanistic insight into this reaction.

5.5.2 Recombinant PRMT5/WD45 methylates Sm proteins B, D1 and D3 *in vitro*

To test its methyltransferase activity, PRMT5/WD45 was incubated on its own or with an excess of Sm protein substrates (D1/D2, F/E/G, D3/B, pICln/D1/D2, 6S and pICln/D3/B) and the radioactively labeled co-factor ^{3}H-S-adenosylmethionine ([^{3}H]-SAM) for 1 h at 37°C. Methylated proteins were separated by SDS-PAGE (Figure 33 A) and the radioactive

signals were visualized by autoradiography (Figure 33 B). For a detailed description of the methylation reaction see Methods 4.3.19, page 71.

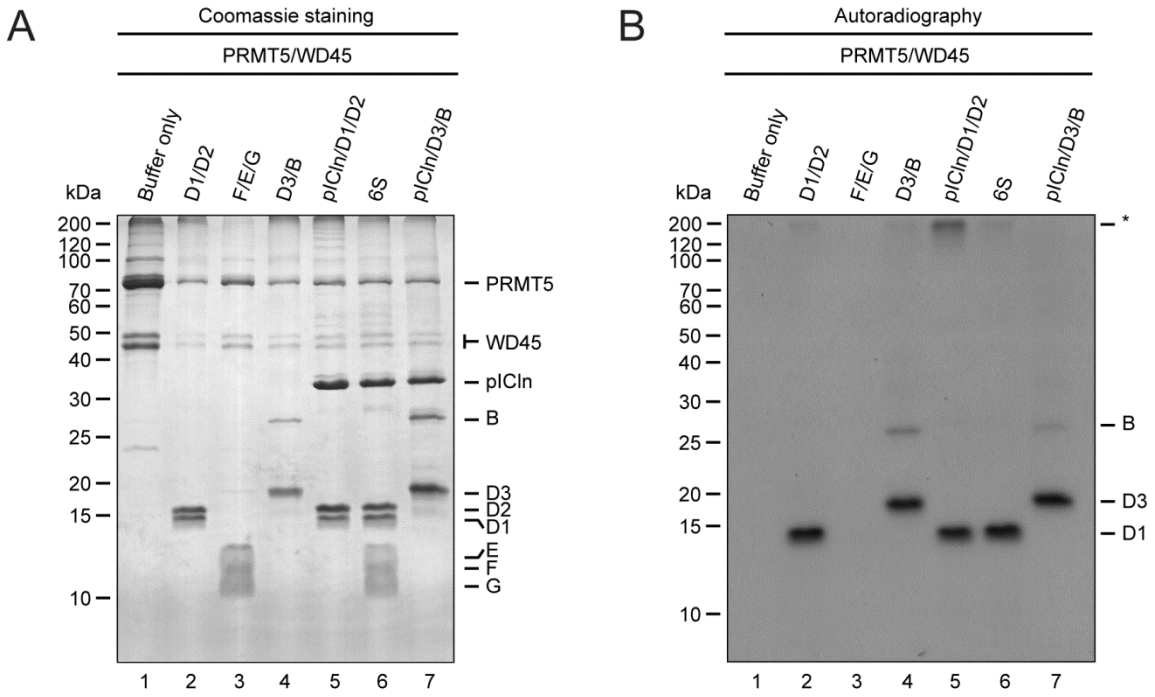

Figure 33 – Baculovirus expressed PRMT5/WD45 methylates Sm protein substrates B, D1 and D3 *in vitro*.

Ten picomoles of recombinant PRMT5/WD45 was incubated with 14 pmol radioactively labeled co-factor ([^{3}H]-SAM) in 1× PBS (pH 7.5), at 37°C for 1 h (lane 1). Additionally, 1 pmol of PRMT5/WD45 and 14 pmol of co-factor were applied to methylate 20 pmol of Sm protein substrates D1/D2 (lane 2), F/E/G (lane 3), D3/B (lane 4), pICln/D1/D2 (lane 5), 6S (lane 6) or pICln/D3/B (lane 7) under the same conditions. Samples were separated by SDS-PAGE **(A)** and radioactive signals were visualized by autoradiography **(B)**.(*) The asterisk indicates a population of SDS resistant Sm protein substrate.

Methylation of the Sm proteins B, D1 and D3 was catalyzed by the recombinant PRMT5/WD45 complex (Figure 33 B). Whereas D1 and D3 had a similar methylation rate, methylation of B was much weaker (compare lanes 2, 5 and 6 with lanes 4 and 7). This effect could also stem from the understoichiometric presence of B in the reconstituted protein complex that served as a methylation substrate (Results 5.3.3, page 97). Also, no methylation occurred in the substrates F/E/G and PRMT5 itself (lanes 1 and 3).

The enzymatic activity was further analyzed with respect to other protein additives as well as storage conditions. Adding increasing amounts of BSA to the methylation reaction and thus decreasing the diffusion rate of methylation reaction partners had no impact on the overall methylation activity (data not shown). Whereas enzymatic activity remained

stable even after a prolonged storage of PRMT5/WD45 at -80°C, incubation at -20°C for as little as one week had a strong effect on methyl transfer activity (data not shown).

In cooperation with Georges Martin it was shown that insect cell-expressed PRMT5/WD45 also methylated the nuclear poly(A) binding protein 1 (PABPN1) and the 68 kDa-large subunit of the mammalian cleavage factor I (CF I_m68). In particular, the formation of symmetrical dimethylarginines was shown by Western blotting using sym10 antibodies in PABPN1 and in a fusion protein of GST and the GAR motif of CF I_m68 (for more information see Martin et al. (2010)).

Until recently, arginine methylation has been understood as an irreversible posttranslational modification. The arginine demethylase Jumonji domain-containing protein 6 (JMJD6) was found to specifically remove methyl groups from asymmetrically as well as symmetrically dimethylated arginine residues in histones H3 and H4 (Chang, 2007). In comparison to Sm proteins, histones contain only a single receptive arginine residue. To test whether JMJD6 also acted on symmetrically dimethylated Sm proteins, the human protein was expressed in bacterial cells and purified to homogeneity. The recombinant JMJD6 protein was unable to demethylate Sm protein substrates (data not shown).

5.5.3 Optimization of methylation buffer conditions

Following the initial identification of recombinant PRMT5/WD45 as a biologically active methyltransferase, the reaction conditions were to be optimized in order to obtain a robust assay system. In enzyme kinetics, increasing amounts of substrates and co-factors are applied to analyze whether a given reaction follows Michaelis-Menten kinetics. The initial methyltransferase activity was verified using 1× PBS (pH 7.5) as the reaction buffer. When the co-factor concentration was increased, however, making up more than 10% of the total volume, the methyltransferase activity declined rapidly and was completely absent at a final co-factor concentration of 25% (v/v) (Figure 34 A).

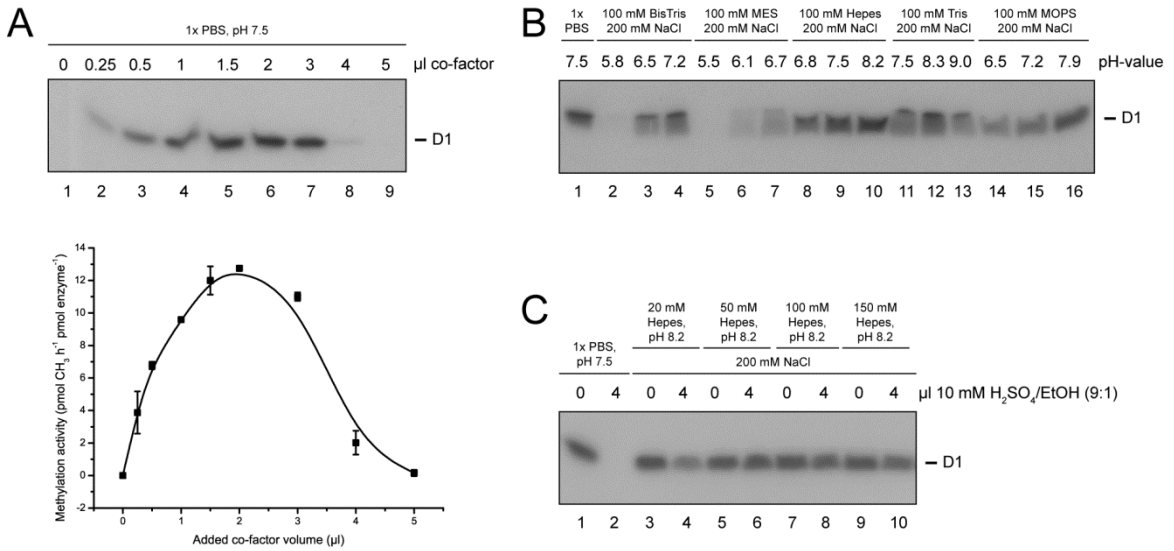

Figure 34 – Optimization of the methylation buffer conditions.

As the methylation co-factor [^{3}H]-SAM was solubilized in 10 mM H_2SO_4 and ethanol (9:1), increasing amounts negatively affected the methylation activity. **(A)** One picomole of PRMT5/WD45 was incubated with 20 pmol of pICln/D1/D2 and increasing amounts of [^{3}H]-SAM (0–5 µl) in 1× PBS (pH 7.5) at 37°C for 1 h. Methylated proteins were separated by SDS-PAGE and analyzed by autoradiography (**A**, upper panel) and densitometry (**A**, lower panel). Values represent the average of two separate experiments. Error bars show the standard errors of the mean. **(B)** One picomole of PRMT5/WD45 was incubated with 20 pmol of pICln/D1/D2 and 14 pmol [^{3}H]-SAM (= 1 µl) at 37°C for 1 h using buffers and pH ranges as indicated. **(C)** Methylation of pICln/D1/D2 applying 1× PBS (pH 7.5) or increasing Hepes concentrations. Reactions were supplemented with 1 µl of co-factor and either 0 or 4 µl of 10 mM H_2SO_4/EtOH (9:1).

The buffer in which the co-factor [^{3}H]-SAM (Perkin Elmer) was delivered contained 10 mM H_2SO_4 and ethanol in a ratio of 9:1. Consequently, various buffers (BisTris, MES, Hepes, Tris and MOPS) and pH values (5.5–8.3) were tested in the methylation of pICln/D1/D2 (Figure 34 B). A buffer consisting of 100 mM Hepes (pH 8.2) and 200 mM NaCl resulted in the strongest methylation signal in autoradiography. Additionally, methylation reactions were carried out using increasing concentrations of Hepes buffer (pH 8.2). These reactions were supplemented with an equal amount of radioactively labeled co-factor in the presence or absence of co-factor dilution buffer (10 mM H_2SO_4:ethanol; 9:1) that could completely inactivate the methyltransferase in 1× PBS buffer (Figure 34 C). A Hepes buffer concentration of at least 50 mM was needed to abolish the effect of the sulfuric acid and ethanol present in the co-factor solution.

To summarize, the addition of methylation co-factor corresponding to 25% of the total volume completely diminished the methylation activity. The choice of the type of buffer, the buffer concentration and the pH value resulted in constant methylation rates even

when high amounts of co-factor were added. Consequently, all upcoming methylation reactions were performed using 100 mM Hepes-NaOH (pH 8.2) and 200 mM NaCl as a reaction buffer.

5.5.4 Quantification of methylation signals

Once the optimized methylation conditions had been identified, a method was needed to reproducibly analyze and compare individual methylation reactions. Methylated proteins were to be analyzed by SDS-PAGE and subsequent autoradiogaphy as shown in the previous paragraph. In enzyme kinetic reactions one measures product formation in a given amount of time. Therefore, a system had to be designed to identify the number of methyl groups that were transferred onto the respective Sm protein substrates according to the autoradiography signal. See Figure 35 for a schematic overview, Figure 36 for exact values and Methods 4.5.3, page 78, for the experimental details.

Increasing amounts of PRMT5/WD45 were used to methylate an excess of pICln/D1/D2 for 1 h at 37°C. Equal amounts of each sample were separated on two SDS-polyacrylamide gels. The first one was incubated in ^{3}H-amplifying solution, dried, exposed to X-ray film for 5, 9 and 15 h (Figure 35 A and Figure 36 A), and submitted to autoradiography as well as densitometry (Figure 35 B and Figure 36 B; see Methods 4.3.15, page 70 and Methods 4.5.1, page 77). The densitometric analysis of the autoradiography signal is shown in the next section (Results 5.5.5, page 117).

The second protein gel was Coomassie-stained and de-stained. Then, the protein bands were excised and dissolved to retrieve the proteins from the gel matrix for subsequent liquid scintillation counting (see Methods 4.3.6, page 65). The resulting numbers of decays per minute were correlated to the initial enzyme concentration of each reaction (Figure 35 C and Figure 36 C). Since both approaches led to values on the basis of the initial enzyme concentration, the determined grayscale value of the densitometric analysis could be directly aligned to the number of decays per minute that were obtained in the liquid scintillation counting (Figure 35 D and Figure 36 D). In a third approach, known concentrations of radioactively labeled co-factor were directly applied to liquid scintillation counting in order to identify the number of decays per minute given by the initial co-factor concentration (Figure 35 E and Figure 36 E). Finally, the result of the two

initial approaches could be combined with the result of the third one to specifically correlate the number of transferred methyl groups to the grayscale value of the densitometric analysis (Figure 35 F and Figure 36 F).

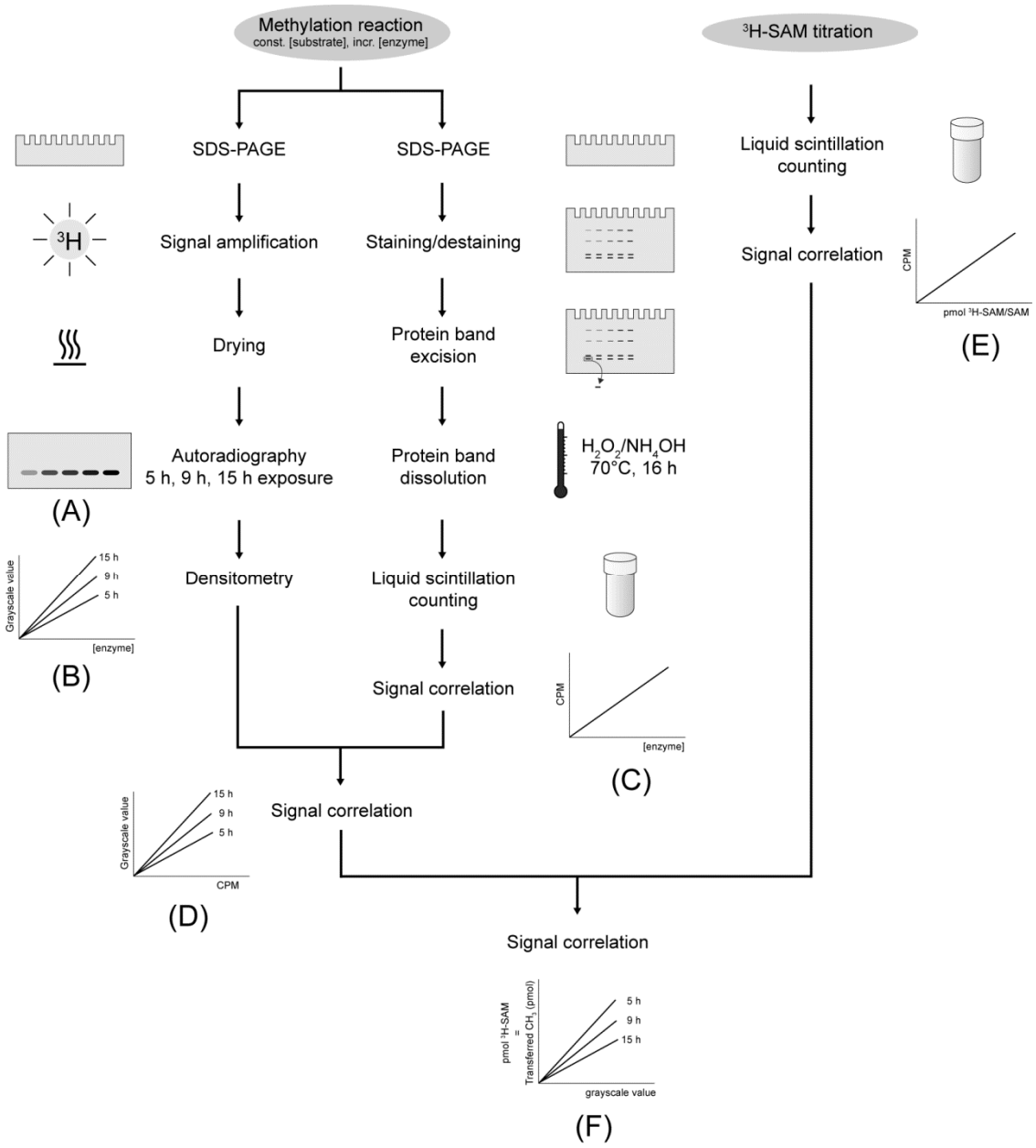

Figure 35 – Outline of the correlation of autoradiography signals and transferred methyl groups.

pICln/D1/D2 was methylated by PRMT5/WD45 using [^{3}H]-SAM as a co-factor. Samples were separated by SDS-PAGE and either processed in autoradiography **(A)** and densitometry **(B)** or gel staining, excision and dissolution of proteins bands followed by liquid scintillation counting **(C)**. Resulting datasets were sequentially correlated with each other **(D)** and with the direct titration of radioactively labeled co-factor **(E)** to identify the relationship between the grayscale value of an autoradiography signal and the amount of transferred methyl groups with respect to the exposure time of the film **(F)**.

Since three different exposure times were included in this, methylation rates could even be compared between samples that had been exposed to X-ray film for different amounts of time.

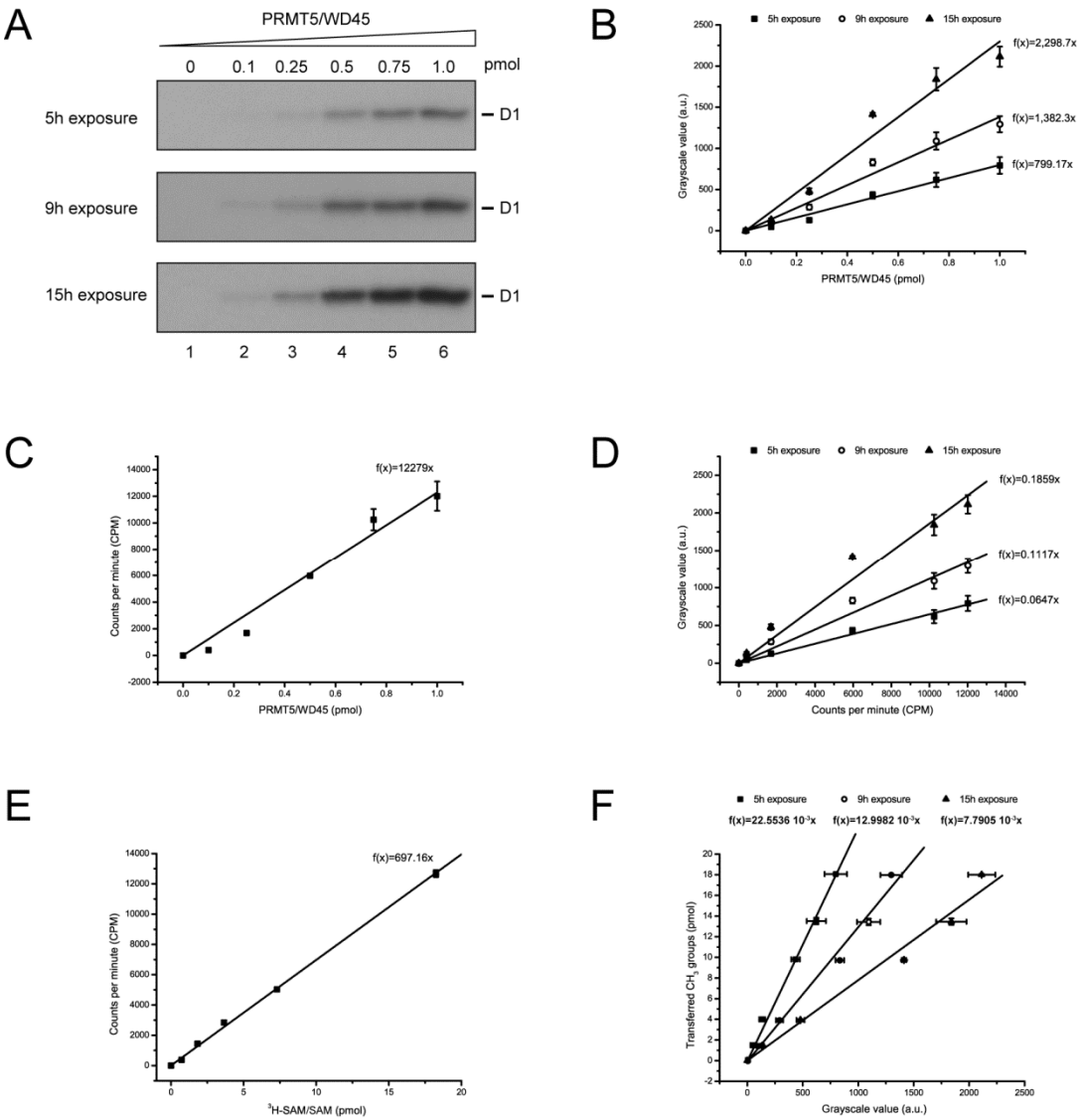

Figure 36 – Correlation of autoradiography signals and transferred methyl groups.

Forty picomoles of pICln/D1/D2 were methylated by 2 pmol PRMT5/WD45 with 438 pmol co-factor at 37°C for 1 h. Data processing was carried out as described in the previous figure depicting the experimental outline. **(A)** Autoradiography of protein gels that were exposed for 5 h (■), 9 h (○) or 16 h (▲). **(B)** Densitometric analysis of the autoradiography signals shown in (A). **(C)** Liquid scintillation counting of the excised and dissolved protein bands. **(D)** Correlation of the data obtained in (B) and (C). **(E)** Liquid scintillation counting of the direct co-factor titration. **(F)** Final correlation of the grayscale value and the number of transferred methyl groups applying the data in (D) and (E). Values represent the average of two separate experiments which were exposed to X-ray films twice. Error bars show the standard errors of the mean.

According to the exposure time of a protein gel to X-ray film, the amount of transferred methyl groups could be calculated. Since the grayscale value of the densitometric analysis was proportional to the amount of methyl groups, correlation coefficients of $22.5536 \cdot 10^{-3}$ (5 h exposure), $12.9982 \cdot 10^{-3}$ (9 h exposure) and $7.7905 \cdot 10^{-3}$ picomoles of methyl groups per grayscale value (15 h exposure) could be obtained. The relationship between the exposure time t (in hours) and the correlation coefficient was exponential ($f(t)= 36.213 \cdot e^{-0.105t}$).

This procedure provided information on the total amount of methyl groups that were introduced to a target protein. More specific information such as what amino acid was methylated and the type of methylation (monomethylation, symmetric/asymmetric dimethylation) could not be obtained.

5.5.5 Densitometric analysis of autoradiography signals using ImageJ

It was previously demonstrated how to correlate a methylation signal that was obtained from autoradiography to the amount of transferred methyl groups. When proteins are separated in SDS-PAGE, the width of each lane of the final gel is not identical and depends on the amount of protein loaded or even the place of application. Protein bands that are applied at the far ends of a gel tend to be distorted and are thus broader than the ones in the middle. In order to reproducibly analyze the signal intensity of a radioactively labeled protein band of varying sizes, an image processing method was devised using the software ImageJ (Figure 37) (see also Methods 4.5.1, page 77).

X-ray films were scanned and saved as 16bit grayscale JPEG (Joint Photographic Experts Group) files. To identify the intensity of a specific radioactive signal, two rectangular shapes of identical size were chosen. Whereas the first covered the radioactive signal, the second exhibited undisturbed background. The actual signal intensity was obtained by correlating the results of the ImageJ-Histogram function and subtracting the background signal from the radioactive one. Since the analysis was independent of the area covered by the signal, band distortion had no influence on the obtained values. Furthermore, evaluating signal intensities at various exposition times provided a means to even process very strong or weak methylation signals.

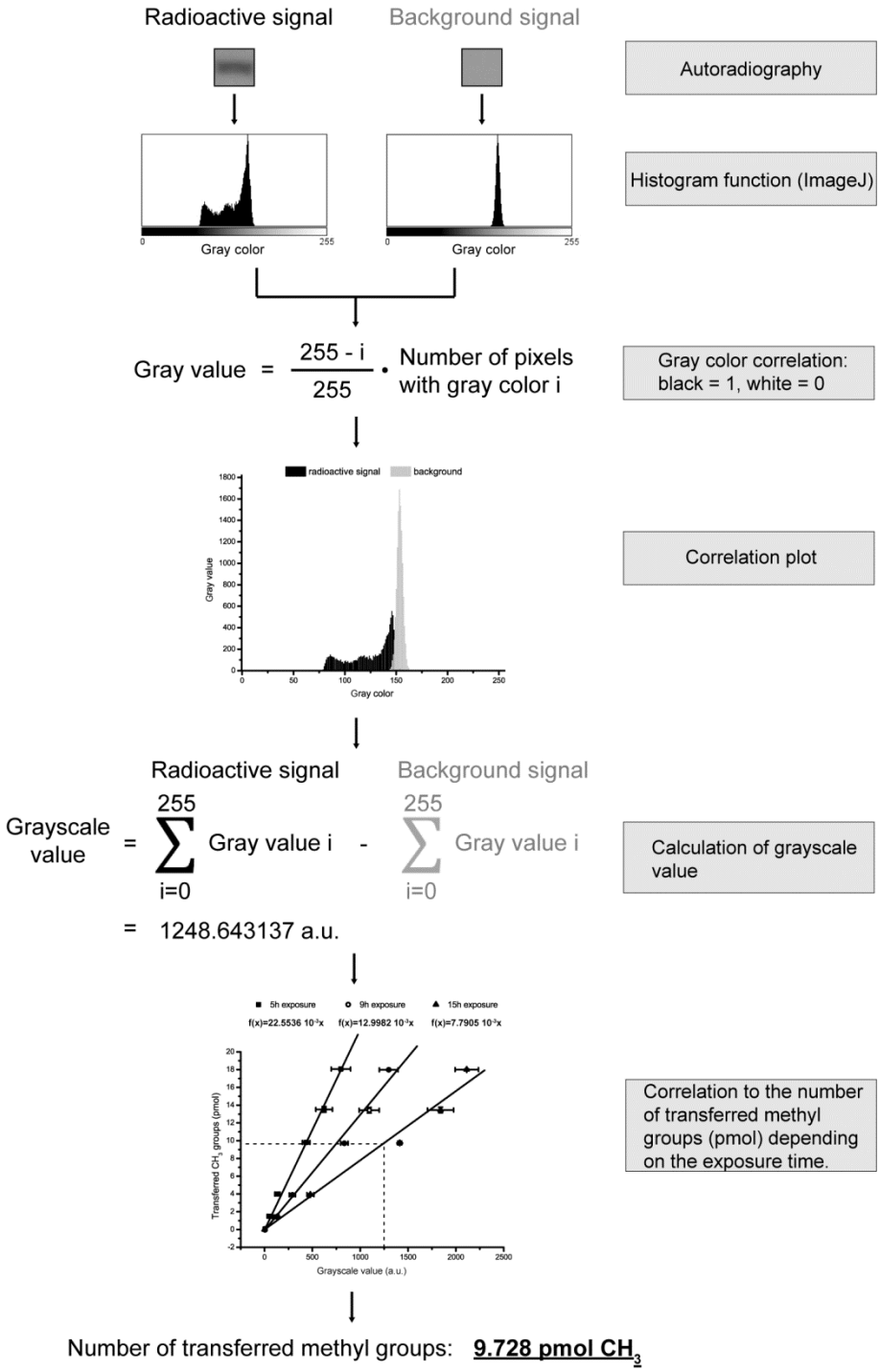

Figure 37 – ImageJ analysis of autoradiography signals.

Methylated proteins were separated by SDS-PAGE and subjected to autoradiography. Scanned films were processed using the software ImageJ as follows: The histogram function of equally sized areas comprising either a radioactive signal or background was run resulting in an array of gray colors [0,255] (0: black, 255: white) and a corresponding number of pixels with this very color. To obtain the gray value, the number of pixels was weighted by a factor between 0 and 1 (0: white, 1: black). The difference of the summed gray values of the radioactive and the background signal corresponds to the grayscale value which is directly proportional to the intensity of the radioactive signal. According to the exposure time of the film, the number of transferred methyl groups can be calculated from the grayscale value. Values represent the average of two separate experiments which were exposed to X-ray films twice. Error bars show the standard errors of the mean.

5.5.6 Determination of the methylation type

In humans, PRMT5 has been identified to be the major type II methyltransferase. Even though PRMT7 and PRMT9 have both been shown to catalyze sDMA formation, the credibility of these results is currently disputed (Zurita-Lopez *et al.*, 2012). Type II methyltransferases mediate the sequential transfer of methyl groups from SAM onto the ω-nitrogens of an arginine residue resulting in monomethylation (MMA) as well as symmetric dimethylation (see Introduction 1.3.2, page 9).

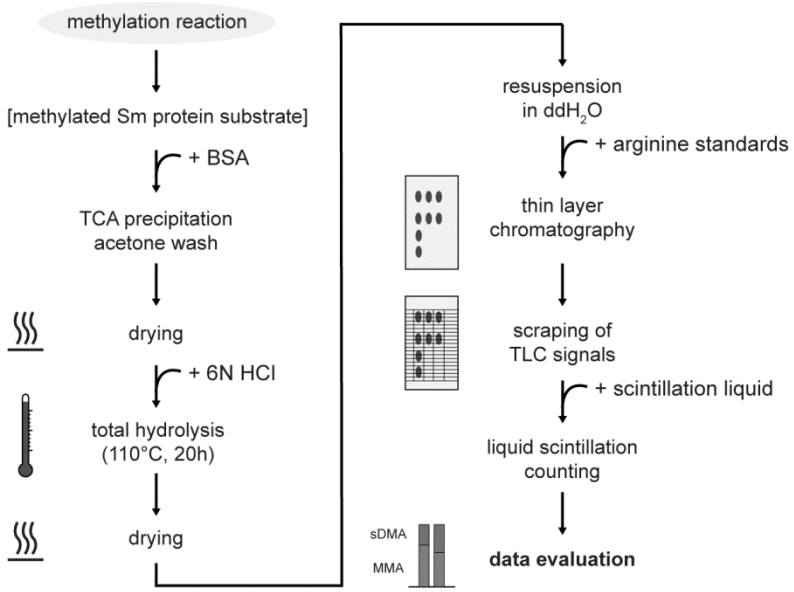

Figure 38 – Schematic overview of methylation type determination.

In order to determine the methylation type conferred by PRMT5, Sm proteins were methylated, supplemented with BSA as a carrier protein and precipitated with 3 volumes of 25% (v/v) TCA overnight at 4°C. Following an acetone wash, samples were dried, supplemented with 100 µl 6N HCl and hydrolyzed for 20 h at 110°C. After drying and resuspension in 50 µl ddH_2O arginine standards were added and the sample applied to thin layer chromatography (see detailed information in Figure 39). Finally, the arginine standards were visualized by ninhydrin staining, the individual lanes were scraped of the plate and analyzed by liquid scintillation counting.

An experimental procedure was to be designed to analyze the type of arginine methylation that is caused by PRMT5. This system was to be based the hydrolysis of the methylated proteins, the separation of individual amino acids using thin layer chromatography (TLC) and the analysis by liquid scintillation counting (Figure 38) (see Methods 4.3.17 and 4.3.18, page 70). Consequently, not only the presence of modified arginine residues could be identified but also the relative abundance of certain modifications. Since type II methyltransferases catalyze both MMA and sDMA formation,

the relative abundance of each type could provide mechanistic details of the methylation reaction.

Sm protein substrates were methylated by PRMT5/WD45, TCA precipitated to remove excess of unused radioactive co-factor and dissociated into individual amino acids by acid hydrolysis. Since all types of modified arginines (L-arginine: L-Arg, mono-methylated arginine: MMA, asymmetrically dimethylated arginine: aDMA and symmetrically dimethylated arginine: sDMA) show a different migration distance in thin layer chromatography, one could deduce the type of methylation inferred by PRMT5/WD45. Hydrolyzed samples were mixed with arginine standards to visualize the migration distance (Figure 39 A). Each lane was then divided into a stack of rectangular shapes of equal size that were scraped off the TLC plate and analyzed for radioactive signals by liquid scintillation counting (Figure 39 B). According to the methylation standards that were co-separated on the same TLC plates, radioactive signals were allocated to the transfer of methyl groups resulting in MMA (R_f = 0.36), aDMA (R_f = 0.43) or sDMA (R_f = 0.50). The recombinant PRMT5/WD45 caused exclusively the formation of MMA and sDMA. When only the co-factor was applied, it interacted strongly with the TLC matrix and had an R_f-value of 0.05. Finally, the relative abundance of transferred methyl groups resulting in MMA and sDMA was calculated (Figure 40).

The co-factor used in the methylation reaction contained 50% of radioactively labeled and 50% unlabeled SAM. Whereas lower amounts of unlabeled co-factor resulted in a final concentration that was too small for enzyme kinetic analyses, higher amounts provided very weak autoradiography signals ([^{3}H]-SAM: 55 µM; SAM: 110 µM). One has to keep in mind that only the arginines carrying a radioactive methyl group are detected in liquid scintillation counting whereas the ones with unlabeled methyl groups are not traceable. Consequently, only half of the methyl groups in the MMA range are detected (Figure 40). The symmetrically dimethylated arginines carry two, one or zero labeled methyl groups. Statistically, the measured radioactive signal was therefore proportional to the number of sDMAs (Figure 40). Finally, these values could be used to calculate the relative abundance of both MMA and sDMA in the methylated protein sample (Figure 40, lower box).

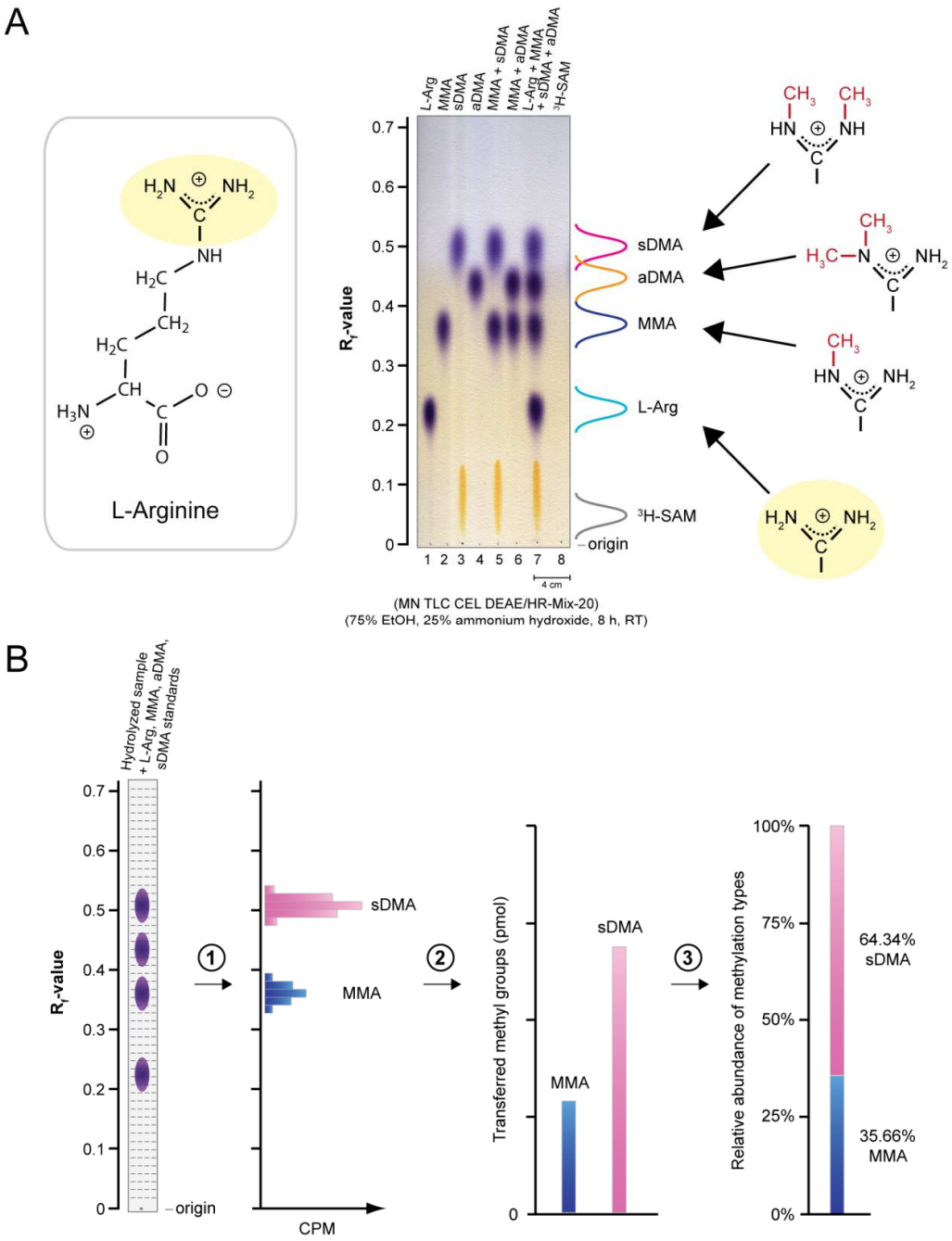

Figure 39 – Thin layer chromatography of methylated and unmethylated arginines.

(A) Type I and type II protein arginine methyltransferases catalyze the transfer of methyl groups onto ω-nitrogen atoms in the arginine side chain. Arginine standards comprising L-arginine (L-Arg), monomethylated (MMA), asymmetrically dimethylated (aDMA) and symmetrically dimethylated arginine (sDMA) were applied to Cellulose DEAE-/HR-Mix-20 (Macherey-Nagel) thin layer chromatography plates and separated using 75% (v/v) ethanol and 25% (v/v) ammonium hydroxide as a running buffer. Amino acids were visualized by ninhydrin staining. The sDMA standard (Sigma-Aldrich) is provided as a di(p-hydroxyazobenzene-p'-sulfonate) salt. This results in a yellow stain on the TLC plate whenever sDMA is applied. **(B)** Analysis of the relative abundance of monomethylated and symmetrically dimethylated arginines. Methylated protein samples were hydrolyzed, mixed with arginine standards, separated by thin layer chromatography and stained with ninhydrin. Equally sized areas of the entire running distance of each lane were scraped off (dashed lines) and analyzed by liquid scintillation counting (1). Signals corresponding to either MMA or sDMA were summed up (2) and finally the relative abundance of either arginine type was calculated as shown in Figure 40 (3).

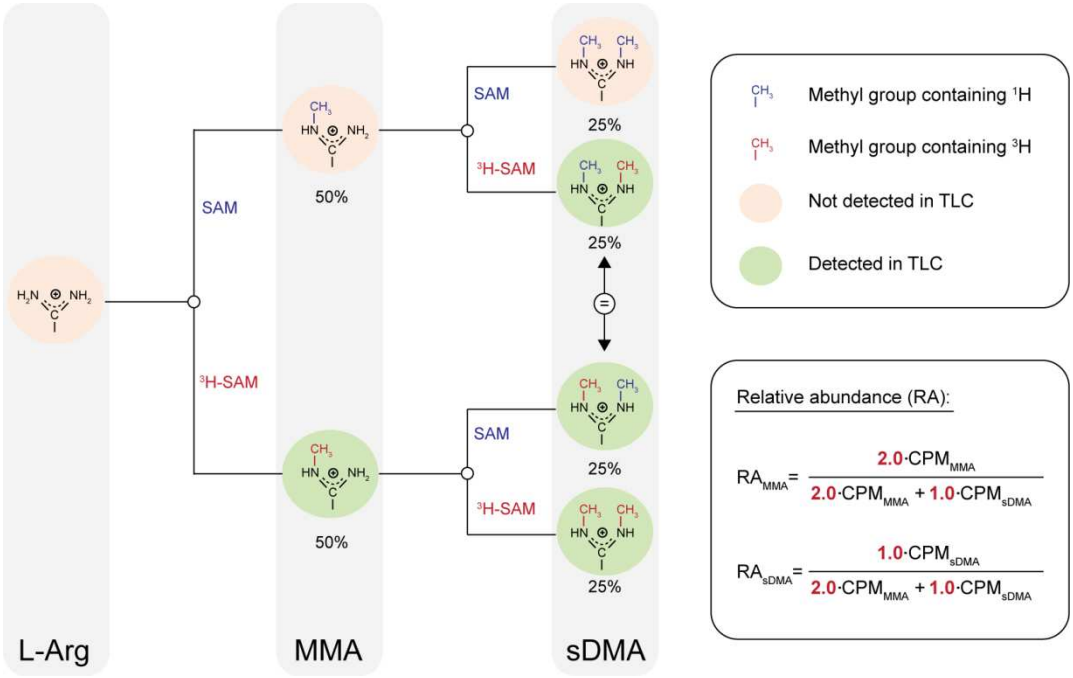

Figure 40 – Determination of the relative abundance of MMAs and sDMAs in thin layer chromatography (TLC).

In Sm protein substrate methylation 50% of the co-factor was radioactively labeled with ^{3}H. In the TLC analysis, only the radioactive methyl group is detected. As the probability of using labeled or unlabeled co-factor is the same in the methylation reaction, only 50% of the actual monomethylation is detected in liquid scintillation counting from thin layer chromatography plates. The amount of symmetrically dimethylated arginine residues has not be adjusted as the event of the transfer of two labeled methyl groups compensates for the event of the incorporation of two unlabeled ones.

In conclusion, an experimental system has been devised to analyze the methylation type that was introduced by a methyltransferase. TLC plates were not routinely analyzed by autoradiography as the exposure time of each experiment augmented to at least 3 weeks (see Appendix 12.12, page 234).

5.5.7 Methylation of Sm protein substrates at increasing time intervals

Once specific techniques had been developed to analyze the overall methylation as well as to determine the methylation type of protein substrates, the kinetics of the methylation reaction could be addressed.

In an enzymatic reaction one commonly measures the formation of product per time shortly after adding the substrate to the enzyme. It is therefore necessary that the

product formation is proportional to the incubation time. Sm protein substrates were to be methylated for 0–90 min in order to identify this linear range.

Furthermore, recombinant PRMT5/WD45 was to be compared with the endogenous PRMT5 complex using cytoplasmic HeLa extract. Consequently, both enzymes were to be used in the methylation reactions. Finally, the formation of MMA and sDMA throughout the entire reaction could be measured.

Recombinant PRMT5/WD45 and Hela cytoplasmic extract were applied to methylate Sm protein substrates pICln/D1/D2, 6S and pICln/D3/B for 0–90 min at 37°C. Reactions were analyzed for overall methylation by SDS-PAGE, autoradiography (Figure 41 A–C and Figure 42 A–C), densitometry (Figure 41 D–F and Figure 42 D–F) and thin layer chromatography (Figure 41 G–I and Figure 42 G–I).

Within the initial 30–60 min, the incorporation of methyl groups was proportional to the incubation time. The methylation rate of B was much lower than the ones of D1 and D3. Both the native and the recombinant protein showed similar methylation properties especially with respect to the methylation type.

Finally, the relative abundance of MMA and sDMA remained stable over the entire reaction (MMA: ≈0.6, sDMA: ≈0.4) (Figure 41 J–L and Figure 42 J–L). In all methylation substrates pICln/D1/D2, 6S and pICln/D3/B the pattern of the relative abundance over time is somewhat different. This pattern will later be used to deduce a possible order in the methylation mechanism (see Results 5.5.13, page 138).

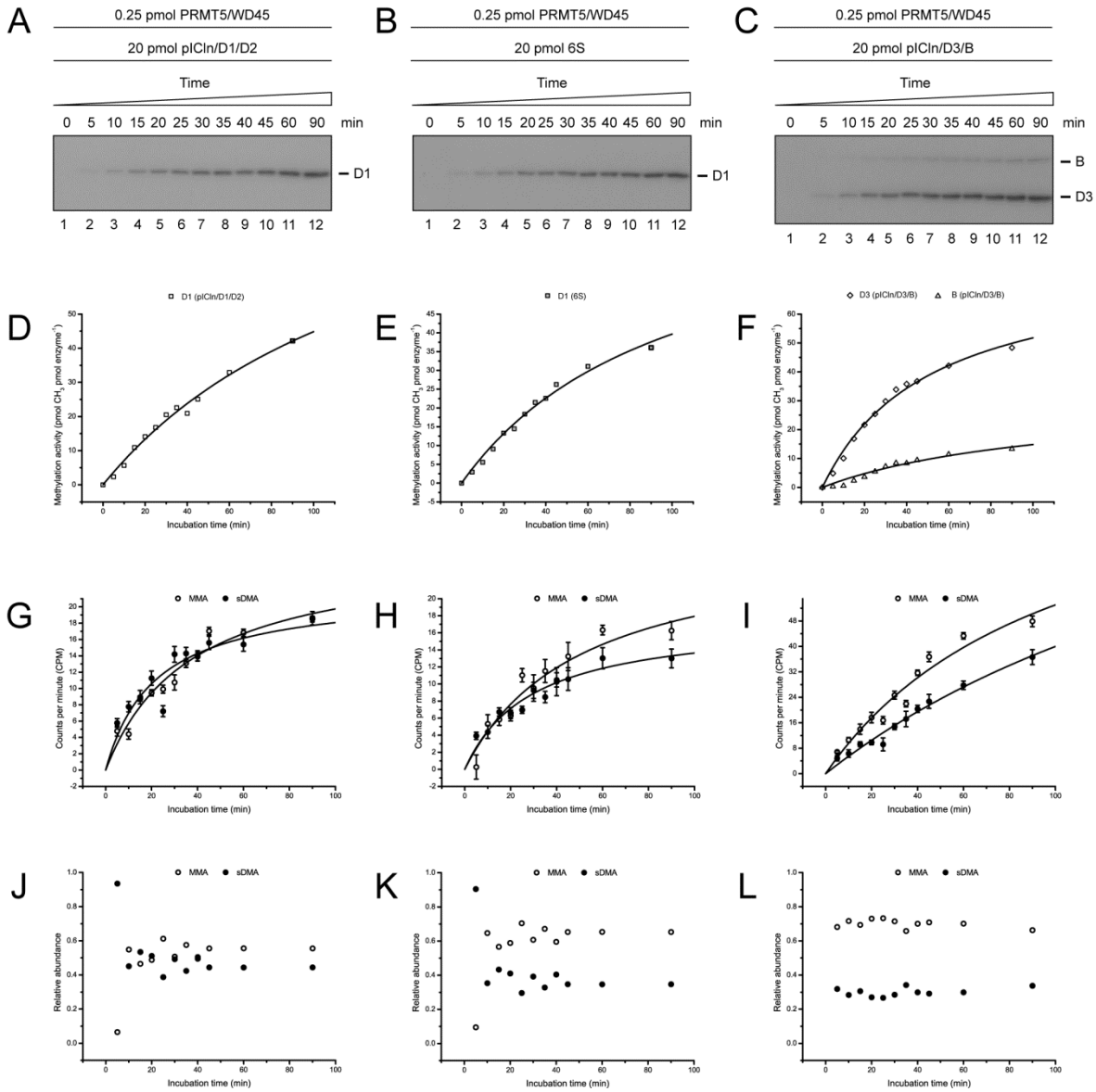

Figure 41 – Methylation of pICln/D1/D2, 6S and pICln/D3/B by recombinant PRMT5/WD45 increasing the incubation time.

Half a picomole of PRMT5/WD45 was used to methylate 40 pmol of pICln/D1/D2 (D1: □), 6S (D1: ■) or pICln/D3/B (D3: ◇, B: △) at 37°C for 0–90 min. Samples were equally split half and either separated by SDS-PAGE and processed in autoradiography **(A–C)** and densitometry **(D–F)** or subjected to total hydrolysis, thin layer chromatography and liquid scintillation counting **(G–I)**. Thus obtained values of radioactive signals in MMA (○) and sDMA (●) were used to calculate the relative abundance of each population at any time point **(J–L)**. Values represent the average of two separate experiments. Error bars show the standard errors of the mean.

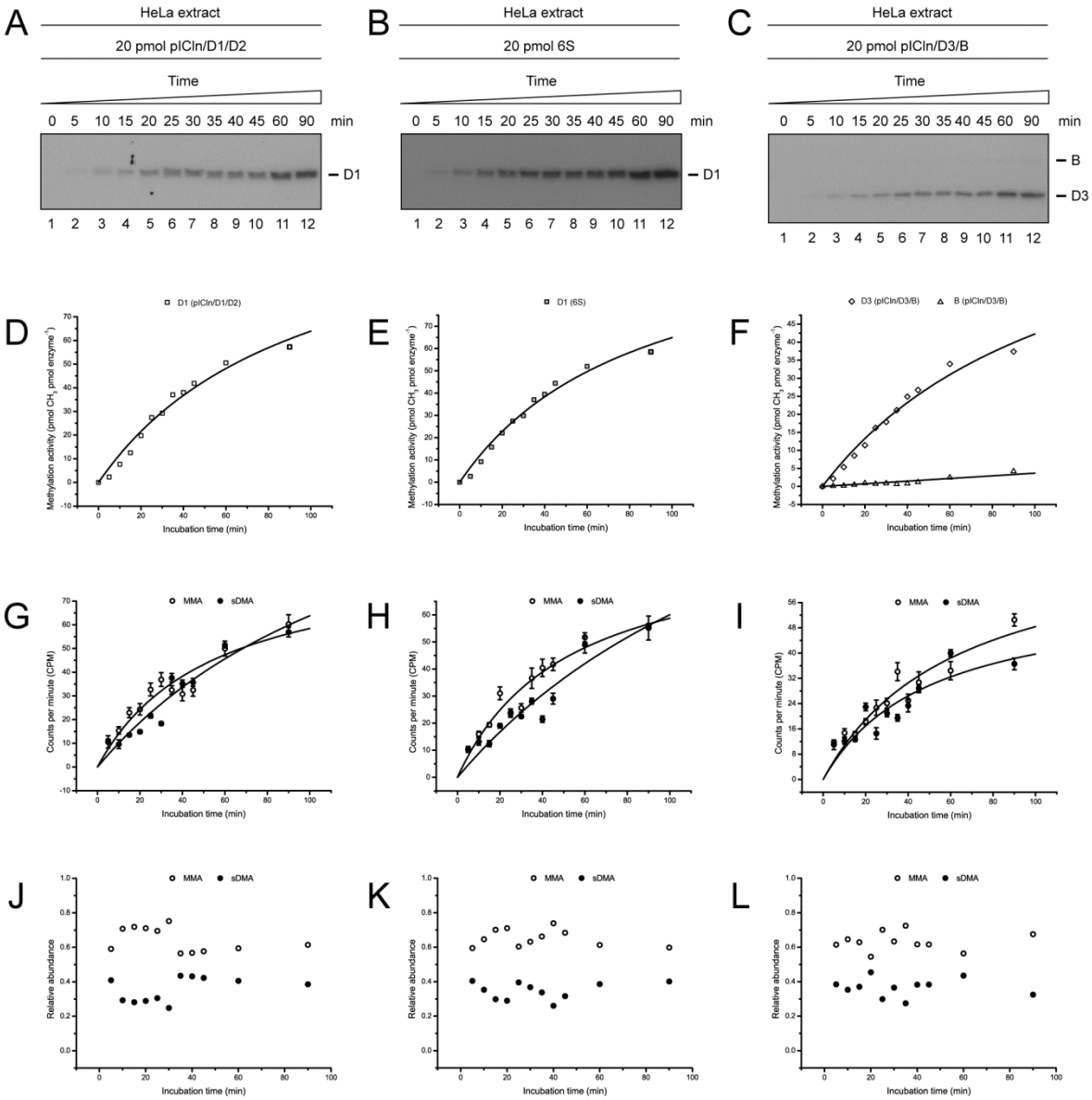

Figure 42 – Methylation of pICln/D1/D2, 6S and pICln/D3/B by total HeLa extract increasing the incubation time.

Total HeLa cell extract was used to methylate pICln/D1/D2 (D1: □), 6S (D1: ■) or pICln/D3/B (D3: ◇, B: △) analogous to the methylation using the recombinant enzyme **(A–C)**. **(D–F)** Densitometric analysis of the autoradiography. **(G–I)** Liquid scintillation counting of MMA (○) and sDMA (●) signals obtained in thin layer chromatography. **(J–L)** Relative abundance of MMA and sDMA over time. Values represent the average of two separate experiments. Error bars show the standard errors of the mean.

5.5.8 Methylation of Sm protein substrates at increasing enzyme concentrations

Both the recombinant and the endogenous enzymes showed similar properties in methylating Sm protein substrates. Only the recombinant one was further used to elucidate the characteristic values of the methylation kinetics.

Individual Sm proteins readily form heterooligomeric complexes *in vivo* which in turn interact with pICln. Since methyl groups can only be transferred onto the Sm proteins B/B', D1 and D3, this leads to five theoretical methylation substrates. Whereas D1/D2, pICln/D1/D2 and 6S contain D1 as a methyl group receptor, both Sm proteins are methylated in D3/B and pICln/D3/B. In the cell, D1/D2 and D3/B most likely do not exist. These substrates are analyzed nevertheless to identify a possible effect of pICln on the methylation reaction.

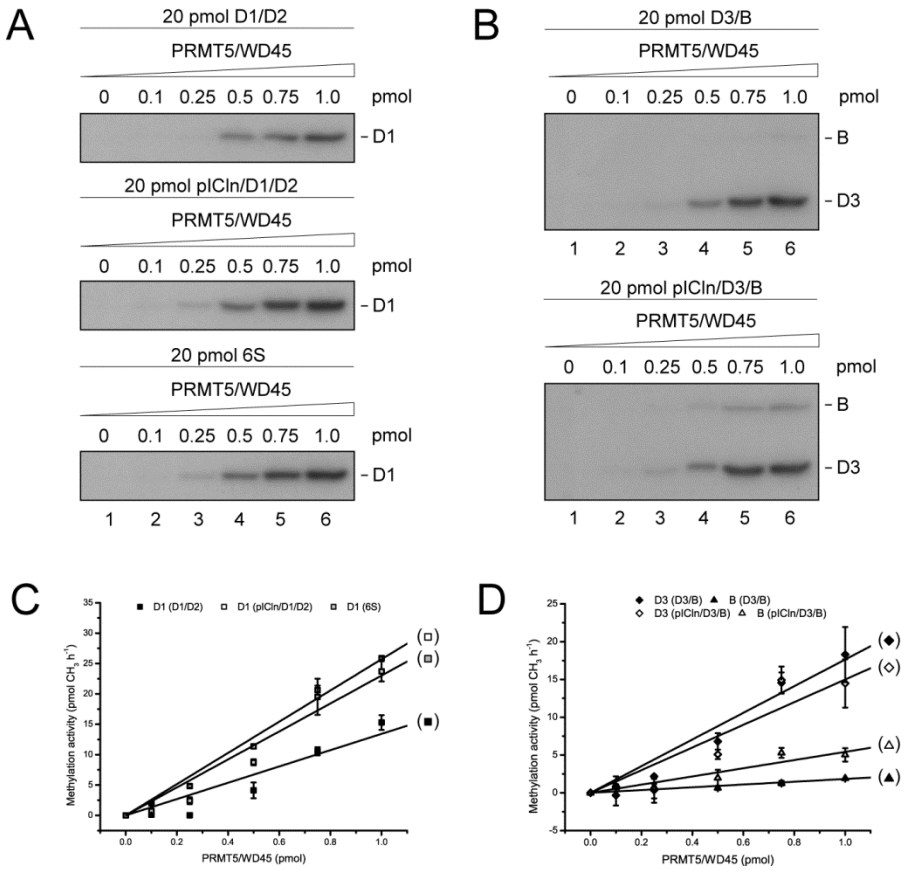

Figure 43 – Titration of recombinant PRMT5/WD45 in Sm protein substrate methylation.

Twenty picomoles of Sm protein substrates D1/D2, pICln/D1/D2 and 6S **(A)**, D3/B and pICln/D3/B **(B)** were methylated by increasing amounts of recombinant PRMT5/WD45 (0–1 pmol) using 219 pmol co-factor for 60 min at 37°C. Radioactive signals were correlated to the number of transferred methyl groups and fitted by linear regression curves. **(C)** D1/D2 (D1: ■), pICln/D1/D2 (D1: □) and 6S (D1: ▩). **(D)** D3/B (D3: ◆, B: ▲) and pICln/D3/B (D3: ◇, B: △). Values represent the average of two separate experiments. Error bars show the standard errors of the mean.

A second prerequisite for the kinetic analysis is a direct relationship between enzyme concentration and enzyme activity. To verify this for PRMT5/WD45, constant amounts of methylation substrates containing D1 (Figure 43 A) and D3/B (Figure 43 B) were

incubated with increasing amounts of recombinant PRMT5/WD45. The number of transferred methyl groups per time (methylation activity) was proportional to the enzyme concentration for each methylation substrate. In the D1-containing group, pICln/D1/D2 was slightly stronger methylated than 6S. D1/D2, on the other hand, received only half as many methyl groups (Figure 43 C). In Sm protein complexes containing D3/B, methylation of D3 was 5-fold stronger than that of B. Additionally, more methyl groups were transferred to D3 in the absence of pICln, whereas for B the case was the opposite (Figure 43 D). The initial protein ratio of D3 to B in the methylation substrates, however, was identical (Figure 25, compare lanes 4 and 8).

5.5.9 Methylation of Sm protein substrates at increasing co-factor concentrations

PRMT5 catalyzes the transfer of methyl groups from S-adenosylmethionine onto an arginine residue of the Sm proteins B, D1 or D3. Consequently, the reaction requires two substrates – an Sm protein and the co-factor. The enzyme kinetics model of Michaelis and Menten is based on the turnover of a single substrate. To verify whether the methylation of Sm protein substrates and the co-factor followed Michaelis-Menten kinetics, one of the two substrates had to be provided in a large excess. By this, either the co-factor or the methylation substrate could be analyzed individually (see Methods 4.3.19.3 and 4.3.19.4, pages 72).

Constant amounts of PRMT5/WD45 were incubated with an excess of pICln/D1/D2 and increasing amounts of a mixture of radioactively labeled and non-labeled co-factor (SAM) for 1 h at 37°C (Figure 44). The methylation activity increased asymptotically towards a maximum value while increasing the co-factor concentration (Figure 44 B). Consequently, the reaction followed the Michaelis-Menten model having a K_m value of 2.58 µM and a V_{max} of 17.83 picomoles of methyl groups per hour and picomole enzyme. Use of the optimized reaction buffer conditions prevented the decline of the methylation rate at higher co-factor concentrations (compare Figure 44 B with Figure 34A).

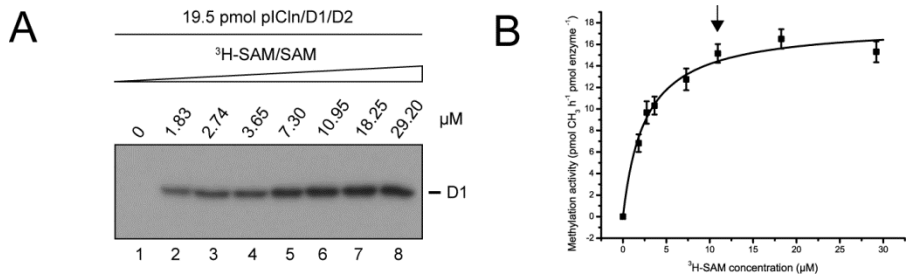

Figure 44 – Methylation of pICln/D1/D2 using increasing co-factor concentrations.

One picomole of PRMT5/WD45 was applied to methylate 19.5 pmol of pICln/D1/D2 with increasing amounts of co-factor (0–29.20 µM) at 37°C for 1 h in the optimized reaction buffer 100 mM Hepes-NaOH, 200 mM NaCl and 5 mM DTT (pH 8.2). Samples were separated in SDS-PAGE and were analyzed by autoradiography **(A)** and densitometry **(B)**. The arrow indicates the smallest amount of co-factor needed to saturate the enzyme with co-factor. Values represent the average of two separate experiments. Error bars show the standard errors of the mean.

5.5.10 Methylation of Sm protein substrates at increasing substrate concentrations

So far, the analysis of the methylation kinetics of the type II methyltransferase PRMT5 has been hampered by the unavailability of a recombinant and biologically active protein. Having insect cell-expressed PRMT5/WD45 at hand, it was to be shown whether the methylation of Sm protein substrates followed Michaelis-Menten kinetics. Furthermore, the specific values of K_m, V_{max} and k_{cat}, as well as the methylation efficiency of each substrate were to be determined. These data provide insight into substrate preference, maximum methylation rates and how efficiently one substrate is methylated in comparison to another one.

PRMT5/WD45 and a large excess of co-factor were incubated with increasing amounts of all five methylation substrates (D1/D2, pICln/D1/D2, 6S, D3/B and pICln/D3/B). Methylation was carried out at 37°C for 1 h and was evaluated by autoradiography and densitometry (Figure 45). In substrates containing D1, the most methyl groups were transferred onto D1/D2, followed by pICln/D1/D2, which in turn was only slightly more methylated than 6S (Figure 45 A and C). The methylation of D3 and B-containing substrates resulted in a better methylation of D3. However, in comparison to the previous enzyme titration, the pICln-bound form received twice as many methyl groups than the unbound one (Figure 45 B and D). Sm protein B was weakly methylated in pICln/D3/B, whereas methylation in D3/B was almost not visible on the X-ray film. Consequently, kinetic data obtained for B were not reliable due to low signal intensity.

The methylation activity asymptotically reached a maximum value when the substrate concentration was increased. Thus, the transfer of methyl groups catalyzed by PRMT5 followed the Michaelis-Menten model. In order to obtain the Michaelis constant K_m, the maximum methylation activity V_{max}, the turn-over number k_{cat} and the efficiency of the methylation reaction ($k_{cat} \cdot K_m^{-1}$), the data points were applied to the Michaelis-Menten equation using non-linear least square fitting (Figure 45 C and D). Linearization of the kinetic data was performed to obtain the above mentioned kinetic constants using the methods of Lineweaver/Burk, Hanes/Woolf and Eadie/Hofstee (Appendix 12.10.1, page 226). Finally, average values stemming from all four methods were calculated (Table 8).

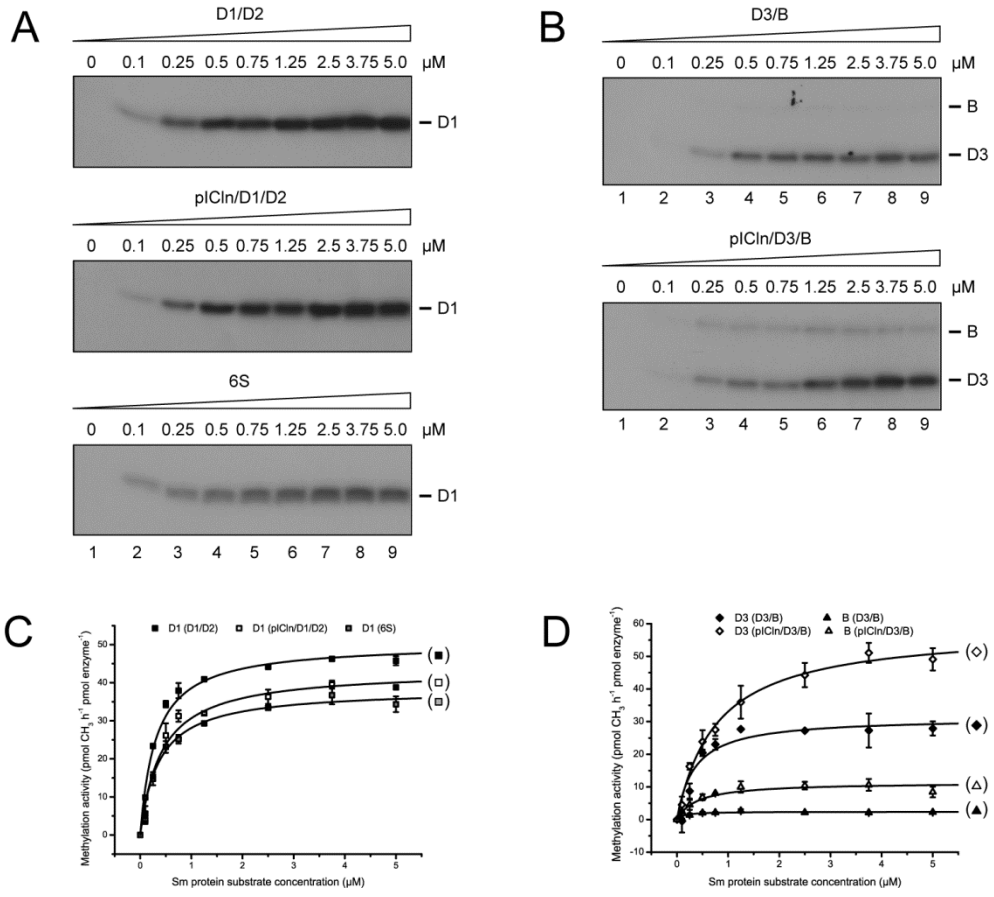

Figure 45 – Methylation of increasing Sm protein substrate concentrations.

One picomole PRMT5/WD45 was used to methylate increasing amounts of Sm protein substrates (0–5 µM) with 11 µM co-factor for 1 h at 37°C. After separation in SDS-PAGE, radioactive signals were visualized by autoradiography and analyzed by densitometry using the ImageJ software. Finally, each data set was fitted to standard Michaelis-Menten kinetics using non-linear regression analysis. **(A)** Autoradiography of D1/D2, pICln/D1/D2 and 6S. **(B)** Autoradiography of D3/B and pICln/D3/B. **(C-D)** Fitted Michaelis-Menten curves of the Sm protein substrate methylation of D1/D2 (D1: ■), pICln/D1/D2 (D1: □) and 6S (D1: ▣) **(C)** and D3/B (D3: ◆, B: ▲) and pICln/D3/B (D3: ◇, B: △) **(D)**. Values represent the average of four separate experiments. Error bars show the standard errors of the mean.

In the D1-containing substrates the maximum methylation rate V_{max}, and consequently the turn-over number k_{cat}, decreased with the increasing size of the substrate. The K_m value of pICln/D1/D2 and 6S were identical and 50% higher than that of D1/D2. Finally, the efficiency of the methylation reaction was twice as high in D1/D2 as in pICln/D1/D2 and 6S.

The maximum methylation activity V_{max} and the turn-over number in D3 and B-containing complexes were 3 to 5-fold higher in the presence of pICln. Similar results were obtained for K_m, which was approximately twice as high. As mentioned above, kinetic data obtained for B were not reliable due to the low signal intensity.

Table 8 – Kinetic data of Sm protein substrate methylation.

Substrate	CH_3-recipient	V_{max} (pmol CH_3 h^{-1} pmol enzyme^{-1})	K_m (µM)	k_{cat} (s^{-1})	k_{cat} K_m^{-1} (s^{-1} $µM^{-1}$)
D1/D2	D1	48.531 (+/- 0.81%)	0.238 (+/- 6.73%)	0.013	0.057
pICln/D1/D2	D1	41.786 (+/- 0.75%)	0.358 (+/- 5.86%)	0.012	0.032
6S	D1	37.857 (+/- 1.28%)	0.347 (+/- 4.04%)	0.011	0.030
D3/B	D3	29.997 (+/- 2.99%)	0.29 (+/- 12.74%)	0.008	0.029
D3/B	B	2.301 (+/- 2.52%)	0.142 (+/- 7.72%)	0.001	0.004
pICln/D3/B	D3	57.804 (+/- 1.52%)	0.701 (+/- 3.14%)	0.016	0.023
pICln/D3/B	B	11.381 (+/- 5.7%)	0.359 (+/- 17.26%)	0.003	0.009

In conclusion, the methylation of Sm protein substrates D1/D2, pICln/D1/D2, 6S, D3/B and pICln/D3/B followed Michaelis-Menten kinetics. D1/D2 and D3/B readily interact with pICln *in vivo* to generate pICln-Sm protein complexes. Consequently, these substrates were analyzed only to identify the effect of pICln-binding has on substrate methylation. Both pICln/D1/D2 and 6S exhibited similar values in K_m, V_{max}, k_{cat} and the methylation efficiency. The presence of pICln caused an increase in the K_m value and in turn a decrease in the efficiency. In the D3/B-containing substrates, addition of pICln increased both the K_m value as well as V_{max}. Consequently, the only common effect of pICln was to increase the K_m value.

5.5.11 Competition of the PRMT5 methylation reaction

In the biochemical analysis of the PRMT5 complex it was shown that 6S is assembled on the PRMT5 complex (Results 5.4.3, page 105). The subsequent kinetic studies resulted in K_m values that were similar for pICln/D1/D2 and 6S. In the literature, the reciprocal K_m value is often associated with the affinity of an enzyme for its substrate. This correlation, however, is oversimplified. More precisely, the K_m value corresponds to a substrate concentration at which catalysis works effectively. In order to differentiate between affinities of PRMT5/WD45 for the various Sm protein substrates, methylation competition experiments were to be carried out.

In an initial experiment, each of the five Sm protein substrates (D1/D2, pICln/D1/D2, 6S, D3/B and pICln/D3/B) was incubated alone (Figure 46 A, lanes 1–5) or with the respective other ones (Figure 46 A, lanes 6–15). Additionally, all five substrates were methylated at the same time (Figure 46 A, lane 16). The number of methyl groups that were transferred onto B, D1 and D3 were identified by SDS-PAGE, autoradiography and densitometry. Finally, the resulting methylation activities could be directly plotting in bar charts (Figure 46 B-G).

Since only the methylation of B, D1 or D3 could be identified, comparison between methylation substrates was only possible if a protein complex contained D1 and the competing one D3/B or *vice versa*. The overall methylation activity was similar in all reactions indicating that the active sites of the enzymes were saturated and competition between substrates could take place. Overall, three major effects could be seen. First, as seen in previous experiments, D3 was more effectively methylated than B. Second, D3/B-containing complexes caused stronger competition when attached to pICln (Figure 46 B-D, lanes 4 and 5). Third, D3/B-containing complexes interfered most strongly with the methylation of 6S, followed by pICln/D1/D2 and D1/D2 (Figure 46 E-F, lanes 2–4).

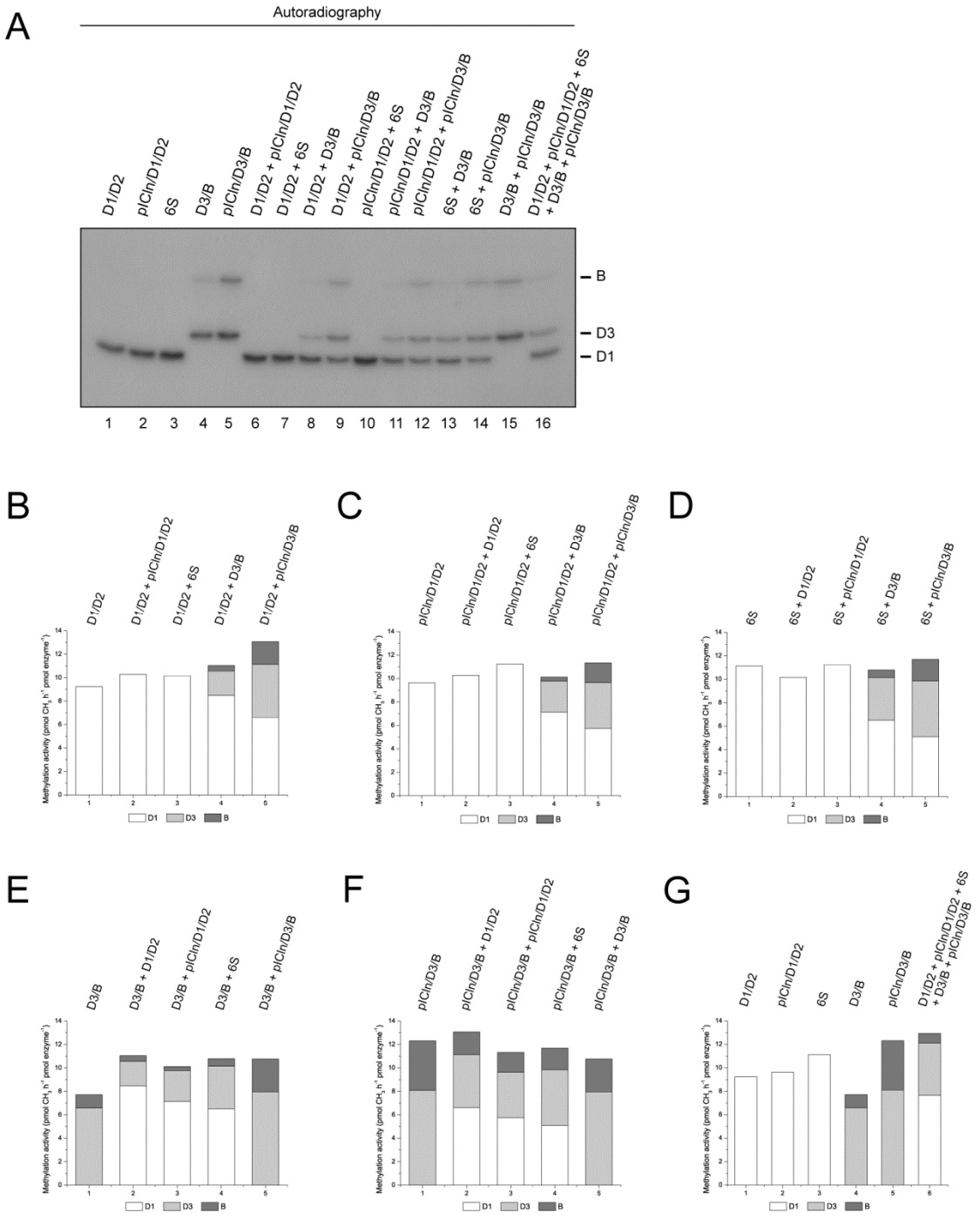

Figure 46 – Methylation of Sm protein substrate mixtures.

Combinations of two Sm protein substrates (5 pmol each) were methylated by 1 pmol of PRMT5/WD45 using 219 pmol co-factor for 60 min at 37°C, separated by SDS-PAGE and analyzed by autoradiography **(A, lanes 1–15)**. Additionally, a mixture of all Sm protein substrates was processed likewise **(A, lane 16)**. The autoradiography signals were subjected to densitometry to directly compare the change of D1 (white), D3 (light gray) and B (dark gray) methylation in each Sm protein substrate in the presence of any other competing methylation substrate: **(B)** D1/D2, **(C)** pICln/D1/D2, **(D)** 6S, **(E)** D3/B, **(F)** pICln/D3/B. Finally, all methylation substrates were compared with each other **(G)**.

Following this preliminary test of whether competition of the methylation reaction by other substrates was possible, constant amounts of Sm protein substrates were methylated in the presence of 0 to 20-fold molar excess of competing substrates.

Substrates D1/D2, pICln/D1/D2 and 6S were competed with D3/B and pICln/D3/B (Figure 47); substrates D3/B and pICln/D3/B with D1/D2, pICln/D1/D2 and 6S (Figure 48). Without a competing substrate a certain number of methyl groups was transferred onto the Sm protein substrate. The higher the competitor concentration needed to decrease the initial methylation rate by 50%, the higher the affinity of the initial substrate towards the enzyme. As the decrease followed a hyperbolic curve, only small changes in competitor concentration were needed for this reduction. The substrate pICln/D3/B was shown to be a much more effective competitor than D3/B since a 20-fold excess of pICln/D3/B was sufficient to fully diminish D1 methylation. Addition of the same amounts of D3/B still enabled D1 modification (Figure 47, compare A–C with D–F)

When using D1-containing Sm protein substrates as a competitor, D1/D2 was most effective, followed by pICln/D1/D2 and 6S (Figure 48). The initial methylation rate of pICln/D1/D2 and 6S was cut in half when adding 1.74 and 0.67-fold molar excess of pICln/D3/B. In the opposite case, when pICln/D3/B methylation was competed with pICln/D1/D2 and 6S, a molar excess of 5.39 and 6.05 was needed, respectively. Consequently, the Sm protein substrate pICln/D1/D2 had a higher affinity towards PRMT5/WD45 than 6S.

In conclusion, PRMT5 is capable of transferring methyl groups onto a variety of Sm proteins substrates. The endogenous 20S complex comprises PRMT5/WD45, pICln/D1/D2 and pICln/D3/B. Competition experiments using equimolar amounts of both substrates indicated that an equal amount of methyl groups was transferred onto each substrate. Further methylation competitions provided evidence that pICln/D1/D2 had a higher affinity towards PRMT5/WD45 than 6S. This finding supports the previous observations that pICln/D1/D2 is capable of releasing 6S from the PRMT5 complex (Results 5.4.4, page 107).

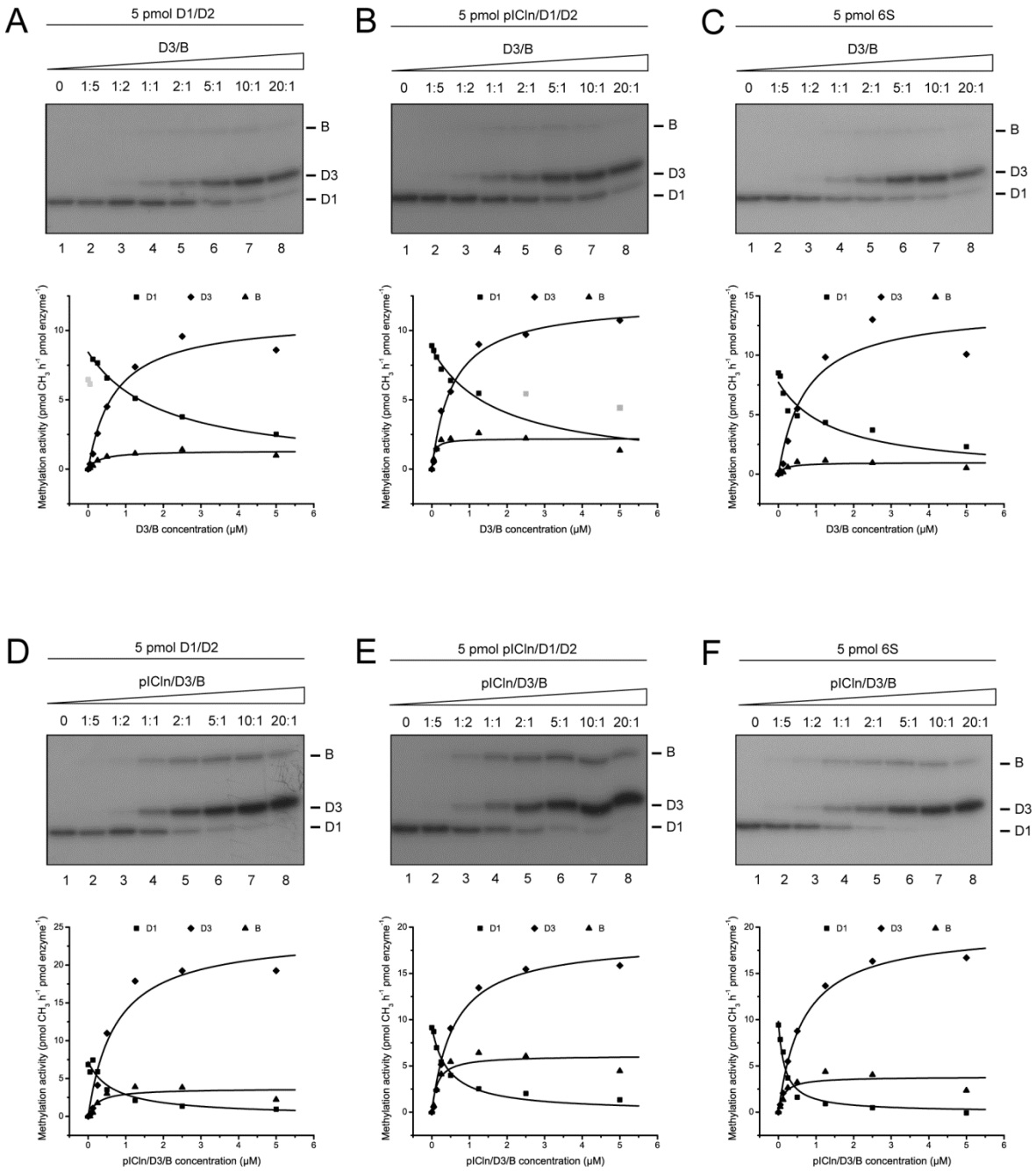

Figure 47 – Methylation competition of D1 containing substrates with D3/B containing ones.

Five picomoles of Sm protein substrates D1/D2 (D1: ■) **(A,D)**, pICln/D1/D2 (D1: ■) **(B,E)** and 6S (D1: ■) **(C,F)** were methylated with 1 pmol PRMT5/WD45 and 219 pmol co-factor for 1 h at 37°C with increasing amounts (0 to 20-fold molar excess) of D3/B (D3: ◆, B: ▲) **(A-C)** or pICln/D3/B (D3: ◆, B: ▲) **(D-F)**. Upper panel: Autoradiography of SDS-PAGE, lower panel: Densitometry of autoradiography signals fitted to saturation kinetics using non-linear regression. Gray data points are outliers and were not considered in the regression analysis.

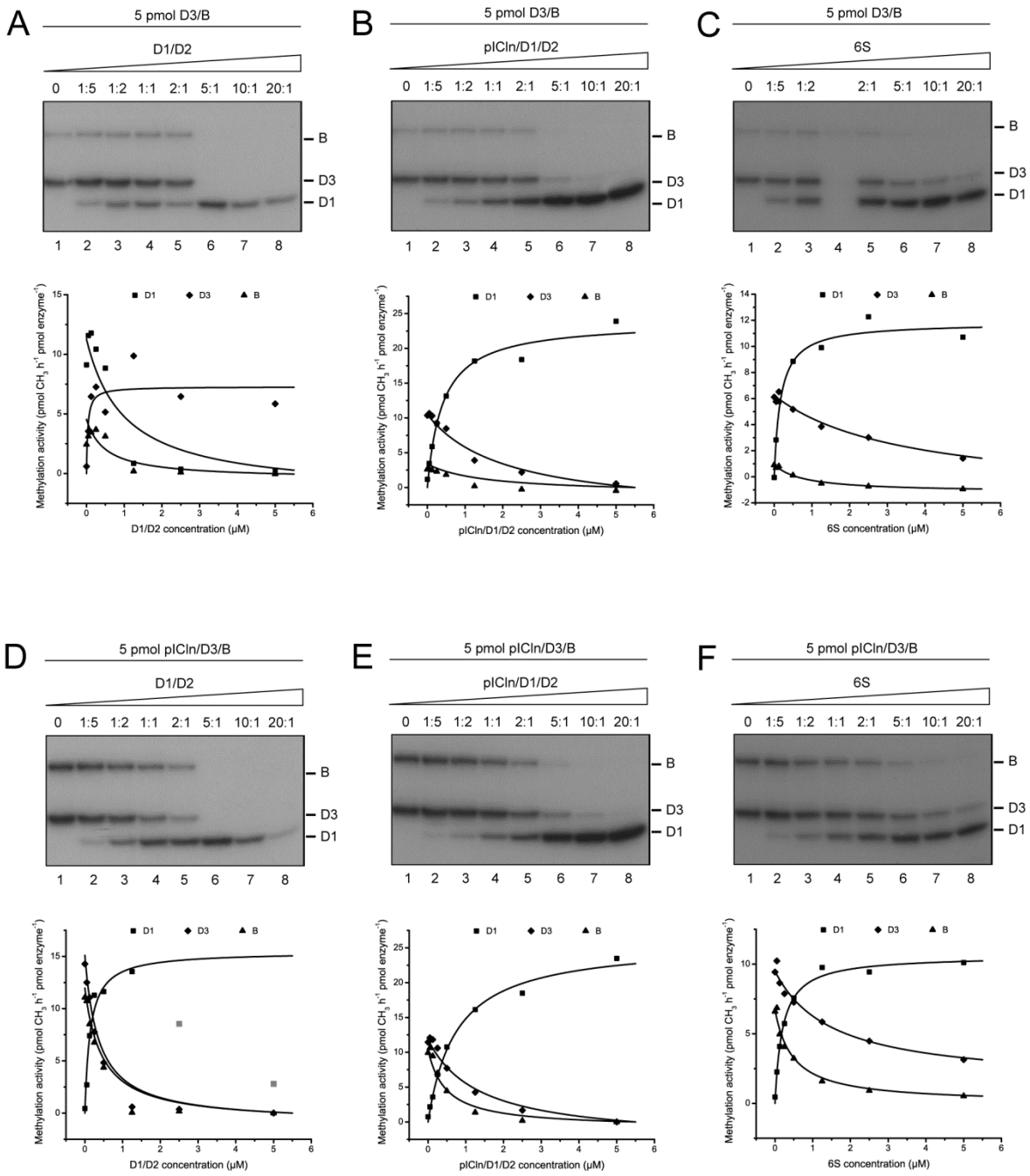

Figure 48 – Methylation competition of D3 and B containing substrates with D1 containing ones.

Five picomoles of Sm protein substrates D3/B (D3: ◆, B: ▲) **(A-C)** and pICln/D3/B (D3: ◆, B: ▲) **(D-F)** were methylated with 1 pmol PRMT5/WD45 and 219 pmol co-factor for 1 h at 37°C with increasing amounts (0 to 20-fold molar excess) of D1/D2 (D1: ■) **(A,D)**, pICln/D1/D2 (D1: ■) **(B,E)** or 6S (D1: ■) **(C,F)**. Upper panel: autoradiography of SDS-PAGE, lower panel: densitometry of autoradiography signals fitted to saturation kinetics using non-linear regression. Gray data points are outliers and were not considered in the regression analysis.

5.5.12 PRMT5 methylates Sm protein substrates distributively

So far it could be shown that recombinant PRMT5/WD45 expressed in insect cells is capable of methylating Sm proteins B, D1 and D3. Furthermore, the enzyme catalyzes both MMA as well as sDMA formation verifying its type II methyltransferase activity. The major difference between Sm protein substrates and histones is the number of receptive arginine residues. Sm proteins B, D1 and D3 contain so-called RG repeats in their C-terminal domains comprising 6, 9 and 4–5 possible methylation sites (Introduction Figure 10, page 16). Consequently, the question arises whether PRMT5 acts processively or distributively on these substrates. In a processive mechanism, PRMT5 could interact with an unmethylated substrate catalyzing the complete dimethylation of all arginine residues. Alternatively, PRMT5 could act distributively, dissociating from the substrate after each methylation reaction.

In principle, a processive and distributive mechanism can be distinguished by methylating a substrate for a short time before adding a large excess of competing substrate. If the enzyme was processive, the initial substrate would remain associated with the enzyme until it was completely methylated. Consequently, the methylation activity of the initial substrate would continue to increase. A distributive enzyme would release the substrate after each reaction, thus stalling any further methylation of the substrate.

In the previous experiment, it was shown that a 20-fold molar excess of pICln/D3/B caused complete methylation inhibition of pICln/D1/D2 and 6S. A 20-fold molar excess of pICln/D1/D2 and a 30-fold molar excess of 6S prevented methylation of pICln/D3/B. To analyze whether recombinant PRMT5/WD45 followed a processive or distributive mechanism with respect to 6S (containing D1 as a methylation substrate) or pICln/D3/B (comprising the methylation substrates D3 and B) methylation, the initial substrate was methylated for 0–90 min. Without competitor, the methylation activity primarily increased proportional to the incubation time and asymptotically reached a maximum value (Figure 49 A and Figure 50 A). Immediately adding a large excess of competitor to the reaction completely inhibited the methylation of the initial substrate (Figure 49 B and Figure 50 B). Finally, the initial substrate was methylated for 15 min before an excess of competitor was supplied. Whereas the methylation rate of the competitor increased over time, the methylation of the initial substrate remained stable. Identical results were obtained for the methylation of pICln/D1/D2 (data not shown). Therefore, PRMT5

exhibits a distributive methylation mechanism for substrates containing D1 as well as D3 and B.

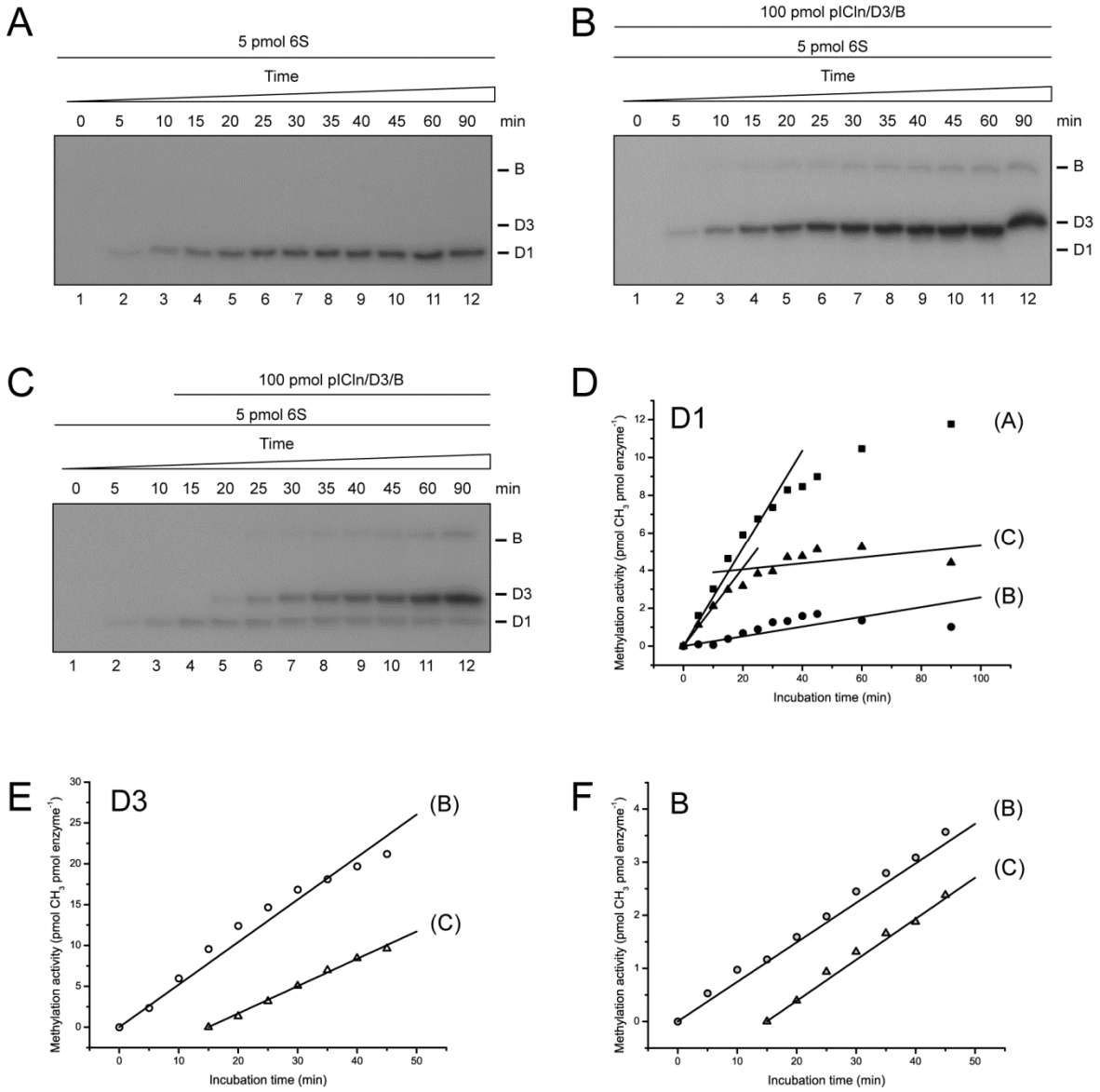

Figure 49 – The 6S complex is methylated distributively by recombinant PRMT5/WD45.

Five picomoles of 6S were methylated by 1 pmol of PRMT5/WD45 with 219 pmol of co-factor at 37°C for 0–90 min **(A)**. The identical reaction was repeated adding a 20-fold molar excess of pICln/D3/B at 0 min **(B)** or 15 min of incubation **(C)**. Samples were analyzed by SDS-PAGE, autoradiography, densitometry and grayscale value correlation. Resulting values of increased methylation were plotted for the individual methylation substrates D1 **(D)**, D3 **(E)** and B **(F)**.

In conclusion, PRMT5 is a type II methyltransferase that acts distributively on Sm protein substrates. After each methylation reaction the substrate is released from the enzyme. For symmetrical dimethylation of a single arginine residue the substrate has to interact with the enzyme twice.

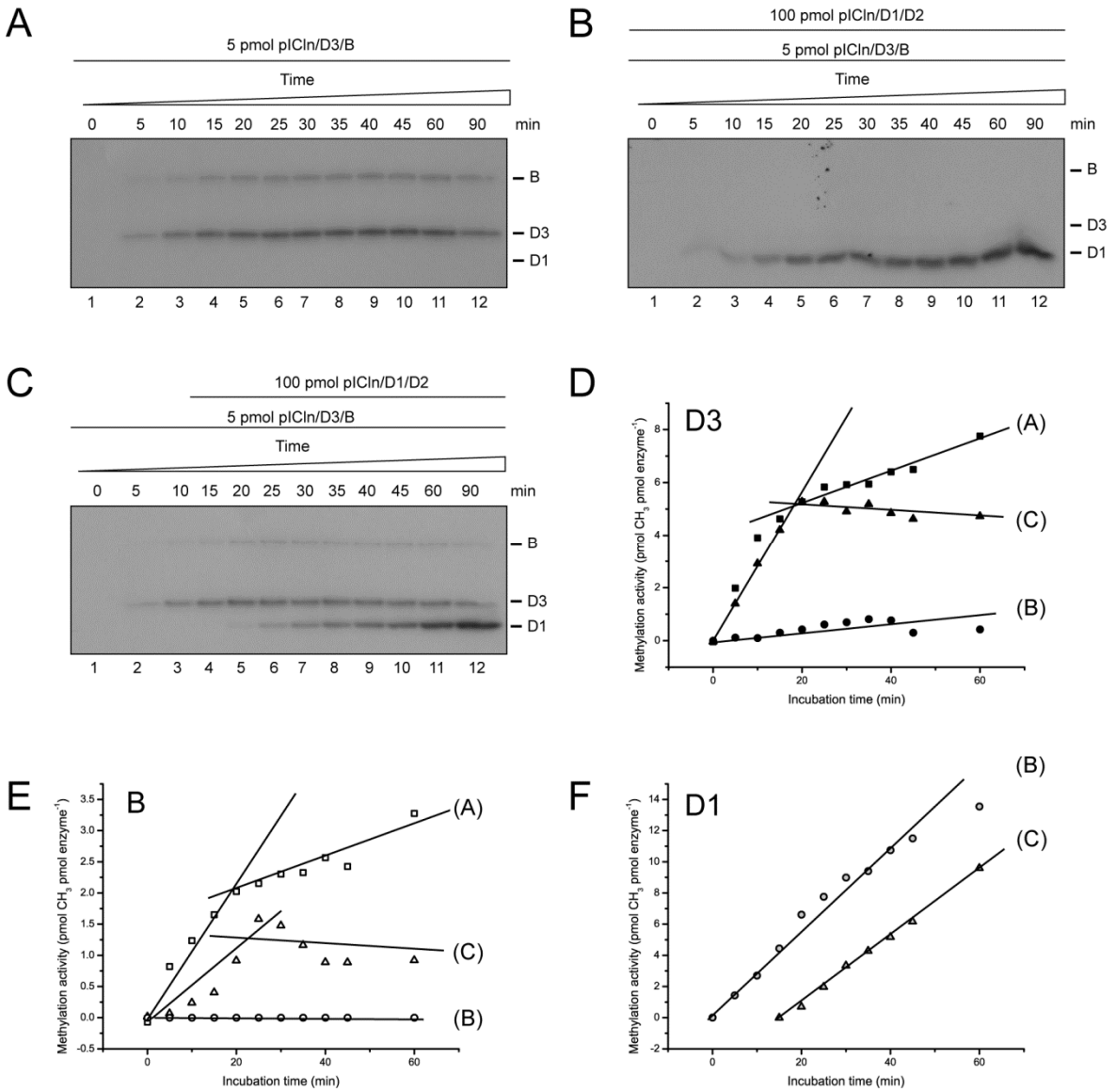

Figure 50 – The pICln/D3/B complex is methylated distributively by recombinant PRMT5/WD45.

Five picomoles of pICln/D3/B were methylated by 1 pmol of PRMT5/WD45 with 219 pmol of co-factor at 37°C for 0–90 min **(A)**. The identical reaction was repeated adding a 20-fold molar excess of pICln/D1/D2 at 0 min **(B)** or 15 min of incubation **(C)**. Samples were analyzed by SDS-PAGE, autoradiography, densitometry and grayscale value correlation. Resulting values of increased methylation were plotted for the individual methylation substrates D3 **(D)**, B **(E)** and D1 **(F)**.

5.5.13 PRMT5 catalyzes MMA and sDMA formation in various substrate proteins

The fact that PRMT5 follows a distributive reaction mechanism indicates that the enzyme has to interact 18 times with D1-containing substrates to achieve complete symmetrical dimethylation. Sm D1 contains nine overlapping GRG motifs that are recognized by PRMT5. So far, it is unknown whether there is a specific reaction order in which the methyl groups are transferred onto Sm proteins. The data obtained in this work do not

provide information on what specific arginine residues are modified. Previously, Sm protein methylation and MMA as well as sDMA formation was measured over time (Results 5.5.7, page 122).

A theoretical model for the methylation of arginine residues was developed in order to identify whether PRMT5 specifically acted on singular substrate molecules or indiscriminately methylated various ones (see Appendix 12.11, page 231). When constant amounts of Sm protein substrates pICln/D1/D2, 6S and pICln/D3/B were methylated by recombinant PRMT5/WD45 and HeLa extract at increasing time intervals, the relative abundance of MMA and sDMA stayed approximately the same over time (Figure 41 and Figure 42). Shortly after the beginning of the methylation reaction, the relative abundance of MMA accounted for 60% and of sDMA for 40% of total modifications.

Monomethylated arginines are generated by the transfer of a methyl group onto a non-modified arginine residue. Formation of symmetrically dimethylatated arginines requires the presence of an MMA receiving a second methyl group. According to the relative abundance of MMA and sDMA directly after the beginning of the reaction, consecutive mono- and dimethylation has to occur on the same substrate. Initially, more unmethylated than monomethylated substrates are present and thus MMA formation is statistically more likely than sDMA formation. Therefore, in the following steps, one or more MMA-causing events but fewer symmetrical dimethylations will occur.

A general model characterizing this sequential methylation of substrates has been devised and is explained in the Appendix 12.11, page 231. According to this model, substrate protein interacts with PRMT5 and receives a single methyl group on an arginine residue. Since PRMT5 acts distributively, the methylated substrate is released from the enzyme. In the next step, the monomethylated substrate associates once more with the enzyme to receive a second methyl group. The MMA is transformed to sDMA and the substrate is once more expelled from the enzyme. These two initial reactions are then followed by various (*n*) monomethylation steps and a single sDMA formation event. For n = 1, each MMA formation would be directly followed by a symmetrical dimethylation resulting in almost only sDMA formation. Since the data obtained for pICln/D1/D2, 6S and pICln/D3/B contain up to 60% MMA, a value greater than n = 1 has to be expected. Scenarios for n = 1,2,3,4 have been calculated and are depicted in the Appendix of this work (Appendix 12.11, page 231). All four scenarios resulted in distinct profiles for the

relative abundance of MMA and sDMA in methylated substrates with respect to increasing numbers of transferred methyl groups.

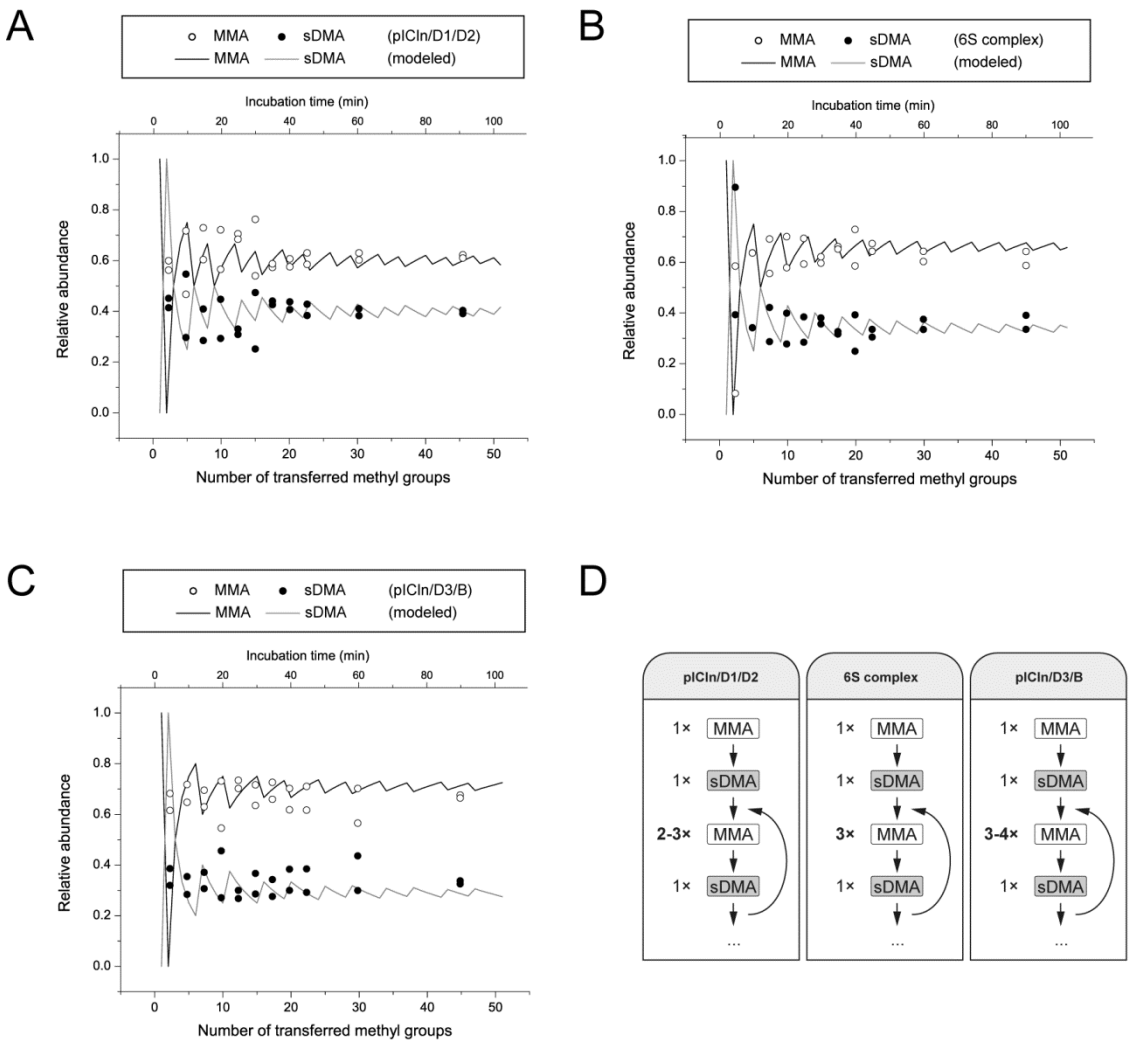

Figure 51 – Methylation order of Sm protein substrates

A theoretical model was devised in which unmethylated Sm protein substrates were once mono- and dimethylated consecutively. Then, iterative n-fold MMA (n = 1 – 4) and single sDMA formation was hypothesized with respect to a continuous transfer of methyl groups (see Appendix 12.11, page 231 for more information). **(A-C)** Graphs of the theoretical model with overlaid the data points of the methylation of pICln/D1/D2 **(A)**, 6S **(B)** and pICln/D3/B **(C)** using recombinant protein as well as HeLa extract as depicted in Figure 41 J–L and Figure 42 J–L. **(D)** Schematic overview of the methylation order most likely occurring in pICln/D1/D2, 6S and pICln/D3/B.

When the Sm protein substrates pICln/D1/D2, 6S and pICln/D3/B were methylated by recombinant PRMT5 and HeLa extract, the methylation rate was proportional to the incubation time within the initial 30–60 min (Figure 41 and Figure 42, pages 124 and 125). Consequently, data observed in this reaction could be explained with the above

mentioned model. The data of the individual substrates were compared with the models for n = 1,2,3,4 and alternating values n = 2/n = 3 (n = 2 – 3) or n = 3/n = 4 (n = 3 – 4). All substrates correlated to the methylation model with slightly different n-values for pICln/D1/D2 (n = 2 – 3), 6S (n = 3) and pICln/D3/B (n = 3 – 4) (Figure 51). This showed that pICln/D1/D2 has a somewhat higher rate of incorporating sDMA than 6S when both are presented separately to the enzyme. The higher the obtained n-values the more monomethylated arginines are generated in comparison to symmetrically dimethylated ones. Consequently, it is unlikely that PRMT5 processes singular substrate molecules until they are completely symmetrically dimethylated. Yet, it cannot be excluded that monomethylation occurs on the same molecule until all receptive arginines carry at least one methyl group. The above stated model only covers the initial phase of methylation and is based on the application of a constant amount of substrate. In later stages of the methylation reaction, most arginines will carry at least one methyl group.

In classical enzyme kinetic reactions increasing amounts of substrate were methylated by PRMT5/WD45 for 60 min (Results 5.5.10, page 128). Apart from deducing the characteristic values of V_{max}, K_m and k_{cat} as well as the methylation efficiency, the relative abundance of MMA and sDMA was determined. This was done by hydrolyzing the methylated proteins and separating the individual amino acids in thin layer chromatography (Appendix 12.10.2 and 12.10.3, page 227 and 229). The lower the substrate concentration was in the reaction, the higher was the relative abundance of sDMA and *vice versa* (see Figure 75 and Figure 77 on pages 228 and 230). This effect was verified by liquid scintillation counting of the scraped TLC plate surface as well as autoradiography (Appendix 12.12, page 234). In all substrates, mostly MMA could be detected in autoradiography as well as in liquid scintillation counting. Therefore, it could be shown that PRMT5 is capable of forming monomethylated as well as symmetrically dimethylated arginines. The type of methylation strongly depended on the initial substrate concentration.

In summary, PRMT5 acts distributively on Sm protein substrates initially causing mono- and symmetrical dimethylation of the same arginine residue. Depending on the substrate to enzyme ratio, PRMT5 catalyzes mainly MMA formation at high and sDMA at low ratios. Finally, it could be shown that Sm protein substrates slightly differ in the order of MMA and sDMA formation indicating that at the same concentration more sDMAs are formed in pICln/D1/D2 than in pICln/D3/B.

5.6 Expression and purification of SMN complex components

5.6.1 Introductory notes

In the early phase of cytoplasmic snRNP assembly, the PRMT5 complex sequesters the Sm proteins and catalyzes the symmetrical dimethylation of B/B', D1 and D3. pICln, an integral component of the PRMT5 complex associates with Sm proteins and thus imposes a kinetic trap that prevents Sm proteins from interacting with snRNA. The late phase of snRNP assembly is characterized by the SMN complex that binds to Sm proteins, expels pICln and thus provides the U snRNP assembly to proceed.

To recapitulate this phase in vitro, all SMN complex components were to be generated in recombinant form. So far, expression and purification of Gemin3, Gemin4 and Gemin5 in bacterial cells previously resulted in insoluble or biologically inactive protein. In order to reconstitute the entire human SMN complex *in vitro*, the central complex components SMN, Gemin2 and Gemin6–8 were to be co-expressed in bacteria and the remaining components Gemin3–5 in insect cells. Having the recombinant complex at hand, the influence of individual subunits could be analyzed by site-directed mutagenesis or the complete removal of specific complex components.

5.6.2 Bacterial expression and purification of SMNΔGemin3–5

The central SMN complex components SMN, Gemin2, Gemin6, Gemin7 and Gemin8 were expressed in bacterial cells (see Methods 4.3.9, page 68). Since specific mutations in the SMN gene result in the disease spinal muscular atrophy (SMA), a common patient

mutation (E134K) was also introduced to SMN to compare the biochemical properties of wild-type and mutated SMN complexes.

Protein complexes were purified via a GST-tag attached to the N-terminus of SMN followed by its proteolytic cleavage (Figure 52). Further purification by gel filtration chromatography often resulted in substoichiometric distribution of individual subunits (data not shown). Consequently, proteins that were used for further complex reconstitutions were only purified via its GST-tag. The SMN (E134K) mutant showed a slightly different migration pattern than the wild-type protein in SDS-PAGE (Figure 52, compare lanes 3 and 6). Purified proteins were further used in the reconstitution of wild-type and mutant SMN complexes (see Results 5.7.4, page 155).

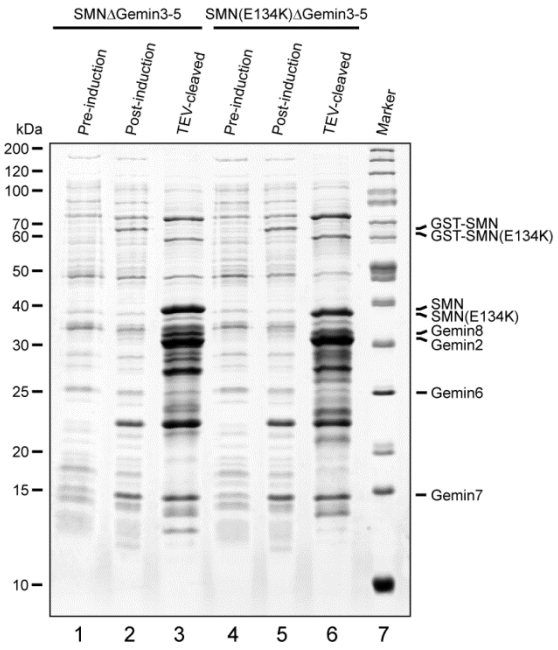

Figure 52 – Expression and purification of wild-type and mutant (E134K) SMNΔGemin3–5.

GST-SMN (either wild-type or E134K mutant), Gemin2, Gemin6, Gemin7 and Gemin8 were co-expressed in bacterial cells. GST-SMN was immobilized on glutathione sepharose (GSH) beads, washed and proteolytically cleaved by tobacco etch virus (TEV) protease. Purified protein was directly used for SMN complex reconstitution experiments.

5.6.3 Insect cell expression and purification of Gemin3, Gemin4 and Gemin5

Since previous expression of Gemin3, Gemin4 and Gemin5 was not successful in bacteria, the MultiBac system was used to generate these proteins in a eukaryotic expression system (see Methods 4.3.7, page 65).

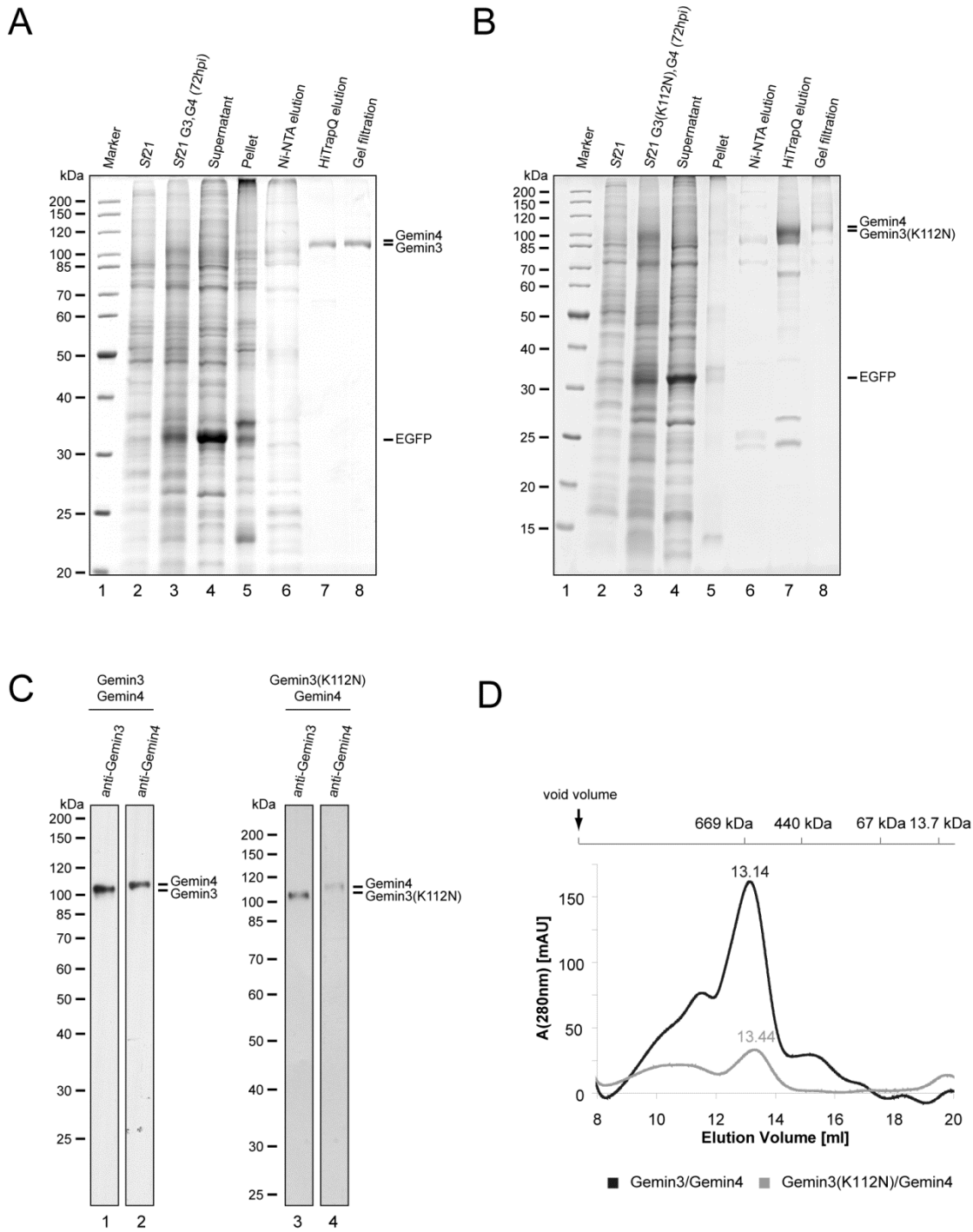

Figure 53 – Expression and purification of Gemin3/Gemin4 and Gemin3(K112N)/Gemin4.

*Sf*21 insect cells were co-infected (3 MOI of each virus) using baculoviruses coding for His_6-Gemin3,EGFP and His_6-Gemin4,EGFP or His_6-Gemin3(K112N),EGFP and His_6-Gemin4,EGFP. After protein expression at 27°C for 72 h, cells were harvested, lyzed and sequentially purified by affinity chromatography (Ni-NTA), anion exchange chromatography (HiTrapQ 1 ml) and gel filtration chromatography (Superose6 10/300GL). **(A)** SDS-PAGE of Gemin3/Gemin4 purification. **(B)** SDS-PAGE of Gemin3(K112N)/Gemin4 purification. **(C)** Western blot analysis of purified Gemin3/Gemin4 (lanes 1 and 2) and Gemin3(K112N)/Gemin4 (lanes 3 and 4) using anti-Gemin3 and anti-Gemin4 antibodies. **(D)** Gel filtration elution profiles of Gemin3/Gemin4 (black) and Gemin3(K112N)/Gemin4 (gray).

In order to express the heterodimer of His_6-Gemin3 and His_6-Gemin4, coding sequences were introduced into transfer vectors under the control of the p10 and polyhedrin promoter, respectively. Whereas Gemin4 could be individually expressed and purified, Gemin3 alone could only be obtained in an insoluble form. Two independent baculoviruses coding for N-terminally tagged Gemin3 and Gemin4 proteins as well as EGFP as a transfection marker were used in the co-infection of *Sf*21 insect.

Since Gemin3 is a putative ATPase and RNA helicase of so far unknown function, the Gemin3 mutant (K112N) was co-expressed with Gemin4 to further elucidate whether the impaired ATP-binding activity has an impact on snRNP assembly. Following a three step protein purification process combining immobilized-metal affinity, anion exchange and gel filtration chromatography (Figure 53 A and B) (see Methods 4.3.8.1, page 66), both proteins could be detected by Western blotting using protein specific antibodies (Figure 53 C). In the gel filtration elution profile the wild-type as well as the mutant protein complexes elute at similar volumes corresponding to a molecular weight of approximately 600 kDa (Figure 53 D). Gemin3 and Gemin4 have a very similar migration pattern in SDS-PAGE. Therefore, depending on the acrylamide/bisacrylamide concentration of the gel, only one protein band might be seen, yet both proteins can be identified in a Western blot. Purified wild-type and mutant Gemin3/Gemin4 complexes were used in ATP cross-linking and ATP hydrolysis assays (Results 5.7.2, page 150).

The co-expression of His_6-tagged Gemin3 and Gemin4 resulted in low amounts of protein. Furthermore, the observation of the complex stoichiometry was hampered by the almost identical migration pattern in SDS-PAGE. To circumvent this problem, baculoviruses were constructed coding for N-terminally GST-tagged wild-type and mutant (K112N) Gemin3.

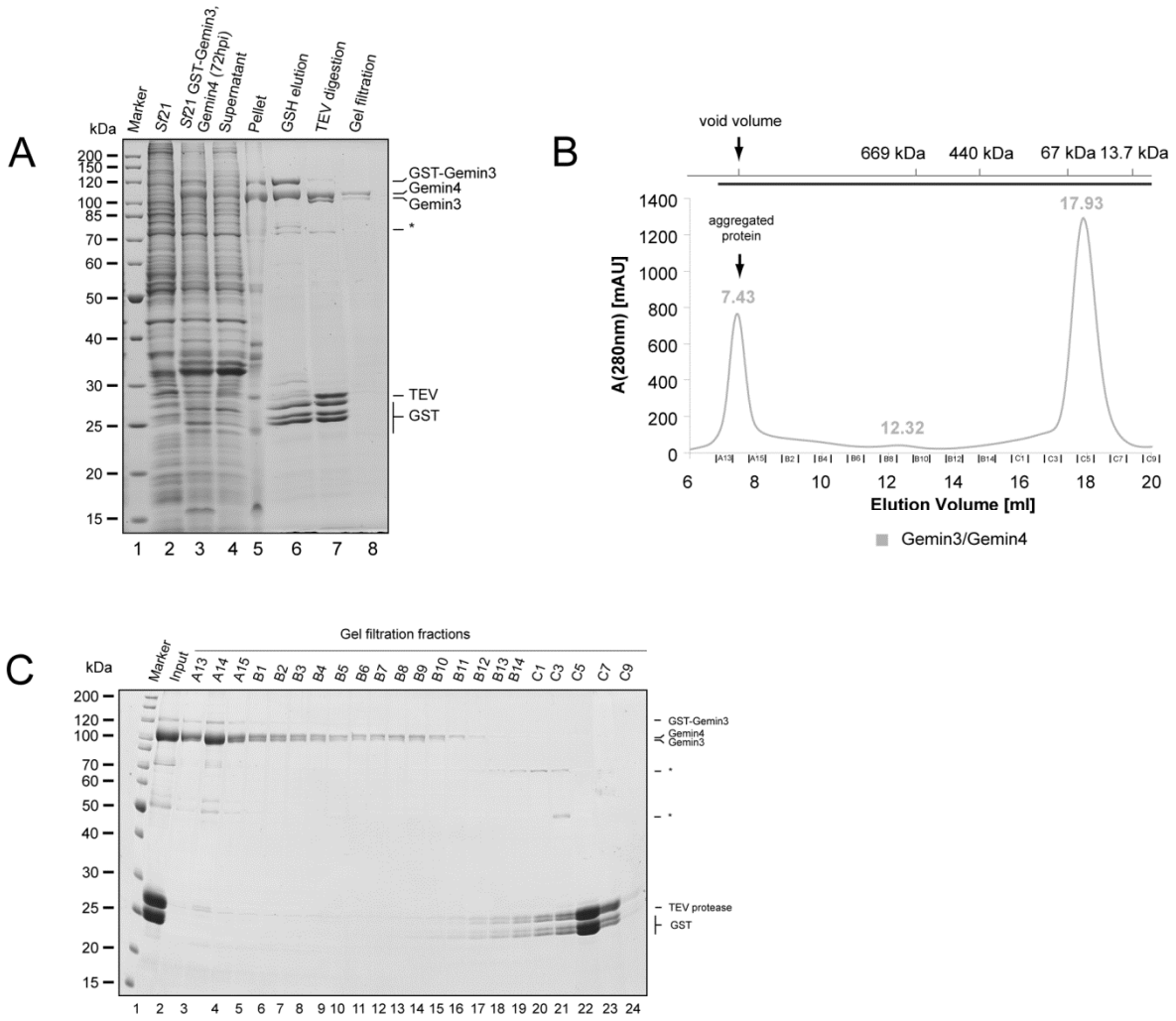

Figure 54 – Expression and purification of GST-tagged Gemin3/Gemin4.

*Sf*21 insect cells were co-infected at 3.0 MOI with baculoviruses coding for GST-Gemin3,EGFP and His_6-Gemin4,EGFP. After protein expression at 27°C for 72 h, cells were harvested, lyzed and proteins were sequentially purified by affinity chromatography (glutathione sepharose), proteolytic cleavage using TEV protease and gel filtration chromatography (Superose6 10/300GL). **(A)** SDS-PAGE of protein purification steps. **(B)** Gel filtration elution profile. **(C)** SDS-PAGE of gel filtration chromatography.

Co-infection using two independent baculoviruses for GST-Gemin3, EGFP and His_6-Gemin4, EGFP resulted in higher expression rates than in His_6-tagged heterodimer. The resulting protein complex could be purified by GSH-sepharose (Figure 54 A). Proteolytic cleavage of the GST-tag on Gemin3 and the His_6-tag on Gemin4, as well as subsequent gel filtration chromatography (Figure 54 B and C) finally led to a complex consisting of stoichiometric amounts of untagged Gemin3 and Gemin4 (Figure 54 C). Aggregated protein in the void volume of the gel filtration column also included Gemin3 and Gemin4 (Figure 54 B). Due to its low absorbance at 280 nm, the heterodimer could not be identified as a singular peak in the elution profile. The resulting protein complexes were

applied to ATP cross-linking, ATP hydrolysis assays and SMN complex reconstitutions (Results 5.7.4, page 155).

Gemin5 is the largest component of the SMN complex and was found to be insoluble following bacterial expression. Therefore, baculoviruses coding for His_6-tagged Gemin5 (p10) and EGFP (polyhedrin) were generated. The expression and purification of Gemin5 was identical to the one applied for the His-tagged heterodimer of Gemin3 and Gemin4. Notably, Gemin5 showed a stronger expression than the co-expressed EGFP and also than Gemin3/Gemin4 (Figure 55 A). According to the elution profile of the gel filtration chromatography, Gemin5 forms a tri- or tetramer (Figure 55 B). The thus prepared Gemin5 protein was analyzed for specific binding of U1 snRNA (Results 5.7.3, page 153) and in the reconstitution of the entire SMN complex (Results 5.7.4, page 155).

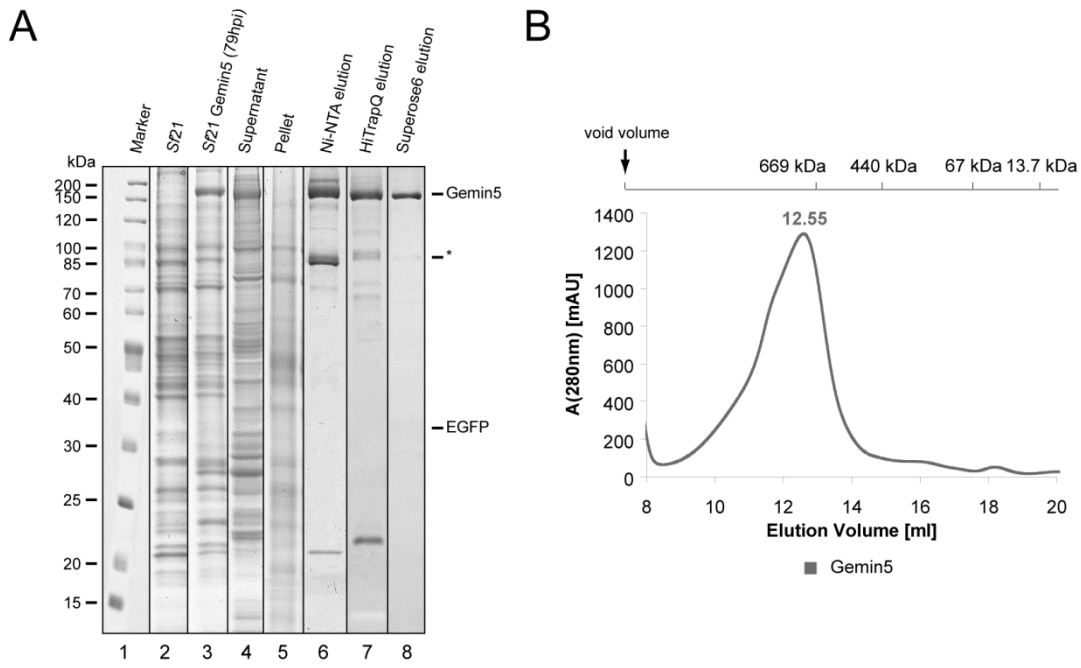

Figure 55 – Expression and purification of Gemin5.

His_6-Gemin5 was expressed in *Sf*21 insect cells at 3.0 MOI and 27°C for 79 h. Cells were harvested, lyzed and sequentially purified by affinity chromatography (Ni-NTA), anion exchange chromatography (HiTrapQ 1 ml) and gel filtration (Superose6 10/300GL). Purified samples were used for SMN complex reconstitution assays and electrophoretic mobility shift assays (EMSA) with U1 snRNA. **(A)** SDS-PAGE of Gemin5 purification. **(B)** Gel filtration elution profile of Gemin5.

Recently, it has been shown that Gemin3, Gemin4 and Gemin5 are capable of forming complexes devoid of SMN *in vivo*. Using this finding, baculoviruses were constructed coding for N-terminally GST-tagged Gemin5 and EGFP. In a co-expression using three independent baculoviruses for the generation of GST-Gemin5, His_6-Gemin3, and His_6-Gemin4, each in combination with EGFP, all recombinant proteins were soluble.

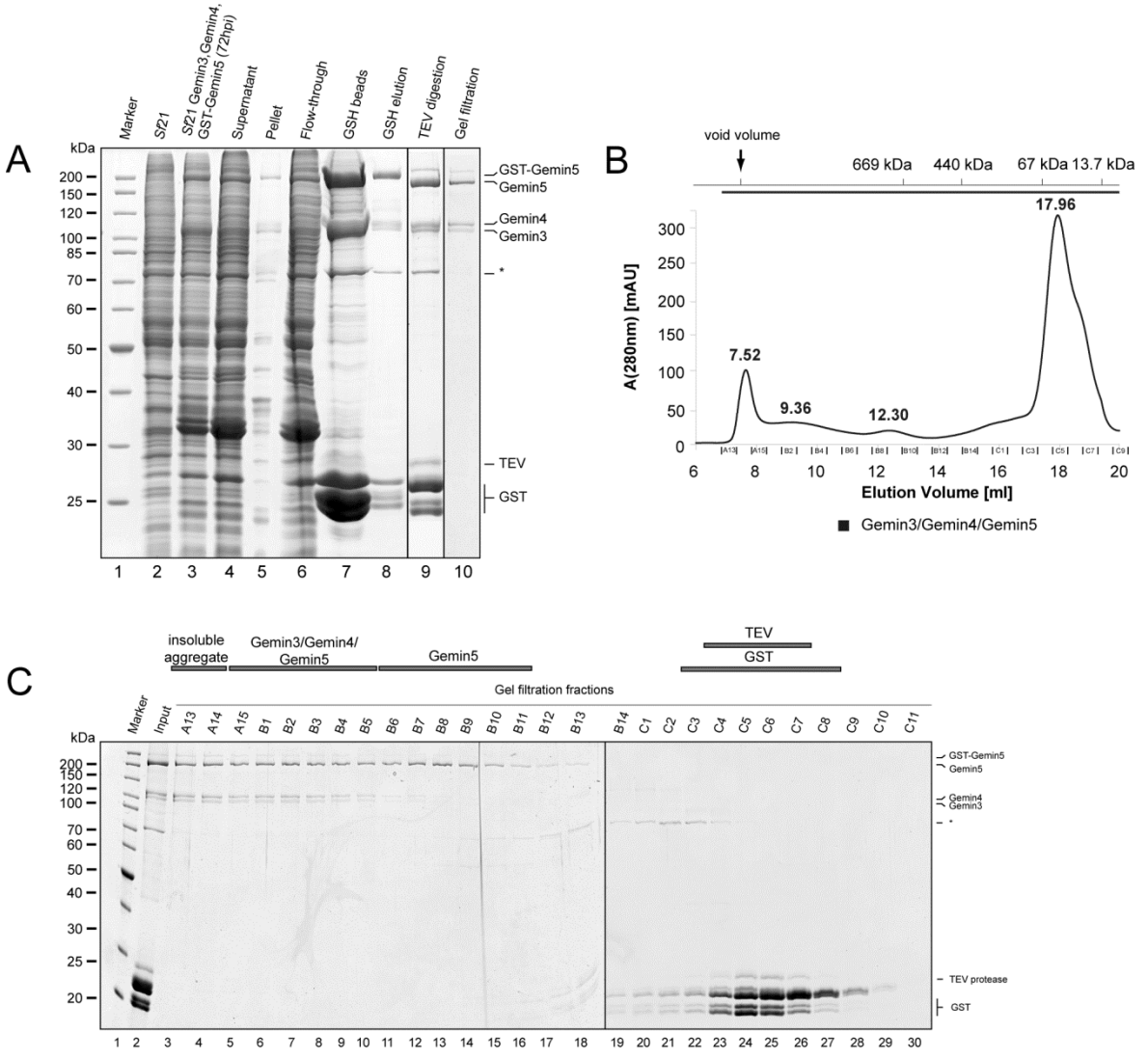

Figure 56 – Expression and purification of GST-tagged Gemin5, Gemin3 and Gemin4.

*Sf*21 insect cells were co-infected at 3.0 MOI with three baculoviruses coding for GST-Gemin5,EGFP, His_6-Gemin3,EGFP and His_6-Gemin4,EGFP. After protein expression at 27°C for 72 h, cells were harvested, lyzed and sequentially purified by affinity chromatography (glutathione sepharose), proteolysis using TEV protease and gel filtration chromatography (Superose6 10/300GL). **(A)** SDS-PAGE of protein purification steps. **(B)** Gel filtration elution profile. **(C)** SDS-PAGE of gel filtration chromatography.

The resulting protein complex was first affinity purified, then proteolytically cleaved by TEV protease to remove the GST and His_6-tags and finally isolated by gel filtration chromatography (Figure 56 A) (see Methods 4.3.8.3, page 67). In the SDS-PAGE analysis of the gel filtration, protein complexes containing Gemin3, Gemin4 and Gemin5 as well as only Gemin5 were identified (Figure 56 C). The elution fraction of Gemin5 alone is identical to the one obtained from the individual expression and purification of His_6-tagged Gemin5 (compare Figure 55 B with Figure 56 B). Thus purified stoichiometric protein complexes were further used in the total reconstitution of the SMN complex (Results 5.7.4, page 155).

5.6.4 Overview of recombinantly expressed SMN complex components

The application of the bacterial and insect cell expression system resulted in the expression and purification of the SMN complex components. The five central proteins of the complex, namely SMN, Gemin2, Gemin6, Gemin7 and Gemin8, were expressed in *E. coli* containing either wild-type (SMNΔGemin3–5; Figure 57, lane 1) or mutated SMN (SMN(E134K)ΔGemin3–5; Figure 57, lane 2), a common patient mutation in SMA. Furthermore, the MultiBac system was used to generate the heterodimer of Gemin3 and Gemin4 including the wild-type (Figure 57, lane 3) and the Walker A mutant (K112N) of Gemin3 devoid of ATP binding (Figure 57, lane 4). Gemin5 was expressed individually (Figure 57 , lane 5). Finally, a complex of the three largest subunits of the SMN complex could be expressed and purified simultaneously using three independent baculoviruses coding for Gemin3–5 (Figure 57, lane 6).

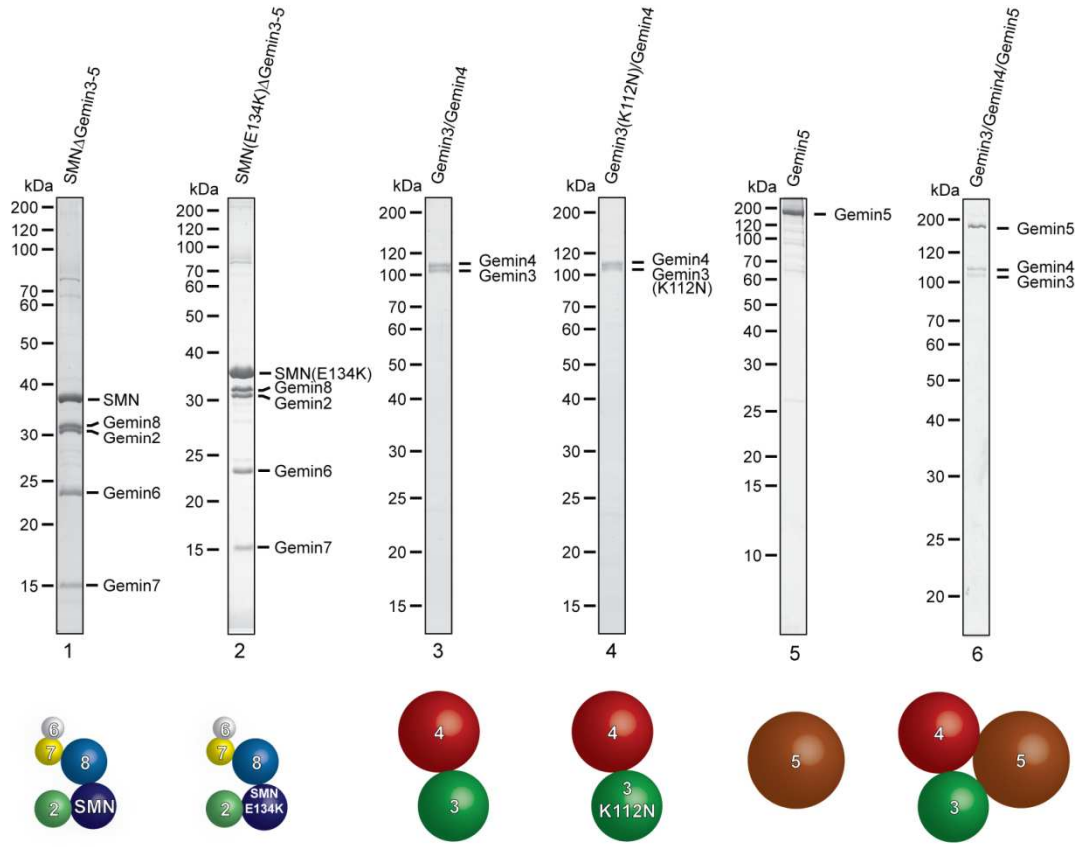

Figure 57 – Overview of purified proteins and protein complexes (SMN complex).

Wild-type SMNΔGemin3–5 (lane 1) and mutant SMN(E134K)ΔGemin3–5 (lane 2) were bacterially co-expressed. Gemin3/Gemin4 (lane 3) as well as Gemin3(K112N)/Gemin4 (lane 4) were co-expressed and Gemin5 (lane 5) individually expressed in insect cells. Gemin3/Gemin4/Gemin5 was co-expressed in insect cells using three independent baculoviruses (lane 6).

5.7 SMN complex biochemistry

5.7.1 Introductory notes

Once all SMN complex components were available in a recombinant form the biochemical activities of these could be analyzed. Since both Gemin3 and Gemin5 have been proposed or shown to play major roles in snRNP assembly, these proteins were to be assessed with respect to their ATPase activity (Gemin3) as well as RNA binding (Gemin5).

5.7.2 Insect-cell expressed Gemin3/Gemin4 is devoid of an ATPase activity

Gemin3 is a putative ATPase and RNA helicase of so far unknown function. Recombinantly co-expressed His_6-tagged Gemin3/Gemin4 was analyzed for ATP binding by ATP cross-

linking (Figure 58) (see Methods 4.3.21, page 74). Whereas radioactively labeled ^{32}P-α-ATP could be covalently linked to T4 DNA ligase, recombinant Gemin3/Gemin4 did not interact with ATP (Figure 58, lanes 3 and 4). The addition of ribooligonucleotides polyA and polyU stimulated the binding of a factor of high molecular weight (Figure 58, lanes 5–9). Increase of the added polyA concentration resulted in the focusing of the obtained signal and caused migration retardation (Figure 58, lanes 10–14), while additional recombinant Gemin3/Gemin4 positively influenced signal intensity (Figure 58, lanes 15–18).

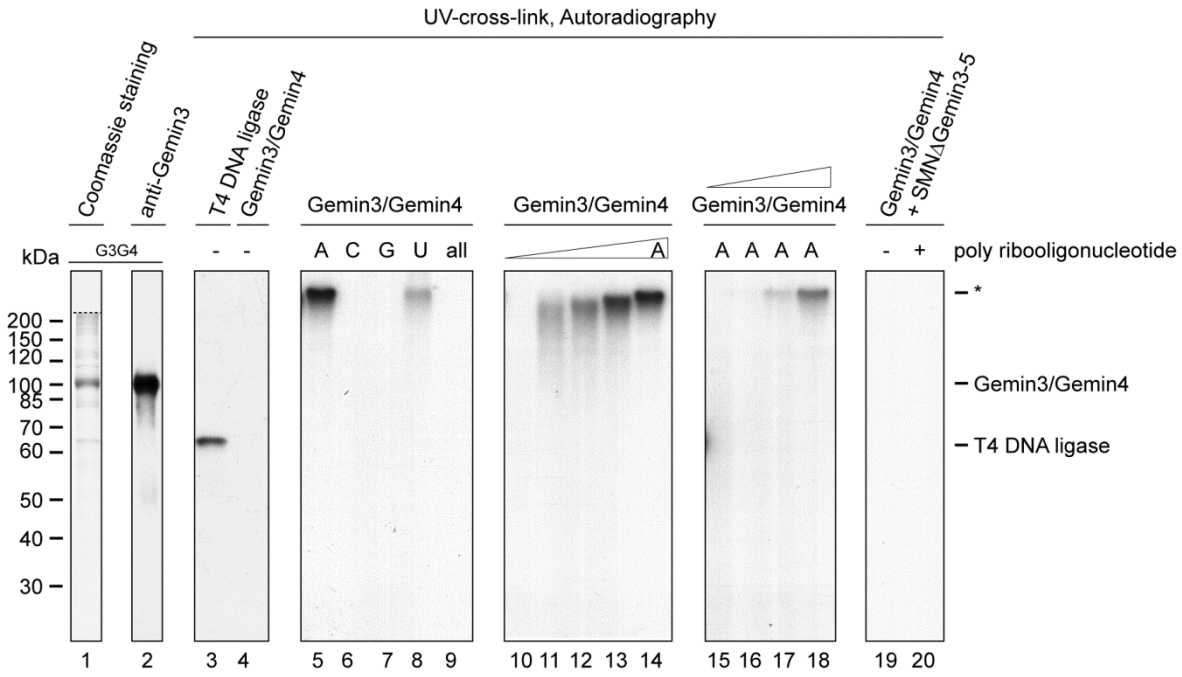

Figure 58 – Gemin3/Gemin4 is devoid of an ATPase activity.

Gemin3 and Gemin4 were co-expressed in insect cells, purified to homogeneity (lane 1) and verified by Western blotting (lane 2). ^{32}P-labelled α-ATP was UV-cross-linked to T4 DNA ligase (lane 3), Gemin3/Gemin4 alone (lane 4) or in the presence of RNA oligomers (lanes 5–9). Furthermore, the influence of an increasing concentration of Gemin3/Gemin4 and polyA as well as the presence of SMNΔGemin3–5 was analyzed.

When the central SMN complex components SMN, Gemin2 and Gemin6–8 were supplemented in the absence or presence of ribooligonucleotides no interaction with ATP was observed (Figure 58, lanes 19-20). Repetition of the UV-cross-linking reaction using GST-purified Gemin3/Gemin4 or Gemin3–5 in combination with the Gemin3 (K112N) mutant also did not result in any signal (data not shown).

In previous reactions, the Gemin3/Gemin4 heterodimer was not capable of interacting with ATP. Nevertheless, it was to be assessed whether this dimer observes and ATPase activity (see Methods 4.3.20, page 73). For this, His_6-tagged Gemin3/Gemin4 was purified by immobilized-metal affinity and anion exchange chromatography (Figure 59 A). To analyze whether the purified proteins were capable of ATP hydrolysis, elution fractions were incubated with ^{32}P-labeled α-ATP and separated by thin layer chromatography (Figure 59 B). An increased ATPase activity was observed in the elution fractions that predominantly contained the Gemin3/Gemin4 heterodimer (Figure 59 A and B, lanes 5–12). In order to remove protein contaminants the His_6-tagged Gemin3/Gemin4 was further purified by gel filtration chromatography (Figure 60 A). The resulting protein fractions, however, were devoid of any ATPase activity (Figure 60 B). Identical results were obtained for the Gemin3(K112N)/Gemin4 complex (data not shown).

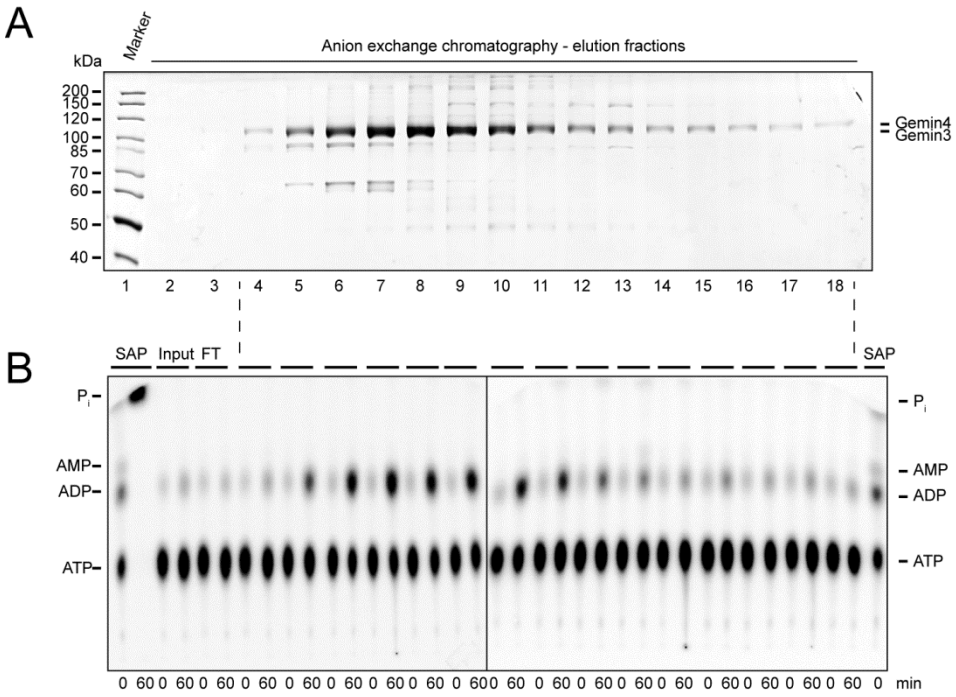

Figure 59 – Gemin3/Gemin4 exhibits an ATPase activity in the anion exchange peak fractions.

Insect cell expressed Gemin3/Gemin4 was purified by immobilized-metal affinity chromatography and anion exchange chromatography **(A)**. Elution fractions harboring recombinant Gemin3 and Gemin4 protein were incubated with ^{32}P-labelled α-ATP. Hydrolyzed nucleotides were separated by thin layer chromatography and subjected to phosphor imaging **(B)**.

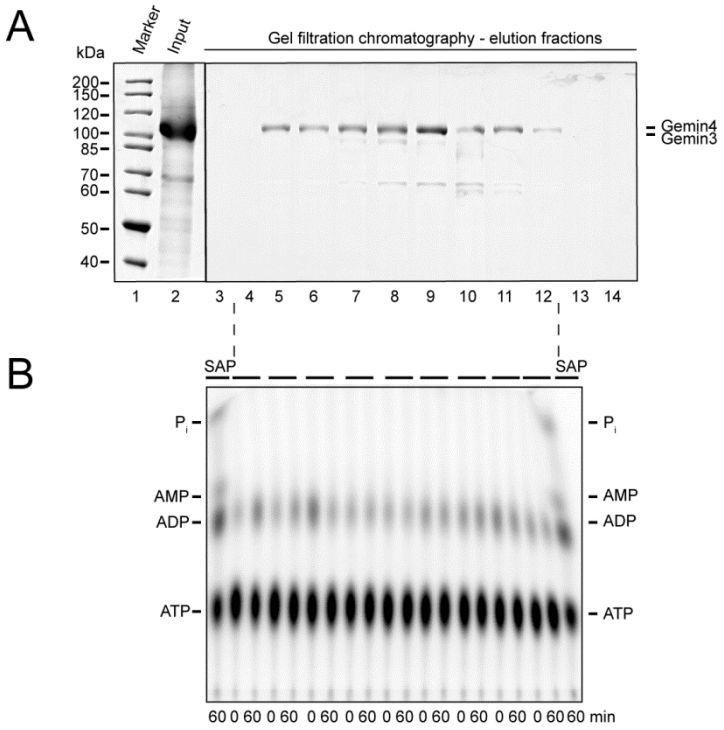

Figure 60 – The ATPase activity of Gemin3/Gemin4 is lost after gel filtration chromatography.

Elution fractions of the anion exchange chromatography were pooled, concentrated and further subjected to gel filtration chromatography **(A)** and reassessed in their ATP hydrolysis capacity **(B)**.

In summary, the heterodimer of Gemin3/Gemin4 could be expressed in a soluble form using either a His_6- or GST-affinity tag for protein purification. The cross-linking of radioactively labeled ATP to Gemin3 was not possible. Whereas an ATPase activity co-migrated with Gemin3/Gemin4 in the anion exchange chromatography peak, this activity was lost following gel filtration chromatography. Consequently, the baculovirus-expressed Gemin3/Gemin4 was soluble, however, showed no biochemical activity.

5.7.3 Recombinant Gemin5 unspecifically interacts with U1 snRNA

Gemin5 was recently shown to specifically identify snRNAs and guide them to the SMN complex. To test this function on the recombinantly expressed protein, Gemin5 was incubated with wild-type U1 snRNA and the mutated forms ΔD (lacking the Sm site to interact with Sm proteins) and ΔE (missing the terminal stem loop) at increasing heparin concentrations (Figure 61 A) (see Methods 4.4.5, page 76). In the absence of heparin a complex of Gemin5 and all three RNAs was formed (Figure 61 A, lanes 2, 8 and 14). Sm proteins D1/D2, F/E/G and D3/B form the so-called “core” structure with the snRNA resulting in a heptameric Sm Protein ring surrounding the Sm site.

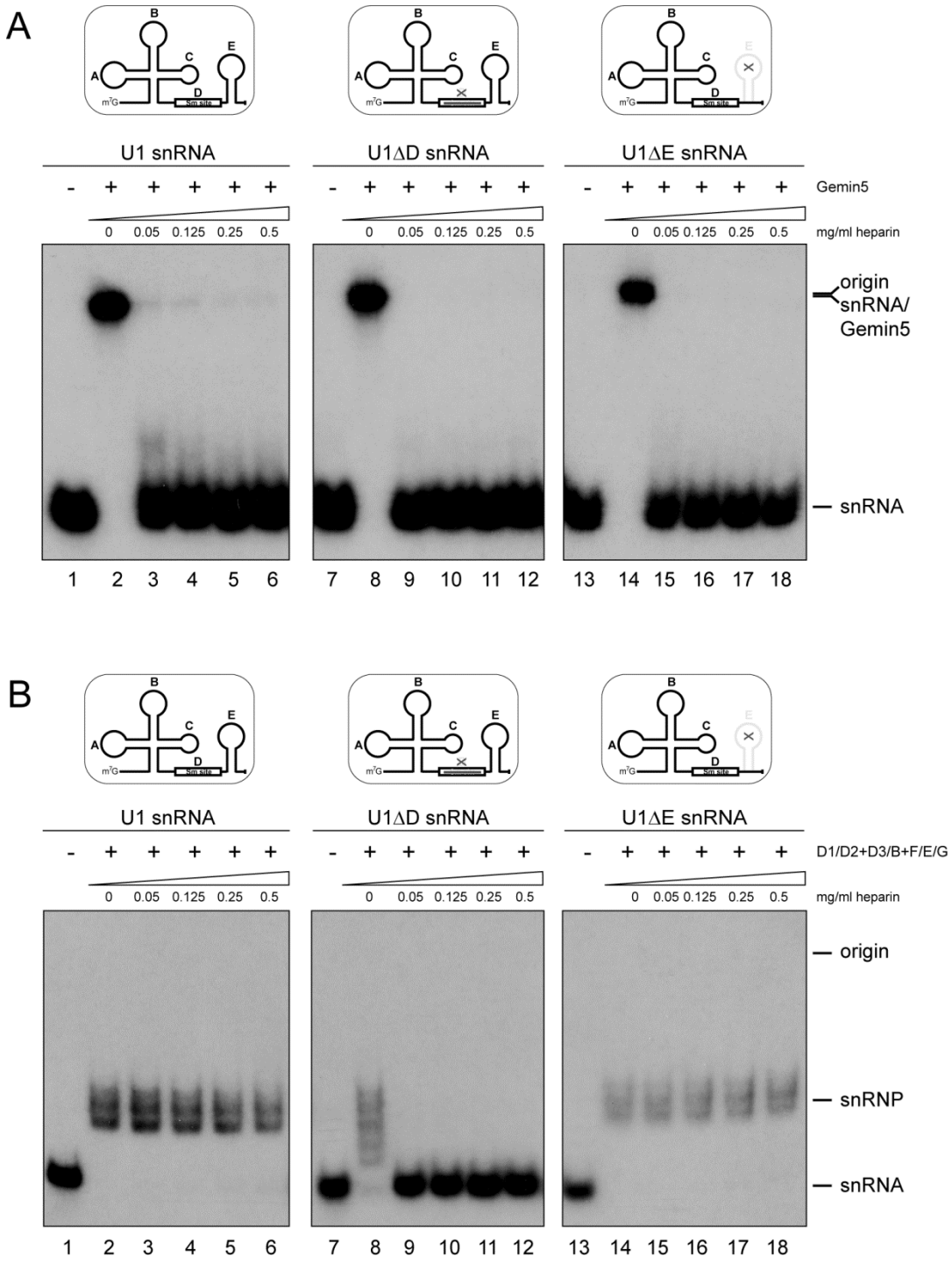

Figure 61 – Recombinant Gemin5 interacts non-specifically with wild-type and mutated snRNAs.

Insect cell expressed Gemin5 was incubated with ^{32}P-labelled *in vitro* transcribed wild-type U1, U1ΔD and U1ΔE snRNA at increasing heparin concentrations **(A)**. The U snRNAs were incubated under identical conditions with the Sm protein heterooligomers D1/D2, D3/B and F/E/G, separated in native gel electrophoresis and analyzed by autoradiography **(B)**.

The incubation of the Sm proteins with the three types of U1 snRNA showed that RNA-protein complexes were assembled in the wild-type and ΔE mutant irrespective of the heparin concentration (Figure 61 B, lanes 1–6 and 13–18). U1ΔD snRNA interacted only with the Sm proteins in the absence of heparin (Figure 61 B, lanes 7–12).

In conclusion, the insect cell-expressed Gemin5 protein was soluble and readily interacted with U1 snRNA. This, however, was found to be unspecific as the addition of minimal amounts of heparin resulted in Gemin5-snRNA dissociation. Despite the lacking biochemical activities in Gemin3/Gemin4 and Gemin5, these complexes were used to reconstitute the entire SMN complex.

5.7.4 Total reconstitution of the human SMN complex from recombinant sources

A major aim of this work was the reconstitution of the human SMN complex *in vitro* in order to analyze its biochemical properties as a whole. The SMN complex catalyzes the formation of snRNPs by sequestering all seven Sm proteins in a pICln-bound state expelling pICln upon binding. The U snRNA is thought to be delivered to the SMN complex by Gemin5 which was recently demonstrated to specifically interact with U snRNAs.

The expression and purification of the individual sub-complexes and interaction partners of the SMN complex have been shown. The central SMN complex components SMN, Gemin2 and Gemin6–8 were bacterially co-expressed comprising either wild-type or E134K mutant SMN protein (Results 5.6.2, page 142). Gemin3/Gemin4, Gemin5 and Gemin3–5 (Results 5.6.3, page 143) were generated in *Sf*21 insect cells. Finally, pICln and the Sm protein heterooligomers D1/D2, D3/B and F/E/G were produced in bacterial cells (Results 5.3.4, page 98) and recombined to form the 6S complex (pICln/D1/D2/F/E/G) and pICln/D3/B (Results 5.3.3, page 97).

For the total reconstitution of the SMN complex, the central proteins SMN, Gemin2 and Gemin6–8 (SMNΔGemin3–5) were supplemented with Gemin3–5. These were then incubated with pICln-Sm protein complexes and immunoprecipitated using 7B10 (anti-SMN) antibody (see Figure 62 A for a schematic).

Initially, four different SMN complexes were formed. The first comprised only the central proteins SMN, Gemin2 and Gemin6–8 (Figure 62 B, lane 2), whereas the second and third were either devoid of Gemin5 (Figure 62 B, lane 6) or Gemin3 and Gemin4 (Figure 62 B,

lane 10). The fourth complex contained all known components of the human SMN complex (Figure 62 B, lane 14). To these complexes either 6S or a combination of 6S and pICln/D3/B were added to transfer the Sm proteins found in the so-called “subcore” (Figure 62 B, lanes 3, 7, 11 and 15) and “core” (Figure 62 B, lanes 4, 8, 12 and 16) complexes *in vivo*. The removal of pICln was verified by Western blotting using anti-pICln antibody (Figure 62 B, lower panel).

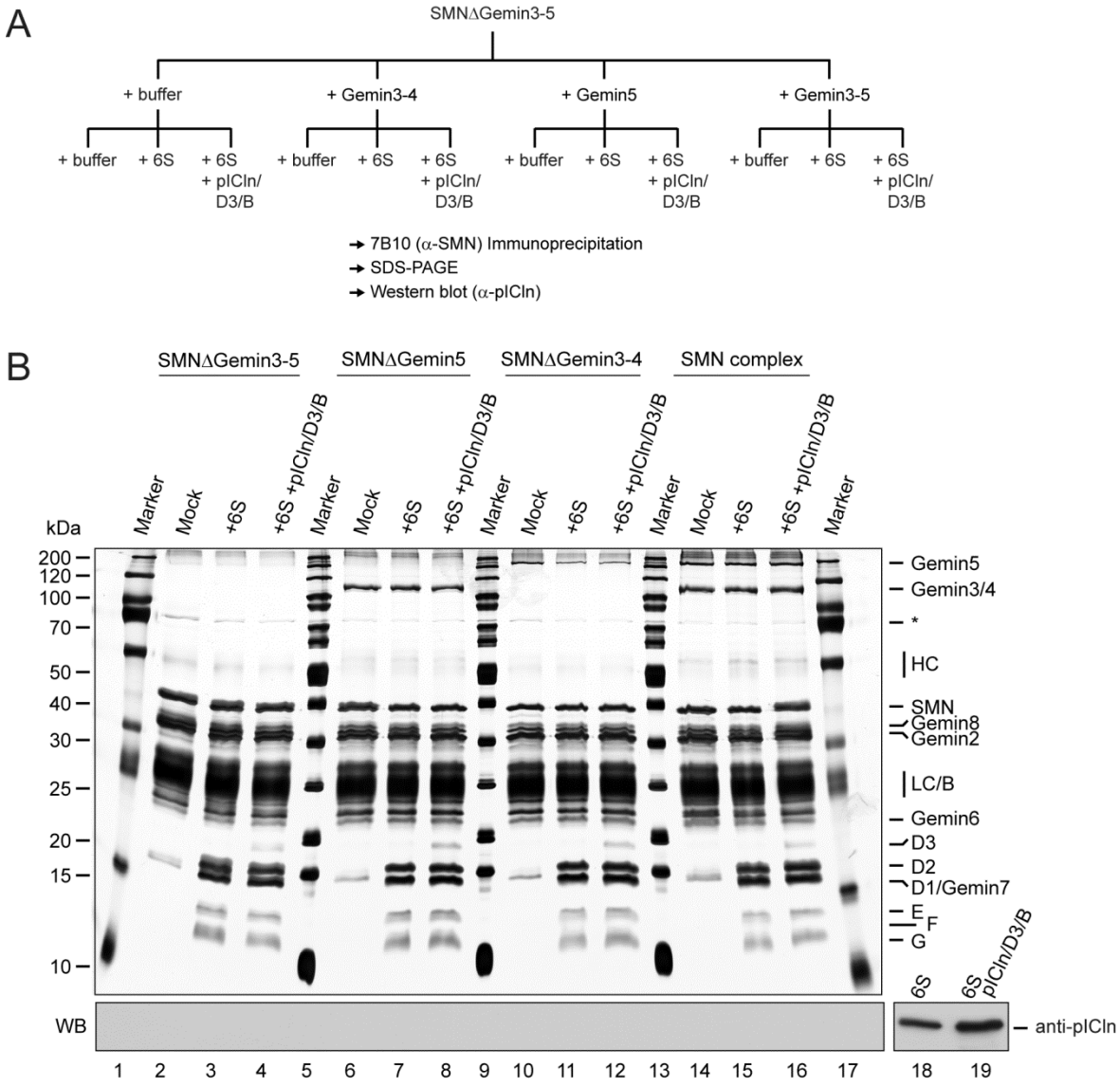

Figure 62 – Total reconstitution of the human wild-type SMN complex from recombinant sources.

(A) Schematic of the experimental outline. **(B)** Recombinant SMNΔGemin3–5 was incubated with buffer alone (lanes 2–4), with Gemin3/Gemin4 (lanes 6–8), Gemin5 (lanes 10–12) or Gemin3/Gemin4/Gemin5 (lanes 14–17) at 4°C overnight. Additionally, no Sm proteins (lanes 2, 6, 10, 14), 6S (lanes 3, 7, 11, 15) or 6S + pICln/D3/B (lanes 4, 8, 12, 16) were added. Protein complexes containing SMN were immunoprecipitated using the 7B10 antibody (α-SMN) and applied to SDS-PAGE. Asterisks indicate degradation products. HC and LC indicate the heavy and the light chain of the antibody, respectively. The exclusion of pICln from the SMN complex was determined by Western blotting (lower panel, WB).

A common patient mutation in the SMN gene that causes SMA is the modification of glutamic acid to lysine at position 134 in the Tudor domain. This domain is known as the interaction platform of SMN with the Sm proteins. The previously shown reconstitution of the SMN complex was recapitulated exchanging the wild-type SMN with the E134K SMN mutant (Figure 63). Despite the minor difference in migration of the two forms of SMN in SDS-PAGE, no difference in SMN complex integrity was observed.

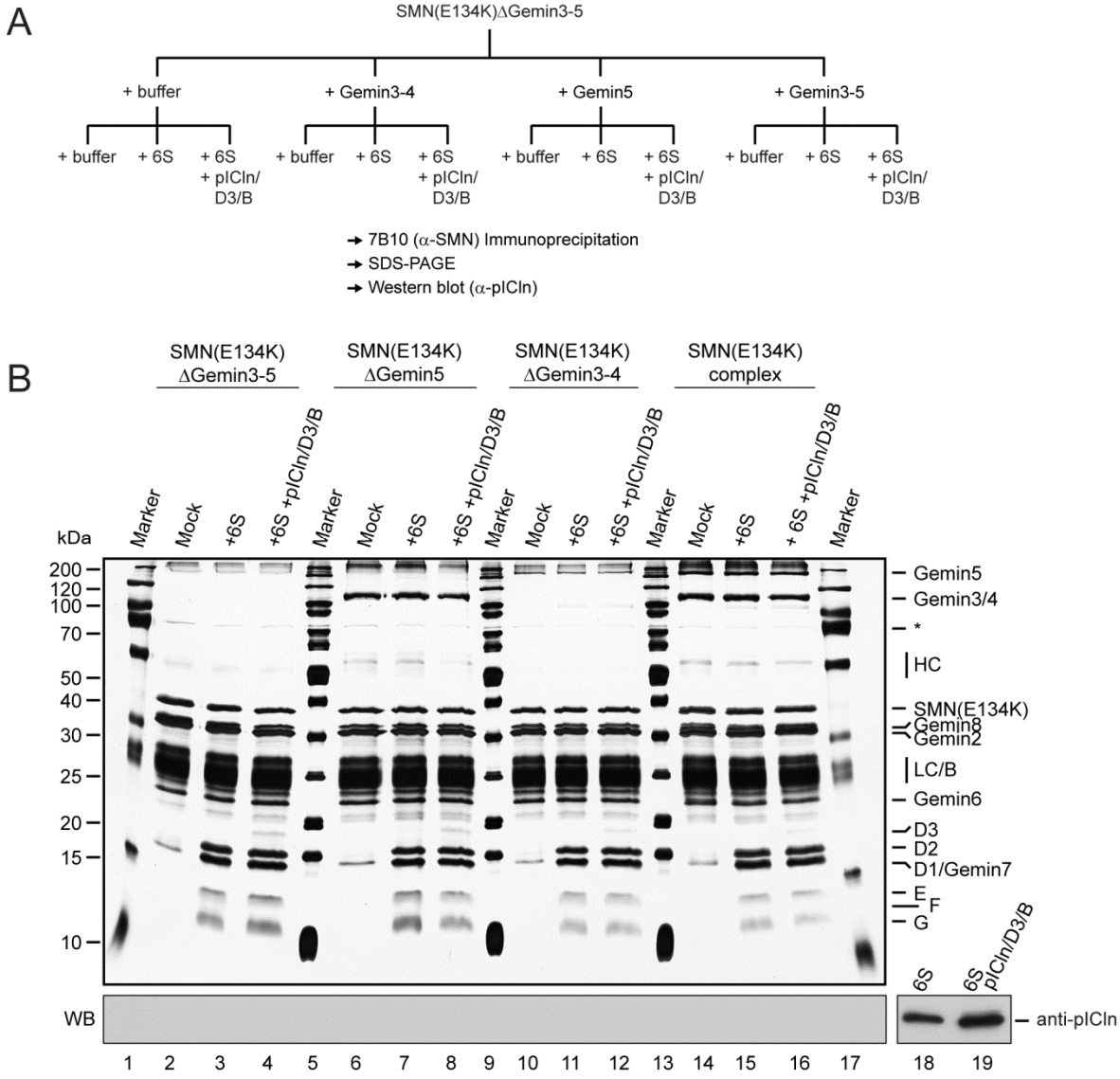

Figure 63 – Total reconstitution of the human mutant SMN(E134K) complex from recombinant sources.

(A) Schematic of the experimental outline. **(B)** Recombinant mutant SMN(E134K)ΔGemin3–5 was incubated with buffer alone (lanes 2–4), with Gemin3/Gemin4 (lanes 6–8), Gemin5 (lanes 10–12) or Gemin3/Gemin4/Gemin5 (lanes 14–17) at 4°C overnight. Additionally, no Sm proteins (lanes 2, 6, 10, 14), 6S (lanes 3, 7, 11, 15) or 6S + pICln/D3/B (lanes 4, 8, 12, 16) were added. Protein complexes containing SMN were immunoprecipitated using the 7B10 antibody (α-SMN) and applied to SDS-PAGE. Asterisks indicate degradation products. HC and LC indicate the heavy and the light chain of the antibody, respectively. The exclusion of pICln from the SMN complex was determined by Western blotting (lower panel, WB).

In conclusion, the entire SMN complex as well as complexes missing individual subunits (Gemin3–5) were reconstituted from recombinant sources. SMN, Gemin2 and Gemin6–8 were expressed in bacterial cells (see Results 5.6.2, page 142), whereas Gemin3–5 were generated using the MultiBac system (see Results 5.6.3, page 143). Despite the lacking biochemical activity of Gemin3 and Gemin5 both proteins specifically interacted with the remaining SMN complex components. Finally, Sm proteins could be transferred from 6S and pICln/D3/B onto the SMN complex, while pICln was released.

5.7.5 The reconstituted SMN complex mediates snRNP assembly *in vitro*

The SMN complex mediates the transfer of Sm proteins onto snRNA *in vivo*. With the above described system to reconstitute the entire SMN complex from recombinant sources novel opportunities arise to identify the contribution of individual complex components in snRNP assembly.

Reconstituted SMN complexes were analyzed for their ability to assemble snRNPs. For this, radioactively labeled, *in vitro* transcribed U1 and U1ΔD snRNA were incubated with the entire SMN complex or the central complex of SMN, Gemin2 and Gemin6–8 in the presence or absence of pICln-Sm protein complexes. Since these pICln-associated proteins are incapable of binding to the RNA, the SMN complex is needed to expel pICln and transfer the Sm proteins unto the RNA (Figure 64).

It could be shown that the central SMN complex specifically mediated the formation of “subcore” (snRNA + D1/D2/F/E/G) and “core” snRNPs (snRNA + D1/D2/F/E/G/D3/B) (Figure 64 A). This assembly activity depended on the presence of the Sm site on the snRNA. Furthermore, the entire human SMN complex exhibited the same activity (Figure 64 B). In preliminary experiments it could be shown that the SMN E134K mutation resulted in a somewhat decreased assembly activity (data not shown). Since the general association with Sm proteins was not affected in this mutant complex, the reduced ability to form snRNPs might be important in the molecular etiology of SMA.

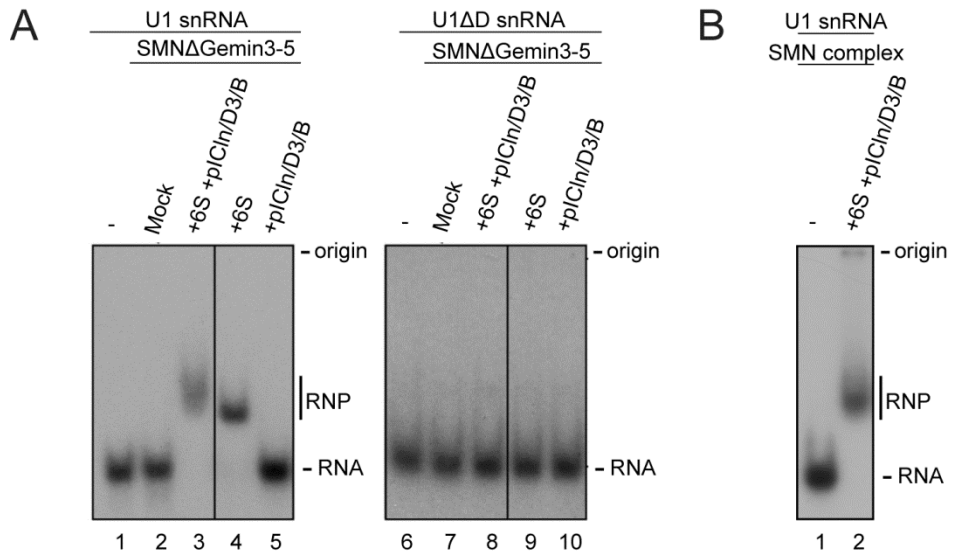

Figure 64 – *In vitro* snRNP assembly is mediated by the SMN complex.

(A) Assembly reactions on ^{32}P-labeled U1 snRNA with recombinant SMNΔGemin3–5 complex without bound Sm proteins (lane 2) or loaded with the indicated pICln-Sm protein complexes (lanes 3–5). Lane 1 shows RNA only; lanes 6–10 show control assembly reactions on ^{32}P-labeled U1ΔD snRNA. (**B)** Assembly reactions on ^{32}P-labeled U1 snRNA with recombinant SMN complex loaded with 6S and pICln/D3/B (lane2). Lane 1 shows RNA only. Experiments have been performed by Ashwin Chari and Clemens Englbrecht. (A) has been adapted from (Chari *et al.*, 2008) with permission from Elsevier.

In conclusion, both the PRMT5 and the SMN complex could be reconstituted from recombinant sources in a soluble and biochemically active form. Whereas PRMT5 was capable of introducing MMA and sDMA in a distributive mechanism to Sm proteins B, D1 and D3, the SMN complex caused the specific transfer of these onto snRNA.

6 Discussion

6.1 Introductory notes

The cytoplasmic assembly of snRNPs can be separated into an early and a late phase. In the early phase, the PRMT5 complex introduces symmetrically dimethylated arginines into specific Sm proteins that are complexed with the adaptor protein pICln. In the late phase, these Sm proteins are transferred onto the SMN complex which catalyzes the specific arrangement of these on the snRNA.

In this work, both protein complexes were recombinantly expressed and purified to recapitulate the cytoplasmic snRNP assembly *in vitro*. To achieve this, a combination of bacterial and insect cell expression systems were applied. Whereas polycistronic expression vectors were used for bacterial expression, the MultiBac system was called upon to generate protein complexes containing posttranslational modifications.
The early phase of snRNP assembly is characterized by the action of the PRMT5 complex. Insect cell-expressed PRMT5/WD45 could be shown to interact with Sm protein substrates and serve as a scaffold for the assembly of the 6S complex, an RNA-free assembly intermediate that has recently been characterized (Chari *et al.*, 2008). Additionally, PRMT5/WD45 observed a type II methyltransferase activity. Experimental procedures were devised to analyze this activity as well as the properties of generating mono- and dimethylated arginines. Applying these techniques, PRMT5 was proven to act distributively on Sm protein substrates.

To analyze the late phase of snRNP assembly, the SMN complex was reconstituted from recombinant sources containing wild-type SMN as well as an SMA patient mutation (SMN E134K). Sm proteins could be readily transferred from pICln-Sm protein intermediates onto both SMN complexes. Finally, these proteins could be arranged onto *in vitro* transcribed snRNA completing the snRNP assembly reaction.

6.2 The PRMT5 complex

6.2.1 PRMT5-interacting proteins mediate the enzymatic activity and enhance substrate specificity

Previous studies identified PRMT5 as a type II methyltransferases (Friesen *et al.*, 2001). The *in intro* analysis of PRMT5 has so far been hampered by the fact that the bacterially expressed enzyme was either insoluble or biologically inactive (Cheng *et al.*, 2004; Friesen *et al.*, 2001; Pal *et al.*, 2003). Similar results have been obtained in this work using His_6-tagged PRMT5 in the insect cell expression system. Opposing findings were made expressing Flag-tagged PRMT5 in *Sf*9 insect cells (Pal *et al.*, 2003). The purified protein was able to methylate histones H3 and H4 leading to the conclusion that posttranslational modifications of PRMT5 might be essential for its activity.

In the cell, PRMT5 associates with pICln and WD45 to form the so-called PRMT5 complex or methylosome (Friesen *et al.*, 2001; Friesen *et al.*, 2002; Meister *et al.*, 2001b). Consequently, one can assume that the enzymatic activity of PRMT5 might be influenced by its interaction partners. It was found that WD45 indeed modulates PRMT5 activity (Friesen *et al.*, 2002). Taking into account the composition of the PRMT5 complex and the findings of previous studies, a strategy was devised to co-express PRMT5 and WD45 in *Sf*21 insect cells. The purified complex was capable of symmetrically dimethylating Sm proteins B, D1 and D3 (Results 5.5.7, page 122) as well as the mammalian pre-mRNA cleavage factor I (CF I_m68) (Martin *et al.*, 2010).

Recently, a model has been proposed founding the enzymatic activity of PRMT5 on enzyme di- or multimerization and association with WD45 (Figure 65) (Krause *et al.*, 2007). This could also be verified by the co-expression of enzymatically active *Xenopus laevis* PRMT5/WD45 (Wilczek *et al.*, 2011). Recombinant protein readily methylated histones H2A and H4 as well as the histone storage chaperone nucleoplasmin on a conserved motif on its unstructured C terminus.

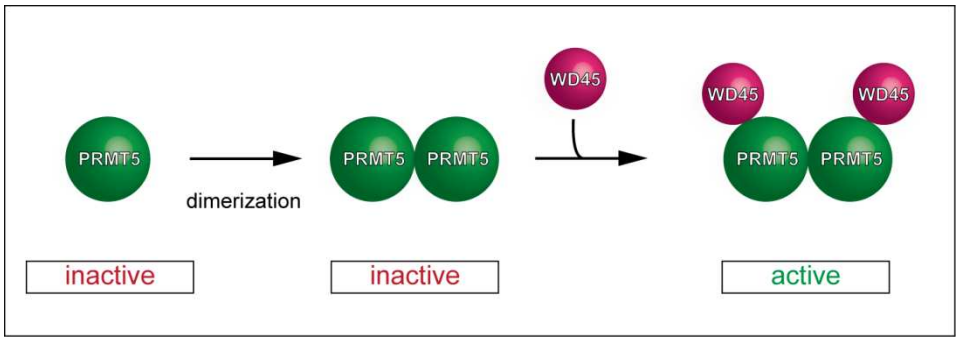

Figure 65 – PRMT5 activity depends on enzyme dimerization and WD45 association

Recombinantly expressed PRMT5 on its own forms homodimeric complexes and is biologically inactive as well as insoluble in bacterial and insect cells. The co-expression of PRMT5 and WD45 results in enzymatically active protein in insect cells but not in bacterial cells. Furthermore, the combination of individually expressed PRMT5 and WD45 does not yield biologically active protein complexes.

In vivo, pICln, as a part of the PRMT5 complex, associates with the Sm protein heterooligomers D1/D2 and D3/B. Furthermore, a ring-shaped complex consisting of pICln/D1/D2/F/E/G, termed 6S complex, has been found (Chari *et al.*, 2008). In either case, the interaction of the Sm proteins with the snRNA is prevented by pICln, functioning as a kinetic trap.

Most cytoplasmic Sm proteins were found to associate with pICln in the cytoplasm (Pu *et al.*, 1999). Consequently, one would expect pICln to have an impact on Sm protein binding to the PRMT5 complex as well as Sm protein methylation. It could be shown in this work that the presence of pICln increased the amount of Sm protein binding to PRMT5/WD45, however, the methylation was only affected in D3/B (Results 5.4.2, page 100). Whereas D1/D2 methylation either in the form of pICln/D1/D2 or 6S showed similar values to D1/D2 methylation alone, the total methylation of D3/B increased when bound to pICln (Results 5.5.10, page 128). Both substrates contain similar numbers of receptive arginine residues (9 in D1, 10–11 in D3/B). While the arginine residues form a singular RG-repeat domain in D1, they are distributed over a wider range in D3/B (Introduction 1.3.7, page 15). Consequently, pICln could stabilize D3/B binding aiding in the presentation of receptive arginine residues to the active site of the enzyme.

Lately, RioK1 has been identified to share the binding site on PRMT5 with pICln (Guderian *et al.*, 2011). RioK1 is a protein kinase that is involved in ribosomal biogenesis by influencing the processing of 18S ribosomal RNA and in the final stages of cytoplasmic maturation of the pre-40S ribosomal subunit (Widmann *et al.*, 2012). Both pICln and RioK1 act as a bridging factor bringing various methylation substrates to PRMT5/WD45 that in turn are symmetrically dimethylated. Whereas pICln provides Sm proteins, RioK1 mediates the interaction with nucleolin (Guderian *et al.*, 2011). Consequently, the substrate specificity of PRMT5/WD45 can be altered by a bridging factor. Nevertheless, the presence of such a factor is no necessity for methylation of substrates such as histone H2A, H3 and H4 (Pal *et al.*, 2004; Pollack *et al.*, 1999; Wilczek *et al.*, 2011).

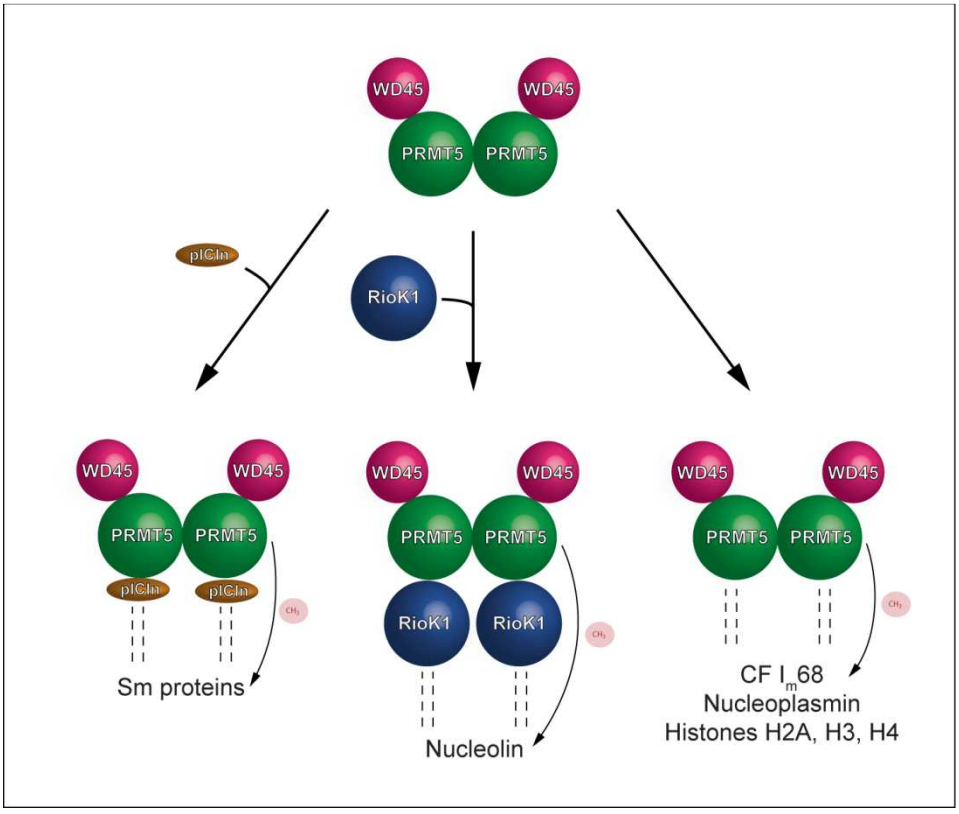

Figure 66 – Bridging factors enhance PRMT5 substrate specificity

The minimal entity of the PRMT5 complex that was found to exhibit a type II methyltransferase activity is PRMT5/WD45. *In vivo*, the adaptor proteins pICln and RioK1 have been found to bind to the enzyme in a mutual exclusive manner. While pICln binds to Sm proteins and RioK1 to nucleolin, the substrate specificity of PRMT5 can be modulated. Still, PRMT5/WD45 is capable of methylating substrates that directly interact with the enzyme.

In summary, the activity of PRMT5 depends on its association with WD45. Substrate protein can directly interact with the enzyme or bind to a bridging factor that might stabilize substrate binding and its presentation to the active site of the enzyme. Even though adaptor proteins cause more substrate to bind to the methyltransferase, the number of transferred methyl groups is only affected in distinct substrates.

6.2.2 6S is formed on the PRMT5 complex

In the cytoplasmic assembly of snRNPs, all seven Sm proteins are specifically arranged as a closed ring onto the Sm site of the snRNA (Fischer *et al.*, 2011; Will and Lührmann, 2011). Newly translated Sm proteins form heterooligomeric complexes containing D1/D2, F/E/G and D3/B (Raker *et al.*, 1996). Whereas D1/D2 and D3/B quantitatively form stable complexes with pICln *in vitro*, F/E/G alone exists as a dimer and necessitates the presence of D1/D2 to engage with pICln (Chari *et al.*, 2008; Pu *et al.*, 1999; Raker *et al.*, 1996). In the cell, the so-called 6S complex, consisting of pICln, D1, D2, F, E and G, does not interact with PRMT5 (Chari *et al.*, 2008). Yet, the arginine residues of D1 exhibit only symmetrically dimethylated arginines (Miranda *et al.*, 2004a). This led to two conclusions concerning the assembly of the 6S complex. First, 6S is no direct substrate of PRMT5 as it does not co-migrate with the enzyme in gel filtration of HeLa cytoplasmic extract (Chari *et al.*, 2008). Second, the methylation D1 has to be accomplished before the assembly of the 6S complex occurs as there are no intermediate monomethylated arginines present in D1 of the cytoplasmic 6S complex (Miranda *et al.*, 2004a).

In this work, the interaction of Sm protein heterooligomers in the presence and absence of pICln with PRMT5/WD45 was analyzed (Results 5.4.2, page 100). It could be shown that D1/D2, and D3/B but not F/E/G were capable of directly associating with PRMT5/WD45. Furthermore, pICln/D1/D2, pICln/D3/B and the 6S complex bound to the enzyme. *In vivo*, pICln is present in two complexes with a sedimentation coefficient of 20S and 6S. Whereas 6S is identical to the above mentioned complex, the 20S complex contains PRMT5, WD45, pICln, D1/D2 and D3/B but not F/E/G. Consequently, PRMT5/WD45 interacts only with pICln/D1/D2 and pICln/D3/B and is therefore most likely capable of fully methylating the arginine residues in D1 before the 6S complex is formed (Figure 67

A). It was shown that the addition of F/E/G to the preformed PRMT5/WD45/pICln/D1/D2 complex led to 6S formation independent of its methylation state. Still, another control mechanism must be present to prevent the immature interaction of F/E/G with the not yet fully methylated pICln/D1/D2 substrate. Further supplementation of pICln/D1/D2 or pICln/D3/B caused the removal of 6S from PRMT5/WD45 (Figure 67 B). The opposite, however, was not possible.

Methylation kinetics were carried out to obtain characteristic values for the maximum reaction velocity (V_{max}), the Michael-Menten constant (K_m), the turn-over number (k_{cat}) and the reaction efficiency ($k_{cat} \cdot K_m^{-1}$) (Results 5.5.10, page 128). It could be shown that the resulting kinetic data of pICln/D1/D2 and 6S were very similar. In order to identify which of the both substrates had the highest affinity for PRMT5/WD45 methylation competition experiments were performed (Results 5.5.11, page 131). In accordance with the ability of pICln/D1/D2 to expel 6S from the enzyme, pICln/D1/D2 was found to bind stronger to PRMT5/WD45 than 6S.

Both approaches, the biochemical reconstitutions and well as the analysis of enzymatic activity, indicate that the assembly of 6S on the PRMT5 complex is a directed process. So far, it remains elusive whether pICln/D3/B dissociates from PRMT5/WD45 after its methylation or whether the Sm proteins are directly transferred onto the SMN complex.

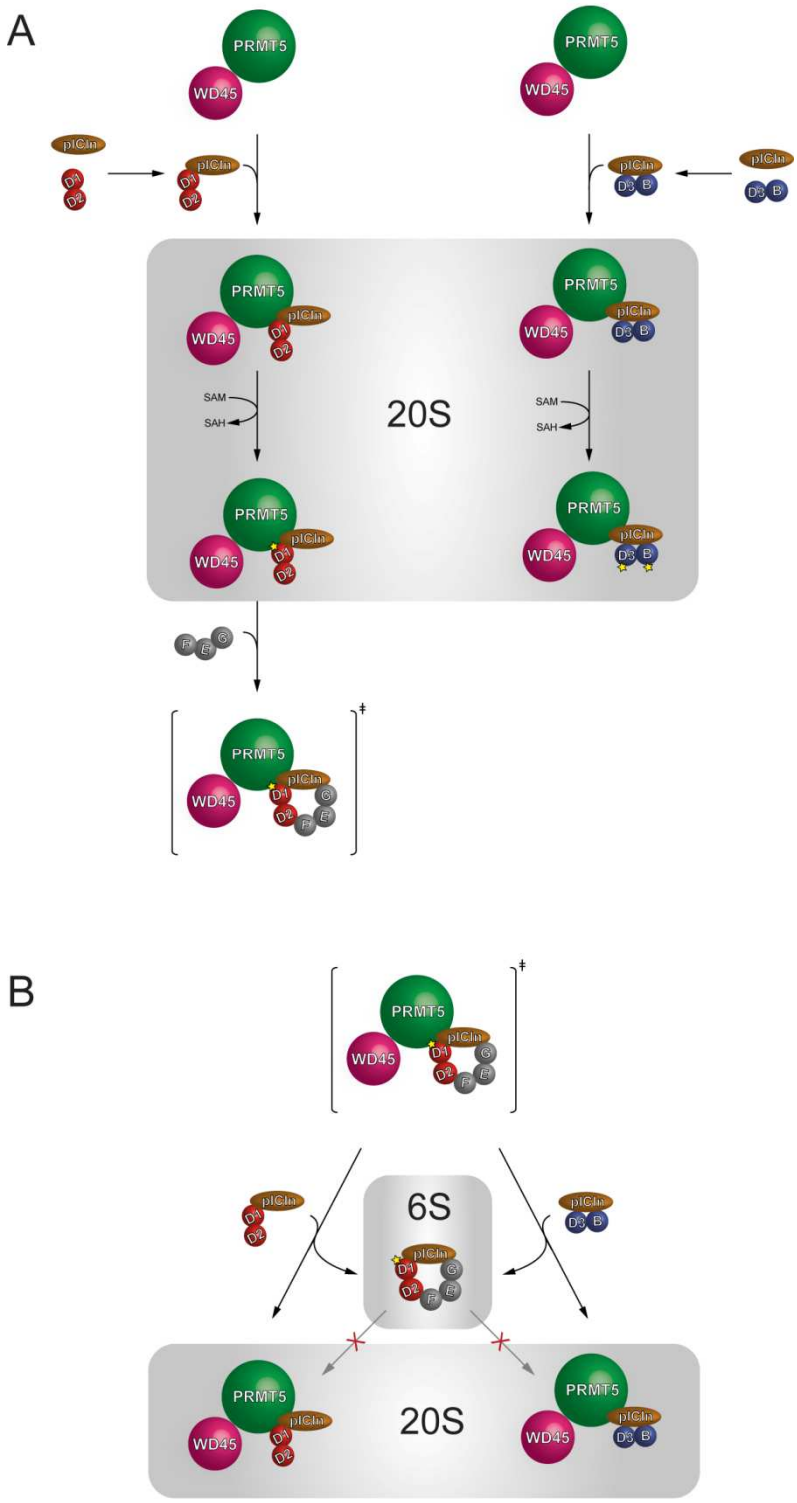

Figure 67 – Formation of 6S on the PRMT5 complex.

(A) Sm protein heterooligomers D1/D2 and D3/B readily interact with pICln *in vivo*. These complexes then associate with PRMT5/WD45 forming the so-called 20S complex receiving symmetrical dimethylarginines in their C-terminal domains. After D1 in pICln/D1/D2 is fully methylated F/E/G is able to bind and form the 6S complex. **(B)** The 6S complex is then released by the addition of yet unmethylated pICln/D1/D2 or pICln/D3/B. The PRMT5/WD45/6S complex is most likely a short-lived transition state since it cannot be observed in cytoplasmic HeLa extracts. Once the 6S complex has been released from PRMT5 reentering is prevented by the presence of pICln/D1/D2 and pICln/D3/B. Stars indicate the methylation of a protein substrate.

6.2.3 PRMT5 methylates Sm protein substrates distributively

PRMT5 methylates a variety of substrates and transfers two (histones) to twenty (coilin) methyl groups onto a single substrate (Hebert *et al.*, 2002; Pollack *et al.*, 1999). Sm proteins B/B', D1 and D3 contain 6, 9 and 4/5 receptive arginine residues (Brahms *et al.*, 2000).

Since PRMT5 introduces several methyl groups onto a single substrate, two possible reaction mechanisms are possible. In a processive mechanism, PRMT5 binds to the substrate molecule and transfers methyl groups until all arginine residues are symmetrically dimethylated. The enzyme stays attached to the substrate throughout the entire reaction. In a distributive mechanism, the enzyme dissociates from the substrate after each methyl group transfer. Accordingly, PRMT5 has to re-associate with a substrate to incorporate one more methyl group.

The sheer number of receptive arginine residues available in D1 and D3/B argues for a processive mechanism. So far, the crystal structures of rat PRMT1 and PRMT3, mouse PRMT4 and worm PRMT5 indicate an important role of the co-factor SAM. It could be shown that the addition of co-factor to the enzyme stabilized a region in the N-terminal domain contributing to the spatial arrangement of the active site of the enzyme (Sun *et al.*, 2011; Yue *et al.*, 2007; Zhang and Cheng, 2003; Zhang *et al.*, 2000). Furthermore, biochemical evidence has been provided that PRMT1, PRMT3 and PRMT6 follow a distributive mechanism (Kolbel *et al.*, 2009; Lakowski and Frankel, 2008).

In this work, methylation competitions provided information on how much D1-containing substrate is necessary to fully stop the methylation of D3/B-containing substrate (Results 5.5.11, page 131). Consequently, the reaction mechanism of PRMT5 could be analyzed and was also found to be distributive (Figure 68) (Results 5.5.12, page 136). Therefore, it is most likely that the co-factor SAM binds to PRMT5 first, stabilizing the active site, followed by the association of the substrate. In the case of the 20S complex this is either pICln/D1/D2 or pICln/D3/B. The enzymatic reaction occurs by transferring a methyl group from SAM onto the arginine residue of the respective Sm protein. In turn, the methylated Sm protein substrate and the modified co-factor (SAH) are released before a new round

of methylation can occur. It is important to state that the overall assembly of the 6S complex on PRMT5/WD45 is not affected by this, since the methylation of D1 is already completed before F/E/G docks to PRMT5.

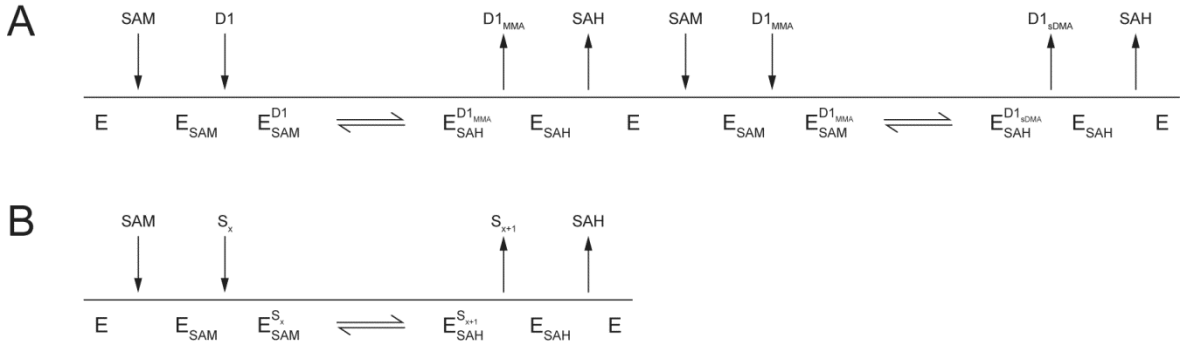

Figure 68 – Distributive mechanism of PRMT5 (Cleland notation)

(A) Formation of a symmetrically dimethylated arginine (sDMA) in D1 by PRMT5 following a distributive mechanism. The co-factor SAM and the substrate D1 bind sequentially to the enzyme. After the transfer of the methyl group, SAH and monomethylated D1 ($D1_{MMA}$) are released. To introduce a second methyl group to form sDMA, SAM and $D1_{MMA}$ associate with the enzyme. The MMA is modified to sDMA before SAH and the symmetrically dimethylated substrate ($D1_{sDMA}$) are expelled. **(B)** Overview of distributive mechanism in substrate methylation by PRMT5. PRMT5 methylates a variety of substrates, some of which contain more than one receptive arginine residue. Consequently, these substrates could harbor various numbers of unmethylated, monomethylated or already symmetrically dimethylated arginines. Independent of the previous methylation state of the substrate, PRMT5 binds SAM and the substrate including x methyl groups (S_x), catalyzes the incorporation of another methyl group on one receptive arginine residue and finally releases SAH and the modified substrate (S_{x+1}). For the transfer of an additional methyl group this process is repeated using the modified substrate and a fresh SAM co-factor.

The distributive mechanism of PRMT5 methylating substrates with several receptive arginine residues brings up the question of how these are processed over time. One could imagine an alternating mechanism introducing MMA and sDMA on the same arginine residue before interacting with the next one. Alternatively, first MMA could be generated in each arginine residue of a substrate before the methylation is completed by sDMA formation.

It could be shown in this work, that the frequency of substrate-enzyme interaction depends on the given substrate concentration. A model has been proposed in which the first substrate protein initially receives two methyl groups in two consecutive reactions generating one sDMA (Results 5.5.13, page 138 and Appendix 12.11, page 231). Then, an

n-fold number of monomethylations occurs before a monomethylarginine is altered to a symmetrically dimethylated one. The higher the substrate concentration was chosen, the more often MMAs were generated and the more likely was the event of methylating various substrate molecules. Reducing the substrate concentration resulted in a higher relative abundance of symmetrically dimethylated arginines (Appendix 12.10.2, page 227 and Appendix 12.10.3, page 229).

The methylation of Sm protein substrates *in vivo* would, therefore, occur most effectively if the local concentration of the substrate in close proximity to the active site was low. This would favor the complete methylation of one substrate as only a limited amount of competing substrates was present. Whereas the methylation data of this study provide a general overview of Sm protein substrate methylation, the exact composition of unmethylated, monomethylated and symmetrically dimethylated arginines at specific amino acid positions remains elusive.

6.2.4 The contribution of PRMT7 and PRMT9 to snRNP assembly

Three protein arginine methyltransferases, PRMT5, PRMT7 and PRMT9, have been described to catalyze sDMA formation in human (Cook *et al.*, 2006; Friesen *et al.*, 2001; Lee *et al.*, 2005c; Miranda *et al.*, 2004b). The by far best characterized of these is PRMT5 playing a major role in the biogenesis of snRNPs. Whereas PRMT7 has been found to serve a similar function as PRMT5, only very little is known about PRMT9 (Gonsalvez *et al.*, 2007; Lee *et al.*, 2005c). A recent study argues that both PRMT7 and PRMT9 do not belong to the type II methyltransferases since the applied technique of using a Flag-affinity tag to obtain these proteins inadvertently led to the co-purification of PRMT5 (Nishioka and Reinberg, 2003; Zurita-Lopez *et al.*, 2012). Consequently, this affects the overall contribution of PRMT5 on the generation of symmetrically dimethylated arginines.

Initially, PRMT7 was identified as a type III methyltransferase by showing that bacterially expressed protein caused only the monomethylation of synthetic peptides but not protein substrates (Miranda *et al.*, 2004b). Shortly after, PRMT7 was identified to symmetrically methylate histones, MBP, GAR and Sm B *in vivo* using Flag-antibody

immunoprecipitated enzyme. D3 was strongly methylated by bacterially expressed PRMT7, whereas D1 was not modified at all. Most altered arginine residues in these experiments exhibited monomethylation (Lee *et al.*, 2005c). A third study proposed PRMT7 to be a type II methyltransferase that can symmetrically dimethylate B and D3 independently of PRMT5 (Gonsalvez *et al.*, 2007). Again, Flag-antibody immunoprecipitation of PRMT5 and PRMT7 was separately applied, however, previously depleting the respective other methyltranferase by RNA interference. To verify sDMA formation the specific antibodies SYM10 and SYM11 were used (Boisvert *et al.*, 2002; Boisvert *et al.*, 2003). Yet, the analysis of any MMA or aDMA formation was fully omitted.

Very recently, bacterially and baculovirus-expressed PRMT7 were shown to produce only MMA but no sDMA, providing evidence of a type III instead of a type II methyltransferase activity (Zurita-Lopez *et al.*, 2012). The substrates comprised MBP, GAR, histones H2A, H2B, H3 and H4, the Sm protein D3 and the heteroligomer D3/B.

Apart from a possible PRMT5 contamination, experimental shortcomings have been stated for the identification of PRMT7 as a type II methyltransferase (Zurita-Lopez *et al.*, 2012). The identification of the type of methylated arginine performed by Lee et al. (2005c) was similar to one applied in this work. Proteins were methylated, split into individual amino acids and separated by thin layer chromatography. Still, four major differences occurred that might have had a strong impact on the identification of the methylation type when comparing both approaches. In this work, methylated proteins were separated from the unused radioactively labeled co-factor by TCA precipitation. Omission of this step could lead to a high background signal which would make an evaluation very difficult. The hydrolyzed sample was dried, resuspended in ddH_2O and mixed with arginine standards (L-Arg, MMA, aDMA and sDMA) (see Figure 39, page 121). Stemming from the hydrochloric acid in the hydrolysis reaction, the pH of the resuspended sample was between 0 and 1. Consequently, R_f values of arginines in the hydrolyzed sample lacking arginine standards and the arginine standards alone are not the same. Other differences between the two experimental approaches were the size of the TLC plate and the applied running buffer.

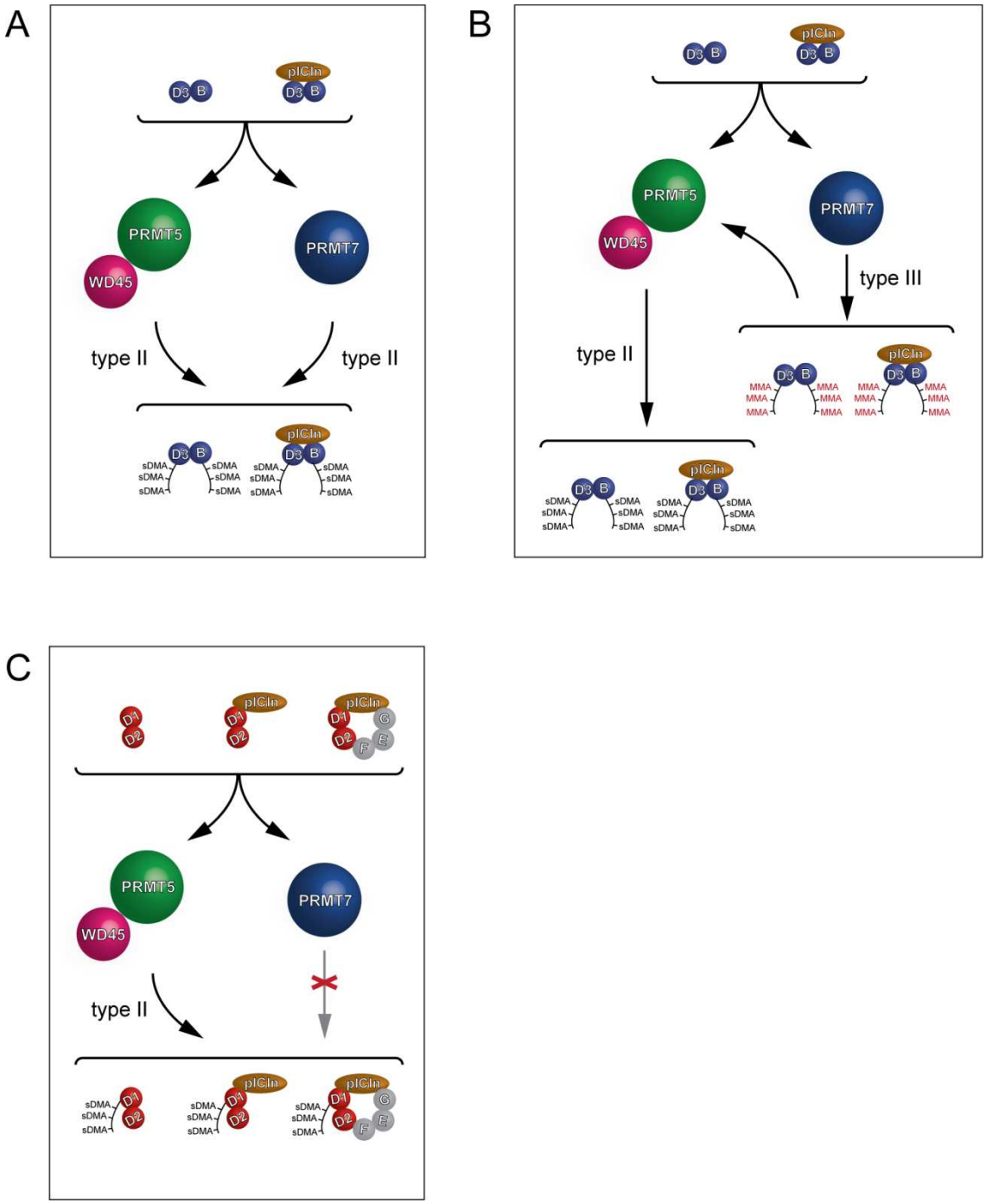

Figure 69 – PRMT7 participation in snRNP biogenesis.

Currently, it is disputable whether PRMT7 is a type II or type III methyltransferase. **(A)** Model 1: PRMT5 and PRMT7 are both type II methyltransferases that are able to symmetrically dimethylate Sm proteins B and D3. **(B)** Model 2: PRMT7 is a type III methyltransferase providing monomethylated precursor forms of B and D1 which are in turn symmetrically dimethylated by PRMT5. **(C)** Influence of PRMT7 in D1 methylation. PRMT5 but not PRMT7 is able to generate sDMAs in D1.

In this work, several TLC running buffers have been evaluated for optimal separation of methylated arginines resulting in a mixture of 25% (v/v) ammonium hydroxide and 75% (v/v) ethanol as the best candidate. The buffer used in the previous study (30% (v/v) ammonium hydroxide, chloroform, methanol, and water (2:0.5:4.5:1) caused only a minor separation of the individual arginine species. Despite the shortcomings in arginine separation, this running buffer has been commonly applied in the analysis of PRMTs by thin layer chromatography (Friesen *et al.*, 2001; Pesiridis *et al.*, 2009). Taking all this together, the omitted precipitation of co-factor, the separate application of arginine standard, the shorter running distance in the TLC and the usage of an inadvertent running buffer makes it nearly impossible to specifically correlate the radioactive signals to the arginine standards.

Ten years ago, PRMT5 was the only known type II methyltransferase in human. Since the later discovered PRMT7 and PRMT9 are at the moment highly disputed or only poorly understood, two possible models arise. If PRMT5 and PRMT7 were type II methyltransferases both enzymes should be able to symmetrically dimethylate B and D3 (Figure 69 A). PRMT7 was shown to influence snRNP biogenesis (Gonsalvez *et al.*, 2007). Oddly, only specific antibodies were applied to identify sDMAs but not MMAs, which are an intermediate product of type II and the main product of type III methyltransferases. Without sufficient data on the generation of MMAs and a possible PRMT5 contamination in the PRMT7 purifications, the type III methyltransferase activity is also likely (Zurita-Lopez *et al.*, 2012). In that case, PRMT7 would still contribute to B and D3 methylation producing only monomethylated arginines. PRMT5 would then be able to complete the methylation reaction by transferring the second methyl group (Figure 69 B). Still, PRMT5 would be capable of introducing MMAs as well as sDMAs to substrate proteins. D1 was found to be no common substrate of PRMT7 (Figure 69 C). Consequently, PRMT5 most likely remains the only type II methyltransferase that affects the biogenesis of snRNPs and the only one involved in the assembly of the 6S complex.

6.3 The SMN complex

6.3.1 Baculovirus expressed Gemin3 and Gemin5 are biochemically inactive

In the late phase of cytoplasmic assembly of snRNPs the SMN complex catalyzes the transfer of Sm proteins onto the Sm site of snRNA. To address this reaction in an *in vitro* system, the central SMN complex components (SMN, Gemin2 and Gemin6–8) were expressed in bacteria and Gemin3–5 using insect cells. Especially the latter ones proved to be difficult to obtain in bacterial expression. Of these, Gemin3 has been identified as a putative ATPase and RNA helicase (Charroux *et al.*, 1999) and Gemin5 has been shown to be responsible for snRNA recognition and guidance to the SMN complex (Battle *et al.*, 2006; Lau *et al.*, 2009).

It was found in this work that the individual expression of Gemin3 yielded only insoluble protein whereas the co-expression of Gemin4 had a positive effect on Gemin3 solubility. Gemin3 and Gemin4 are components of two different complexes, the SMN complex as well as miRNPs (Dostie *et al.*, 2003; Fischer *et al.*, 2011; Mourelatos *et al.*, 2002). Therefore, it is likely that one protein necessitates the presence of the other one in order to obtain its correct three-dimensional orientation.

The ATPase and RNA helicase activity that has been proclaimed for Gemin3 could not be identified using the insect cell-expressed protein (Results 5.7.2, page 150). In comparison, no such activity has been found in recombinantly expressed human Gemin3 (Charroux *et al.*, 1999). Immunoprecipitation of Gemin3 from HeLa extract could prove an ATP hydrolyzing activity (Grundhoff *et al.*, 1999). The recombinantly expressed mouse homolog of Gemin3 (dp103, 82.1% sequence identity with human Gemin3), however, was able to hydrolyze ATP as well as unwind synthetic RNA substrates (Yan *et al.*, 2003). So far, it is not proven that Gemin3 is responsible for the ATP hydrolysis that occurs in snRNP assembly. A yet unknown kinase that phosphorylates a component of the SMN complex is also likely to consume the ATP.

The second component of the SMN complex that was proposed to possess a specific function is Gemin5 (Battle *et al.*, 2006). This protein was shown to interact with snRNA in

a sequence-dependent manner via its N-terminal WD-repeat domain (Lau *et al.*, 2009). In this work, Gemin5 was either individually expressed or co-expressed with Gemin3 and Gemin4 in insect cells. Both cases have been identified to exist *in vivo*. Singular Gemin5 protein has been proposed to capture free snRNA and guide it to the SMN complex (Workman *et al.*, 2012). Also, a complex of Gemin3–5 was identified in gradient centrifugations of HeLa cytoplasmic extracts (Battle *et al.*, 2007). Recombinantly expressed Gemin5 in this work behaved as a trimer in gel filtration chromatography as was predicted in the initial identification of Gemin5 (Gubitz *et al.*, 2002). Interestingly, this protein interacted only unspecifically with RNA (Results 5.7.3, page 153). Correspondingly, the activity that has been previously shown for Gemin5 could not be identified using the insect cell-expressed protein.

Even though no biochemical activity could be observed in either Gemin3 or Gemin5, both proteins interacted specifically with Gemin4 or Gemin3/Gemin4, respectively. Furthermore, these three proteins could complement SMN, Gemin2 and Gemin6–8 to form the entire human SMN complex (see next paragraph). Consequently, at least the protein domains responsible for protein-protein interaction must be correctly folded.

6.3.2 *In vitro* reconstitution of wild-type and mutant human SMN complexes

The entire human SMN complex could be reconstituted *in vitro* containing wild-type SMN as well as SMN protein harboring a mutation found in SMA patients (E134K). In both complexes the transfer of Sm proteins from the 6S complex and pICln/D3/B was feasible even in the absence of Gemin3–5. This indicates that Gemin3–5 is not essential for Sm protein binding. Evidence has been provided that the tudor domain of SMN is responsible for the specific binding of symmetrically dimethylated Sm proteins *in vivo* possibly regulating the kinetics and fidelity of snRNP assembly (Meister *et al.*, 2001a; Tripsianes *et al.*, 2011). Using an *in vitro* system, on the other hand, showed that Sm proteins were capable of binding to SMN even in the absence of sDMA (Chari *et al.*, 2008).

Recently, Gemin2 was shown to make extensive contacts with an N-terminal helix of SMN and a pentameric Sm protein complex consisting of D1/D2/F/E/G (Zhang *et al.*, 2011). The

Sm proteins are arranged on Gemin2 in an open ring conformation. Paradoxically, Gemin2 was the only component in previous studies that was shown not to interact with Sm proteins (Baccon *et al.*, 2002; Carissimi *et al.*, 2006a; Charroux *et al.*, 1999; Charroux *et al.*, 2000; Gubitz *et al.*, 2002; Pellizzoni *et al.*, 2002). This finding resulted most likely from the application of individual Sm proteins in interaction studies rather than the application of heterooligomers of D1/D2, F/E/G and D3/B that have been identified *in vivo* (Raker *et al.*, 1996).

The exact binding site of D3/B is so far unknown. According to the data obtained in this work SMN, Gemin2 and Gemin6–8 might be solely responsible for Sm protein interaction. A minimal complex of SMN and Gemin2 has been found to be conserved in evolution that is capable of snRNP assembly (Kroiss *et al.*, 2008). Whereas D3/B directly bound to recombinantly expressed *Drosophila* SMN/Gemin2, its association could be increased by the presence of the remaining Sm proteins indicating a stabilizing effect of these proteins. It can be envisaged that the Sm protein pentamer D1/D2/F/E/G is held as an open ring on Gemin2. Addition of the snRNA via its Sm site might cause a transformational change in protein structure that enables the closure of the Sm core ring. In this work, it could be shown that both the central SMN complex consisting of SMN, Gemin2 and Gemin6–8 as well as the entire SMN complex are capable of snRNP formation (Results 5.7.5, page 158). Preliminary data indicated that the heterotrimeric Gemin3–5 has a positive effect on Sm core formation. Finally, SMN complexes harboring a mutated SMN protein that is also present in SMA patients could be used to obtain novel insight into the etiology of SMA.

7 Perspectives and Outlook

For the first time, the cytoplasmic snRNP assembly machinery consisting of the PRMT5 and SMN complexes has been reconstituted *in vitro* from recombinant sources. The combined application of bacterial as well as insect cell expression systems proved successful in generating the human PRMT5 complex that was capable of distributively introducing symmetrically dimethylated arginines into Sm proteins B, D1 and D3. Additionally, the assembly of 6S could be shown to occur on the PRMT5 complex. Finally, the recombinant SMN complex was able to remove pICln from the kinetically trapped Sm proteins and transfer them onto snRNA.

Having this *in vitro* system at hand provides the opportunity not only to analyze the modification of PRMT5 substrates present in spliceosomal snRNP formation but also involved in other cellular functions such as in histone modification and many more.

The reconstituted complexes could further be used to determine structural features applying cryo-electron microscopy and X-ray crystallography. Insight into the three-dimensional orientation of the PRMT5 complex alone or in combination with substrate proteins would offer detailed information on the methylation mechanism. Also, the influence of WD45 on the enzymatic activity and possible substrate binding could be determined. Recently, the crystal structure of *C. elegans* PRMT5 has been solved (Sun *et al.*, 2011). Direct comparison with the human amino acid sequence revealed only 28% identity. The domain responsible for PRMT5 dimerization was shown to be much smaller in the human homolog.

The SMN complex consists of 9 proteins several of which have been shown to oligomerize. Consequently, structural information could provide a better understanding of the actual composition of the functional SMN complex. Introducing patient mutations such as D44V, Y272C or T274I into the SMN protein could give further biochemical insight into the molecular etiology of spinal muscular atrophy. The most likely aspects that could be disrupted are SMN oligomerization affecting the overall composition of the complex and the actual transfer of Sm proteins onto snRNA.

8 References

Achsel, T., Brahms, H., Kastner, B., Bachi, A., Wilm, M., and Lührmann, R. (1999). A doughnut-shaped heteromer of human Sm-like proteins binds to the 3'-end of U6 snRNA, thereby facilitating U4/U6 duplex formation *in vitro*. *EMBO J* **18**, 5789-5802.

Baccon, J., Pellizzoni, L., Rappsilber, J., Mann, M., and Dreyfuss, G. (2002). Identification and characterization of Gemin7, a novel component of the survival of motor neuron complex. *J Biol Chem* **277**, 31957-31962.

Bachand, F. (2007). Protein arginine methyltransferases: from unicellular eukaryotes to humans. *Eukaryot Cell* **6**, 889-898.

Baillat, D., Hakimi, M.A., Naar, A.M., Shilatifard, A., Cooch, N., and Shiekhattar, R. (2005). Integrator, a multiprotein mediator of small nuclear RNA processing, associates with the C-terminal repeat of RNA polymerase II. *Cell* **123**, 265-276.

Battle, D.J., Kasim, M., Wang, J., and Dreyfuss, G. (2007). SMN-independent subunits of the SMN complex. Identification of a small nuclear ribonucleoprotein assembly intermediate. *J Biol Chem* **282**, 27953-27959.

Battle, D.J., Lau, C.K., Wan, L., Deng, H., Lotti, F., and Dreyfuss, G. (2006). The Gemin5 protein of the SMN complex identifies snRNAs. *Mol Cell* **23**, 273-279.

Bedford, M.T., and Clarke, S.G. (2009). Protein arginine methylation in mammals: who, what, and why. *Mol Cell* **33**, 1-13.

Berger, I., Fitzgerald, D.J., and Richmond, T.J. (2004). Baculovirus expression system for heterologous multiprotein complexes. *Nat Biotechnol* **22**, 1583-1587.

Bergin, A., Kim, G., Price, D.L., Sisodia, S.S., Lee, M.K., and Rabin, B.A. (1997). Identification and characterization of a mouse homologue of the spinal muscular atrophy-determining gene, survival motor neuron. *Gene* **204**, 47-53.

Boisvert, F.M., Cote, J., Boulanger, M.C., Cleroux, P., Bachand, F., Autexier, C., and Richard, S. (2002). Symmetrical dimethylarginine methylation is required for the localization of SMN in Cajal bodies and pre-mRNA splicing. *J Cell Biol* **159**, 957-969.

Boisvert, F.M., Cote, J., Boulanger, M.C., and Richard, S. (2003). A proteomic analysis of arginine-methylated protein complexes. *Mol Cell Proteomics* **2**, 1319-1330.

Boisvert, F.M., Dery, U., Masson, J.Y., and Richard, S. (2005). Arginine methylation of MRE11 by PRMT1 is required for DNA damage checkpoint control. *Genes Dev* **19**, 671-676.

Brahms, H., Raymackers, J., Union, A., de Keyser, F., Meheus, L., and Lührmann, R. (2000). The C-terminal RG dipeptide repeats of the spliceosomal Sm proteins D1 and D3 contain symmetrical dimethylarginines, which form a major B-cell epitope for anti-Sm autoantibodies. *J Biol Chem* **275**, 17122-17129.

Branscombe, T.L., Frankel, A., Lee, J.H., Cook, J.R., Yang, Z., Pestka, S., and Clarke, S. (2001). PRMT5 (Janus kinase-binding protein 1) catalyzes the formation of symmetric dimethylarginine residues in proteins. *J Biol Chem* **276**, 32971-32976.

Bühler, D., Raker, V., Lührmann, R., and Fischer, U. (1999). Essential role for the tudor domain of SMN in spliceosomal U snRNP assembly: implications for spinal muscular atrophy. *Hum Mol Genet* **8**, 2351-2357.

Bullock, W.O., Fernandez, J.M., and Short, J.M. (1987). XL1-Blue: A high efficiency plasmid transforming recA *Escherichia coli* strain with beta-galactosidase selection. *Biotechniques* **5**, 376-379.

Burghes, A.H., and Beattie, C.E. (2009). Spinal muscular atrophy: why do low levels of survival motor neuron protein make motor neurons sick? *Nat Rev Neurosci* **10**, 597-609.

Carissimi, C., Baccon, J., Straccia, M., Chiarella, P., Maiolica, A., Sawyer, A., Rappsilber, J., and Pellizzoni, L. (2005). Unrip is a component of SMN complexes active in snRNP assembly. *FEBS Lett* **579**, 2348-2354.

Carissimi, C., Saieva, L., Baccon, J., Chiarella, P., Maiolica, A., Sawyer, A., Rappsilber, J., and Pellizzoni, L. (2006a). Gemin8 is a novel component of the survival motor neuron complex and functions in small nuclear ribonucleoprotein assembly. *J Biol Chem* **281**, 8126-8134.

Carissimi, C., Saieva, L., Gabanella, F., and Pellizzoni, L. (2006b). Gemin8 is required for the architecture and function of the survival motor neuron complex. *J Biol Chem* **281**, 37009-37016.

Carvalho, T., Almeida, F., Calapez, A., Lafarga, M., Berciano, M.T., and Carmo-Fonseca, M. (1999). The spinal muscular atrophy disease gene product, SMN: A link between snRNP biogenesis and the Cajal (coiled) body. *J Cell Biol* **147**, 715-728.

Cauchi, R.J., Davies, K.E., and Liu, J.L. (2008). A motor function for the DEAD-box RNA helicase, Gemin3, in *Drosophila*. *PLoS Genet* **4**, e1000265.

Chang, B., Chen, Y., Zhao, Y., and Bruick, R.K. (2007). JMJD6 is a histone arginine demethylase. *Science* **318**, 444-447.

Chari, A., Golas, M.M., Klingenhager, M., Neuenkirchen, N., Sander, B., Englbrecht, C., Sickmann, A., Stark, H., and Fischer, U. (2008). An assembly chaperone collaborates with the SMN complex to generate spliceosomal SnRNPs. *Cell* **135**, 497-509.

Charroux, B., Pellizzoni, L., Perkinson, R.A., Shevchenko, A., Mann, M., and Dreyfuss, G. (1999). Gemin3: A novel DEAD box protein that interacts with SMN, the spinal muscular atrophy gene product, and is a component of gems. *J Cell Biol* **147**, 1181-1194.

Charroux, B., Pellizzoni, L., Perkinson, R.A., Yong, J., Shevchenko, A., Mann, M., and Dreyfuss, G. (2000). Gemin4. A novel component of the SMN complex that is found in both gems and nucleoli. *J Cell Biol* **148**, 1177-1186.

Chen, C., Nott, T.J., Jin, J., and Pawson, T. (2011). Deciphering arginine methylation: Tudor tells the tale. *Nat Rev Mol Cell Biol* **12**, 629-642.

Chen, D., Ma, H., Hong, H., Koh, S.S., Huang, S.M., Schurter, B.T., Aswad, D.W., and Stallcup, M.R. (1999). Regulation of transcription by a protein methyltransferase. *Science* **284**, 2174-2177.

Cheng, D., Yadav, N., King, R.W., Swanson, M.S., Weinstein, E.J., and Bedford, M.T. (2004). Small molecule regulators of protein arginine methyltransferases. *J Biol Chem* **279**, 23892-23899.

Coady, T.H., and Lorson, C.L. (2011). SMN in spinal muscular atrophy and snRNP biogenesis. *Wiley Interdiscip Rev RNA* **2**, 546-564.

Cook, J.R., Lee, J.H., Yang, Z.H., Krause, C.D., Herth, N., Hoffmann, R., and Pestka, S. (2006). FBXO11/PRMT9, a new protein arginine methyltransferase, symmetrically dimethylates arginine residues. *Biochem Biophys Res Commun* **342**, 472-481.

Dahlberg, J.E., Yang, H., Neuman de Vegvar, H., and Lund, E. (1990). Formation of the 3 end of U1 snRNA. *Mol Biol Rep* **14**, 161-162.

Darzacq, X., Jady, B.E., Verheggen, C., Kiss, A.M., Bertrand, E., and Kiss, T. (2002). Cajal body-specific small nuclear RNAs: a novel class of 2'-O-methylation and pseudouridylation guide RNAs. *EMBO J* **21**, 2746-2756.

Dostie, J., Mourelatos, Z., Yang, M., Sharma, A., and Dreyfuss, G. (2003). Numerous microRNPs in neuronal cells containing novel microRNAs. *RNA* **9**, 180-186.

Emma, F., Breton, S., Morrison, R., Wright, S., and Strange, K. (1998). Effect of cell swelling on membrane and cytoplasmic distribution of pICln. *Am J Physiol* **274**, C1545-1551.

Fischer, U., Darzynkiewicz, E., Tahara, S.M., Dathan, N.A., Lührmann, R., and Mattaj, I.W. (1991). Diversity in the signals required for nuclear accumulation of U snRNPs and variety in the pathways of nuclear transport. *J Cell Biol* **113**, 705-714.

Fischer, U., Englbrecht, C., and Chari, A. (2011). Biogenesis of spliceosomal small nuclear ribonucleoproteins. *Wiley Interdiscip Rev RNA* **2**, 718-731.

Fischer, U., Liu, Q., and Dreyfuss, G. (1997). The SMN-SIP1 complex has an essential role in spliceosomal snRNP biogenesis. *Cell* **90**, 1023-1029.

Fischer, U., and Lührmann, R. (1990). An essential signaling role for the m3G cap in the transport of U1 snRNP to the nucleus. *Science* **249**, 786-790.

Fitzgerald, D.J., Berger, P., Schaffitzel, C., Yamada, K., Richmond, T.J., and Berger, I. (2006). Protein complex expression by using multigene baculoviral vectors. *Nat Methods* **3**, 1021-1032.

Frankel, A., Yadav, N., Lee, J., Branscombe, T.L., Clarke, S., and Bedford, M.T. (2002). The novel human protein arginine N-methyltransferase PRMT6 is a nuclear enzyme displaying unique substrate specificity. *J Biol Chem* **277**, 3537-3543.

Friesen, W.J., Paushkin, S., Wyce, A., Massenet, S., Pesiridis, G.S., Van Duyne, G., Rappsilber, J., Mann, M., and Dreyfuss, G. (2001). The methylosome, a 20S complex containing JBP1 and pICln, produces dimethylarginine-modified Sm proteins. *Mol Cell Biol* **21**, 8289-8300.

Friesen, W.J., Wyce, A., Paushkin, S., Abel, L., Rappsilber, J., Mann, M., and Dreyfuss, G. (2002). A novel WD repeat protein component of the methylosome binds Sm proteins. *J Biol Chem* **277**, 8243-8247.

Gharahdaghi, F., Weinberg, C.R., Meagher, D.A., Imai, B.S., and Mische, S.M. (1999). Mass spectrometric identification of proteins from silver-stained polyacrylamide gel: a method for the removal of silver ions to enhance sensitivity. *Electrophoresis* **20**, 601-605.

Gonsalvez, G.B., Rajendra, T.K., Tian, L., and Matera, A.G. (2006). The Sm-protein methyltransferase, dart5, is essential for germ-cell specification and maintenance. *Curr Biol* **16**, 1077-1089.

Gonsalvez, G.B., Tian, L., Ospina, J.K., Boisvert, F.M., Lamond, A.I., and Matera, A.G. (2007). Two distinct arginine methyltransferases are required for biogenesis of Sm-class ribonucleoproteins. *J Cell Biol* **178**, 733-740.

Granados, R.R., Guoxun, L., Derksen, A.C.G., and McKenna, K.A. (1994). A new insect cell line from *Trichoplusia ni* (BTI-Tn-5B1-4) susceptible to *Trichoplusia ni* single enveloped nuclear polyhedrosis virus. *Journal of Invertebrate Pathology* **64**, 260-266.

Grimmler, M., Otter, S., Peter, C., Muller, F., Chari, A., and Fischer, U. (2005). Unrip, a factor implicated in cap-independent translation, associates with the cytosolic SMN complex and influences its intracellular localization. *Hum Mol Genet* **14**, 3099-3111.

Grundhoff, A.T., Kremmer, E., Tureci, O., Glieden, A., Gindorf, C., Atz, J., Mueller-Lantzsch, N., Schubach, W.H., and Grasser, F.A. (1999). Characterization of DP103, a novel DEAD box protein that binds to the Epstein-Barr virus nuclear proteins EBNA2 and EBNA3C. *J Biol Chem* **274**, 19136-19144.

Gubitz, A.K., Feng, W., and Dreyfuss, G. (2004). The SMN complex. *Exp Cell Res* **296**, 51-56.

Gubitz, A.K., Mourelatos, Z., Abel, L., Rappsilber, J., Mann, M., and Dreyfuss, G. (2002). Gemin5, a novel WD repeat protein component of the SMN complex that binds Sm proteins. *J Biol Chem* **277**, 5631-5636.

Guderian, G., Peter, C., Wiesner, J., Sickmann, A., Schulze-Osthoff, K., Fischer, U., and Grimmler, M. (2011). RioK1, a new interactor of protein arginine methyltransferase 5 (PRMT5), competes with pICln for binding and modulates PRMT5 complex composition and substrate specificity. *J Biol Chem* **286**, 1976-1986.

Hamm, J., Darzynkiewicz, E., Tahara, S.M., and Mattaj, I.W. (1990a). The trimethylguanosine cap structure of U1 snRNA is a component of a bipartite nuclear targeting signal. *Cell* **62**, 569-577.

Hamm, J., Dathan, N.A., Scherly, D., and Mattaj, I.W. (1990b). Multiple domains of U1 snRNA, including U1 specific protein binding sites, are required for splicing. *EMBO J* **9**, 1237-1244.

Hebert, M.D., Shpargel, K.B., Ospina, J.K., Tucker, K.E., and Matera, A.G. (2002). Coilin methylation regulates nuclear body formation. *Dev Cell* **3**, 329-337.

Hebert, M.D., Szymczyk, P.W., Shpargel, K.B., and Matera, A.G. (2001). Coilin forms the bridge between Cajal bodies and SMN, the spinal muscular atrophy protein. *Genes Dev* **15**, 2720-2729.

Hericourt, F., Blanc, S., Redeker, V., and Jupin, I. (2000). Evidence for phosphorylation and ubiquitinylation of the turnip yellow mosaic virus RNA-dependent RNA polymerase domain expressed in a baculovirus-insect cell system. *Biochem J* **349**, 417-425.

Hodder, A.N., Crewther, P.E., Matthew, M.L., Reid, G.E., Moritz, R.L., Simpson, R.J., and Anders, R.F. (1996). The disulfide bond structure of Plasmodium apical membrane antigen-1. *J Biol Chem* **271**, 29446-29452.

Horii, T., Ogawa, T., and Ogawa, H. (1980). Organization of the recA gene of *Escherichia coli*. *Proc Natl Acad Sci U S A* **77**, 313-317.

Izaurralde, E., Lewis, J., Gamberi, C., Jarmolowski, A., McGuigan, C., and Mattaj, I.W. (1995). A cap-binding protein complex mediating U snRNA export. *Nature* **376**, 709-712.

Jady, B.E., Darzacq, X., Tucker, K.E., Matera, A.G., Bertrand, E., and Kiss, T. (2003). Modification of Sm small nuclear RNAs occurs in the nucleoplasmic Cajal body following import from the cytoplasm. *EMBO J* **22**, 1878-1888.

Jarmolowski, A., and Mattaj, I.W. (1993). The determinants for Sm protein binding to *Xenopus* U1 and U5 snRNAs are complex and non-identical. *EMBO J* **12**, 223-232.

Jelinic, P., Stehle, J.C., and Shaw, P. (2006). The testis-specific factor CTCFL cooperates with the protein methyltransferase PRMT7 in H19 imprinting control region methylation. *PLoS Biol* **4**, e355.

Jones, S., Daley, D.T., Luscombe, N.M., Berman, H.M., and Thornton, J.M. (2001). Protein-RNA interactions: a structural analysis. *Nucleic Acids Res* **29**, 943-954.

Junge, K.-W., and Hübner, G. (1989). Fotografische Chemie, Vol 5. verb. Aufl. (Leipzig, VEB Fotokinoverlag).

Kakker, N.K., Mikhailov, M.V., Nermut, M.V., Burny, A., and Roy, P. (1999). Bovine leukemia virus Gag particle assembly in insect cells: formation of chimeric particles by domain-switched leukemia/lentivirus Gag polyprotein. *Virology* **265**, 308-318.

Kambach, C., Walke, S., Young, R., Avis, J.M., de la Fortelle, E., Raker, V.A., Lührmann, R., Li, J., and Nagai, K. (1999). Crystal structures of two Sm protein complexes and their implications for the assembly of the spliceosomal snRNPs. *Cell* **96**, 375-387.

Kapust, R.B., Tozser, J., Copeland, T.D., and Waugh, D.S. (2002). The P1' specificity of tobacco etch virus protease. *Biochem Biophys Res Commun* **294**, 949-955.

Katsanis, N., Yaspo, M.L., and Fisher, E.M. (1997). Identification and mapping of a novel human gene, HRMT1L1, homologous to the rat protein arginine N-methyltransferase 1 (PRMT1) gene. *Mamm Genome* **8**, 526-529.

Kolbel, K., Ihling, C., Bellmann-Sickert, K., Neundorf, I., Beck-Sickinger, A.G., Sinz, A., Kuhn, U., and Wahle, E. (2009). Type I Arginine Methyltransferases PRMT1 and PRMT-3 Act Distributively. *J Biol Chem* **284**, 8274-8282.

Krause, C.D., Yang, Z.H., Kim, Y.S., Lee, J.H., Cook, J.R., and Pestka, S. (2007). Protein arginine methyltransferases: evolution and assessment of their pharmacological and therapeutic potential. *Pharmacol Ther* **113**, 50-87.

Kroiss, M., Schultz, J., Wiesner, J., Chari, A., Sickmann, A., and Fischer, U. (2008). Evolution of an RNP assembly system: a minimal SMN complex facilitates formation of UsnRNPs in *Drosophila melanogaster*. *Proc Natl Acad Sci U S A* **105**, 10045-10050.

Kuhn, P., and Xu, W. (2009). Protein Arginine Methyltransferases: Nuclear Receptor Coregulators and Beyond. *Progress in Molecular Biology and translational science Regulatory mechanisms in transcriptional signaling* **87**, 299-342.

L'Annunziata, M.F. (2003). Handbook of Radioactivity Analysis, Vol 2nd ed. (Sandiego, CA, USA, Academic Press).

Lacroix, M., El Messaoudi, S., Rodier, G., Le Cam, A., Sardet, C., and Fabbrizio, E. (2008). The histone-binding protein COPR5 is required for nuclear functions of the protein arginine methyltransferase PRMT5. *EMBO Rep* **9**, 452-458.

Laemmli, U.K. (1970). Cleavage of structural proteins during the assembly of the head of bacteriophage T4. *Nature* **227**, 680-685.

Lakowski, T.M., and Frankel, A. (2008). A kinetic study of human protein arginine N-methyltransferase 6 reveals a distributive mechanism. *J Biol Chem* **283**, 10015-10025.

Lau, C.K., Bachorik, J.L., and Dreyfuss, G. (2009). Gemin5-snRNA interaction reveals an RNA binding function for WD repeat domains. *Nat Struct Mol Biol* **16**, 486-491.

Lee, D.Y., Teyssier, C., Strahl, B.D., and Stallcup, M.R. (2005a). Role of protein methylation in regulation of transcription. *Endocr Rev* **26**, 147-170.

Lee, J., Sayegh, J., Daniel, J., Clarke, S., and Bedford, M.T. (2005b). PRMT8, a new membrane-bound tissue-specific member of the protein arginine methyltransferase family. *J Biol Chem* **280**, 32890-32896.

Lee, J.H., Cook, J.R., Yang, Z.H., Mirochnitchenko, O., Gunderson, S.I., Felix, A.M., Herth, N., Hoffmann, R., and Pestka, S. (2005c). PRMT7, a new protein arginine methyltransferase that synthesizes symmetric dimethylarginine. *J Biol Chem* **280**, 3656-3664.

Lefebvre, S., Burglen, L., Reboullet, S., Clermont, O., Burlet, P., Viollet, L., Benichou, B., Cruaud, C., Millasseau, P., Zeviani, M.*, et al.* (1995). Identification and characterization of a spinal muscular atrophy-determining gene. *Cell* **80**, 155-165.

Lefebvre, S., Burlet, P., Liu, Q., Bertrandy, S., Clermont, O., Munnich, A., Dreyfuss, G., and Melki, J. (1997). Correlation between severity and SMN protein level in spinal muscular atrophy. *Nat Genet* **16**, 265-269.

Lin, W.J., Gary, J.D., Yang, M.C., Clarke, S., and Herschman, H.R. (1996). The mammalian immediate-early TIS21 protein and the leukemia-associated BTG1 protein interact with a protein-arginine N-methyltransferase. *J Biol Chem* **271**, 15034-15044.

Liu, F., Zhao, X., Perna, F., Wang, L., Koppikar, P., Abdel-Wahab, O., Harr, M.W., Levine, R.L., Xu, H., Tefferi, A.*, et al.* (2011). JAK2V617F-mediated phosphorylation of PRMT5 downregulates its methyltransferase activity and promotes myeloproliferation. *Cancer Cell* **19**, 283-294.

Liu, Q., and Dreyfuss, G. (1996). A novel nuclear structure containing the survival of motor neurons protein. *EMBO J* **15**, 3555-3565.

Liu, Q., Fischer, U., Wang, F., and Dreyfuss, G. (1997). The spinal muscular atrophy disease gene product, SMN, and its associated protein SIP1 are in a complex with spliceosomal snRNP proteins. *Cell* **90**, 1013-1021.

Lorson, C.L., and Androphy, E.J. (2000). An exonic enhancer is required for inclusion of an essential exon in the SMA-determining gene SMN. *Hum Mol Genet* **9**, 259-265.

Lorson, C.L., Strasswimmer, J., Yao, J.M., Baleja, J.D., Hahnen, E., Wirth, B., Le, T., Burghes, A.H., and Androphy, E.J. (1998). SMN oligomerization defect correlates with spinal muscular atrophy severity. *Nat Genet* **19**, 63-66.

Lunn, M.R., and Wang, C.H. (2008). Spinal muscular atrophy. *Lancet* **371**, 2120-2133.

Ma, Y., Dostie, J., Dreyfuss, G., and Van Duyne, G.D. (2005). The Gemin6-Gemin7 heterodimer from the survival of motor neurons complex has an Sm protein-like structure. *Structure* **13**, 883-892.

Markowitz, J.A., Singh, P., and Darras, B.T. (2012). Spinal muscular atrophy: a clinical and research update. *Pediatr Neurol* **46**, 1-12.

Martin, G., Ostareck-Lederer, A., Chari, A., Neuenkirchen, N., Dettwiler, S., Blank, D., Ruegsegger, U., Fischer, U., and Keller, W. (2010). Arginine methylation in subunits of mammalian pre-mRNA cleavage factor I. *RNA* **16**, 1646-1659.

McBride, A.E., and Silver, P.A. (2001). State of the arg: protein methylation at arginine comes of age. *Cell* **106**, 5-8.

Meister, G., Bühler, D., Laggerbauer, B., Zobawa, M., Lottspeich, F., and Fischer, U. (2000). Characterization of a nuclear 20S complex containing the survival of motor neurons (SMN) protein and a specific subset of spliceosomal Sm proteins. *Hum Mol Genet* **9**, 1977-1986.

Meister, G., Bühler, D., Pillai, R., Lottspeich, F., and Fischer, U. (2001a). A multiprotein complex mediates the ATP-dependent assembly of spliceosomal U snRNPs. *Nat Cell Biol* **3**, 945-949.

Meister, G., Eggert, C., Bühler, D., Brahms, H., Kambach, C., and Fischer, U. (2001b). Methylation of Sm proteins by a complex containing PRMT5 and the putative U snRNP assembly factor pICln. *Curr Biol* **11**, 1990-1994.

Meister, G., Eggert, C., and Fischer, U. (2002). SMN-mediated assembly of RNPs: a complex story. *Trends Cell Biol* **12**, 472-478.

Merril, C.R., Dunau, M.L., and Goldman, D. (1981). A rapid sensitive silver stain for polypeptides in polyacrylamide gels. *Anal Biochem* **110**, 201-207.

Metcalf, W.W., Jiang, W., and Wanner, B.L. (1994). Use of the rep technique for allele replacement to construct new *Escherichia coli* hosts for maintenance of R6K gamma origin plasmids at different copy numbers. *Gene* **138**, 1-7.

Meywald, T., Scherthan, H., and Nagl, W. (1996). Increased specificity of colloidal silver staining by means of chemical attenuation. *Hereditas* **124**, 63-70.

Miranda, T.B., Khusial, P., Cook, J.R., Lee, J.H., Gunderson, S.I., Pestka, S., Zieve, G.W., and Clarke, S. (2004a). Spliceosome Sm proteins D1, D3, and B/B' are asymmetrically dimethylated at arginine residues in the nucleus. *Biochem Biophys Res Commun* **323**, 382-387.

Miranda, T.B., Miranda, M., Frankel, A., and Clarke, S. (2004b). PRMT7 is a member of the protein arginine methyltransferase family with a distinct substrate specificity. *J Biol Chem* **279**, 22902-22907.

Morse, R., Shaw, D.J., Todd, A.G., and Young, P.J. (2007). Targeting of SMN to Cajal bodies is mediated by self-association. *Hum Mol Genet* **16**, 2349-2358.

Mourelatos, Z., Dostie, J., Paushkin, S., Sharma, A., Charroux, B., Abel, L., Rappsilber, J., Mann, M., and Dreyfuss, G. (2002). miRNPs: a novel class of ribonucleoproteins containing numerous microRNAs. *Genes Dev* **16**, 720-728.

Najbauer, J., Johnson, B.A., Young, A.L., and Aswad, D.W. (1993). Peptides with sequences similar to glycine, arginine-rich motifs in proteins interacting with RNA are efficiently recognized by methyltransferase(s) modifying arginine in numerous proteins. *J Biol Chem* **268**, 10501-10509.

Narayan, R. (2009). Biomedical Materials (New York, Springer).

Narayanan, U., Ospina, J.K., Frey, M.R., Hebert, M.D., and Matera, A.G. (2002). SMN, the spinal muscular atrophy protein, forms a pre-import snRNP complex with snurportin1 and importin beta. *Hum Mol Genet* **11**, 1785-1795.

Neuenkirchen, N., Chari, A., and Fischer, U. (2008). Deciphering the assembly pathway of Sm-class U snRNPs. *FEBS Lett* **582**, 1997-2003.

Niewmierzycka, A., and Clarke, S. (1999). S-Adenosylmethionine-dependent methylation in Saccharomyces cerevisiae. Identification of a novel protein arginine methyltransferase. *J Biol Chem* **274**, 814-824.

Nishioka, K., and Reinberg, D. (2003). Methods and tips for the purification of human histone methyltransferases. *Methods* **31**, 49-58.

Novy, R., Drott, D., Yaeger, K., and Mierendorf, R. (2001). Overcoming the codon bias of *E. coli* for enhanced protein expression. *inNovations* **12**, 1-3.

O'Reilly, D.R., Miller, L.K., and Luckow, V.A. (1993). Baculovirus Expression Vectors: A Laboratory Manual (Oxford, Oxford University Press).

Ogawa, C., Usui, K., Aoki, M., Ito, F., Itoh, M., Kai, C., Kanamori-Katayama, M., Hayashizaki, Y., and Suzuki, H. (2007). Gemin2 plays an important role in stabilizing the survival of motor neuron complex. *J Biol Chem* **282**, 11122-11134.

Ogawa, C., Usui, K., Ito, F., Itoh, M., Hayashizaki, Y., and Suzuki, H. (2009). Role of survival motor neuron complex components in small nuclear ribonucleoprotein assembly. *J Biol Chem* **284**, 14609-14617.

Ohno, M., Segref, A., Bachi, A., Wilm, M., and Mattaj, I.W. (2000). PHAX, a mediator of U snRNA nuclear export whose activity is regulated by phosphorylation. *Cell* **101**, 187-198.

Otter, S., Grimmler, M., Neuenkirchen, N., Chari, A., Sickmann, A., and Fischer, U. (2007). A comprehensive interaction map of the human survival of motor neuron (SMN) complex. *J Biol Chem* **282**, 5825-5833.

Paik, W.K., and Kim, S. (1967). Enzymatic methylation of protein fractions from calf thymus nuclei. *Biochem Biophys Res Commun* **29**, 14-20.

Paik, W.K., and Kim, S. (1980). Natural occurrence of various methylated amino acid derivatives. In Protein Methylation, A. Meister, ed. (New York, John Wiley & Sons), pp. 8-22.

Pal, S., Vishwanath, S.N., Erdjument-Bromage, H., Tempst, P., and Sif, S. (2004). Human SWI/SNF-associated PRMT5 methylates histone H3 arginine 8 and negatively regulates expression of ST7 and NM23 tumor suppressor genes. *Mol Cell Biol* **24**, 9630-9645.

Pal, S., Yun, R., Datta, A., Lacomis, L., Erdjument-Bromage, H., Kumar, J., Tempst, P., and Sif, S. (2003). mSin3A/histone deacetylase 2- and PRMT5-containing Brg1 complex is involved in transcriptional repression of the Myc target gene cad. *Mol Cell Biol* **23**, 7475-7487.

Patel, A.A., and Steitz, J.A. (2003). Splicing double: insights from the second spliceosome. *Nat Rev Mol Cell Biol* **4**, 960-970.

Pawson, T., and Scott, J.D. (2005). Protein phosphorylation in signaling--50 years and counting. *Trends Biochem Sci* **30**, 286-290.

Pellizzoni, L., Baccon, J., Rappsilber, J., Mann, M., and Dreyfuss, G. (2002). Purification of native survival of motor neurons complexes and identification of Gemin6 as a novel component. *J Biol Chem* **277**, 7540-7545.

Pellizzoni, L., Charroux, B., and Dreyfuss, G. (1999). SMN mutants of spinal muscular atrophy patients are defective in binding to snRNP proteins. *Proc Natl Acad Sci U S A* **96**, 11167-11172.

Pesiridis, G.S., Diamond, E., and Van Duyne, G.D. (2009). Role of pICLn in methylation of Sm proteins by PRMT5. *J Biol Chem* **284**, 21347-21359.

Phan, J., Zdanov, A., Evdokimov, A.G., Tropea, J.E., Peters, H.K., 3rd, Kapust, R.B., Li, M., Wlodawer, A., and Waugh, D.S. (2002). Structural basis for the substrate specificity of tobacco etch virus protease. *J Biol Chem* **277**, 50564-50572.

Phillips, T.A., VanBogelen, R.A., and Neidhardt, F.C. (1984). lon gene product of *Escherichia coli* is a heat-shock protein. *J Bacteriol* **159**, 283-287.

Plessel, G., Fischer, U., and Lührmann, R. (1994). m3G cap hypermethylation of U1 small nuclear ribonucleoprotein (snRNP) *in vitro*: evidence that the U1 small nuclear RNA-(guanosine-N2)-methyltransferase is a non-snRNP cytoplasmic protein that requires a binding site on the Sm core domain. *Mol Cell Biol* **14**, 4160-4172.

Pollack, B.P., Kotenko, S.V., He, W., Izotova, L.S., Barnoski, B.L., and Pestka, S. (1999). The human homologue of the yeast proteins Skb1 and Hsl7p interacts with Jak kinases and contains protein methyltransferase activity. *J Biol Chem* **274**, 31531-31542.

Pu, W.T., Krapivinsky, G.B., Krapivinsky, L., and Clapham, D.E. (1999). pICln inhibits snRNP biogenesis by binding core spliceosomal proteins. *Mol Cell Biol* **19**, 4113-4120.

Puck, T.T., Marcus, P.I., and Cieciura, S.J. (1956). Clonal growth of mammalian cells *in vitro*; growth characteristics of colonies from single HeLa cells with and without a feeder layer. *J Exp Med* **103**, 273-283.

Raijmakers, R., Zendman, A.J., Egberts, W.V., Vossenaar, E.R., Raats, J., Soede-Huijbregts, C., Rutjes, F.P., van Veelen, P.A., Drijfhout, J.W., and Pruijn, G.J. (2007). Methylation of arginine residues interferes with citrullination by peptidylarginine deiminases in vitro. *J Mol Biol* **367**, 1118-1129.

Raker, V.A., Plessel, G., and Lührmann, R. (1996). The snRNP core assembly pathway: identification of stable core protein heteromeric complexes and an snRNP subcore particle *in vitro*. *EMBO J* **15**, 2256-2269.

Reddy, R., Singh, R., and Shimba, S. (1992). Methylated cap structures in eukaryotic RNAs: structure, synthesis and functions. *Pharmacol Ther* **54**, 249-267.

Reed, L.J., and Muench, H. (1938). A simple method of estimating fifty percent endpoints. *The American Journal of Hygiene* **27**, 493-497.

Rho, J., Choi, S., Seong, Y.R., Cho, W.K., Kim, S.H., and Im, D.S. (2001). Prmt5, which forms distinct homo-oligomers, is a member of the protein-arginine methyltransferase family. *J Biol Chem* **276**, 11393-11401.

Rino, J., and Carmo-Fonseca, M. (2009). The spliceosome: a self-organized macromolecular machine in the nucleus? *Trends Cell Biol* **19**, 375-384.

Robin-Lespinasse, Y., Sentis, S., Kolytcheff, C., Rostan, M.C., Corbo, L., and Le Romancer, M. (2007). hCAF1, a new regulator of PRMT1-dependent arginine methylation. *J Cell Sci* **120**, 638-647.

Rossoll, W., and Bassell, G.J. (2009). Spinal muscular atrophy and a model for survival of motor neuron protein function in axonal ribonucleoprotein complexes. *Results Probl Cell Differ* **48**, 289-326.

Sakharkar, M.K., Chow, V.T., and Kangueane, P. (2004). Distributions of exons and introns in the human genome. *In Silico Biol* **4**, 387-393.

Schneider, C., Newman, R.A., Sutherland, D.R., Asser, U., and Greaves, M.F. (1982). A one-step purification of membrane proteins using a high efficiency immunomatrix. *J Biol Chem* **257**, 10766-10769.

Scorilas, A., Black, M.H., Talieri, M., and Diamandis, E.P. (2000). Genomic organization, physical mapping, and expression analysis of the human protein arginine methyltransferase 1 gene. *Biochem Biophys Res Commun* **278**, 349-359.

Selenko, P., Sprangers, R., Stier, G., Bühler, D., Fischer, U., and Sattler, M. (2001). SMN tudor domain structure and its interaction with the Sm proteins. *Nat Struct Biol* **8**, 27-31.

Singh, R., and Reddy, R. (1989). Gamma-monomethyl phosphate: a cap structure in spliceosomal U6 small nuclear RNA. *Proc Natl Acad Sci U S A* **86**, 8280-8283.

Singh, V., Miranda, T.B., Jiang, W., Frankel, A., Roemer, M.E., Robb, V.A., Gutmann, D.H., Herschman, H.R., Clarke, S., and Newsham, I.F. (2004). DAL-1/4.1B tumor suppressor interacts with protein arginine N-methyltransferase 3 (PRMT3) and inhibits its ability to methylate substrates *in vitro* and *in vivo*. *Oncogene* **23**, 7761-7771.

Sivaraman, T., Kumar, T.K.S., Jayaraman, G., and Yu, C. (1997). The Mechanism of 2,2,2-Trichloroacetic Acid-Induced Protein Precipitation. *Journal of Protein Chemistry* **16**, 291-297.

Smith, D.B., and Johnson, K.S. (1988). Single-step purification of polypeptides expressed in *Escherichia coli* as fusions with glutathione S-transferase. *Gene* **67**, 31-40.

Smith, G.E., Ju, G., Ericson, B.L., Moschera, J., Lahm, H.W., Chizzonite, R., and Summers, M.D. (1985). Modification and secretion of human interleukin 2 produced in insect cells by a baculovirus expression vector. *Proc Natl Acad Sci U S A* **82**, 8404-8408.

Stark, H., Dube, P., Lührmann, R., and Kastner, B. (2001). Arrangement of RNA and proteins in the spliceosomal U1 small nuclear ribonucleoprotein particle. *Nature* **409**, 539-542.

Strahl, B.D., Briggs, S.D., Brame, C.J., Caldwell, J.A., Koh, S.S., Ma, H., Cook, R.G., Shabanowitz, J., Hunt, D.F., Stallcup, M.R*., et al.* (2001). Methylation of histone H4 at arginine 3 occurs *in vivo* and is mediated by the nuclear receptor coactivator PRMT1. *Curr Biol* **11**, 996-1000.

Sun, L., Wang, M., Lv, Z., Yang, N., Liu, Y., Bao, S., Gong, W., and Xu, R.M. (2011). Structural insights into protein arginine symmetric dimethylation by PRMT5. *Proc Natl Acad Sci U S A* **108**, 20538-20543.

Talken, B.L., Schafermeyer, K.R., Bailey, C.W., Lee, D.R., and Hoffman, R.W. (2001). T cell epitope mapping of the Smith antigen reveals that highly conserved Smith antigen motifs are the dominant target of T cell immunity in systemic lupus erythematosus. *J Immunol* **167**, 562-568.

Tang, J., Gary, J.D., Clarke, S., and Herschman, H.R. (1998). PRMT 3, a type I protein arginine N-methyltransferase that differs from PRMT1 in its oligomerization, subcellular localization, substrate specificity, and regulation. *J Biol Chem* **273**, 16935-16945.

Taylor, R.G., Walker, D.C., and McInnes, R.R. (1993). *E. coli* host strains significantly affect the quality of small scale plasmid DNA preparations used for sequencing. *Nucleic Acids Res* **21**, 1677-1678.

Tripsianes, K., Madl, T., Machyna, M., Fessas, D., Englbrecht, C., Fischer, U., Neugebauer, K.M., and Sattler, M. (2011). Structural basis for dimethylarginine recognition by the Tudor domains of human SMN and SPF30 proteins. *Nat Struct Mol Biol* **18**, 1414-1420.

Urlaub, H., Raker, V.A., Kostka, S., and Lührmann, R. (2001). Sm protein-Sm site RNA interactions within the inner ring of the spliceosomal snRNP core structure. *EMBO J* **20**, 187-196.

Vaughn, J.L., Goodwin, R.H., Tompkins, G.J., and McCawley, P. (1977). The establishment of two cell lines from the insect *Spodoptera frugiperda* (Lepidoptera; Noctuidae). *In Vitro* **13**, 213-217.

Walsh, C. (2006). Posttranslational Modification Of Proteins: Expanding Nature's Inventory (Greenwood Village, Colorado, USA, Roberts and Company Publishers).

Wang, H., Huang, Z.Q., Xia, L., Feng, Q., Erdjument-Bromage, H., Strahl, B.D., Briggs, S.D., Allis, C.D., Wong, J., Tempst, P.*, et al.* (2001). Methylation of histone H4 at arginine 3 facilitating transcriptional activation by nuclear hormone receptor. *Science* **293**, 853-857.

Wang, X., Zhang, Y., Ma, Q., Zhang, Z., Xue, Y., Bao, S., and Chong, K. (2007). SKB1-mediated symmetric dimethylation of histone H4R3 controls flowering time in Arabidopsis. *EMBO J* **26**, 1934-1941.

Wang, Y.C., and Li, C. (2012). Evolutionarily conserved protein arginine methyltransferases in non-mammalian animal systems. *FEBS J*.

Widmann, B., Wandrey, F., Badertscher, L., Wyler, E., Pfannstiel, J., Zemp, I., and Kutay, U. (2012). The kinase activity of human Rio1 is required for final steps of cytoplasmic maturation of 40S subunits. *Mol Biol Cell* **23**, 22-35.

Wiesner, J. (2011). Quantitative Analyse des Survival of Motor Neuron(SMN)-Komplexes unter Verwendung von Absoluter Quantifizierung SMN-Komplex-spezifischer Peptide durch synthetische stabilisotopenmarkierte Peptidanaloga (Dortmund, Technische Universität Dortmund), pp. 171.

Wilczek, C., Chitta, R., Woo, E., Shabanowitz, J., Chait, B.T., Hunt, D.F., and Shechter, D. (2011). Protein arginine methyltransferase Prmt5-Mep50 methylates histones H2A and H4 and the histone chaperone nucleoplasmin in *Xenopus laevis* eggs. *J Biol Chem* **286**, 42221-42231.

Will, C.L., and Lührmann, R. (2001). Spliceosomal UsnRNP biogenesis, structure and function. *Curr Opin Cell Biol* **13**, 290-301.

Will, C.L., and Lührmann, R. (2011). Spliceosome structure and function. *Cold Spring Harb Perspect Biol* **3**.

Winkler, C., Eggert, C., Gradl, D., Meister, G., Giegerich, M., Wedlich, D., Laggerbauer, B., and Fischer, U. (2005). Reduced U snRNP assembly causes motor axon degeneration in an animal model for spinal muscular atrophy. *Genes Dev* **19**, 2320-2330.

Wolf, S.S. (2009). The protein arginine methyltransferase family: an update about function, new perspectives and the physiological role in humans. *Cell Mol Life Sci* **66**, 2109-2121.

Workman, E., Kolb, S.J., and Battle, D.J. (2012). Spliceosomal small nuclear ribonucleoprotein biogenesis defects and motor neuron selectivity in spinal muscular atrophy. *Brain Res*.

Xu, W., Cho, H., Kadam, S., Banayo, E.M., Anderson, S., Yates, J.R., 3rd, Emerson, B.M., and Evans, R.M. (2004). A methylation-mediator complex in hormone signaling. *Genes Dev* **18**, 144-156.

Xu, Z., Xie, Q., and Zhou, H.-M. (2003). Trichloroacetic Acid-Induced Molten Globule State of Aminoacylase from Pig Kidney. *Journal of Protein Chemistry* **22**, 669-675.

Yan, X., Mouillet, J.F., Ou, Q., and Sadovsky, Y. (2003). A novel domain within the DEAD-box protein DP103 is essential for transcriptional repression and helicase activity. *Mol Cell Biol* **23**, 414-423.

Yong, J., Golembe, T.J., Battle, D.J., Pellizzoni, L., and Dreyfuss, G. (2004). snRNAs contain specific SMN-binding domains that are essential for snRNP assembly. *Mol Cell Biol* **24**, 2747-2756.

Young, P.J., Le, T.T., Dunckley, M., Nguyen, T.M., Burghes, A.H., and Morris, G.E. (2001). Nuclear gems and Cajal (coiled) bodies in fetal tissues: nucleolar distribution of the spinal muscular atrophy protein, SMN. *Exp Cell Res* **265**, 252-261.

Yue, W.W., Hassler, M., Roe, S.M., Thompson-Vale, V., and Pearl, L.H. (2007). Insights into histone code syntax from structural and biochemical studies of CARM1 methyltransferase. *EMBO J* **26**, 4402-4412.

Zeller, R., Carri, M.T., Mattaj, I.W., and De Robertis, E.M. (1984). *Xenopus laevis* U1 snRNA genes: characterisation of transcriptionally active genes reveals major and minor repeated gene families. *EMBO J* **3**, 1075-1081.

Zhang, R., So, B.R., Li, P., Yong, J., Glisovic, T., Wan, L., and Dreyfuss, G. (2011). Structure of a key intermediate of the SMN complex reveals Gemin2's crucial function in snRNP assembly. *Cell* **146**, 384-395.

Zhang, X., and Cheng, X. (2003). Structure of the Predominant Protein Arginine Methyltransferase PRMT1 and Analysis of Its Binding to Substrate Peptides. *Structure* **11**, 509-520.

Zhang, X., Zhou, L., and Cheng, X. (2000). Crystal structure of the conserved core of protein arginine methyltransferase PRMT3. *EMBO J* **19**, 3509-3519.

Zhao, Q., Rank, G., Tan, Y.T., Li, H., Moritz, R.L., Simpson, R.J., Cerruti, L., Curtis, D.J., Patel, D.J., Allis, C.D.*, et al.* (2009). PRMT5-mediated methylation of histone H4R3 recruits DNMT3A, coupling histone and DNA methylation in gene silencing. *Nat Struct Mol Biol* **16**, 304-311.

Zurita-Lopez, C.I., Sandberg, T., Kelly, R., and Clarke, S.G. (2012). Human protein arginine methyltransferase 7 (PRMT7) is a type III enzyme forming omega-NG-monomethylated arginine residues. *J Biol Chem* **287**, 7859-7870.

9 Acronyms and Abbreviations

Acronym/Abbreviation	Definition
%	Percent
α	Alpha
β	Beta
β-ME	β-mercaptoethanol ($HOCH_2CH_2SH$)
γ	Gamma
°C	Degree Celsius
µ	Micro
µg	Micrograms
µM	Micromolar
7B10	Anti-SMN antibody
aa	Amino acid
ADH	Alcohol dehydrogenase
aDMA	Asymmetrical dimethyl-L-arginine (ω-N^G,N^G-Dimethyl-L-arginine)
AEBSF	4-(2-Aminoethyl) benzenesulfonyl fluoride
APS	Ammonium persulfate
ATP	Adenosine-5‘-triphosphate
ATPase	Adenosine-5‘-triphosphatase
BEVS	Baculovirus Expression Vector System
BisTris	2-bis(2-hydroxyethyl)amino-2-(hydroxymethyl)-1,3-propanediol
bp	Base pairs
Bq	Becquerel (s^{-1})
BSA	Bovine serum albumin
CBC	Cap binding complex
CBP	Cap binding protein
cDNA	Complementary DNA
Ci	Curie (1 Ci = 3.7×10^{10} Bq = 37 GBq)
cm	Centimeter
cpm / CPM	Counts per minute
CRM1	Chromosome region maintenance 1 protein homolog (Exp1)
C-terminal	Carboxyl terminal
CTP	Cytidine-5‘-triphosphate
Da	Dalton
dATP	Deoxyadenosine-5‘-triphosphate
dCTP	Deoxycytidine-5‘-triphosphate
ddH_2O	Double-distilled water
DEPC	Diethylpyrocarbonate
dGTP	Deoxyguanosine-5‘-triphosphate
DMEM	Dulbecco’s Modified Eagle Medium
DMF	N,N-Dimethylformamide
DMP	Dimethyl pimelimidate
DMSO	Dimethyl sulfoxide

DNA	Deoxyribonucleic acid
dNTP	Deoxyribonucleoside-5‘-triphosphosphate
dpi	Days post infection
ds	Double-stranded
DTT	Dithiothreitol
dTTP	Deoxythymidine-5‘-triphosphate
E	Enzyme
E. coli	*Escherichia coli*
ECACC	European Collection of Cell Cultures
ECL	Enhanced chemiluminescence
EDTA	Ethylenediaminetetraacetic acid
EGFP	Enhanced green fluorescent protein
EtOH	Ethanol
FCS	Fetal calf serum
Fig.	Figure
FITC	Fluorescein-5-isothiocyanate
g	Gram
g	Gravity
GDP	Guanosine-5‘-diphosphate
GRG	Glycine-arginine-glycine tripeptide
GSH	Glutathione sepharose
GST	Glutathione-S-transferase
GTP	Guanosine-5‘-triphosphate
h	hours
HAc	Acetic acid
HCl	Hydrochloric acid
HEK293	Human embryonic kidney 293 (cell line)
HeLa	Henrietta Lacks
Hepes	*N*-2-hydroxyethylpiperazine-*N*'-2-ethane sulfonic acid
His_6	Hexahistidine tag
hpi	Hours post infection
IMAC	Immobilized metal affinity chromatography
IP	Immunoprecipitation
IPTG	Isopropyl-ß-D-thiogalactoside
JMJD6	Jumonji-domain-containing protein 6 (JMJD6)
k	Kilo
kb	Kilobase
KCl	Potassium chloride
kDa	Kilo Dalton
l	Litre
L-Arg	L-arginine
LB	Luria Bertani
m	Meter
M	Molar
m_3G	2,2,7- trimethylguanosine

m^7G	7- monomethylguanosine
mA	Milliampére
MCS	Multiple cloning site
MeOH	Methanol
MEP50	Methylosome protein 50 (= WD45, WDR77)
MES	2-(N-morpholino)ethanesulfonic acid
$MgCl_2$	Magnesium chloride
$MgSO_4$	Magnesium sulphate
min	Minute
MM	Multiplication module
mM	Millimolar
MMA	Monomethyl-L-arginine (ω-N^G -Monomethyl-L-arginine)
MOI	Multiplicity of infection
MOPS	3-(N-morpholino)propanesulfonic acid
mRNA	Messenger RNA
MW	Molecular weight
MWCO	Molecular weight cut off
NaCl	Sodium chloride
NaOH	Sodium hydroxide
NES	Nuclear export signal
NET	Sodium/EDTA/Tris
Ni-NTA	Nickel-nitrilotriacetic acid
NPC	Nuclear pore complex
N-terminal	Amino terminal
O.D./OD	Optical density
OD_{600}	Optical density at 600 nm
ORF	Open reading frame
p10	p10 promoter
PAAG	Polyacrylamide gel
PAGE	Polyacrylamide gel electrophoresis
PBS	Phosphate buffered saline
PCR	Polymerase chain reaction
PEI	Polyethylenimine
pFBDM	Plasmid DNA of FastBac Dual with Multiplication Module
pfu	Plaque forming unit
Pfu	*Pyrococcus furiosus*
PHAX	Phosphorylated adapter RNA export protein
pI	Isoelectric point
pICln	Integral component of a nucleotide-sensitive chloride channel
PIPES	Piperazine-N,N'-bis(2-ethanesulfonic acid
pmol	Picomole
PMSF	Phenylmethylsulfonyl fluoride
pol	Polyhedrin promoter
PRMT	Protein arginine methyltransferase
pUCDM	Plasmid DNA stemming from pUC-vector with Multiplication Module

PVDF	Polyvinylidene Fluoride
RanGDP	GDP-bound nuclear protein Ran
RanGTP	GTP-bound nuclear protein Ran
R_f	Relative migration distance of a compound in TLC
RNA	Ribonucleic acid
RNase A	Ribonuclease A
RNAsin	RNase inhibitor
RNP	Ribonuleoprotein particle (RNA-protein particle)
rpm	Revolutions per minute
RS	Restriction site
RT	Room temperature
s	Second
SAH	S-adenosylhomocysteine (= AdoHcy)
SAM	S-adenosylmethionine (= AdoMet)
sDMA	Symmetrical dimethyl-L-arginine (ω-N^G,N'^G-Dimethyl-L-arginine)
SDS	Sodium dodecyl sulphate
SDS-PAAG	SDS-polyacrylamide gel
SDS-PAGE	Sodium dodecyl sulphate polyacrylamide gel electrophoresis
*Sf*21	*Spodoptera frugiperda* 21 (insect cell line)
*Sf*9	*Spodoptera frugiperda* 9 (insect cell line)
SLE	Systemic Lupus Erythematosus
Sm	Smith
SMA	Spinal muscular atrophy
SMN	Survival motor neuron
snoRNA	Small nucleolar ribonucleic acid
snoRNP	Small nucleolar ribonucleoprotein particle
snRNA	Small nuclear ribonucleic acid
snRNP	Small nuclear ribonucleoprotein particle
SPN1	Snurportin-1
ss	Single-stranded
Taq	*Thermus aquaticus*
TBE	Tris borate EDTA
TCA	Trichloroacetic acid
TCEP	Tris(2-carboxyethyl)phosphine
$TCID_{50}$	50% tissue culture infectious dose
TE	Tris/EDTA
TEMED	N,N,N',N',-tetramethylethylenediamine
TEV	Tobacco etch virus
Tgs1	Trimethylguanosine synthase
TLC	Thin Layer Chromatography
*Tn*5	*Trichoplusia ni*, High Five™ cells(insect cell line)
Tn7	Transposon 7
Tris	2-Amino-2-(hydroxymethyl)-1,3-propanediol
tRNA	Transfer RNA
UTP	Uridine-5'-triphosphate

UV	Ultraviolet
V	Volt
v/v	Volume-volume percentage
w/v	Weight-volume percentage
WD45	WD-repeat domain 45 (= MEP50, WDR77)
WDR77	WD-repeat containing protein 77
wt	Wild-type
X-Gal	Bromo-chloro-indolyl-galactopyranoside
YE	Yeast extract

10 Table of Figures

11 Table of Tables

12 Appendix

12.1 Nucleotide bases and amino acids

Table 9 – Nucleotide bases

A	Adenine
C	Cytosine
G	Guanine
T	Thymine (DNA only)
U	Uracil (RNA only)

Table 10 – Amino acids: 1-letter code abbreviations

A	Alanine	**M**	Methionine
C	Cysteine	**N**	Asparagine
D	Aspartic acid	**P**	Proline
E	Glutamic acid	**Q**	Glutamine
F	Phenylalanine	**R**	Arginine
G	Glycine	**S**	Serine
H	Histidine	**T**	Threonine
I	Isoleucine	**V**	Valine
K	Lysine	**W**	Tryptophan
L	Leucine	**Y**	Tyrosine

12.2 PRMT5 (20S) and 6S complex components

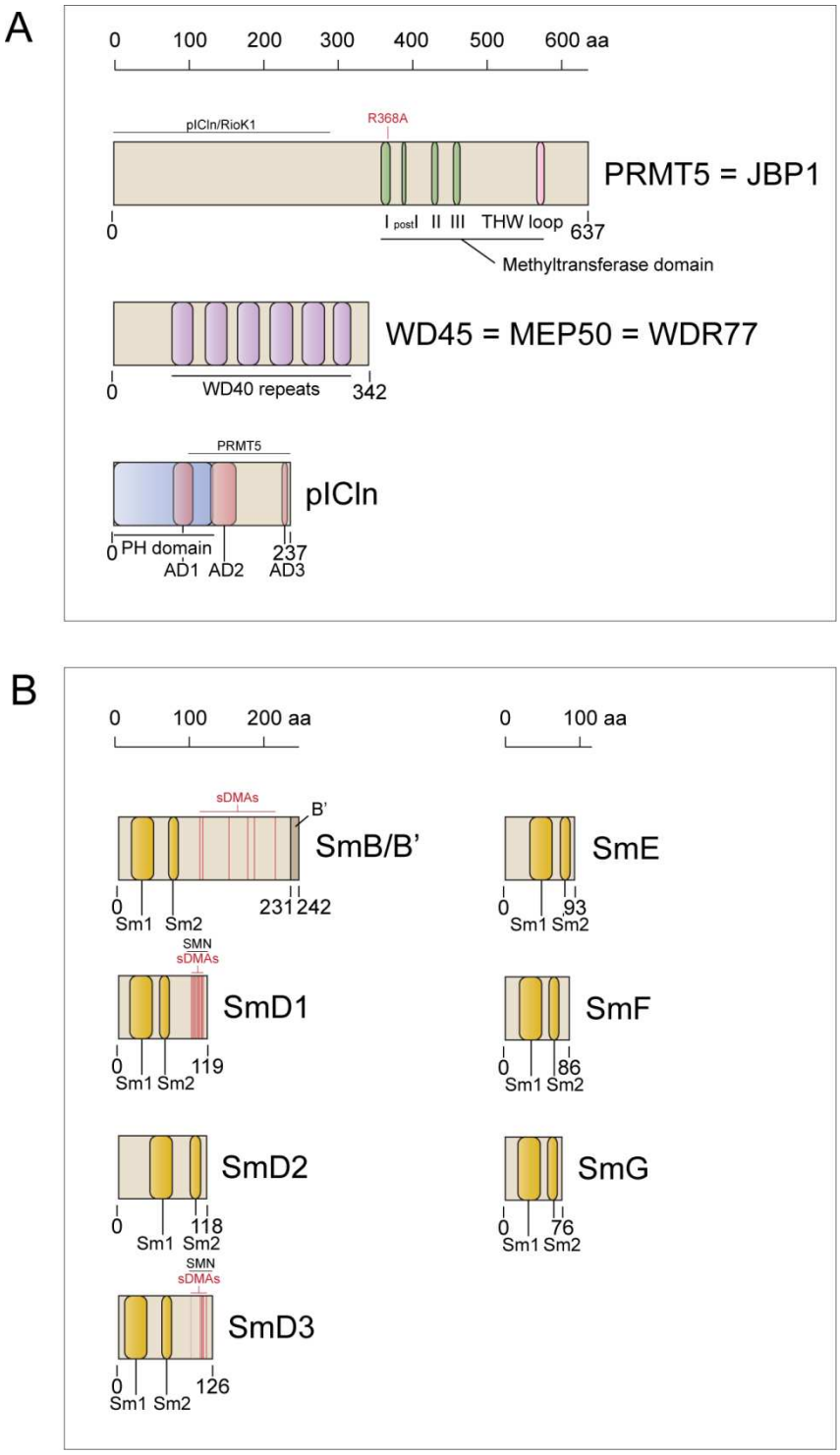

Figure 70 – Schematic of PRMT5 (20S) and 6S complex components.

(A) PRMT5 complex components. **(B)** Sm proteins. The primary sequences of individual proteins are depicted as rectangular shapes of various sizes with respect to their number of amino acids. Protein motifs and domains are indicated as colored boxes and specified underneath. Arginine residues in Sm proteins B/B', D1 and D3 that are symmetrically dimethylated (sDMA) are highlighted by red lines. Interaction partners are shown in black above the protein. A mutation inactivating the methyltransferase activity (R368A) is given in red. Detailed information of this presentation is provided in the following table.

Table 11 – PRMT5 (20S) and 6S complex component protein motifs and domains

Protein	Amino acids	Motif/Domain/Mutation
PRMT5	1–291	pICln binding
	359–371	MT domain I
	368	R368A mutant
	387–392	MT domain post I
	427–435	MT domain II
	456–465	MT domain III
	571–581	THW domain
WD45	5	Phosphorylation site
	78–107	WD-repeat
	123–153	WD-repeat
	166–196	WD-repeat
	210–241	WD-repeat
	253–284	WD-repeat
	295–319	WD-repeat
pICln	1-–34	PH-domain
	84–120	AD1
	134–168	AD2
	230–237	AD3
	137–237	PRMT5 binding
B/B‘	17–47	Sm1
	67–80	Sm2
	108, 112, 147, 172, 181, 209	sDMA sites
D1	15–45	Sm1
	55–68	Sm2
	91–119	SMN binding
	98, 100, 102, 104, 106, 108, 110, 112, 114	sDMA sites
D2	42–72	Sm1
	96–110	Sm2
D3	18–48	Sm1
	58–71	Sm2
	95–126	SMN binding
	97	possible sDMA site
	110, 112, 114, 118	sDMA sites
E	33–63	Sm1
	74–87	Sm2
F	19–49	Sm1
	59–72	Sm2
G	17–47	Sm1
	57–70	Sm2

Table 12 – PRMT5 (20S) and 6S complex component properties

Protein	Amino acids	Molecular weight	Molar extinction coefficient ($M^{-1} \cdot cm^{-1}$)	Isoelectric point
PRMT5	637	72679.87	109260	5.76
WD45	342	36833.41	63580	5.01
pICln	237	26213.28	17570	3.97
B	231	23654.74	2920	10.91
B‘	242	24835.11	2920	11.20
D1	119	13281	1280	11.56
D2	118	13526.31	7210	10.84
D3	126	13915.46	4080	11.92
E	92	10802.89	10930	9.46
F	86	9724.38	12210	4.64
G	76	8495.8	120	8.99

>PRMT5

```
  1 MAAMAVGGAG GSRVSSGRDL NCVPEIADTL GAVAEQGFDF LCMPVFHPRF
 51 KREFIQEPAK NRPGPQTRSD LLLSGRDWNT LIVGKLSPWI RPDSKVEKIR
101 RNSEAAMLQE LNFGAYLGLP AFLLPLNQED NTNLARVLTN HIHTGHHSSM
151 FWMRVPLVAP EDLRDDIIEN APTTHTEEYS GEEKTWMWWH NFRTLCDYSK
201 RIAVALEIGA DLPSNHVIDR WLGEPIKAAI LPTSIFLTNK KGFPVLSKMH
251 QRLIFRLLKL EVQFIITGTN HHSEKEFCSY LQYLEYLSQN RPPPNAYELF
301 AKGYEDYLQS PLQPLMDNLE SQTYEVFEKD PIKYSQYQQA IYKCLLDRVP
351 EEEKDTNVQV LMVLGAGRGP LVNASLRAAK QADRRIKLYA VEKNPNAVVT
401 LENWQFEEWG SQVTVVSSDM REWVAPEKAD IIVSELLGSF ADNELSPECL
451 DGAQHFLKDD GVSIPGEYTS FLAPISSSKL YNEVRACREK DRDPEAQFEM
501 PYVVRLHNFH QLSAPQPCFT FSHPNRDPMI DNNRYCTLEF PVEVNTVLHG
551 FAGYFETVLY QDITLSIRPE THSPGMFSWF PILFPIKQPI TVREGQTICV
601 RFWRCSNSKK VWYEWAVTAP VCSAIHNPTG RSYTIGL
```

>WD45

```
  1 MRKETPPPLV PPAAREWNLP PNAPACMERQ LEAARYRSDG ALLLGASSLS
 51 GRCWAGSLWL FKDPCAAPNE GFCSAGVQTE AGVADLTWVG ERGILVASDS
101 GAVELWELDE NETLIVSKFC KYEHDDIVST VSVLSSGTQA VSGSKDICIK
151 VWDLAQQVVL SSYRAHAAQV TCVAASPHKD SVFLSCSEDN RILLWDTRCP
201 KPASQIGCSA PGYLPTSLAW HPQQSEVFVF GDENGTVSLV DTKSTSCVLS
251 SAVHSQCVTG LVFSPHSVPF LASLSEDCSL AVLDSSLSEL FRSQAHRDFV
301 RDATWSPLNH SLLTTVGWDH QVVHHVVPTE PLPAPGPASV TE
```

>pICln

```
  1 MSFLKSFPPP GPAEGLLRQQ PDTEAVLNGK GLGTGTLYIA ESRLSWLDGS
 51 GLGFSLEYPT ISLHALSRDR SDCLGEHLYV MVNAKFEEES KEPVADEEEE
101 DSDDDVEPIT EFRFVPSDKS ALEAMFTAMC ECQALHPDPE DEDSDDYDGE
151 EYDVEAHEQG QGDIPTFYTY EEGLSHLTAE GQATLERLEG MLSQSVSSQY
201 NMAGVRTEDS IRDYEDGMEV DTTPTVAGQF EDADVDH
```

>B/B‘

```
  1 MTVGKSSKML QHIDYRMRCI LQDGRIFIGT FKAFDKHMNL ILCDCDEFRK
 51 IKPKNSKQAE REEKRVLGLV LLRGENLVSM TVEGPPPKDT GIARVPLAGA
101 AGGPGIGRAA GRGIPAGVPM PQAPAGLAGP VRGVGGPSQQ VMTPQGRGTV
151 AAAAAAATAS IAGAPTQYPP GRGGPPPPMG RGAPPPGMMG PPPGMRPPMG
201 PPMGIPPGRG TPMGMPPPGM RPPPPGMRGL LPPPPGMRPP RP
```

* **R**: symmetrically dimethylated arginines (sDMA)
* N: B’ contains 11 amino acids more than B

>D1

```
  1 MKLVRFLMKL SHETVTIELK NGTQVHGTIT GVDVSMNTHL KAVKMTLKNR
 51 EPVQLETLSI RGNNIRYFIL PDSLPLDTLL VDVEPKVKSK KREAVAGRGR
101 GRGRGRGRGR GRGRGGPRR
```

* **R**: symmetrically dimethylated arginines (sDMA)

>D2

```
  1 MSLLNKPKSE MTPEELQKRE EEEFNTGPLS VLTQSVKNNT QVLINCRNNK
 51 KLLGRVKAFD RHCNMVLENV KEMWTEVPKS GKGKKKSKPV NKDRYISKMF
101 LRGDSVIVVL RNPLIAGK
```

>D3

```
  1 MSIGVPIKVL HEAEGHIVTC ETNTGEVYRG KLIEAEDNMN CQMSNITVTY
 51 RDGRVAQLEQ VYIRGSKIRF LILPDMLKNA PMLKSMKNKN QGSGAGRGKA
101 AILKAQVAAR GRGRGMGRGN IFQKRR
```

* **R**: symmetrically dimethylated arginines (sDMA)

>E

```
  1 MAYRGQGQKV QKVMVQPINL IFRYLQNRSR IQVWLYEQVN MRIEGCIIGF
 51 DEYMNLVLDD AEEIHSKTKS RKQLGRIMLK GDNITLLQSV SN
```

>F

```
  1 MSLPLNPKPF LNGLTGKPVM VKLKWGMEYK GYLVSVDGYM NMQLANTEEY
 51 IDGALSGHLG EVLIRCNNVL YIRGVEEEEE DGEMRE
```

>G

```
  1 MSKAHPPELK KFMDKKLSLK LNGGRHVQGI LRGFDPFMNL VIDECVEMAT
 51 SGQQNNIGMV VIRGNSIIML EALERV
```

Table 13 – Properties of protein complexes

Protein complex	Molecular weight (Da)	Molar extinction coefficient ($M^{-1} \cdot cm^{-1}$)
His_6(TEV)-PRMT5 WD45	111834.5	174120
D1 D2	26807.31	8490
pICln D1 D2	53020.59	26060
F E G	29023.1	23260
pICln D1 D2 F E G (= 6S complex)	82154.6	49320
D3 B	37570.2	7000
pICln D3 B	63783.48	24570
His_6(TEV)-PRMT5 WD45 D1 D2	138641.8	182610
His_6(TEV)-PRMT5 WD45 pICln D1 D2	164855.1	200180
His_6(TEV)-PRMT5 WD45 pICln D1 D2 F E G	193878.2	223440
His_6(TEV)-PRMT5 WD45 D3 B	149404.7	181120
His_6(TEV)-PRMT5 WD45 pICln D3 B	175618	198690

12.3 SMN complex components

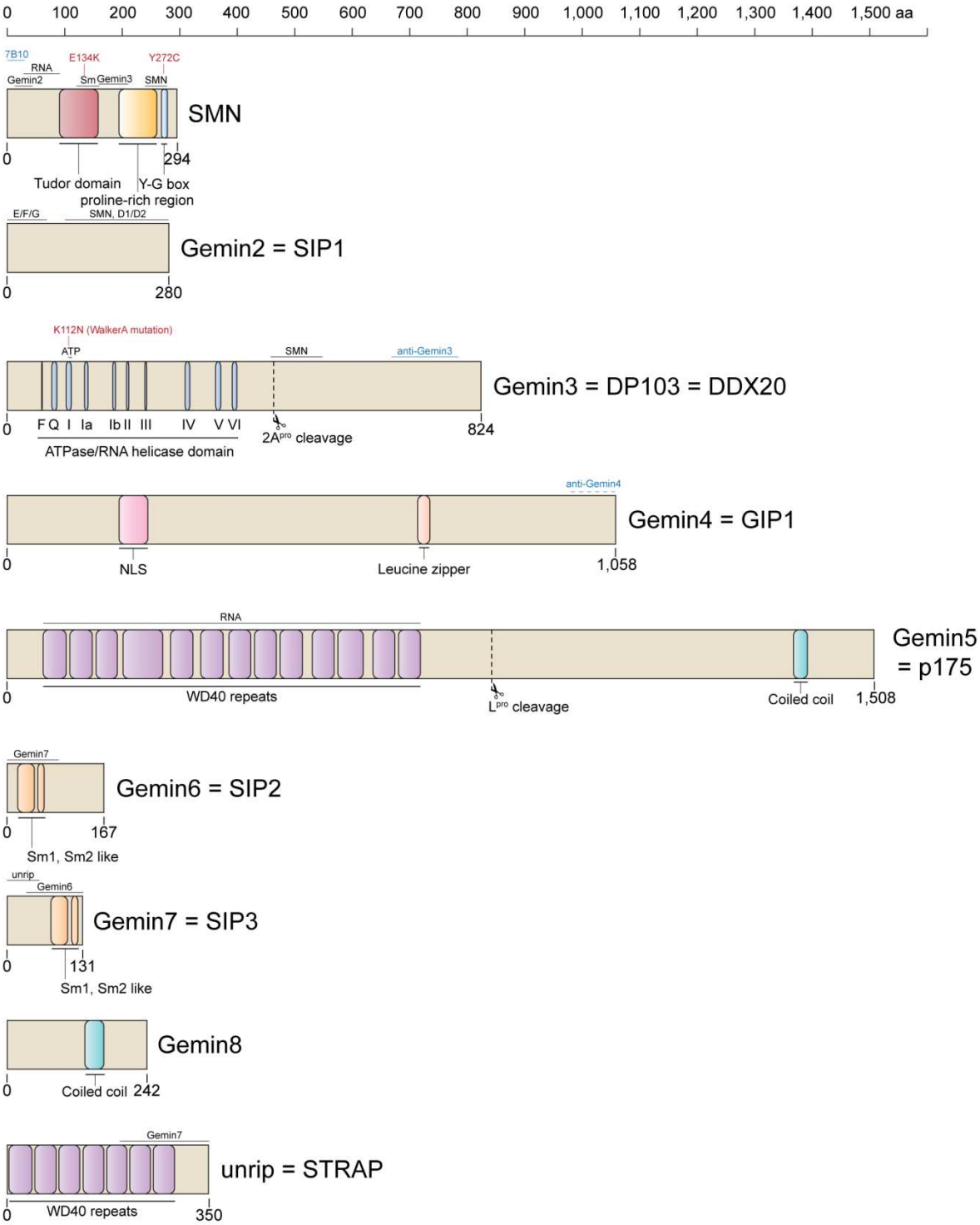

Figure 71 – Schematic of SMN complex components.

The primary sequences of individual proteins are depicted as rectangular shapes of various sizes with respect to their number of amino acids. Protein motifs and domains are indicated as colored boxes and specified underneath. Interaction partners are shown in black, sequence motifs recognized by specific antibodies in light blue above the protein. SMN patient mutations E134K and Y272C as well as Walker A mutation K112N in Gemin3 are given in red. Viral proteinase cleavage sites are indicated by a dashed line. Detailed information of this presentation is provided in the following table.

Table 14 – SMN complex component protein motifs and domains

Protein	Amino acids	Motif/Domain/Mutation
SMN	1–30	7B10 (anti-SMN) antibody recognition
	13–43	Gemin2 binding
	28–91	RNA binding
	91–158	Tudor domain
	120–159	Sm protein binding
	134	E134K
	159–210	Gemin3 binding
	194–259	proline-rich region
	240–267	SmB binding
	268–278	Y-G box
	272	Y272K
Gemin2	1–69	F/E/G binding
	100–280	D1/D2 binding
	100–280	SMN binding
Gemin3	64	F
	89	Q
	93–264	ATPase domain
	106–114	I
	106–113	ATP binding
	112	WalkerA/K112N
	138–143	Ia
	187–191	Ib
	211–214	II/WalkerB
	243–245	III
	299–447	Helicase domain
	313–320	IV
	366–374	V
	395–402	VI
	460–464	Poliovirus proteinase $2A^{pro}$ cleavage site (VHT↓YG)
	456–547	SMN binding
	667–783	anti-Gemin3
Gemin4	194–243	Nuclear localization signal (NLS)
	714–734	Leucine zipper
Gemin5	62–720	RNA binding
	62–104	WD-repeat
	107–148	WD-repeat
	150–189	WD-repeat
	193–264	WD-repeat
	280–321	WD-repeat
	333–374	WD-repeat
	377–417	WD-repeat
	424–464	WD-repeat
	468–509	WD-repeat
	533–573	WD-repeat
	576–622	WD-repeat
	637–677	WD-repeat
	680–720	WD-repeat
	843–846	FMDV proteinase L^{pro} cleavage site (RKAR)
	1366–1392	Coiled-coil
Gemin6	1–92	Gemin7 binding
	20–51	Sm1 like
	55–68	Sm2 like
Gemin7	1–56	unrip binding
	30–131	Gemin6 binding
	78–109	Sm1 like
	114–127	Sm2 like
Gemin8	135–167	Coiled-coil
unrip	3–45	WD-repeat
	48–87	WD-repeat

90–128	WD-repeat
132–170	WD-repeat
173–210	WD-repeat
195–350	Gemin7 binding
213–251	WD-repeat
254–293	WD-repeat

Table 15 – SMN complex component protein properties

Protein	Amino acids	Molecular weight	Molar extinction coefficient ($M^{-1}\cdot cm^{-1}$)	Isoelectric point
SMN	294	31957.54	45340	6.15
SMN(E134K)	294	31845.62	45340	6.15
Gemin2	280	31694.3	42780	5.43
Gemin3	824	92160.09	83040	6.52
Gemin3(K112N)	824	92146.02	83040	6.44
Gemin4	1058	119984.5	162040	5.74
Gemin5	1508	168551.3	251430	6.15
Gemin6	167	18934.08	29520	5.02
Gemin7	131	14646.74	4080	7.03
Gemin8	242	28744.84	55220	6.33
unrip	350	38435.55	55910	4.98

>SMN

```
  1 MAMSSGGSGG GVPEQEDSVL FRRGTGQSDD SDIWDDTALI KAYDKAVASF
 51 KHALKNGDIC ETSGKPKTTP KRKPAKKNKS QKKNTAASLQ QWKVGDKCSA
101 IWSEDGCIYP ATIASIDFKR ETCVVVYTGY GNREEQNLSD LLSPICEVAN
151 NIEQNAQENE NESQVSTDES ENSRSPGNKS DNIKPKSAPW NSFLPPPPPM
201 PGPRLGPGKP GLKFNGPPPP PPPPPPHLLS CWLPPFPSGP PIIPPPPPIC
251 PDSLDDADAL GSMLISWYMS GYHTGYYMGF RQNQKEGRCS HSLN
```

>Gemin2

```
  1 MRRAELAGLK TMAWVPAESA VEELMPRLLP VEPCDLTEGF DPSVPPRTPQ
 51 EYLRRVQIEA AQCPDVVVAQ IDPKKLKRKQ SVNISLSGCQ PAPEGYSPTL
101 QWQQQQVAQF STVRQNVNKH RSHWKSQQLD SNVTMPKSED EEGWKKFCLG
151 EKLCADGAVG PATNESPGID YVQIGFPPLL SIVSRMNQAT VTSVLEYLSN
201 WFGERDFTPE LGRWLYALLA CLEKPLLPEA HSLIRQLARR CSEVRLLVDS
251 KDDERVPALN LLICLVSRYF DQRDLADEPS
```

>Gemin3

```
  1 MAAAVEASGA LAAVATAMPA EHVAVQVPAP EPTPGPVRIL RTAQDLSSPR
 51 TRTGDVLLAE PADFESLLLS RPVLEGLRAA GFERPSPVQL KAIPLGRCGL
101 DLIVQAKSGT GKTCVFSTIA LDSLVLENLS TQILILAPTR EIAVQIHSVI
151 TAIGIKMEGL ECHVFIGGTP LSQDKTRLKK CHIAVGSPGR IKQLIELDYL
201 NPGSIRLFIL DEADKLLEEG SFQEQINWIY SSLPASKQML AVSATYPEFL
251 ANALTKYMRD PTFVRLNSSD PSLIGLKQYY KVVNSYPLAH KVFEEKTQHL
301 QELFSRIPFN QALVFSNLHS RAQHLADILS SKGFPAECIS GNMNQNQRLD
351 AMAKLKHFHC RVLISTDLTS RGIDAEKVNL VVNLDVPLDW ETYMHRIGRA
401 GRFGTLGLTV TYCCRGEEEN MMMRIAQKCN INLLPLPDPI PSGLMEECVD
```

```
 451 WDVEVKAAVH TYGIASVPNQ PLKKQIQKIE RTLQIQKAHG DHMASSRNNS
 501 VSGLSVKSKN NTKQKLPVKS HSECGIIEKA TSPKELGCDR QSEEQMKNSV
 551 QTPVENSTNS QHQVKEALPV SLPQIPCLSS FKIHQPYTLT FAELVEDYEH
 601 YIKEGLEKPV EIIRHYTGPG DQTVNPQNGF VRNKVIEQRV PVLASSSQSG
 651 DSESDSDSHS SRTSSQSKGN KSYLEGSSDN QLKDSESTPV DDRISLEQPP
 701 NGSDTPNPEK YQESPGIQMK TRLKEGASQR AKQSRRNLPR RSSFRLQTEA
 751 QEDDWYDCHR EIRLSFSDTY QDYEEYWRAY YRAWQEYYAA ASHSYYWNAQ
 801 RHPSWMAAYH MNTIYLQEMM HSNQ
```

>Gemin4

```
   1 MDLGPLNICE EMTILHGGFL LAEQLFHPKA LAELTKSDWE RVGRPIVEAL
  51 REISSAAAHS QPFAWKKKAL IIIWAKVLQP HPVTPSDTET RWQEDLFFSV
 101 GNMIPTINHT ILFELLKSLE ASGLFIQLLM ALPTTICHAE LERFLEHVTV
 151 DTSAEDVAFF LDIWWEVMKH KGHPQDPLLS QFSAMAHKYL PALDEFPHPP
 201 KRLRSDPDAC PTMPLLAMLL RGLTQIQSRI LGPGRKCCAL ANLADMLTVF
 251 ALTEDDPQEV SATVYLDKLA TVISVWNSDT QNPYHQQALA EKVKEAERDV
 301 SLTSLAKLPS ETIFVGCEFL HHLLREWGEE LQAVLRSSQG TSYDSYRLCD
 351 SLTSFSQNAT LYLNRTSLSK EDRQVVSELA ECVRDFLRKT STVLKNRALE
 401 DITASIAMAV IQQKMDRHME VCYIFASEKK WAFSDEWVAC LGSNRALFRE
 451 PDLVLRLLET VIDVSTADRA IPESQIRQVI HLILECYADL SLPGKNKVLA
 501 GILRSWGRKG LSEKLLAYVE GFQEDLNTTF NQLTQSASEQ GLAKAVASVA
 551 RLVIVHPEVT VKKMCSLAVV NLGTHKFLAQ ILTAFPALRF VEVQGPNSSA
 601 TFMVSCLKET VWMKFSTPKE EKQFLELLNC LMSPVKPQGI PVAALLEPDE
 651 VLKEFVLPFL RLDVEEVDLS LRIFIQTLEA NACREEYWLQ TCSPFPLLFS
 701 LCQLLDRFSK YWPLPKEKRC LSLDRKDLAI HILELLCEIV SANAETFSPD
 751 VWIKSLSWLH RKLEQLDWTV GLRLKSFFEG HFKCEVPATL FEICKLSEDE
 801 WTSQAHPGYG AGTGLLAWME CCCVSSGISE RMLSLLVVDV GNPEEVRLFS
 851 KGFLVALVQV MPWCSPQEWQ RLHQLTRRLL EKQLLHVPYS LEYIQFVPLL
 901 NLKPFAQELQ LSVLFLRTFQ FLCSHSCRNW LPLEGWNHVV KLLCGSLTRL
 951 LDSVRAIQAA GPWVQGPEQD LTQEALFVYT QVFCHALHIM AMLHPEVCEP
1001 LYVLALETLT CYETLSKTNP SVSSLLQRAH EQRFLKSIAE GIGPEERRQT
1051 LLQKMSSF
```

>Gemin5

```
   1 MGQEPRTLPP SPNWYCARCS DAVPGGLFGF AARTSVFLVR VGPGAGESPG
  51 TPPFRVIGEL VGHTERVSGF TFSHHPGQYN LCATSSDDGT VKIWDVETKT
 101 VVTEHALHQH TISTLHWSPR VKDLIVSGDE KGVVFCYWFN RNDSQHLFIE
 151 PRTIFCLTCS PHHEDLVAIG YKDGIVVIID ISKKGEVIHR LRGHDDEIHS
 201 IAWCPLPGED CLSINQEETS EEAEITNGNA VAQAPVTKGC YLATGSKDQT
 251 IRIWSCSRGR GVMILKLPFL KRRGGGIDPT VKERLWLTLH WPSNQPTQLV
 301 SSCFGGELLQ WDLTQSWRRK YTLFSASSEG QNHSRIVFNL CPLQTEDDKQ
 351 LLLSTSMDRD VKCWDIATLE CSWTLPSLGG FAYSLAFSSV DIGSLAIGVG
 401 DGMIRVWNTL SIKNNYDVKN FWQGVKSKVT ALCWHPTKEG CLAFGTDDGK
 451 VGLYDTYSNK PPQISSTYHK KTVYTLAWGP PVPPMSLGGE GDRPSLALYS
 501 CGGEGIVLQH NPWKLSGEAF DINKLIRDTN SIKYKLPVHT EISWKADGKI
 551 MALGNEDGSI EIFQIPNLKL ICTIQQHHKL VNTISWHHEH GSQPELSYLM
 601 ASGSNNAVIY VHNLKTVIES SPESPVTITE PYRTLSGHTA KITSVAWSPH
 651 HDGRLVSASY DGTAQVWDAL REEPLCNFRG HQGRLLCVAW SPLDPDCIYS
 701 GADDFCVHKW LTSMQDHSRP PQGKKSIELE KKRLSQPKAK PKKKKKPTLR
 751 TPVKLESIDG NEEESMKENS GPVENGVSDQ EGEEQAREPE LPCGLAPAVS
 801 REPVICTPVS SGFEKSKVTI NNKVILLKKE PPKEKPETLI KKRKARSLLP
 851 LSTSLDHRSK EELHQDCLVL ATAKHSRELN EDVSADVEER FHLGLFTDRA
 901 TLYRMIDIEG KGHLENGHPE LFHQLMLWKG DLKGVLQTAA ERGELTDNLV
 951 AMAPAAGYHV WLWAVEAFAK QLCFQDQYVK AASHLLSIHK VYEAVELLKS
1001 NHFYREAIAI AKARLRPEDP VLKDLYLSWG TVLERDGHYA VAAKCYLGAT
1051 CAYDAAKVLA KKGDAASLRT AAELAAIVGE DELSASLALR CAQELLLANN
```

```
1101 WVGAQEALQL HESLQGQRLV FCLLELLSRH LEEKQLSEGK SSSSYHTWNT
1151 GTEGPFVERV TAVWKSIFSL DTPEQYQEAF QKLQNIKYPS ATNNTPAKQL
1201 LLHICHDLTL AVLSQQMASW DEAVQALLRA VVRSYDSGSF TIMQEVYSAF
1251 LPDGCDHLRD KLGDHQSPAT PAFKSLEAFF LYGRLYEFWW SLSRPCPNSS
1301 VWVRAGHRTL SVEPSQQLDT ASTEETDPET SQPEPNRPSE LDLRLTEEGE
1351 RMLSTFKELF SEKHASLQNS QRTVAEVQET LAEMIRQHQK SQLCKSTANG
1401 PDKNEPEVEA EQPLCSSQSQ CKEEKNEPLS LPELTKRLTE ANQRMAKFPE
1451 SIKAWPFPDV LECCLVLLLI RSHFPGCLAQ EMQQQAQELL QKYGNTKTYR
1501 RHCQTFCM
```

>Gemin6

```
   1 MSEWMKKGPL EWQDYIYKEV RVTASEKNEY KGWVLTTDPV SANIVLVNFL
  51 EDGSMSVTGI MGHAVQTVET MNEGDHRVRE KLMHLFTSGD CKAYSPEDLE
 101 ERKNSLKKWL EKNHIPITEQ GDAPRTLCVA GVLTIDPPYG PENCSSSNEI
 151 ILSRVQDLIE GHLTASQ
```

>Gemin7

```
   1 MQTPVNIPVP VLRLPRGPDG FSRGFAPDGR RAPLRPEVPE IQECPIAQES
  51 LESQEQRARA ALRERYLRSL LAMVGHQVSF TLHEGVRVAA HFGATDLDVA
 101 NFYVSQLQTP IGVQAEALLR CSDIISYTFK P
```

>Gemin8

```
   1 MAAVKASTSK ATRPWYSHPV YARYWQHYHQ AMAWMQSHHN AYRKAVESCF
  51 NLPWYLPSAL LPQSSYDNEA AYPQSFYDHH VAWQDYPCSS SHFRRSGQHP
 101 RYSSRIQAST KEDQALSKEE EMETESDAEV ECDLSNMEIT EELRQYFAET
 151 ERHREERRRQ QQLDAERLDS YVNADHDLYC NTRRSVEAPT ERPGERRQAE
 201 MKRLYGDSAA KIQAMEAAVQ LSFDKHCDRK QPKYWPVIPL KF
```

>unrip

```
   1 MAAVKASTSK ATRPWYSHPV YARYWQHYHQ AMAWMQSHHN AYRKAVESCF
  51 NLPWYLPSAL LPQSSYDNEA AYPQSFYDHH VAWQDYPCSS SHFRRSGQHP
 101 RYSSRIQAST KEDQALSKEE EMETESDAEV ECDLSNMEIT EELRQYFAET
 151 ERHREERRRQ QQLDAERLDS YVNADHDLYC NTRRSVEAPT ERPGERRQAE
 201 MKRLYGDSAA KIQAMEAAVQ LSFDKHCDRK QPKYWPVIPL KF
```

Table 16 – Properties of protein complexes (SMN)

Protein complex	Molecular weight (Da)	Molar extinction coefficient ($M^{-1} \cdot cm^{-1}$)
SMN Gemin2 His_6(Thrombin)-Gemin6 Gemin7 Gemin8	129783.7	176940
SMN(E134K) Gemin2 His_6(Thrombin)-Gemin6 Gemin7 Gemin8	129671.8	176940
Gemin3 Gemin4	212144.6	245080
Gemin3 Gemin4 Gemin5	380695.9	496510
Gemin3(K112N) Gemin4	212130.5	245080
Gemin3(K112N) Gemin4 Gemin5	380681.8	496510
SMN Gemin2 Gemin3 Gemin4 Gemin5 His_6(Thrombin)-Gemin6 Gemin7 Gemin8	510479.6	673450
SMN(E134K) Gemin2 Gemin3 Gemin4 Gemin5 His_6(Thrombin)-Gemin6 Gemin7 Gemin8	510367.7	673450

12.4 Insect cell transfection marker (EGFP)

>EGFP

```
  1 MVSKGEELFT GVVPILVELD GDVNGHKFSV SGEGEGDATY GKLTLKFICT
 51 TGKLPVPWPT LVTTLTYGVQ CFSRYPDHMK QHDFFKSAMP EGYVQERTIF
101 FKDDGNYKTR AEVKFEGDTL VNRIELKGID FKEDGNILGH KLEYNYNSHN
151 VYIMADKQKN GIKVNFKIRH NIEDGSVQLA DHYQQNTPIG DGPVLLPDNH
201 YLSTQSALSK DPNEKRDHMV LLEFVTAAGI TLGMDELYKS GLRSRAQASN
251 SAVDGTAGPG STGSR
```

Table 17 – EGFP properties

Protein	Amino acids	Molecular weight	Molar extinction coefficient ($M^{-1} \cdot cm^{-1}$)	Isoelectric point
EGFP	266	29479.8	20010	5.86

12.5 Affinity-tagged proteins

12.5.1 GST affinity tag

>GST

```
  1 MSPILGYWKI KGLVQPTRLL LEYLEEKYEE HLYERDEGDK WRNKKFELGL
 51 EFPNLPYYID GDVKLTQSMA IIRYIADKHN MLGGCPKERA EISMLEGAVL
101 DIRYGVSRIA YSKDFETLKV DFLSKLPEML KMFEDRLCHK TYLNGDHVTH
151 PDFMLYDALD VVLYMDPMCL DAFPKLVCFK KRIEAIPQID KYLKSSKYIA
201 WPLQGWQATF GGGDHPPTSG SGGGGGWMS
```

Table 18 – GST properties

Protein	Amino acids	Molecular weight	Molar extinction coefficient ($M^{-1} \cdot cm^{-1}$)	Isoelectric point
GST	229	26390.24	46850	5.91

12.5.2 Protein affinity tags with proteolytic cleavage site

GST-TEV: M…SSDENLYQF↓GM…*

GST-PreScission: M…PKSDLEVLFQ↓GPLGSPEFM…*

His_6-TEV: MHHHHHHENLYQF↓GM…*

His_6-Thrombin: MGSSHHHHHHSSGLVPR↓GSHMASMTGGQQMGRGSEFPM...*

The recognition site of the protease is underlined.

↓ indicates the position of proteolytic cleavage

M…* represents the coding sequence starting with a methionine and ending in a stop codon

12.5.3 Properties of tagged proteins

For simplified purification protein affinity tags were introduced at the N-termini of several proteins.

Table 19 – Properties of recombinant, affinity-tagged proteins

Protein	Amino acids	Molecular weight (Da)	Molar extinction coefficient ($M^{-1} \cdot cm^{-1}$)	Isoelectric point
GST(TEV)-SMN	532	59269.81	93470	6.01
GST(TEV)-SMN(E134K)	532	59268.87	93470	6.27
His_6(TEV)-Gemin3	840	94133.94	84320	6.55
GST(TEV)-Gemin3	1063	119694.32	131170	6.37
His_6(TEV)-Gemin3(K112N)	840	94119.87	84320	6.48
GST(TEV)-Gemin3(K112N)	1063	119680.25	131170	6.31
His_6(TEV)-Gemin4	1076	122305.71	163320	5.84
His_6(TEV)-Gemin5	1524	170525.19	252710	6.18
GST(TEV)-Gemin5	1746	195974.59	299560	6.12
His_6(Thrombin)-Gemin6	204	22740.26	29520	5.82
His_6(TEV)-PRMT5	655	75001.12	110540	5.91
His_6GST(TEV)-PRMT5	889	102003.91	157390	5.91
GST(PreScission)-pICln	237	26213.28	17570	3.97

The respective protease cleavage sites are indicated in brackets after the affinity tag.

12.6 Gel filtration calibration graphs

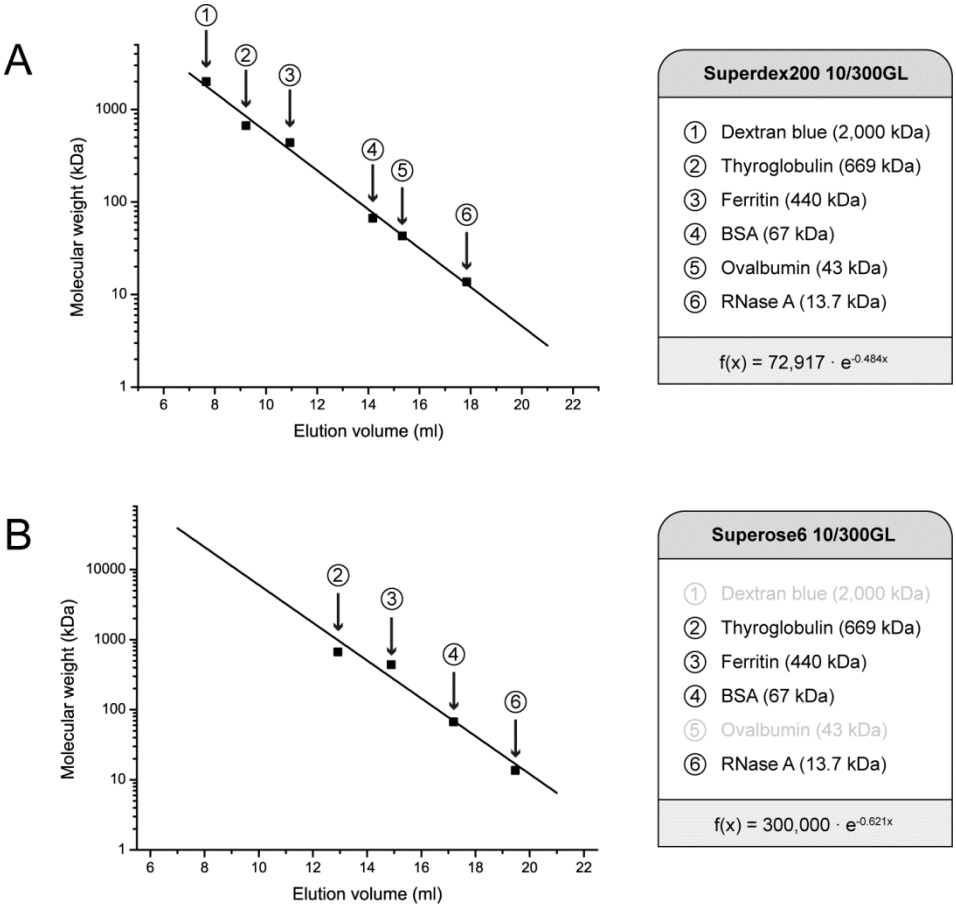

Figure 72 – Gel filtration calibration graphs

Calibration standards of known molecular weight were individually applied to a Superdex200 10/300GL **(A)** and a Superose6 10/300GL **(B)** gel filtration column. The molecular weight was plotted against the elution volume and an exponential regression curve was calculated. Loaded standards: (1) 2.5 mg Dextran blue, (2) 2.5 mg Thyroglobulin, (3) 0.2 mg Ferritin, (4) 4.0 mg BSA, (5) 2.5 mg Ovalbumin, (6) 2.5 mg RNase A.

12.7 Small nuclear ribonucleic acids

The U1 snRNA and respective mutated forms used in this work stemmed from *Xenopus laevis* (Results 5.7.3, page 153, and Results 5.7.5, page 158). Sequence identities of the human and frog RNA are highlighted in gray.

> U1 snRNA

```
                                1                                                  50
  U1_snRNA_(Homo_sapiens)     (1) AUACUUACCUGGCAGGGGAGAUACCAUGAUCACGAAGGUGGUUUUCCCAG
U1_snRNA_(Xenopus_laevis)     (1) AUACUUACCUGGCAGGGGAGAUACCAUGAUCACGAAGGUGGUUCUCCCAG
                               51                                                 100
  U1_snRNA_(Homo_sapiens)    (51) GGCGAGGCUUAUCCAUUGCACUCCGGAUGUGCUGACCCCUGCGAUUUCCC
U1_snRNA_(Xenopus_laevis)    (51) GGCGAGGCUCAGCCAUUGCACUCCGGCCGUGCUGACCCCUGCGAUUUCCC
                              101                                                 150
  U1_snRNA_(Homo_sapiens)   (101) CAAAUGUGGGAAACUCGACUGCAUAAUUUGUGGUAGUGGGGGACUGCGUU
U1_snRNA_(Xenopus_laevis)   (101) CAAAUGCGGGAAAGUCGACUGCAUAAUUUCUGGUAGUGGGGGACUGCGUU
                              151        164         Sm-site
  U1_snRNA_(Homo_sapiens)   (151) CGCGCUUUCCCCUG
U1_snRNA_(Xenopus_laevis)   (151) CGCGCUUUCCCCUG
```

> U1 ΔD snRNA

```
                                1                                                  50
  U1_snRNA_△D_(Homo_sapiens)     (1) AUACUUACCUGGCAGGGGAGAUACCAUGAUCACGAAGGUGGUUUUCCCAG
U1_snRNA_△D_(Xenopus_laevis)     (1) AUACUUACCUGGCAGGGGAGAUACCAUGAUCACGAAGGUGGUUCUCCCAG
                               51                                                 100
  U1_snRNA_△D_(Homo_sapiens)    (51) GGCGAGGCUUAUCCAUUGCACUCCGGAUGUGCUGACCCCUGCGAUUUCCC
U1_snRNA_△D_(Xenopus_laevis)    (51) GGCGAGGCUCAGCCAUUGCACUCCGGCCGUGCUGACCCCUGCGAUUUCCC
                              101                                                 150
  U1_snRNA_△D_(Homo_sapiens)   (101) CAAAUGUGGGAAACUCGACUGCACUCGAGGUGGUAGUGGGGGACUGCGUU
U1_snRNA_△D_(Xenopus_laevis)   (101) CAAAUGCGGGAAAGUCGACUGCACUCGAGCUGGUAGUGGGGGACUGCGUU
                              151        164     modified Sm-site
  U1_snRNA_△D_(Homo_sapiens)   (151) CGCGCUUUCCCCUG
U1_snRNA_△D_(Xenopus_laevis)   (151) CGCGCUUUCCCCUG
```

> U1 ΔE snRNA

```
                                1                                                  50
  U1_snRNA_△E_(Homo_sapiens)     (1) AUACUUACCUGGCAGGGGAGAUACCAUGAUCACGAAGGUGGUUUUCCCAG
U1_snRNA_△E_(Xenopus_laevis)     (1) AUACUUACCUGGCAGGGGAGAUACCAUGAUCACGAAGGUGGUUCUCCCAG
                               51                                                 100
  U1_snRNA_△E_(Homo_sapiens)    (51) GGCGAGGCUUAUCCAUUGCACUCCGGAUGUGCUGACCCCUGCGAUUUCCC
U1_snRNA_△E_(Xenopus_laevis)    (51) GGCGAGGCUCAGCCAUUGCACUCCGGCCGUGCUGACCCCUGCGAUUUCCC
                              101                                                 150
  U1_snRNA_△E_(Homo_sapiens)   (101) CAAAUGUGGGAAACUCGACUGCAUAAUUUGUGGUAGUGGGGGAAGAAUCC
U1_snRNA_△E_(Xenopus_laevis)   (101) CAAAUGCGGGAAAGUCGACUGCAUAAUUUCUGGUAGUGGGGGAAGAAUCC
                              151        Sm-site
  U1_snRNA_△E_(Homo_sapiens)   (151) CCUG
U1_snRNA_△E_(Xenopus_laevis)   (151) CCUG
```

12.8 Evaluation of baculovirus titer screen using end-point dilution

Table 20 – Determination of baculovirus titer concentration

	A	B	C	D	E	F	G	H	I	J
1	**Dilutions**	**Number of Infected Wells**	**Number of Unifected Wells**	**Total Number Infected**	**Total number Uninfected**	**% Total infected**	**Above 0.5**	**% Above 0.5**	**% Below 0.5**	**Log Dilution Above 50%**
2	1.00E-02	12	0	64	0	100.00	true	0.00	0.00	0.00
3	1.00E-03	12	0	52	0	100.00	true	0.00	0.00	0.00
4	1.00E-04	12	0	40	0	100.00	true	0.00	0.00	0.00
5	1.00E-05	12	0	28	0	100.00	true	0.00	0.00	0.00
6	1.00E-06	11	1	16	1	94.12	true	94.12	0.00	-6.00
7	1.00E-07	5	7	5	8	38.46	false	0.00	38.46	0.00
8	1.00E-08	0	12	0	20	0.00	false	0.00	0.00	0.00
9	1.00E-09	0	12	0	32	0.00	false	0.00	0.00	0.00
10										
11	**Num. wells**	12					**SUM**	94.12	38.46	-6
12	**mls/well**	0.01								
13										
14	**Prop. Dist.**	0.793								
15	**Log TCID**	-6.793								
16	**TCID50**	1.61E-07								
17	**1/TCID50**	6.20E+06								
18	**TCID50/ml**	6.20E+08								
19										
20	**pfu/ml**	**4.30E+08**								

Table 21 – Determination of baculovirus titer concentration (displayed formulas)

	A	B	C	D	E	F	G	H	I	J
1	Dilutions	Number of Infected Wells	Number of Unifected Wells	Total Number Infected	Total number Uninfected	% Total infected	Above 0.5	% Above 0.5	% Below 0.5	Log Dilution Above 50%
2	0.01	12	=$B$11-B2	=SUM(B2:$B$9)	=SUM($C$2:C2)	=D2/(D2+E2)*100	=IF(F2>59;"true";"false")	=IF(AND(G2="true";G3="false");F2;0)	=IF(AND(G1="true";G2="false");F2;0)	=IF(H2>0;LOG(A2);0)
3	0.001	12	=$B$11-B3	=SUM(B3:$B$9)	=SUM($C$2:C3)	=D3/(D3+E3)*100	=IF(F3>59;"true";"false")	=IF(AND(G3="true";G4="false");F3;0)	=IF(AND(G2="true";G3="false");F3;0)	=IF(H3>0;LOG(A3);0)
4	0.0001	12	=$B$11-B4	=SUM(B4:$B$9)	=SUM($C$2:C4)	=D4/(D4+E4)*100	=IF(F4>59;"true";"false")	=IF(AND(G4="true";G5="false");F4;0)	=IF(AND(G3="true";G4="false");F4;0)	=IF(H4>0;LOG(A4);0)
5	0.00001	12	=$B$11-B5	=SUM(B5:$B$9)	=SUM($C$2:C5)	=D5/(D5+E5)*100	=IF(F5>59;"true";"false")	=IF(AND(G5="true";G6="false");F5;0)	=IF(AND(G4="true";G5="false");F5;0)	=IF(H5>0;LOG(A5);0)
6	0.000001	11	=$B$11-B6	=SUM(B6:$B$9)	=SUM($C$2:C6)	=D6/(D6+E6)*100	=IF(F6>59;"true";"false")	=IF(AND(G6="true";G7="false");F6;0)	=IF(AND(G5="true";G6="false");F6;0)	=IF(H6>0;LOG(A6);0)
7	0.0000001	5	=$B$11-B7	=SUM(B7:$B$9)	=SUM($C$2:C7)	=D7/(D7+E7)*100	=IF(F7>59;"true";"false")	=IF(AND(G7="true";G8="false");F7;0)	=IF(AND(G6="true";G7="false");F7;0)	=IF(H7>0;LOG(A7);0)
8	0.00000001	0	=$B$11-B8	=SUM(B8:$B$9)	=SUM($C$2:C8)	=D8/(D8+E8)*100	=IF(F8>59;"true";"false")	=IF(AND(G8="true";G9="false");F8;0)	=IF(AND(G7="true";G8="false");F8;0)	=IF(H8>0;LOG(A8);0)
9	0.000000001	0	=$B$11-B9	=SUM(B9:$B$9)	=SUM($C$2:C9)	=D9/(D9+E9)*100	=IF(F9>59;"true";"false")	=IF(AND(G9="true";G10="false");F9;0)	=IF(AND(G8="true";G9="false");F9;0)	=IF(H9>0;LOG(A9);0)
10										
11	**Num. wells**	12					**SUM**	=SUM(H2:H9)	=SUM(I2:I9)	=SUM(J2:J9)
12	**mls/well**	0.01								
13										
14	**Prop. Dist.**	=(H11-50)/(H11-I11)								
15	**Log TCID**	=J11-B14								
16	**TCID50**	=10^B15								
17	**1/TCID50**	=1/B16								
18	**TCID50/ml**	=B17/B12								
19										
20	**pfu/ml**	**=B18*LN(2)**								

12.9 Calculation of grayscale value in methylation reactions

Table 22 – Calculation of grayscale value

	A	B	C	D	E	F
1		**0 pmol**	**x pmol**	**Gray value factor**	**0 pmol**	**x pmol**
2	0	ImageJ	values	=(255-A2)/255	=B2*D2	=C2*D2
3	1	...	...	=(255-A3)/255	=B3*D3	=C3*D3
...	...	...	...	...	...	...
...	...	...	...	...	...	...
...	...	...	...	...	...	...
256	254	...	...	=(255-A256)/255	=B256*D256	=C256*D256
257	255	ImageJ	values	=(255-A257)/255	=B257*D257	=C257*D257
258						
259				**Gray value**	=SUM(E2:E257)	=SUM(F2:F257)
260				**Grayscale value**	=E257-$E$257	=F257-$E$257

12.10 Enzyme kinetics of Sm protein substrate methylation

12.10.1 Enzyme kinetic models

Recombinant PRMT5/WD45 was used to methylate Sm protein substrates D1/D2, pICln/D1/D2, 6S, D3/B and pICln/D3/B providing a large excess of [^{3}H]-SAM co-factor. Consequently, the methylation followed a first order reaction depending on only the Sm protein substrate concentration. For specific reaction conditions see Methods 4.3.19.4, page 72. The resulting methylation activities were plotted as shown below.

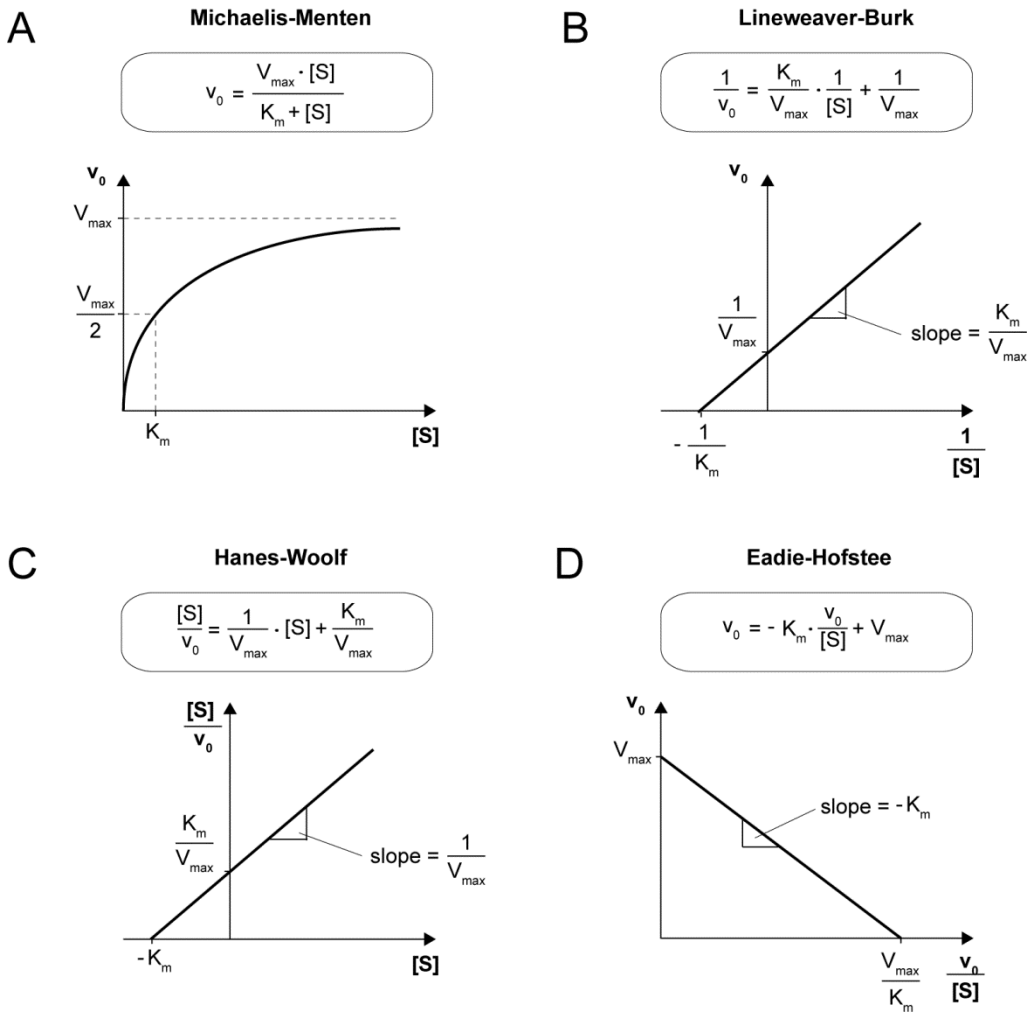

Figure 73 – Graphical analysis of enzyme kinetic reactions.

The substrate concentration and reaction velocity were plotted according to mathematical models derived from Michaelis-Menten kinetics. **(A)** Michaelis-Menten plot. **(B)** Lineweaver-Burk plot. **(C)** Hanes-Woolf plot. **(D)** Eadie-Hofstee plot.

12.10.2 Enzyme kinetic analysis of D1-containing Sm protein substrates

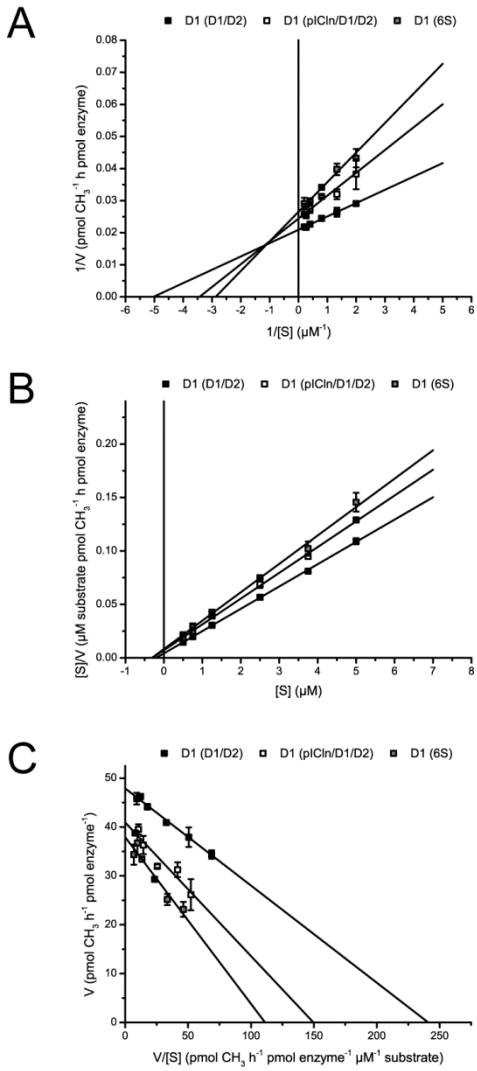

Figure 74 – Enzyme kinetic analysis of D1-containing Sm protein substrates.

Increasing amounts of Sm protein substrates D1/D2 (D1: ■), pICln/D1/D2 (D1: □) and 6S (D1: ▩) were methylated, separated by SDS-PAGE and analyzed by autoradiography and densitometry. The resulting methylation rates are depicted in enzyme kinetic plots following the models of Lineweaver-Burk **(A)**, Hanes-Woolf **(B)** and Eadie-Hofstee **(C)**. From these, the corresponding enzyme kinetic constants K_m and V_{max} were obtained and are listed in the following table. Values represent the average of four separate experiments. Error bars show the standard errors of the mean.

Table 23 – Enzyme kinetic data of D1-containing Sm protein substrate methylation.

		Michaelis-Menten	Lineweaver-Burk	Hanes-Woolf	Eadie-Hofstee
D1/D2	K_m	0.3065	0.1989	0.1989	0.1988
	V_{max}	50.3673	47.9400	47.9400	47.8946
pICln/D1/D2	K_m	0.4203	0.2917	0.2967	0.2735
	V_{max}	43.4272	40.9566	41.4927	40.9383
6S	K_m	0.3452	0.3481	0.3097	0.3409
	V_{max}	38.0384	37.7048	37.6499	37.9174

[K_m] = µM, [V_{max}] = pmol methyl groups per 1 pmol enzyme and hour

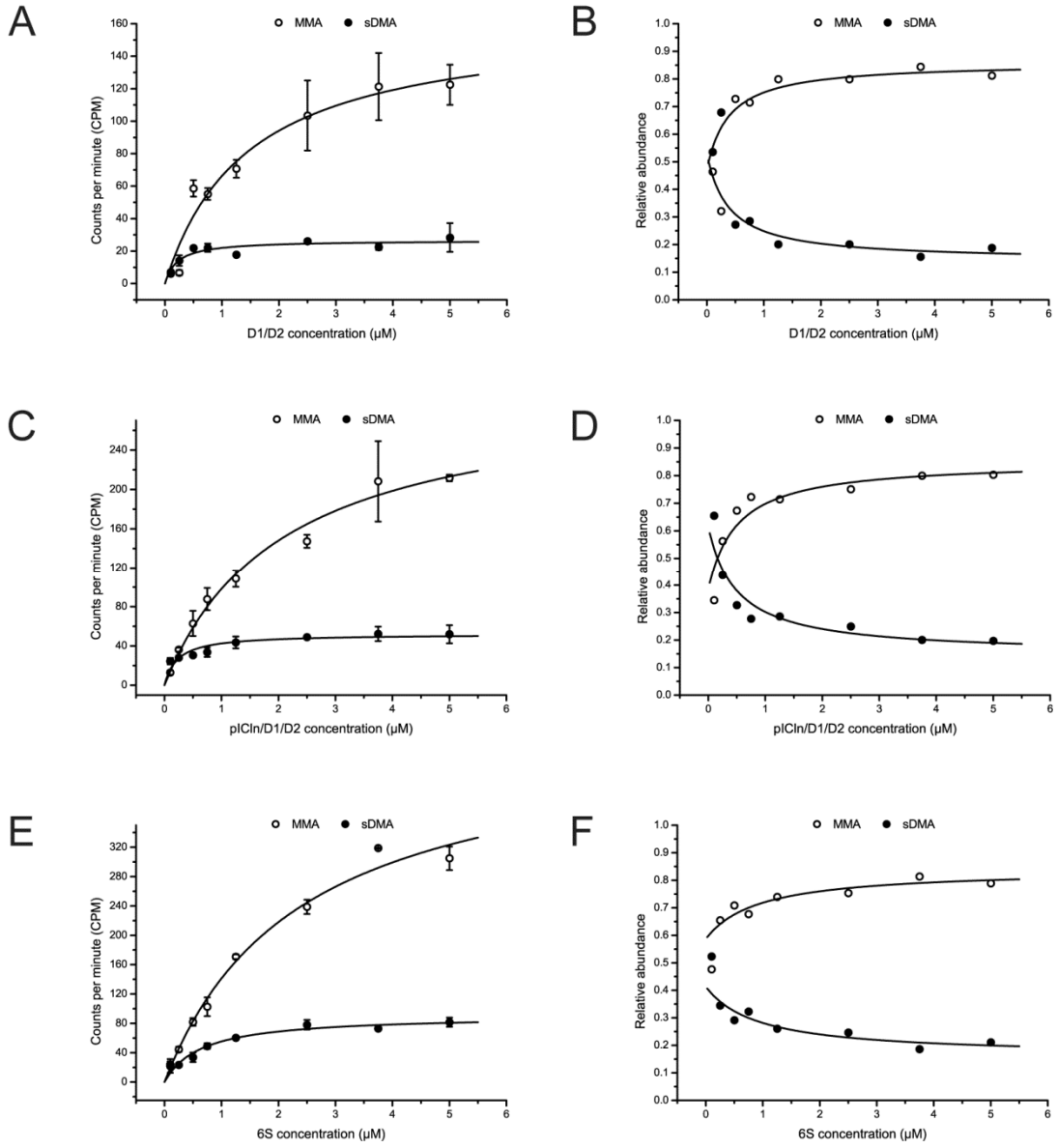

Figure 75 – Relative abundance of MMA and sDMA in D1-containing Sm protein substrate methylation.

Increasing amounts of Sm protein substrates D1/D2 **(A, B)**, pICln/D1/D2 **(C, D)** and 6S **(E, F)** were methylated, TCA-precipitated, hydrolyzed into individual amino acids and analyzed by thin layer chromatography and liquid scintillation counting. The resulting radioactive signals corresponding to methyl groups in monomethylated (MMA: ○) and symmetrically dimethylated (sDMA: ●) arginines were plotted against the initial substrate concentration **(A, C, E)**. Finally, the relative abundance of both arginine modifications was calculated and depicted likewise **(B, D, F)**. Values represent the average of four separate experiments. Error bars show the standard errors of the mean.

12.10.3 Enzyme kinetic analysis of D3/B-containing Sm protein substrates

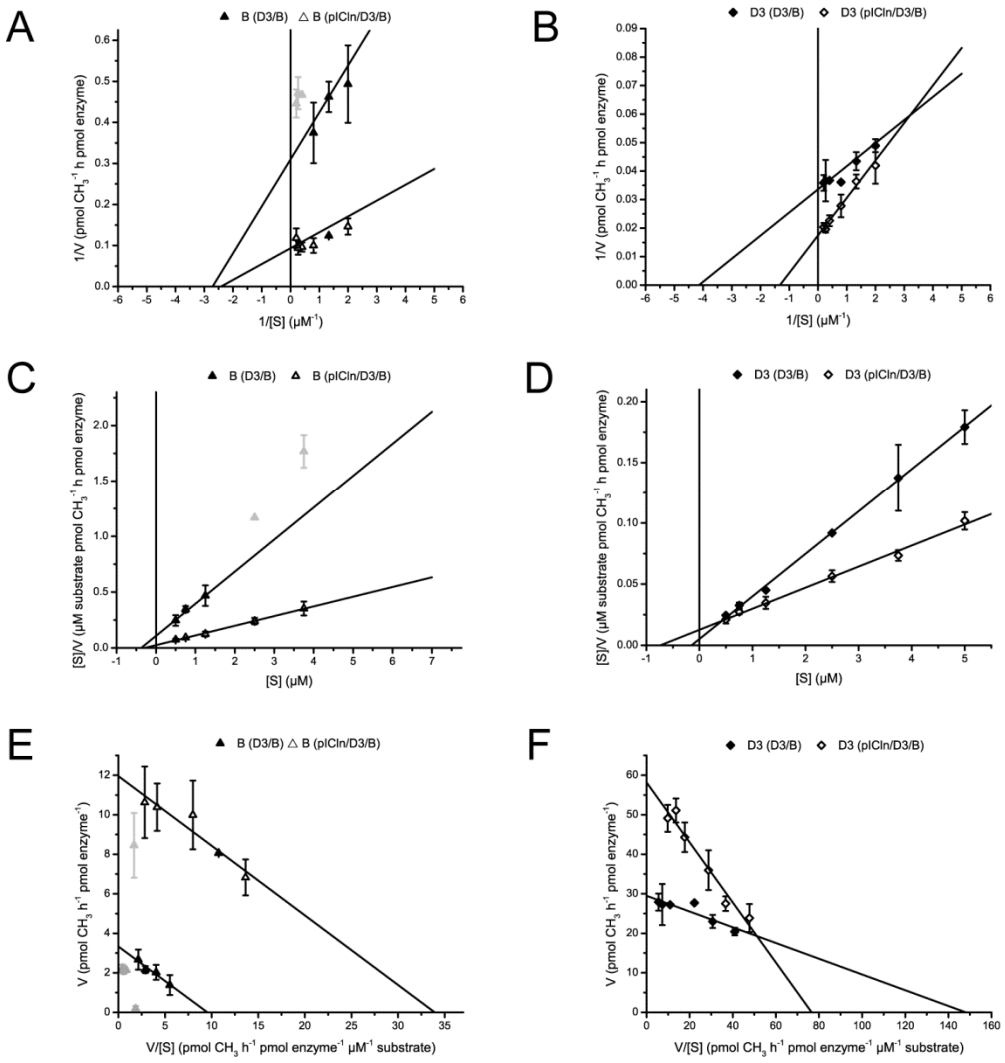

Figure 76 – Enzyme kinetic analysis of D3/B-containing Sm protein substrates.

Increasing amounts of Sm protein substrates D3/B (D3: ◆, B: ▲) and pICln/D3/B (D3: ◇, B: △) were methylated, separated by SDS-PAGE and analyzed by autoradiography and densitometry. The resulting methylation rates are depicted in enzyme kinetic plots by Lineweaver-Burk **(A, B)**, Hanes-Woolf **(C, D)** and Eadie-Hofstee **(E, F)** showing either the modification B **(A, C, E)** or D3 **(B, D, F)**. From these, the corresponding enzyme kinetic constants K_m and V_{max} were obtained and are listed in the following table. Gray data points are outliers and were not considered in the regression analysis. Values represent the average of four separate experiments. Error bars show the standard errors of the mean.

Table 24 – Enzyme kinetic data of D3/B-containing Sm protein substrate methylation.

		Michaelis-Menten	Lineweaver-Burk	Hanes-Woolf	Eadie-Hofstee
D3/B*	K_m	0.1424	0.6917**	0.3739	0.0190
	V_{max}	2.5615	2.2815	2.0947	2.2647
D3*/B	K_m	0.3837	0.2415	0.1478	0.1991
	V_{max}	31.8677	29.7616	28.6920	29.4892
pICln/D3/B*	K_m	0.2577	0.4130	0.2886	0.3521
	V_{max}	10.8889	10.6909	11.5404	11.9517
pICln/D3*/B	K_m	0.7395	0.7562	0.7339	0.7592
	V_{max}	57.9735	57.4503	58.0076	58.1513

[K_m] = µM, [V_{max}] = pmol methyl groups per 1 pmol enzyme and hour

* In D3/ B-containing substrates both proteins can be methylated. The respective substrate is indicated by an asterisk.

** Excluded from enzyme kinetic analyses.

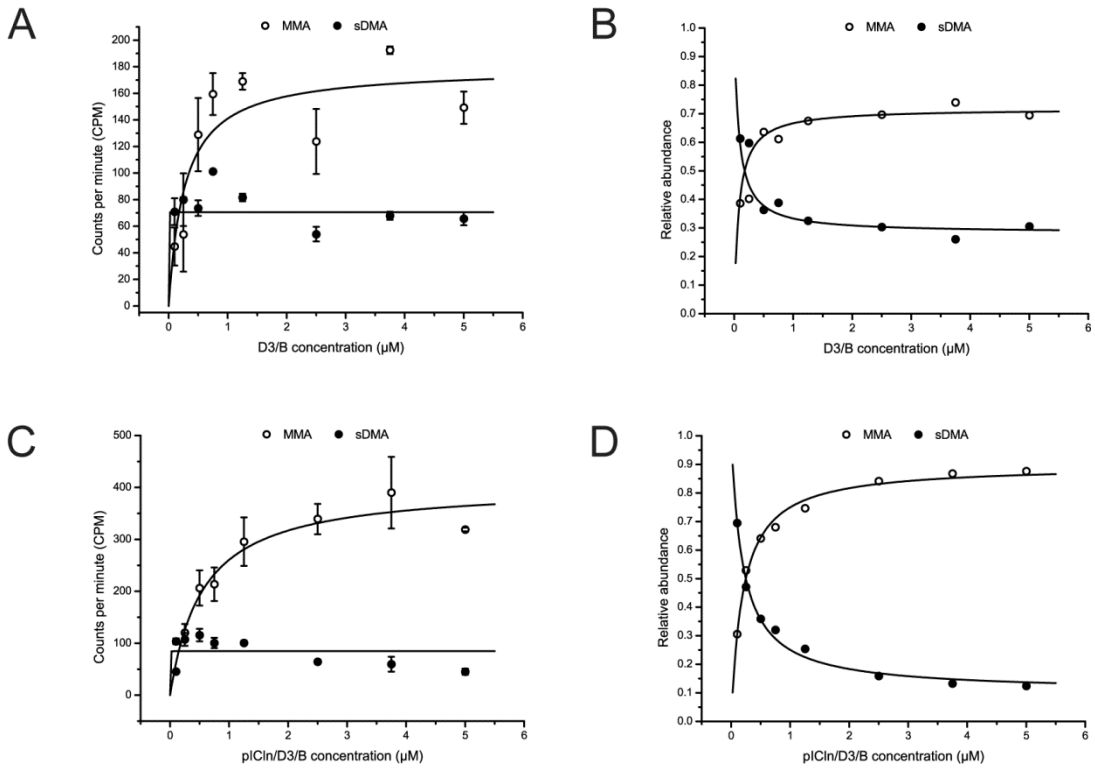

Figure 77 – Relative abundance of MMA and sDMA in D3/B-containing Sm protein substrate methylation.

Increasing amounts of Sm protein substrates D3/B **(A, B)** and pICln/D3/B **(C, D)** were methylated, TCA-precipitated, hydrolyzed into individual amino acids and analyzed by thin layer chromatography and liquid scintillation counting. The resulting radioactive signals corresponding to methyl groups in monomethylated (MMA: ○) and symmetrically dimethylated (sDMA: ●) arginines were plotted against the initial substrate concentration **(A, C)**. Finally, the relative abundance of both arginine modifications was calculated and depicted likewise **(B, D)**. Values represent the average of four separate experiments. Error bars show the standard errors of the mean.

12.11 Order of MMA and sDMA formation

Sm proteins B/B', D1 and D3 contain 6, 9 and 4–5 arginine residues that are symmetrically dimethylated in snRNPs *in vivo*. The order in which methyl groups are incorporated to form monomethylated (MMAs) and symmetrically dimethylated arginines (sDMAs) dictates the relative abundance of both methylation products.

In the beginning, neither MMA nor sDMA are present. Following a distributive mechanism, methyl groups are added one at a time necessitating the intermediate release of the substrate. In each reaction, either MMA or sDMA is formed, whereas sDMA is generated only by the transfer of a second methyl group onto MMA. Depending on the amount of transferred MMA and sDMA, the relative abundance of each product can be calculated from the experimental data.

A theoretical model has been developed to deduce the order and number of mono- and dimethylations (Results 5.5.13, page 138; Discussion 6.2.3, page 168). Initially, the substrate protein is once mono- and dimethylated resulting in a large fluctuation of the relative abundance of MMA and sDMA. Further reactions are iterative and consist of several (n-fold) monomethylations and a subsequent singular dimethylation. Consequently, the number of these monomethylation reactions has a strong influence on the relative abundance of MMA and sDMA. In a theoretical model, the effect of one to four of these monomethylations was analyzed (Figure 78 and Figure 79). The relative abundance of MMA and sDMA in methylation reactions with increasing incubation times can therefore be applied to deduce the number of monomethylations that are made before sDMA is formed. If a methylation substrate contains only one receptive arginine residue, a raised relative abundance of MMA indicates the monomethylation of several substrate molecules before some of these receive a second methyl group. Consequently, it is possible to deduce whether the enzyme interacts with only a single substrate molecule to generate sDMA in all possible methylation sites or whether several molecules carrying various numbers of methyl groups are processed. In the first scenario, one would expect a majority of sDMA to occur throughout the entire reaction. All arginine residues of a substrate molecule would be first altered to MMA and then to sDMA. This would reduce the number of still unmodified arginine residues. The next substrate molecule could only be processed after the first one was completely symmetrically dimethylated. In

the second scenario, the large excess of unmethylated substrate would primarily result in MMA formation.

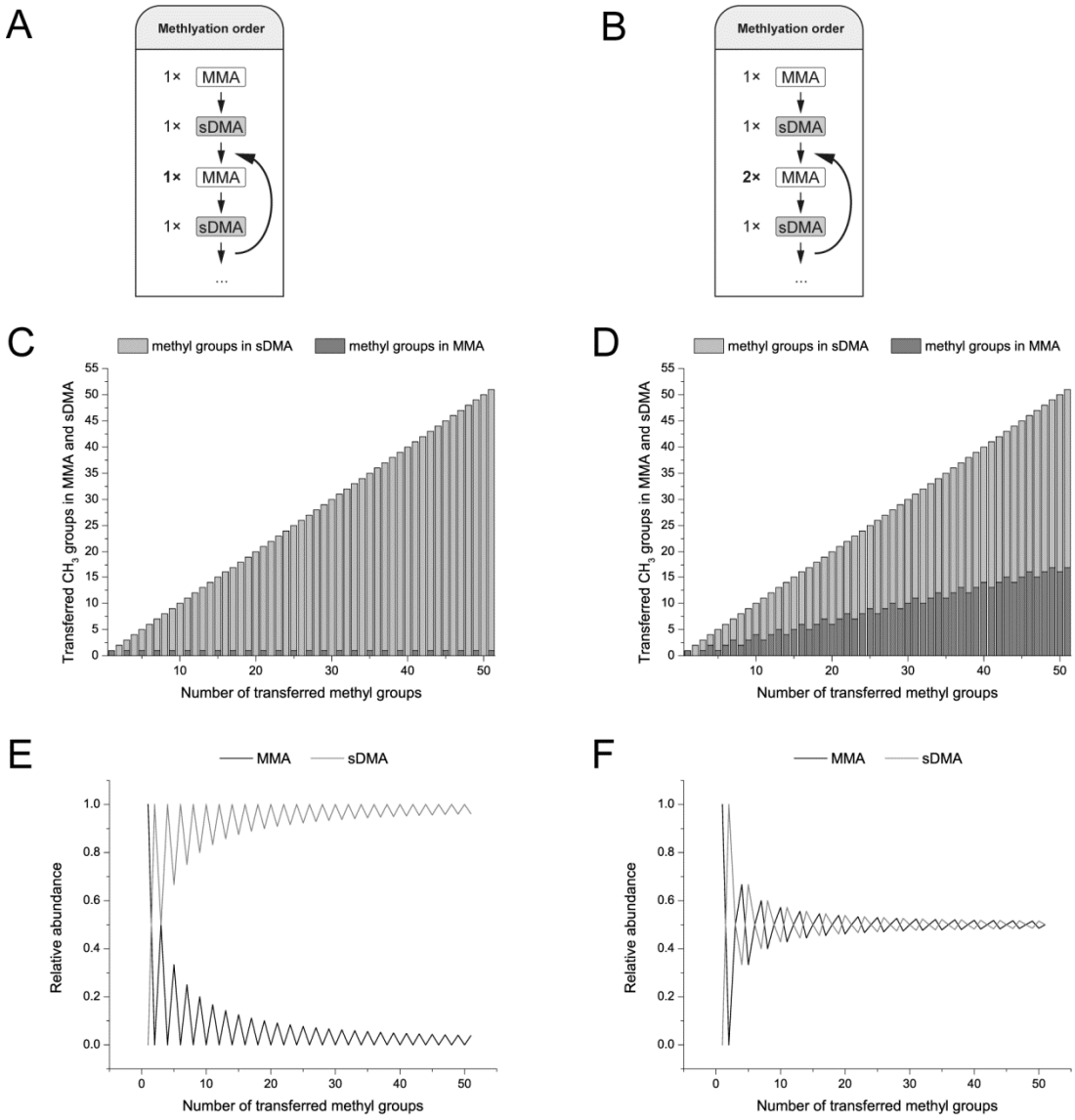

Figure 78 – Order of MMA and sDMA formation dictates its relative abundance (1× and 2× MMA)

In a theoretical approach, substrates were once mono- and dimethylated. In the following reactions, either one MMA and one sDMA **(A, C, E)** or two MMAs and one sDMA **(B, D, F)** were formed consecutively. **(A, B)** Order of MMA and sDMA incorporation. **(C, D)** Incorporated methyl groups forming MMA (dark gray bars) and sDMA (light gray bars). **(E, F)** Predicted relative abundance of MMA (black line) and sDMA (gray line).

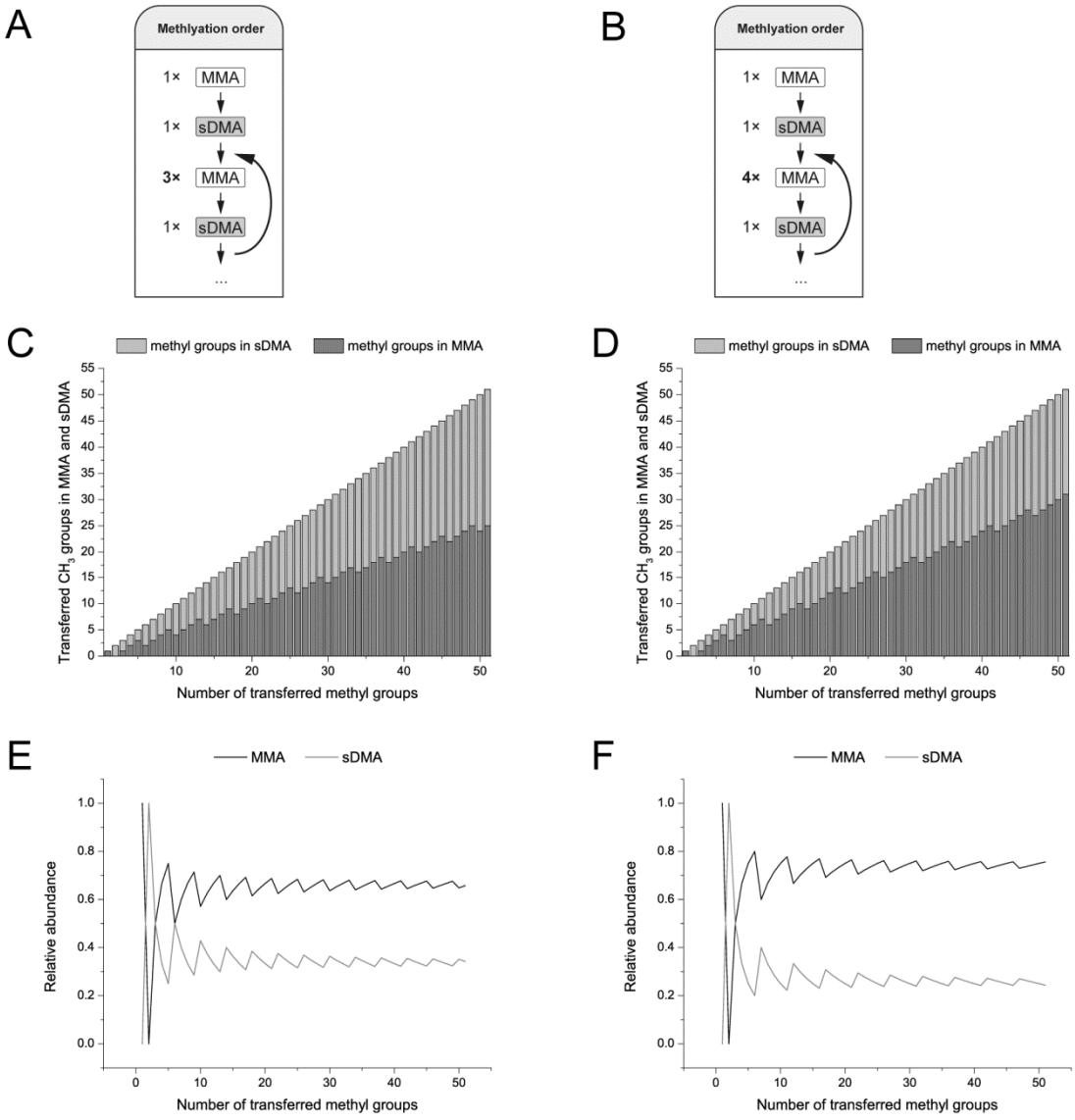

Figure 79 – Order of MMA and sDMA formation dictates its relative abundance (3× and 4× MMA).

In a theoretical approach, substrates were once mono- and dimethylated. In the following reactions, either three MMA and one sDMA **(A, C, E)** or four MMAs and one sDMA **(B, D, F)** were formed consecutively. **(A, B)** Order of MMA and sDMA incorporation. **(C, D)** Incorporated methyl groups forming MMA (dark gray bars) and sDMA (light gray bars). **(E, F)** Predicted relative abundance of MMA (black line) and sDMA (gray line).

12.12 Evaluation of thin layer chromatography of amino acids

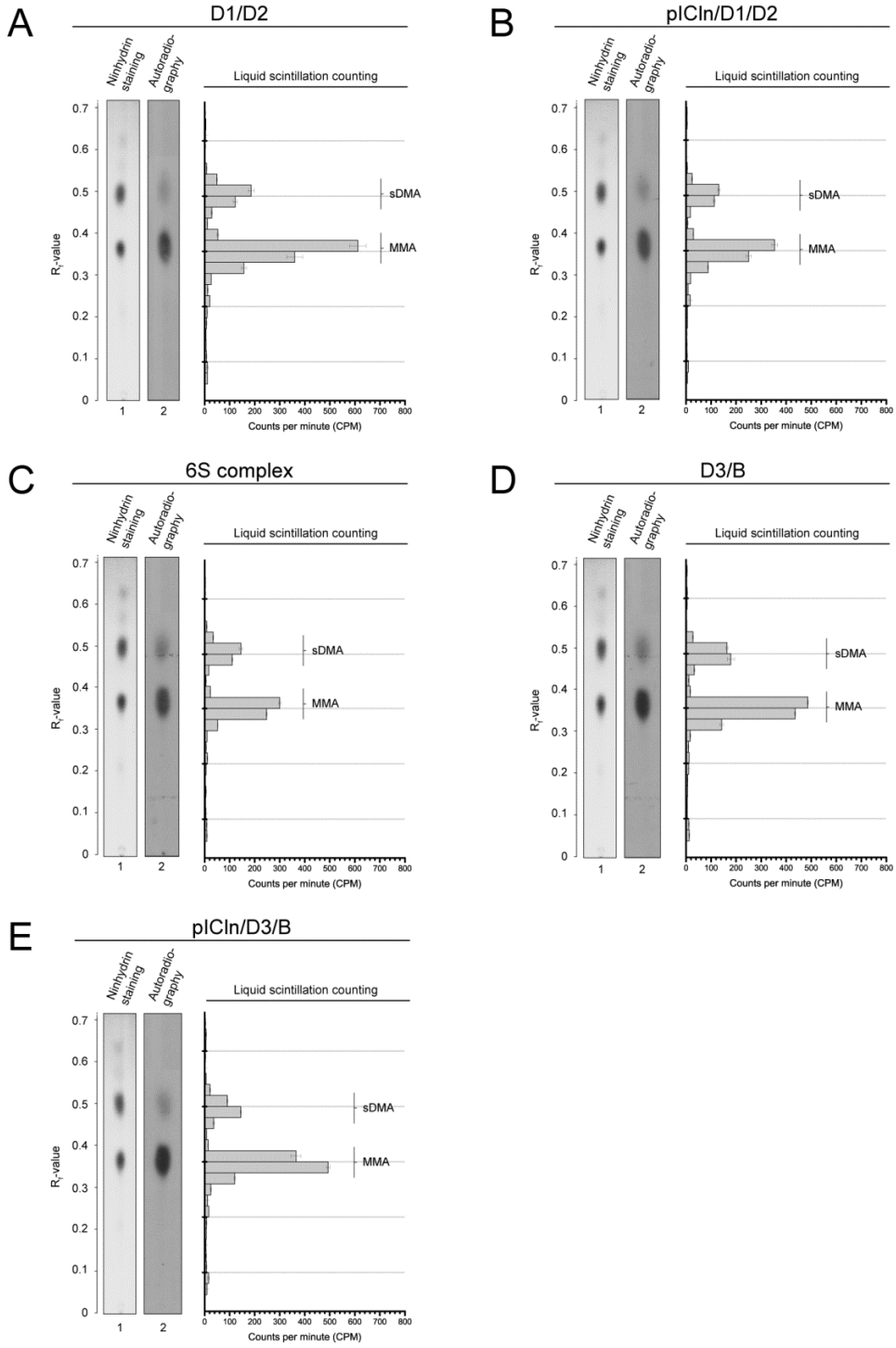

Figure 80 – Thin layer chromatography of methylated Sm protein substrates.

One hundred picomoles Sm protein substrates (**A**: D1/D2, **B**: pICln/D1/D2, **C**: 6S, **D**: D3/B, **E**: pICln/D3/B) were methylated by 5 pmol PRMT5/WD45 in 100 mM Hepes (pH 8.2) using 1 nmol [^{3}H]-SAM as a co-factor for 60 min at 37°C. After TCA precipitation and total hydrolysis, the samples were mixed with monomethylated and symmetrically dimethylated arginine standards and applied to thin layer chromatography and ninhydrin staining. Finally, the surface of the TLC plate was scraped off and analyzed by liquid scintillation counting. Lane 1: Ninhydrin staining of TLC plate; Lane 2: Autoradiography of TLC plate (3 weeks exposure); Right panel: Diagram showing the evaluation of the liquid scintillation counting.

13 Publications

Parts of this dissertation have been published in the following articles. Articles are listed in chronological order of their publication date.

Otter, S., Grimmler, M., **Neuenkirchen, N.**, Chari, A., Sickmann, A., and Fischer, U. (2007). A comprehensive interaction map of the human survival of motor neuron (SMN) complex. **J Biol Chem** *282*, 5825–5833.

Neuenkirchen, N., Chari, A., and Fischer, U. (2008). Deciphering the assembly pathway of Sm-class U snRNPs. **FEBS Lett** *582*, 1997–2003.

Chari, A., Golas, M. M., Klingenhager, M., **Neuenkirchen, N.**, Sander, B., Englbrecht, C., Sickmann, A., Stark, H., and Fischer, U. (2008). An assembly chaperone collaborates with the SMN complex to generate spliceosomal SnRNPs. **Cell** *135*, 497–509.

Martin G., Ostareck-Lederer A., Chari A., **Neuenkirchen N.**, Dettwiler S., Blank D., Rüegsegger U., Fischer U., and Keller W. (2010). Arginine methylation in subunits of mammalian pre-mRNA cleavage factor I. **RNA** 16, 1646–1659.

Gross, H., Hennard, C., Marouris, I., Barth, S., Stober-Grässer, U., Moritz, B., Ostareck, D., Ostareck-Lederer, A., **Neuenkirchen, N.**, Fischer, U., Deng, W., Leonhardt, H., Noessner, E., Kremmer, E., and Graesser, F.A. (2012). Binding of the heterogeneous ribonucleoprotein K (hnRNP K) to the Epstein-Barr virus nuclear antigen 2 (EBNA2) enhances its transcriptional activation. **PLoS One, submitted**.

14 Acknowledgements

I would like to express my thanks to the people who have been very helpful to me during the time of my PhD:

- Prof. Utz Fischer for being my PhD advisor and guiding me throughout the course of this work.
- Prof. Alexander Buchberger for being the second examiner of the dissertation.
- Prof. Manfred Gessler for being the third member of the oral defence commission.
- All people from the lab who contributed to this work.
- And finally my family for supporting me.